AD-A107 255 AIR FORCE INST OF TECH WRIGHT-PATTERSON AFB OH F/G 11/6
MECHANISMS OF RECOVERING LOW CYCLE FATIGUE DAMAGE IN INCOLOY 90--ETC(U)
1979 R E SCHAFRIK
UNCLASSIFIED AFIT-CI-79-212D NL

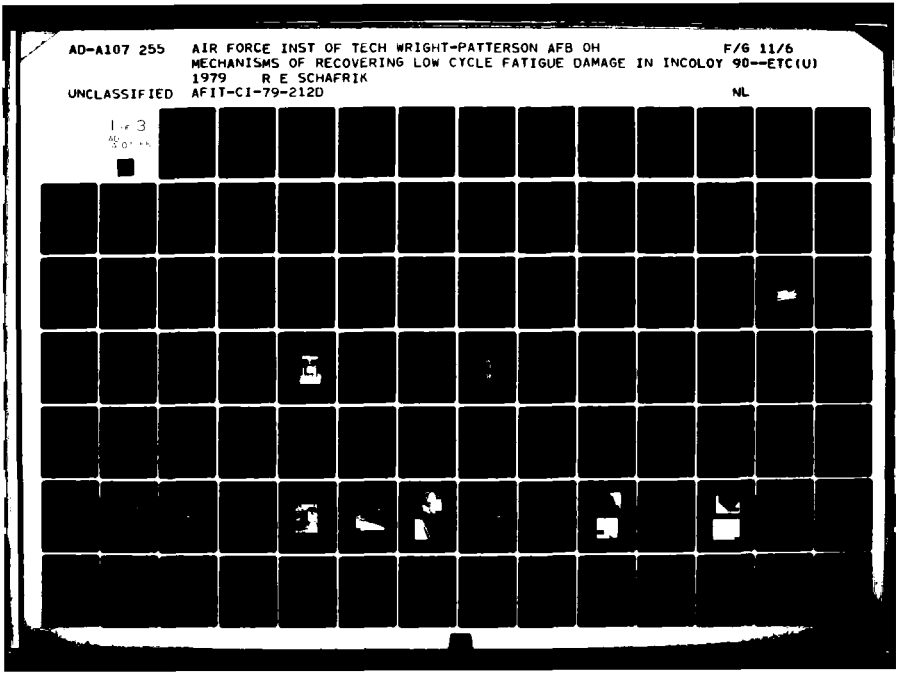

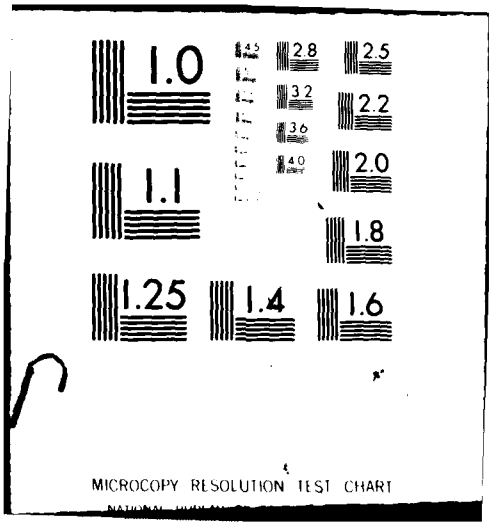
1.0
1.1
1.25
1.4
1.6
1.8
2.0
2.2
2.5
2.8
3.2
3.6
4.0
MICROCOPY RESOLUTION TEST CHART

UNCLASS

SECURITY CLASSIFICATION OF THIS PAGE (When Data Entered)

REPORT DOCUMENTATION PAGE

READ INSTRUCTIONS BEFORE COMPLETING FORM

1. REPORT NUMBER: 79-212D
2. GOVT ACCESSION NO.: AD-A107 255
3. RECIPIENT'S CATALOG NUMBER:
4. TITLE (and Subtitle): Mechanisms of Recovering Low Cycle Fatigue Damage in Incoloy 901
5. TYPE OF REPORT & PERIOD COVERED: ~~THESIS~~/DISSERTATION
6. PERFORMING ORG. REPORT NUMBER:
7. AUTHOR(s): Capt Robert E. Schafrik
8. CONTRACT OR GRANT NUMBER(s):
9. PERFORMING ORGANIZATION NAME AND ADDRESS: AFIT STUDENT AT: The Ohio State University
10. PROGRAM ELEMENT, PROJECT, TASK AREA & WORK UNIT NUMBERS:
11. CONTROLLING OFFICE NAME AND ADDRESS: AFIT/NR, WPAFB OH 45433
12. REPORT DATE: 1979
13. NUMBER OF PAGES: 239
14. MONITORING AGENCY NAME & ADDRESS (if different from Controlling Office)
15. SECURITY CLASS. (of this report): UNCLASS
15a. DECLASSIFICATION/DOWNGRADING SCHEDULE

LEVEL II

AD A107255

DTIC ELECTE NOV 13 1981 H

16. DISTRIBUTION STATEMENT (of this Report)

APPROVED FOR PUBLIC RELEASE; DISTRIBUTION UNLIMITED

17. DISTRIBUTION STATEMENT (of the abstract entered in Block 20, if different from Report)

22OCT 1981

Fredric C. Lynch

FREDRIC C. LYNCH, Major, USAF
Director of Public Affairs
Air Force Institute of Technology (ATC)
Wright-Patterson AFB, OH 45433

18. SUPPLEMENTARY NOTES

APPROVED FOR PUBLIC RELEASE: IAW AFR 190-17

19. KEY WORDS (Continue on reverse side if necessary and identify by block number)

20. ABSTRACT (Continue on reverse side if necessary and identify by block number)

ATTACHED

FILE COPY

81 10 30 051

DD FORM 1 JAN 73 1473 EDITION OF 1 NOV 65 IS OBSOLETE

UNCLASS

SECURITY CLASSIFICATION OF THIS PAGE (When Data Entered)

MECHANISMS OF RECOVERING LOW CYCLE FATIGUE DAMAGE
IN INCOLOY 901
BY

Robert E. Schafrik, Capt. USAF (Ph.D.)
The Ohio State University, 1979
Professor James A. Begley, Adviser

ABSTRACT

The effect of thermal treatment and hot isostatic pressing (HIP) on eliminating low cycle fatigue (LCF) damage in the iron-nickel superalloy, Incoloy 901, was investigated. Testing was done in air at 500°F at a total strain range of 0.75%. The mechanisms of crack initiation and crack propagation in baseline specimens were determined and used as the basis of comparison for the rejuvenated specimens.

Crack initiation in the baseline specimens was due to decohering of blocky grain boundary carbides. Pre-crack initiation damage consisted of extrusions and intrusions formed at persistent slip bands and partially decohered grain boundary carbides.

A pre-rejuvenation damage level of 800 cycles (60% of crack initiation) was selected. Some specimens to be HIP processed were ceramic coated; the rest were left uncoated. Post-HIP testing revealed that LCF properties were adversely affected by surface microstructural damage caused by the HIP processing.

Thermal rejuvenation, consisting of a standard solution treatment and double aging, was partially successful in recovering fatigue properties with a pre-rejuvenation damage level of 800 cycles. Initiation life was extended by 400 cycles and cycles to failure was extended by 600 cycles. This behavior is explained in terms of microstructural damage which is resistant to thermal treatment.

Total Pages - 259

Selected Bibliography

1. M.N. Menon and W.H. Reiman, "Low Cycle Fatigue Crack Initiation Study in Renè 95", J. Mater. Sci. 10, 1571-1581 (1975).

2. B. Leis and A. Clauer, Investigation of Rejuvenation of Fatigue Damage in IN-718, AFML TR-78-90, Wright-Patterson AFB, OH.

3. H.F. Merrick, "The Low Cycle Fatigue of Three Wrought Nickel-Base Alloys", Met Trans 5, 891-897 (1976).

4. C. Laird, Mechanisms and Theories of Fatigue, presented at the Materials Science Seminar, ASM, St. Louis Mo. (1978).

MECHANISMS OF RECOVERING LOW CYCLE FATIGUE DAMAGE IN INCOLOY 901

DISSERTATION

Presented in Partial Fulfillment of the Requirements for the Degree Doctor of Philosophy in the Graduate School of The Ohio State University

By

Robert E. Schafrik, B.S.Met., M.S.

* * * * *

The Ohio State University

1979

Reading Committee:

Dr. G. W. Powell

Dr. J. P. Hirth

Dr. J. A. Begley

Approved By

James A. Begley

Adviser

Department of Metallurgical Engineering

DEDICATION

To my wife, Mary; and to my children: Catherine, Frances, Robert Jr., and Steven.

ACKNOWLEDGEMENTS

The author wishes to express his sincere appreciation to Dr. J. A. Begley of The Ohio State University for his guidance and encouragement throughout this project. The author is thankful for the constructive comments of the following individuals in the early stages of this effort: Dr. B. Wilshire of University College, University of Wales; A. Adair, Dr. W. Reimann, and Dr. H. A. Lipsitt of the Air Force Materials Laboratory, Wright-Patterson Air Force Base; Drs. A. Clauer and B. Leis, Battelle-Columbus Laboratories; and Dr. J. C. Williams, Carnegie-Mellon University. Also, the author is grateful for the excellent training in practical aspects of transmission electron microscopy provided by Dr. J. C. Williams.

Appreciation is due to Captain P. Martin and R. Kerans of the Air Force Materials Laboratory for helpful advice, instruction, and troubleshooting assistance in using the many different pieces of laboratory equipment required to complete this dissertation; and for helpful discussions on the research work throughout the project. Also, appreciation is due to Mr. Dwelle Butts of the Air Force Materials Laboratory for his efforts in obtaining necessary supplies.

I wish to thank my wife, Mary, and our four children for their support and extreme patience throughout my graduate education.

The author is obliged to the following for supplying materials: M. M. Allen, Government Products Division, Pratt-Whitney Aircraft Co.,

for providing a section of a compressor shaft forging; P. Bailey, Aircraft Engine Group, General Electric Co., for providing ceramic coating for some specimens; and D. Weaver, Kelsey-Hayes, Detroit, for a piggybacked hot-isostatic-pressing run.

I would like to recognize the cooperation and help of the following: S. Leffler, J. Henry, M. Henry, G. Cornish, and J. Barlowe. Many thanks are due to Ms. S. Ehlers for typing this manuscript.

Able assistance in transferring my fatigue data from paper punch tape format to computer disk file was provided by Captain D. Summer and Ms. C. Johnson of the Air Force Materials Laboratory.

This research was performed under the auspices of the Air Force Materials Laboratory. I am appreciative of the moral and financial support provided by Dr. H. A. Lipsitt, and for his helpful advice during various stages in this project. I am likewise appreciative of the encouragement given me by Dr. H. Burte and L. Hjelm of the Air Force Materials Laboratory.

Finally, I wish to thank the Air Force Institute of Technology and the U. S. Air Force for the opportunity to complete my graduate education. I would like to acknowledge the administrative assistance provided by my Program Managers, Captains S. Brown and D. Cain.

VITA

February 6, 1946	Born - Cleveland, Ohio
1963-1967	B.S.Met., Case-Western Reserve University, Cleveland, Ohio
1967-1968	Applications Engineer, American Air Filter Co., Louisville, KY
1968	Commissioned and entered U. S. Air Force
1968-1972	Base Civil Engineer, Hanscom Air Force Base, Bedford, MA
1972-1974	M.S., Aerospace Engineering, Air Force Institute of Technology, Wright-Patterson Air Force Base, Ohio
1974-1975	Materials Development Engineer, Metallurgy and Ceramics Laboratory, Aerospace Research Laboratories, Wright-Patterson Air Force Base, Ohio
1975-1977	Assistant Branch Chief, Metals Branch, Manufacturing Technology, Air Force Materials Laboratory, Wright-Patterson Air Force Base, Ohio

PUBLICATIONS

"Determination of Texture Pole Figures Using Picker FACS-1 Apparatus," with L. A. Jacobson, ARL TR 75-0190, Aerospace Research Laboratories, Wright-Patterson Air Force Base, Ohio (1975).

"The Deformation and Fracture of TiAl at Elevated Temperatures," with H. A. Lipsitt and D. S. Schechtman, Met. Trans. A 6A, 1991-1996 (1975).

"Dynamic Elastic Moduli of the Titanium Aluminides," Met. Trans. A 8A, 1003-1006 (1977).

"Manufacture of TiAl by Extrusion of Blended Elemental Powders," Met. Trans. B 7B, 713-716 (1976).

"Manufacture of TiAl by Extrusion of Blended Elemental Powders," DDC Report AD-780630, Defence Documentation Center, Arlington, VA (1974).

TABLE OF CONTENTS

TABLE OF CONTENTS (CONT'D)

TABLE OF CONTENTS (CONT'D)

LIST OF TABLES

LIST OF FIGURES

LIST OF FIGURES (CONT'D)

LIST OF FIGURES (CONT'D)

LIST OF FIGURES (CONT'D)

LIST OF FIGURES (CONT'D)

Chapter 1

INTRODUCTION

The modern gas turbine engine demands the ultimate in performance from materials. Typical material requirements include high strength and stiffness at operating temperatures, good oxidation resistance, low creep rates and high stress rupture values, and good low-cycle and high-cycle fatigue resistance. Since the results of component failure, especially of rotating components, usually are catastrophic, design approaches and material specifications tend to be conservative (1,3,4,61).

A turbine disk is that component which transmits the work done by hot, expanding gases on the turbine blades to the power shaft of the engine. Experience has indicated that turbine disks can fail either by stress rupture at the rim where the blades are attached with dovetail slots; or, as is usually the case, by low-cycle fatigue at cross-sectional changes or at bolt holes (10). The low-cycle fatigue results from vibration, changing engine operating speeds and thermal gradients (3,12). When a turbine disk is limited by low-cycle fatigue (LCF) life, the design approach is to establish a probability of failure of 0.5%, with failure defined as extension of a detectable crack and not component disintegration. Therefore, most turbine disks reach their LCF life with a high probability of additional life remaining (1). Since these disks are quite expensive, there is a great deal of interest in processing the disks in some manner (i.e., rejuvenating the disks)

to remove the microstructural damage which leads to LCF failure, so that the disks can be returned to service safely and reliably at low cost (2).

This investigation was undertaken to determine how the LCF process causes crack initiation in Incoloy 901, and to find which rejuvenation treatments can lead to recovery of the initiation life. Incoloy 901 was selected for study because it is a commonly used superalloy and, thus, there are many disks which potentially can be returned to service after rejuvenation.

Subsequent portions of this introduction will briefly review LCF crack initiation and propagation in superalloys, the physical metallurgy of Incoloy 901, and rejuvenation.

I. CRACK INITIATION

Dieter divides the fatigue process into four steps: crack initiation, Stage I crack growth, Stage II crack growth, and ultimate ductile failure (14). This classification will be used in the following discussion.

The mechanisms for LCF crack initiation generally involve the interaction between the deformation processes and the alloy microstructures (1,4,5,6,7,8,9,11,46,64,67,68). The mode of crack nucleation depends on such factors as the amount of deformation, the degree of slip dispersal, test temperature and environment, and the amount and type of microstructural defects (carbo-nitrides, borides, porosity, brittle second phases, etc.). Kim and Laird point out that in pure metals, crack initiation occurs at persistent slip bands at low stress ranges and at grain boundaries at high stress ranges exclusive of severe

environmental effects (47). In lower temperature regimes (less than about 700°F or 370°C), superalloys deform by planar slip which is heterogeneous in nature (4). Kuhlmann-Wilsdorf and Laird have developed a dislocation model to explain how persistent slip bands can lead to the formation of instrusions and extrusions on the specimen surface which in turn lead to crack initiation (49,46). This model presents the rationale for the simple stress-raiser mechanism proposed by Wood 20 years ago (50).

At high cyclic ranges, cracks generally initiate at the grain boundaries. Recent work by Kim and Laird (47,48) have developed three criteria for crack initiation in pure metals at grain boundaries: (a) The grain boundaries must have a high degree of lattice mismatch; (b) The slip on the active slip system in either one or both of the adjacent grains should be directed at the intersection of the boundary with the specimen surface; and (c) The trace of the boundary at the free surface should lie at an angle of 30-90° with respect to the stress axis. Kim and Laird also observed grain boundary sliding in their LCF experiments on pure copper (47). The cracks were observed to have initiated at grain boundary steps.

Superalloys contain a substantial amount of carbides, carbo-nitrides, and borides intentionally added to control the grain size, improve creep resistance, increase grain boundary strength, and to vitiate the adverse effects of trace elements (17). Unfortunately, it has been found that these nonmetallic inclusions serve as favorable sites for crack initiation. In a study by Gell and Leverant on the LCF behavior of Mar-M200, it was found that metal carbides played a key role in

determining the crack initiation life (8). The carbides can be pre-cracked due to differential contraction during the solidification process or during the various metalworking processes. Also, the carbides can de-cohere from the matrix, especially at the surface, leading to a localized strain concentration region. As recently shown by Reimann and Menon, carbides provide a preferential path for developing LCF cracks in René 95 and seem to be associated with initiation of the cracks themselves (1).

Many investigators have found coherent twin boundaries to be significant sites for crack initiation at lower stress ranges (4).

II. STAGE I CRACK PROPAGATION

There is some disagreement in the literature about a definition of Stage I cracking. Coffin suggests that Stage I is early growth of a crack to some detectable limit and then propagation through a plastic regime (12). A more accepted definition is that Stage I cracking is that stage where cracks propagate along specific crystallographic planes which are oriented near 45° to the applied stress axis (46). But Laird points out that this definition is not strictly applicable to LCF where crack nucleation and growth may occur along sections which are not crystallographic (47).

Since persistent slip bands develop on the most active slip plane, cracks initiated at them generally continue to propagate along them (46). Thus, a persistent slip band can lead to the development of intrusions/extrusions, to a crack nucleus, and finally to crack propagation.

Similarly, cracks nucleated at grain boundaries tend to grow along the boundary both on the surface and into the bulk (47). Thus, the

crack front develops a thumbnail shape. Also, Kim and Laird predicted and observed a crack path which is asymmetric with respect to the boundary, with the crack occurring in that grain with the most favorably oriented active slip system (48).

III. STAGE II CRACK PROPAGATION

Coffin proposes that Stage I cracking leads to Stage II cracking when the crack overcomes the plastic zone which envelops it during its early stages, and thus it begins to grow elastically (12).

Usually, however, Stage II is denoted as the transition of the crack from growing along the maximum shear direction to growing normal to the applied stress direction. At high stress ranges, the crack will almost immediately propagate by Stage II processes (46).

It is during Stage II crack growth that fatigue striations are generated, although not all materials develop a striation pattern. Striations are usually observed in superalloys (53). It is generally accepted that each striation represents the propagation distance of a fatigue crack during each cycle. A crack plastic blunting process proposed by Laird requiring two slip systems (51) is a very reasonable explanation for the formation of striations (52).

Stage II continues until the crack becomes long enough to cause the final instability. In brittle materials, the crack begins to propagate unstably after a critical length is reached. In ductile materials, the crack grows until a tensile overload occurs, at which time fracture occurs by shear rupture on planes inclined 45° to the tensile axis (52).

IV. PHYSICAL METALLURGY OF INCOLOY 901

Incoloy 901 is an iron-nickel superalloy widely used as a turbine disk material since the early 1960's (17). Its nominal composition is (in weight percent): Ni-42.5, Fe-36.0, Cr-12.5, Mo-5.7, Ti-2.8, Al-0.2, C-0.05, and B-0.015. Since it is fairly strong and ductile at intermediate temperatures (up to 1000°F/540°C) and contains substantial iron and relatively low chromium, it is widely used due to its comparatively low cost. It also possesses the advantage of being in that group of superalloys which can be forged and machined fairly conventionally (19).

Incoloy 901 has an austenitic (γ-f.c.c.) iron-nickel-chromium matrix. Molybdenum, titanium, carbon, and boron are the other principal substitutional solid-solution strengtheners of the matrix (17). The stacking fault energy is not known, but from data presented by Decker and Floreen, it can be estimated to be greater than 60 ergs/cm^2 (18).

The primary precipitate is γ', an intermetallic compound of the type Cu_3Au, possessing a Strukturbericht structure type $L1_2$. Its stoichiometric composition is Ni_3Al with a lattice parameter of 3.60 Å. In actual fact, γ' contains some iron on the nickel lattice sites, and some titanium on the aluminum lattice sites, so that γ' is usually denoted as $(Ni,Fe)_3(Al,Ti)$. The lattice mismatch between γ' and the γ matrix is low, so that the γ' nucleates homogeneously. The γ' grows in a spherical morphology which indicates that the lattice misfit is less than 0.5% (17,20). The solvus temperature is 1725°F (940°C) (17).

Actually, in Incoloy 901, γ' is a metastable precipitate (18). The equilibrium precipitate is η, an h.c.p.-ordered intermetallic compound with a Strukturbericht structure type DO_{24}. It has the stoichiometric

composition Ni_3Ti. Unlike γ', it does not dissolve substantial amounts of other elements (20). The precipitation of η may occur in two forms: at the grain boundaries in a cellular morphology or intergranularly as plates (22,20). The cellular precipitation nucleates at a lower temperature than the plate-shaped precipitates. The solvus temperature for η is 1825°F (996°C)(17). Significant precipitation occurs in the temperature range 1500-1750°F (816-954°C), with the most rapid precipitation rate in the temperature region 1600-1650°F (871-899°C) (25).

The cellar precipitation reaction consi-ts of alternating lamellae of γ and η. These cells have a random orientation with respect to the grain into which they are growing. But the close-packed planes and directions of the h.c.p. η and the f.c.c. γ are parallel to one another (20). These orientation relationships are also true for the plate morphology which are thought to nucleate on stacking faults in γ' (18). The interface between γ and η is semi-coherent, with a lattice mismatch of 0.65% (19). The η phase is associated with severe degradation in mechanical properties. Not only is the phase itself brittle, but also it grows at the expense of the γ'. However, η has successfully been used to control the grain size of Incoloy 901 during forging by the utilization of special thermomechanical processing (25).

Carbides play a key role in superalloys. They help to control grain size since some carbide types are stable nearly to the melting point of the alloys. Also, the carbides which precipitate in the grain boundary greatly increase stress rupture strength at elevated temperatures. And, carbides can increase the chemical stability of the matrix by removing reacting elements (26). MC carbides form shortly after freezing and,

hence, they occur as discrete particles distributed homogeneously throughout the alloy. In Incoloy 901, these MC carbides have the composition TiC with an f.c.c. structure. Some molybdenum can substitute on the titanium lattice sites, so that a carbide of the type (Ti,Mo)C is possible (26,70).

Although carbides of the type $M_{23}C_6$ usually form in superalloys during low-temperature heat treatment and service in the temperature range 1400-1800°F (760-980°C), they are not found in Incoloy 901. Instead, MC carbides of the type (Ti,Mo)C precipitate at the grain boundaries during the stabilization portion of the heat treatment (70). The morphology of these grain boundary carbides is similar to that for a Laves phase and they have been incorrectly identified as Laves phases (24).

The formation of carbo-nitrides and titanium nitrides has been reported (24). Cubic TiN is as thermally inert in the superalloy as is TiC.

The boron which is added to improve creep properties results in the precipitation of hard, refractory M_3B_2 borides (26). Typical composition of these borides is: $(Mo,Ti,Al,Cr,Fe,Ni,Si)_3B_2$ (24,69).

In addition to the intentional precipitates, various topologically close-packed (t.c.p.) intermetallic compounds form in superalloys due to solid-state bonding phenomena (t.c.p. phases are also referred to as "Hume-Rothery compounds" and "electron compounds"). A hexagonal Laves phase of the type $(Fe,Cr,Mn,Si)_2(Mo,Ti,Cb)$ has been found in Incoloy 901 after aging for long times in the temperature range 1200-2000°F (649-1093°C). The morphology varies from general intergranular to grain

boundary precipitation (24,23,18). The trigonal μ phase has been observed in Incoloy 901 with high boron additions (0.1 weight percent) (24). This phase has a close structural relationship to the M_6C carbides and, thus, it may be that M_6C can precipitate in this alloy, although it has not been reported. The chemical composition of the μ phase can be quite complex. It is, in general, $(Ti,Mo)_6(Fe,Ni)_7$ (24). The precipitation is intragranular as thin platelets parallel to γ close-packed planes.

V. REJUVENATION

Metallurgical engineers who are responsible for the maintenance of turbine engines have long expressed a desire to be able to restore at least a portion of the design life of expensive engine components through some sort of processing operation. This process has been given the name "rejuvenation." Recent advances made by Wilshire and others have shown that thermal treatments are successful in recovering the creep life of superalloys (28,29). Wilshire found that the onset of tertiary creep is caused either by development and growth of grain boundary cavities or by microstructural changes which cause changes in volume fraction and morphology of the γ' (28). Thus, suitable heat treatments could be devised to sinter out the cavities in the first case, or to restore the original microstructure in the second case in order to recover the creep life.

The success with creep damage has given impetus to finding suitable processing conditions for recovering the low-cycle fatigue (LCF) life of superalloys. The use of hot-isostatic-pressing (HIP) technology to consolidate metal powders has been quite successful (31) and it was

inferred that this technology would be useful in heatling LCF damage. The HIP process involves the introduction of high pressure gas into an autoclave at elevated temperature. Thus, some mechanical energy is available as well as thermal energy.

Researchers at the Stellite Division of the Cabot Corporation obtained some preliminary data on turbine blades which indicated that some recovery of creep and fatigue properties was possible with HIP processing (30). An Air Force funded study on HIP rejuvenation in IN-718 concluded that there was no rejuvenation of pre-crack initiated damage, but that there was some rejuvenation of post-crack initiation life due to the closure and bonding of fatigue cracks (2). However, this work was not conclusive because the HIP cycle chosen for the rejuvenation effort substantially changed the baseline properties of the material, and there was relatively little effort devoted to microstructural characterization.

It is the purpose of this dissertation to report the results of the experimental investigation to recover some portion of pre-crack initiated LCF life using thermal and HIP processing. Pertinent aspects of the physical metallurgy of Incoloy 901 are presented. The LCF behavior of Incoloy 901 at various strain ranges is reported. The microstructural mechanisms of LCF damage and the resultant effects of the rejuvenation processes are detailed.

Chapter 2

EXPERIMENTAL PROCEDURE

I. METALLOGRAPHY TECHNIQUES

A. Optical Microscopy

The samples to be examined were mounted in Bakelite, hand polished through 600-grit silicon carbide paper using water as a lubricant, and polished successively with 6-μ, 1-μ, and 1/4-μ diamond paste. Several different etchants were utilized. ASTM Etchant 105 (32) was most generally used to reveal microstructural details. It was freshly mixed each time in these proportions: 92% HCl, 5% H_2SO_4, and 3% HNO_3. Immersion for 5-30 seconds was usually sufficient. Marble's Reagent (ASTM Etchant 25) was effective in highlighting the grain boundaries. It was mixed in these proportions: 10 g $CuSO_4$, 50 ml HCl, and 50 ml water (32). Etchant times were generally 10-30 seconds. Glyceregia (ASTM Etchant 87) was useful in highlighting microstructural details when the other etchants were not adequate. It was freshly mixed each time according to the formula: 10 ml HNO_3, 50 ml HCl, 30 ml glycerin (32). The samples were bathed in hot water prior to immersion in the glyceregia. Etchant times depended on the surface temperature of the specimen. Average times were between 20 seconds and 1 minute. Sometimes the samples were immersed in HF for a few seconds to remove a passive layer prior to etching.

After the samples were satisfactorily etched, they were thoroughly rinsed in water and bathed in a saturated sodium bicarbonate solution placed in an ultrasonic cleaner for several minutes. This step was necessary to prevent etching of the microscope objective piece. The etched surface was then dried using a methanol wash and a blower. The samples were examined and photographed in a Bausch and Lomb Research II Metallograph using a xenon light source.

B. Transmission Electron Microscopy

Thin slices of Incoloy 901, approximately 0.010 inch thick, were cut using a thin abrasive cut-off wheel. These slices were then ground flat on 240- and 320-grit silicon carbide paper using water as a lubricant. The slices were attached to the bottom of a stainless steel mount using balsam wax. The slice was further ground down to a thickness of 5-6 mils on 320- and 400-grit silicon carbide paper using a water lubricant. The thin slices were then dismounted and the residual balsam was removed by slight grinding on the 400-grit paper. A punch-out die, with a 3-mm opening, was used to cut out the disks. In the case of the fatigue specimens where the disks were taken normal to the longitudinal axis, the above procedure was simplified somewhat since the fatigue specimens had a nominal 3-mm diameter.

Electropolishing was done with a dual-jet Tenupol. The electrolyte had the following composition: 600 ml methanol, 250 ml butanol, and 60 ml perchloric acid (70%). The electrolyte was maintained at a temperature of about -60°C by constantly adding liquid nitrogen to a methanol bath surrounding the electrolyte.

The controls on the polisher were set for minimum flow rate and maximum sensitivity of the photocell detector which turned off the

electrolyte pump after perforation of the disk. A two-step polishing sequence worked best. Electropolishing for 15-30 minutes at 30 volts followed by final polishing at 16-20 volts produced dished disks with holes close to the center. After electropolishing, the disks were washed in methanol. Great care was taken in handling to prevent inducing artifact dislocations into the structure.

C. Scanning Electron Microscopy (SEM)

An AMR Model 1000 Scanning Electron Microscope was used in this investigation. An Energy Dispersive Analysis of X-Rays (EDAX) attachment to the SEM was used to identify chemical elements. Sample preparation involved cutting the LCF specimen just below the extensometer flange, and mounting it on an aluminum stud using a silver paste.

D. Surface Replication

Acetyl cellulose replicating film was used to replicate the surface in the gauge section of the low-cycle fatigue specimen. The replication was done on loose specimens and while the specimens were mounted in the Instron Hydraulic Testing Machine (37). The replicating film, 0.034 mm thick (1.34 mils), was cut into strips 0.30 in. wide (the approximate length of the gauge section). The strips were cut into lengths 0.25-0.30 in. long. Strips of this length covered about 75% of the gauge length area. A reference line was made on the LCF specimen above the extensometer flange so that the location of each replica could be noted. At least six replicas were made for each gauge length, with adequate overlap of areas between adjacent replicas. Thus, the gauge section was completely replicated about three times. This provided insurance against an artifact in the replica obscuring a vital surface detail.

The replicating film was prepared for use by submerging it in acetone for 8-10 seconds, holding a corner with tweezers. The film was removed from the acetone and quickly applied to the surface. The film "grabbed" onto the surface almost immediately. The film dried on the surface for 5-10 minutes, and then was stripped off with tweezers. It was placed on a piece of double-sided sticky tape mounted on a glass slide. The position of the reference mark on the LCF specimen with respect to the replica was scribed into the sticky tape at the appropriate position. A piece of masking tape on the reverse of the glass contained the identification data. Two glass slides at a time were then placed in a vacuum evaporator, and the belljar evacuated to 2×10^{-5} torr. The slides were rotated and a uniform thin coating of 99.99% purity aluminum was applied. The replicas were then examined using a light microscope or a scanning electron microscope.

II. AGING RESPONSE OF INCOLOY 901

A. Material Specification

The Incoloy 901 was received in the form of a segment of a partially finished compressor shaft. The shaft had been cast, forged, and pierced. A chemical analysis is presented in Table 1. A band saw with a bi-metal blade was used to cut pieces of material for study. The material was received in solution-treated and double-aged condition. The commercial heat treatment specification is shown in Table 2 (34).

B. Thermal Treatments

Heat treating studies were conducted in two different furnaces. A vertical tube drop Marshall furnace was used when rapid quenching

TABLE 1

CHEMICAL ANALYSIS OF BILLET

Element	Weight Percent	Atomic Percent
C	0.034	0.162
Mn	0.10	0.104
P	0.019	0.035
S	0.005	0.009
Si	0.10	0.203
Cr	12.41	13.63
Ni	41.33	40.21
Mo	5.31	3.16
Ti	2.99	3.57
Al	0.29	0.61
Cu	0.09	0.08
Co	0.29	0.28
Bi	0.00005	0.00001
Pb	0.0003	0.00008
B	0.015	0.079
Fe	Balance (37.02)	37.86

TABLE 2

COMMERCIAL HEAT TREATMENT SPECIFICATION
FOR INCOLOY 901

SOLUTION	Heat to 1975-2025 F
	Hold within ±25 F for 2 hours
	Cool at rate equivalent to air cool or faster
STABILIZATION	Heat to 1400-1475 F
	Hold within ±15 F for 2-4 hours
	Cool in air or quench in water
PRECIPITATION	Heat to 1300-1375 F
	Hold within ±15 F for 24 hours
	Cool in air

Reference: Pratt & Whitney Aircraft Specification 1003H, 20 Nov. 1973.

of the specimen was desired. A thin piece of alumel wire was used to suspend a tantalum specimen basket in the furnace hot zone. The alumel wire was formed into a loop and each end was connected to a metal post in a cap at the top of the furnace. Heavy gauge nichrome wire, bent at each end in the form of a "U", was used to connect the basket to the alumel wire. Helium gas was passed through a gas train to remove impurities and then introduced into the top cap of the tube. The bottom tube opening was covered with a thin sheet of plastic held in place by a rubber band wrapped around the tube. Tygon tubing, connected to a side tap in the tube, near the bottom, directed the helium gas into a beaker of vacuum pump oil. Minimal pressure and flow rate of the gas was maintained, i.e., only sufficient pressure to generate a bubble every few seconds in the oil was used. A chromel-alumel thermocouple placed at the same height in the tube as the basket was used to monitor temperature. When the heat treatment was completed, the thin alumel wire loop was broken by passing a 110-volt line current through it. The basket, with the specimen in it, fell out the bottom of the tube, easily penetrating the plastic membrane on the bottom. A pail of water was placed under the tube to serve as the quenching medium.

A Brew High Vacuum Furnace was also used for heat treatment studies. Vacuums on the order of 10^{-6} torr were easily obtainable at the temperatures used in this study. A platinum/platinum-10% rhodium thermocouple was used to monitor temperature. The hot zone of the furnace was 6 inches in diameter by 14 inches high. Tantalum heating elements and shields were used. The furnace design was of the cold wall type. Temperature was controlled within ± 5°F. The specimens were either

cooled in vacuo or by backfilling the furnace chamber with helium gas, which passed through the gas train, to a partial pressure of 640 torr (about 0.83 atmosphere). The cooling rates, as measured by a thermocouple, for the vacuum cool and the helium quench, are presented in Table 3.

III. LOW-CYCLE FATIGUE

A. LCF Specimen Design and Manufacture

The specimen design is shown in Figure 1. The outstanding feature of the specimen is the extensometer ridges located on either side of the gauge section. This allows accurate measurement of displacement and the ability to maintain constant, uniform temperature in the gauge section using a clamshell furnace. The disadvantages of the system are the long times required for the entire system to reach equilibrium (typically 2-3 hours) and the fact that the calculation of strain necessarily involves the application of effective gauge lengths. The details of the load train, the strain measuring system, and the equations required to convert displacement to strain are discussed in following sections.

The specimens were manufactured by Metcut Research Associates from blanks sawed from a portion of a forged shaft. Figure 2(a) shows a photograph of the shaft segment. Specimen blanks were sawed from this segment parallel to the shaft axis. A typical cutout configuration is depicted in Figure 2(b). The blanks were then rounded by straight wheel grinding, and rough machined to ~ 0.020 in. oversize in the gauge section. The specimens were given a standard heat treatment, designated as STA 3A

TABLE 3

FURNACE COOLING RATES

Vacuum Cool

A. Heat Treatment Temperature: 1975 F

Temperature (°F)	Average Cooling Rate (°F/min.)
1400	192.0
1299	97.6
1072	72.2
893	55.8
709	47.8
509	27.1

B. Heat Treatment Temperature: 1400 F

1299	100.0
1072	50.5
893	40.2
709	28.2
509	15.1

C. Heat Treatment Temperature: 1300 F

1072	46.5
893	35.4
709	25.1
509	33.7

TABLE 3 (CONT'D)

Helium Gas Quench (640 torr)

A. Heat Treatment Temperature: 1975 F

Temperature (°F)	Average Cooling Rate (°F/min.)
1400	243.4
1299	214.6
1072	166.2
893	137.4
709	120.0
509	116.4

B. Heat Treatment Temperature: 1400 F

1299	85.5
1072	104.1
893	92.0
709	83.6
509	75.4

C. Heat Treatment Temperature: 1300 F

1072	82.7
893	86.1
709	75.1
509	67.0

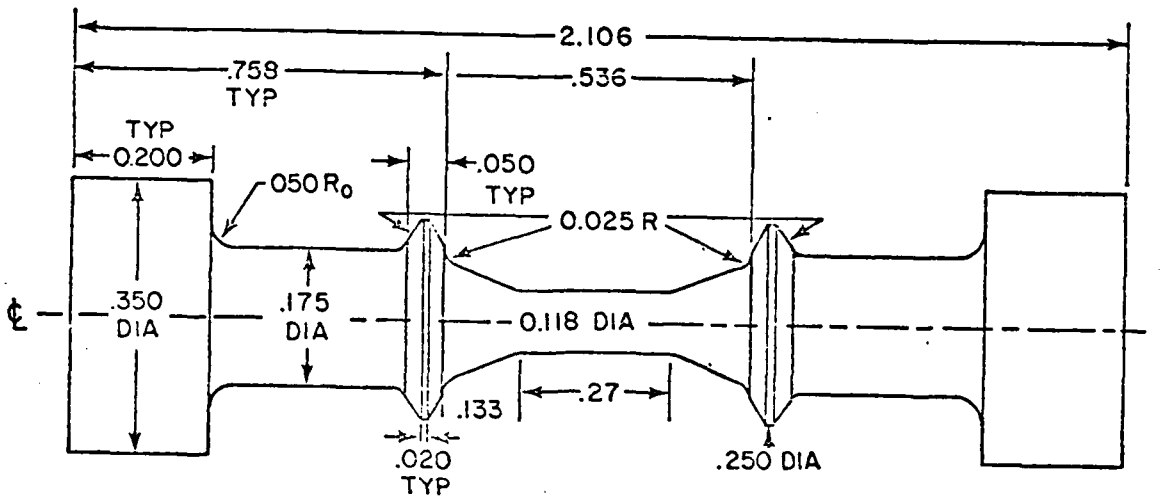

SCALE:

ALL DIMENSIONS IN INCHES

Figure 1. Low-Cycle Fatigue Specimen Design

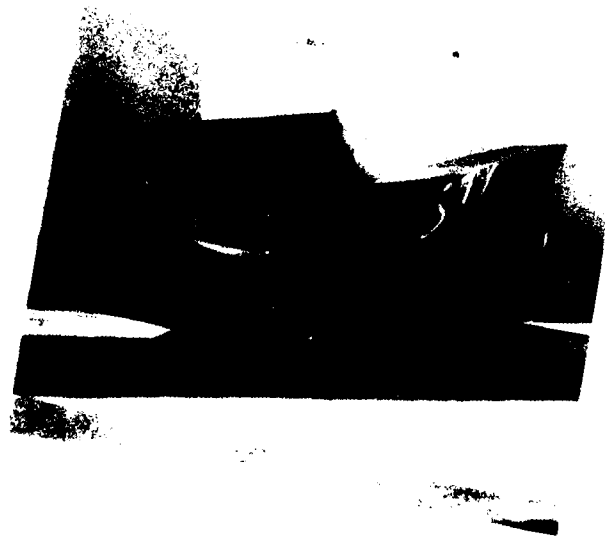

Figure 2a. Incoloy 903 Shaft Forging Photograph

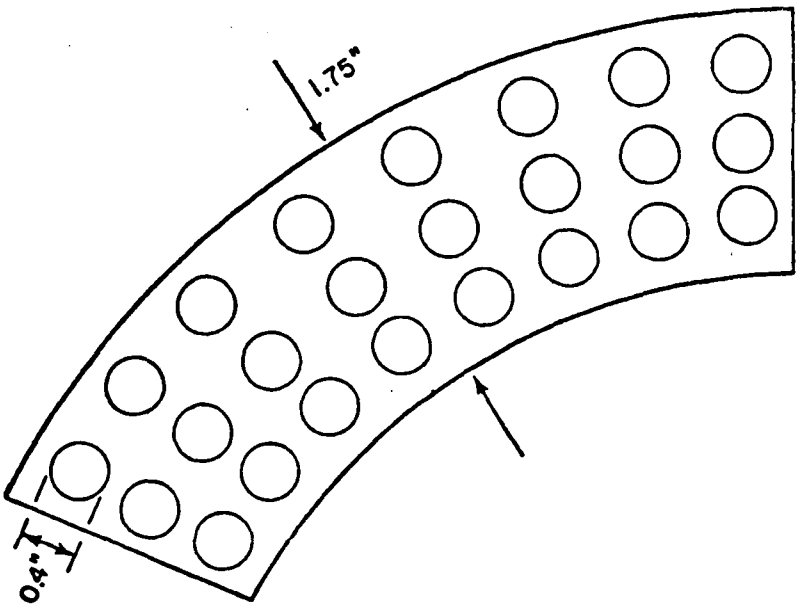

Figure 2b. Incoloy 901 Shaft Forging Segment Indicating Cut-Out Pattern for LCF Test Specimens

prior to final machining. The heat treatment parameters for STA 3A are contained in Table 4. The specimens, in groups of nine, were heat treated in a Brew High Vacuum Furnace. The fixture used to support the specimens in the furnace chamber is described in Section V of this chapter.

Final machining of the gauge section was done using a low-stress grinding approach (35). The machining parameters are summarized in Table 5. Final polishing of the gauge section was done with 400-grit silicon carbide paper using water as a lubricant, followed by 3/0 and 4/0 Emery polishing paper using Buehler Isocut Fluid as a lubricant. The paper was cut into strips approximately 0.20 inches wide, and polishing was done axially with the specimen chucked in a jeweler's lathe.

B. Ceramic Coating Procedure

A gas-tight ceramic coating, Solaramic 5210, was applied to the gauge sections of some specimens at General Electric's Materials and Processing Laboratory in Evendale, Ohio. Before the coating was applied, the gauge section was vapor blasted; this procedure entailed impinging fine alumina powder (Novacite 1250/150, supplied by Malvern Minerals) in a water stream at 0.31 MPa at the specimen surface. The specimen-to-surface distance was kept at about 5 cm, and total honing time was approximately 1 minute. The surface had a bright matte finish after the vapor blasting.

The ceramic coating was then applied, and baked in air at 1750°F for 20 minutes, and air cooled. The gauge section was inspected for spallation of the coating.

TABLE 4

STANDARD HEAT TREATMENT STA 3A
FOR INCOLOY 901

SOLUTION	Heat to 1975 °F in vacuum Hold within ±4 F for 2 hours Backfill furnace with helium gas to a partial pressure of 640 torr
STABILIZATION	Heat to 1400 °F in vacuum Hold within ±4 F for 2 hours Backfill furnace with helium gas to a partial pressure of 640 torr
PRECIPITATION	Heat to 1300 °F in vacuum Hold within ±4 F for 24 hours Backfill furnace with helium gas to a partial pressure of 640 torr

TABLE 5

LOW STRESS GRINDING PARAMETERS

SPEEDS	Work surface: 8-26 ft/min.
	Table speed: 7 in./min.
	Wheel speed for traverse grinding: 2800-3250 ft/min.
FEEDS	Traverse grinding
	Roughing: 0.001 in./pass
	Finishing: Last 0.010 in. (250 μm)
	First 0.0080 in.: 0.0005 in./pass
	Next 0.0008 in. : 0.0004 in./pass
	Final 0.0012 in.: 0.0002 in./pass
	Plung grinding: 0.00002 to 0.00008 in./rev.

C. Specimen Preparation after Rejuvenation

After the specimens were thermally rejuvenated (see Section V-A), the gauge section was axially repolished with 3/0 and 4/0 emery polishing paper as described above in Section III-A. This provided a good quality surface for replication; an oxided surface could not be replicated without loss of detail.

After the specimens were HIP rejuvenated (see Section V-B), those specimens which were ceramic coated were mechanically polished with 240-grit polishing paper to remove the coating. The specimens were given the standard STA 3A (Table 5) to restore the morphology of the precipitates in the matrix. The gauge length was then lightly polished through 4/0 emery polishing paper as previously described.

D. Load Train Configuration

A photograph of the load train is shown in Figure 3(a). Note that a resistance-wound clamshell furnace was used for heating. A sketch of the load train with the various components labelled is illustrated in Figure 3(b). The grip design is contained in Figure 4. A molybdenum di-sulfide lubricant was effective in preventing binding in the grips.

E. Strain Measuring System

Although commonly referred to as a strain measuring system, the system employed actually measured displacement which must then be converted to strain. The necessary equations to accomplish this are described in Sections III-F and IV-C. Figure 5 is a photograph of the extensometer system used in this investigation. The system features a Satek PSH-8MS High Temperature Extensometer with a Microformer (Linear

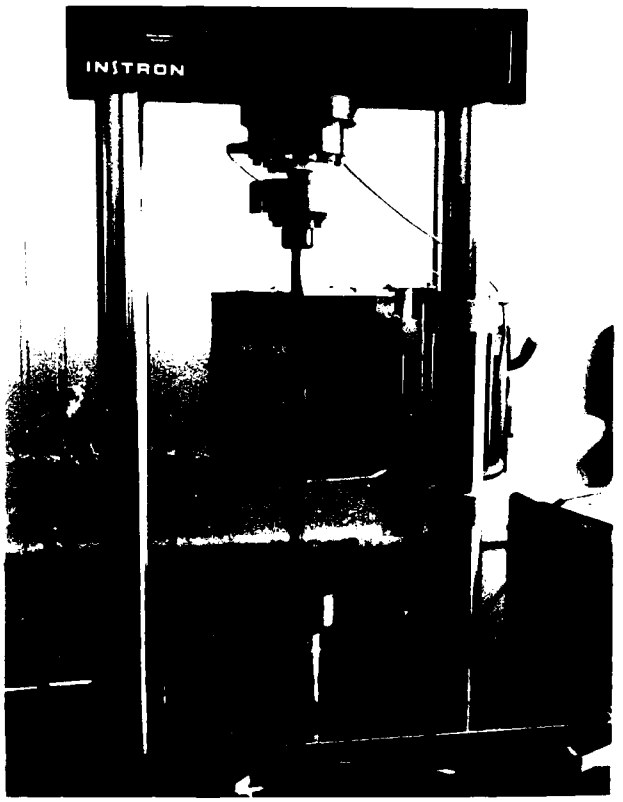

Figure 3a. Photograph of Load Train

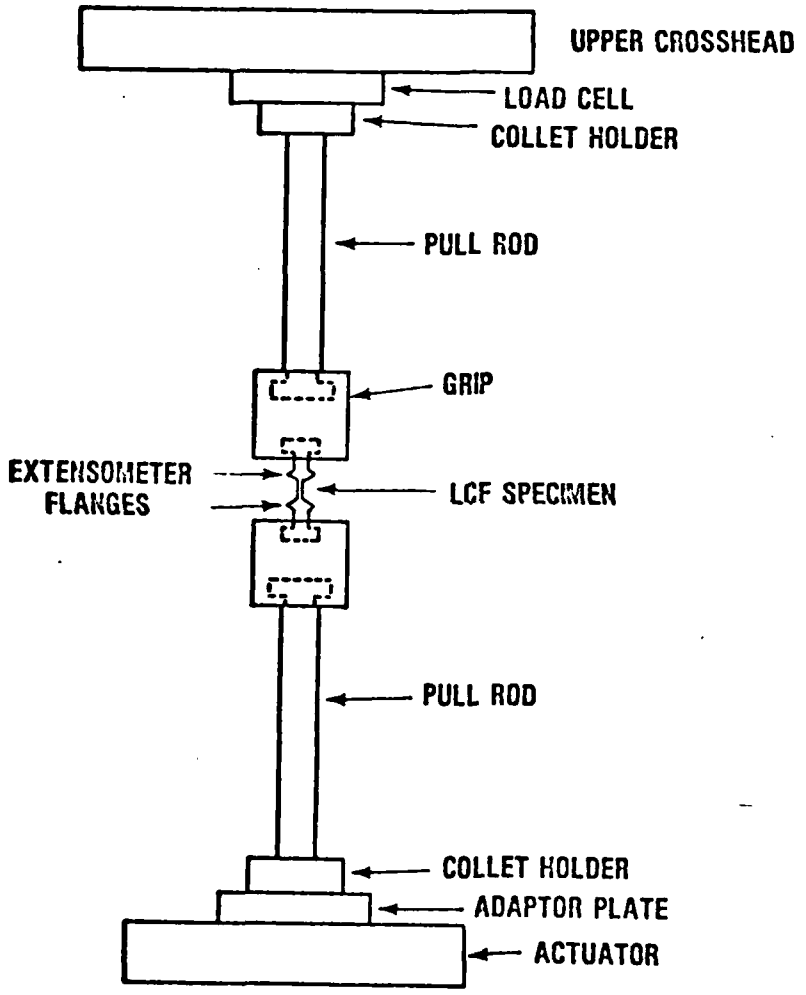

Figure 3b. Sketch of Load Train

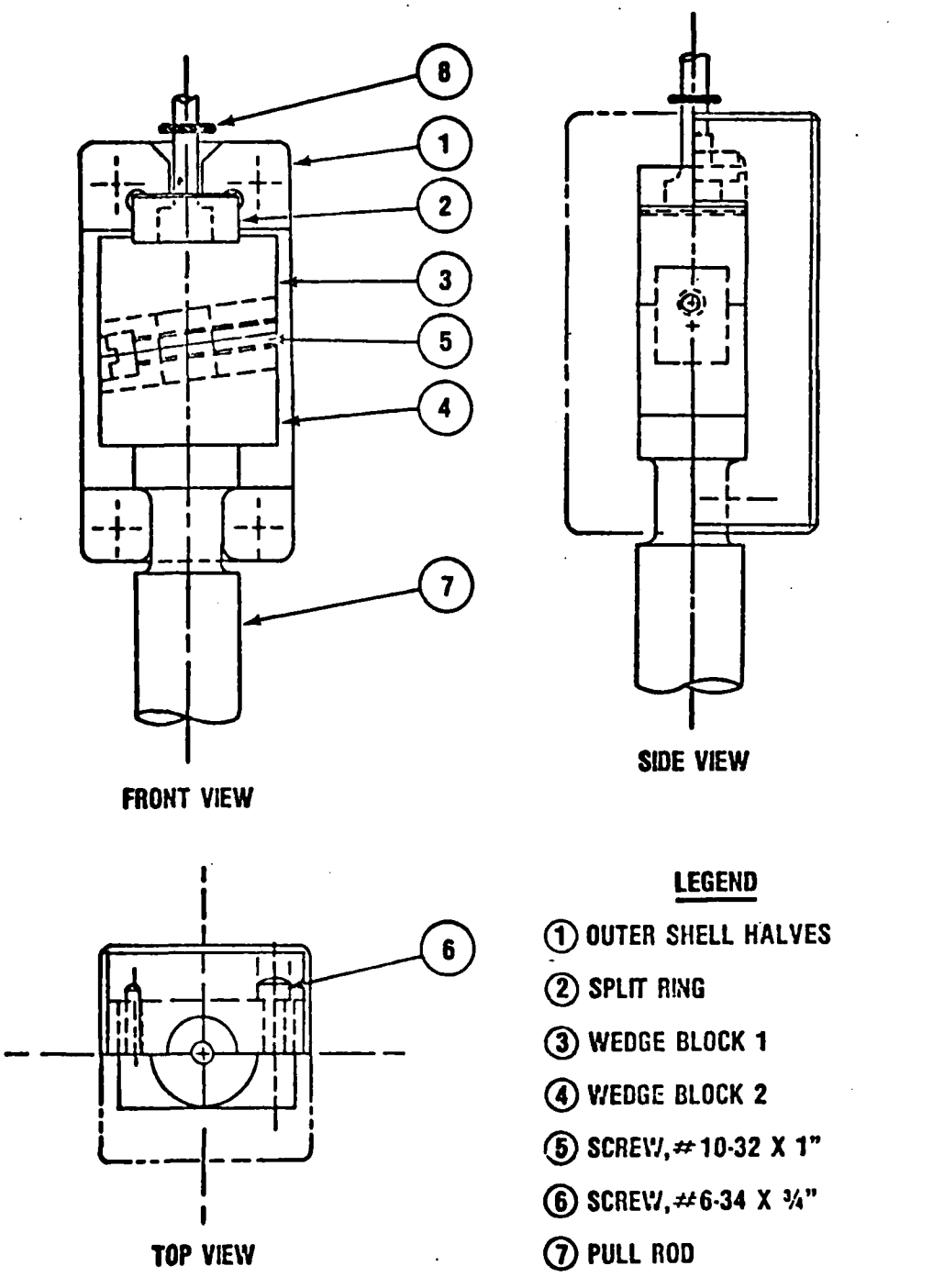

Figure 4. LCF Specimen Grip Design

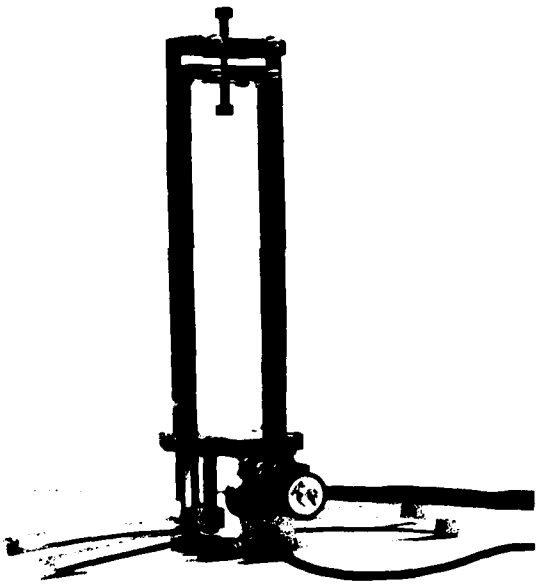

Figure 5. Photograph of Strain Measuring System

Variable Differential Transducer or "LVDT") to measure displacement. The suspension arms, which lock into the extensometer fixture, bolt around the flanges on the LCF specimen and effectively transmit the displacement of the specimen to the LVDT located beneath the furnace. The length of the suspension arms was governed by two criteria: (a) adequate length to allow the center of the specimen gauge length to be located in the center of the furnace hot zone with a one-inch clearance between the top of the extensometer fixture and the bottom of the furnace; and (b) proper difference in length between the top and bottom arms so that they would lock into the fixture for the particular flange separation distance used for the LCF specimen.

Calibration of the strain measuring system was accomplished as follows: The extensometer system was mounted in a Boeckeler Instrument Calibration Fixture. The top extension arm remained fixed and the bottom arm was movable using a dial calibrated in increments of 0.0001 inch. The LVDT was connected to an Instron Model 602A Stroke Controller. A Resistance-Capacitance (R-C) balancing network was adjusted to compensate for the resistive and capacitive characteristics of the system.

The zero suppression control was used to give a zero voltage when the LVDT core was in the center position of the LVDT. Output was read as a voltage on a digital voltmeter. Voltage readings were then taken as the dial was advanced in increments of a thousandths of an inch from 0 mils to 10 mils to -10 mils, and back to 0 mils. These 41 data points were then used to compute a linear least-square error line of the form $y - mx + b$ (36) where y is the displacement in volts, x is the displacement in mils, m is the slope of the line in volts/mil, and b is the y-intercept value. Table 6 contains typical data obtained from a

TABLE 6

TYPICAL LVDT CALIBRATION CURVE DATA

Inches × 10^3	Output Voltage	Inches × 10^3	Output Voltage
0.0	0.003	-1.0	-0.687
1.0	0.723	-2.0	-1.397
2.0	1.429	-3.0	-2.120
3.0	2.129	-4.0	-2.835
4.0	2.828	-5.0	-3.552
5.0	3.534	-6.0	-4.269
6.0	4.230	-7.0	-4.991
7.0	4.927	-8.0	-5.707
8.0	5.622	-9.0	-6.428
9.0	6.320	-10.0	-7.153
10.0	6.994	-9.0	-6.421
9.0	6.324	-8.0	-5.700
8.0	5.630	-7.0	-4.980
7.0	4.926	-6.0	-4.258
6.0	4.243	-5.0	-3.538
5.0	3.553	-4.0	-2.821
4.0	2.848	-3.0	-2.110
3.0	2.130	-2.0	-1.396
2.0	1.421	-1.0	-0.678
1.0	0.721	0.0	0.023
0.0	0.007		

calibration run. The data is plotted in Figure 6. Note that it is very linear. The inverse slope of this graph, or 1/m, is the desired calibration factor, λ, in volts per mil. These calibration runs were typically done before and after each LCF test.

F. Low Cycle Fatigue Testing

All LCF testing was performed on an Instron Dynamic Materials Testing System. The testing was done using a saw-tooth wave form at a frequency of 0.4 Hz under strain control (actually displacement control, as explained above) with zero mean level (i.e., fully reversed). The signal cable connecting the actuator LVDT with the Stroke Controller was disconnected and attached to the extensometer LVDT by means of an adapter cable. Specimen displacement thus served as the feedback to the controller. Command signals to the servovalve were generated by two different techniques: (a) Instron Model 860 Function Generator (i.e., an analog computer), and (b) Instron Series 900 Computer System, utilizing a Computer Automation Alpha 16 Minicomputer. Load-displacement hysteresis loops were plotted on a Hewlett Packard Model 7004B X-Y Plotter.

The load train alignment was checked and the load cell calibrated prior to each test. To begin the actual testing, the specimen was loaded into the grips, the extension arms were attached, and a chromel-alumel thermocouple was placed in close proximity to the LCF specimen surface in the center of the gauge length. Then the clamshell furnace was placed around the assembly. All testing was done at 500°F. Temperature was controlled using a West Guardsman Controller. The specimen was heated under load control at a tensile stress of ~ 3 ksi.

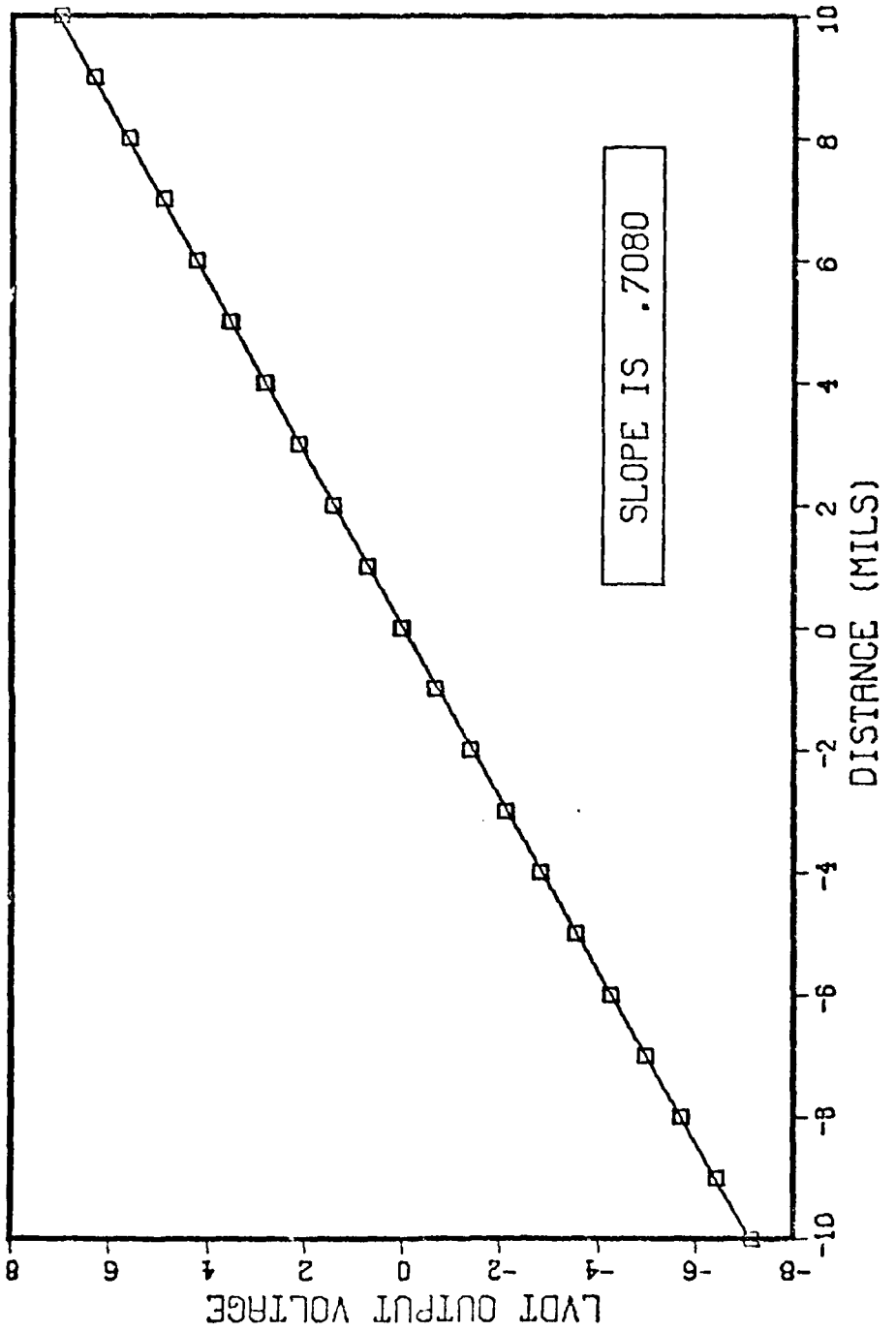

Figure 6. LVDT Calibration Curve

Once the temperature and the indicated specimen displacement readings had equilibrated, the Stroke Zero Suppression control was used to obtain zero voltage output of the LVDT at zero load.

The operation of the Function Generator was fairly straightforward. The proper amplitude setting to provide the desired strain range was empirically determined, using several specimens.

Testing under computer control required the use of a computer program. Instron's Low Cycle Fatigue Application Program APP-900-A3A8 (1974) was modified to provide more frequent and better formatted data output. The Appendix contains the source listing of the modified program. The address locations are in hexadecimal notation. The program was assembled using an Alpha 16 Assembler. Program parameters were entered via a teletype keyboard. Output was accomplished by teletype printer and punched paper tape. The frequency of data output was governed only by the speed of the paper tape punch. The fastest rate that data could be recorded was every three cycles at the test strain rate. The data on paper tape was processed by another program, written in Fortran, on a CDC 6600 computer. This program provided data, typically every five cycles, in tabular format for the following parameters: total displacement, plastic displacement, maximum elongation, minimum elongation, stress range, maximum stress, minimum stress, the ratio of maximum stress to minimum stress, elastic strain range, plastic strain range, and total strain range. Also, the program generated plots of stress range versus cycles, ratio of maximum stress to minimum stress versus cycles, and strain range versus cycles. A source listing of the computer program is contained in the Appendix.

The Instron computer program required a specification of strain rate, rather than frequency. Equation 1 is the appropriate expression relating frequency to strain rate:

$$\dot{u} = 2\nu\,\Delta u \tag{1}$$

where $\dot{u}$ is "strain" rate (actually displacement rate) in mils per second, ν is frequency in hertz (cycles per second), and Δu is displacement in mils.

The instron was capable of controlling displacements to ±0.00004 in. A typical plot of displacement versus cycles is shown in Figure 7.

G. Computation of Strain Range and Stress Range

As previously explained, the strain measuring system actually measured displacement. Since the cross-section of the LCF specimen between the extensometer flanges was not uniform, as is apparent from Figure 1, the computation of strain involved consideration of an effective gauge length. An effective gauge length is defined as that gauge length of uniform cross-sectional area which produces the same displacement under the application of a given load as does the gauge section of variable geometry. Use of the effective gauge length concept is made in the following equation which allows the computation of strain from displacement data:

$$\Delta\varepsilon_t = \Delta\varepsilon_e + \Delta\varepsilon_p = \frac{u_t - u_p}{L^e_{eff}} + \frac{u_p}{L^p_{eff}} \tag{2}$$

where $\Delta\varepsilon_t$ is the total strain range, $\Delta\varepsilon_e$ is the elastic strain range, $\Delta\varepsilon_p$ is the plastic strain range, u_t is the total specimen displacement (in inches), u_p is the plastic displacement (in inches), L^e_{eff} is the effective gauge length in the elastic regime (in inches), and L^p_{eff} is

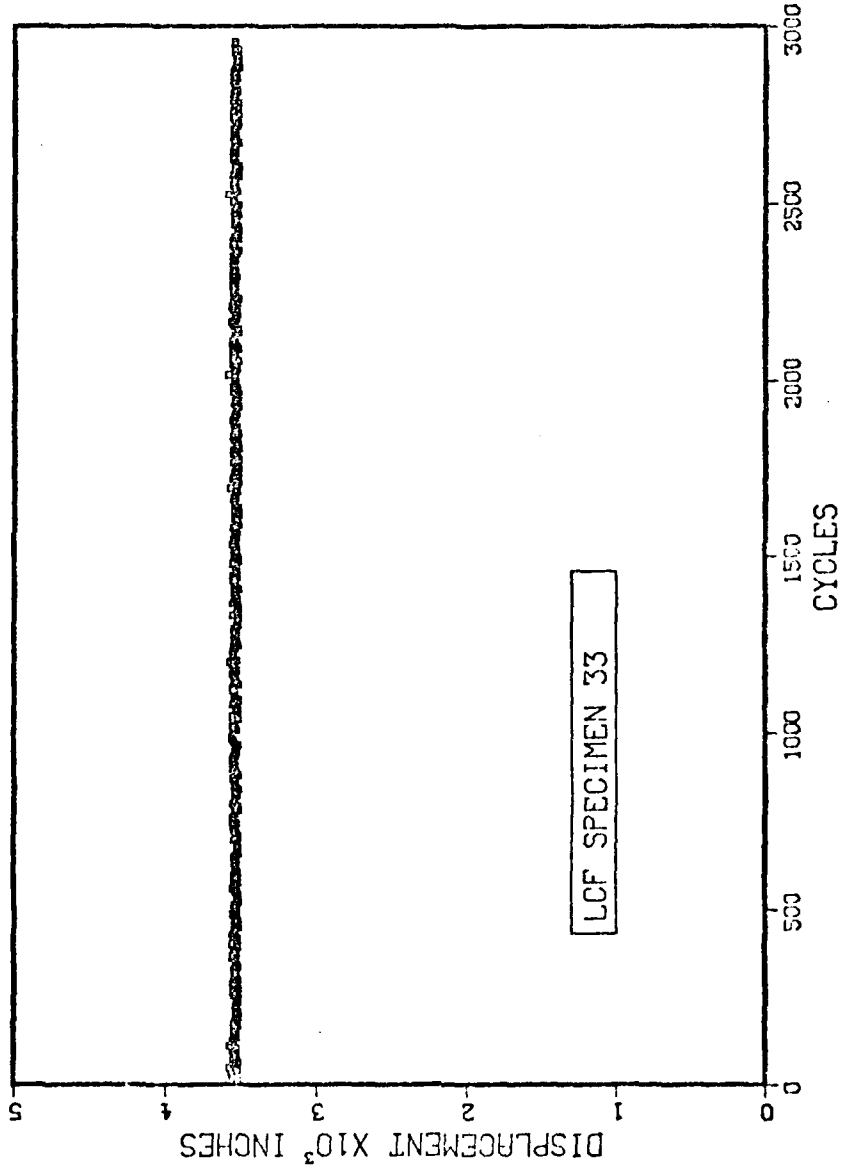

Figure 7. Plot of Displacement vs Cycles

the effective gauge length in the plastic regime (in inches). Now, u_t and u_p can be measured directly from the hysteresis loop plots or can be obtained from the computer data.

Equation 3 was used to compute displacement in thousandths of an inch when displacement distances were measured from hysteresis loop plots:

$$u = \lambda \cdot s \cdot \ell_D \tag{3}$$

where u is displacement (in mils), λ is the LVDT calibration factor, m^{-1} (in mils/volt), s is the plotter chart scale factor (in volts/inch of chart), and ℓ_D is the measured chart distance along the displacement axis of the hysteresis loop plot (in inches).

The plastic effective gauge length, L^p_{eff}, was assumed to be the straight portion of gauge length. This straight segment was measured for each specimen using a traveling microscope. Measurements were made along the top and bottom surfaces of a specimen supported horizontally; these were then averaged and rounded off to two significant figures.

The experimental determination of the elastic effective gauge length, L^e_{eff}, involved comparing the slope of a stress-displacement curve to a known elastic modulus value. The equation of interest was:

$$L^e_{eff} = \frac{E_{ACT}}{\Delta\sigma/\Delta u} \tag{4}$$

where L^e_{eff} is the effective elastic gauge length (in inches), E_{ACT} is the known Young's Modulus (in psi), $\Delta\sigma$ is the stress range (in psi), and Δu is the displacement range (in inches).

The calculation of stress, using distances measured along the load axis on the fatigue hysteresis loop, was done by applying Equation 5:

$$\sigma = k \cdot (1/d_o^2) \cdot t \cdot \ell_L \qquad (5)$$

where σ is stress (in psi), k is a constant = 6.367×10^2 when the full scale load is 5000 lbs, d_o is the specimen diameter (in inches), t is the plotter chart scale factor (in volts/inch of chart), and ℓ_L is the measured chart distance (in inches) along the load axis of the hysteresis loop plot.

H. In Situ Surface Replication

When it was necessary to interrupt a fatigue test in order to replicate the gauge length of the specimen, the specimen was not removed from the load train but rather replicated in place in order to maintain the same alignment (37). The procedure is detailed below.

After the LCF test was halted, while the specimen was going into compression, the system was placed in Load Control with a mean level of zero. Then the stroke value was recorded. A mean tensile stress of about 3 ksi was then imposed on the specimen. The furnace was removed and a small fan was used to speed the cooling of the load train. After the system was at room temperature, the actuator was turned off, the thermocouple pulled back, and the extensometer removed. These procedures exposed the gauge section. The gauge section was cleaned with acetone and the replication was accomplished as explained in Section I-D.

In order to restart the test, the extensometer was reattached and the thermocouple placed back in position. The actuator was turned on, and a mean tensile stress of about 3 ksi was imposed. The furnace was placed back around the load train. When the system was equilibrated, both with respect to temperature and dimensions, a zero mean level was

imposed and the Stroke Zero Suppression Control was used to set the same stroke value which was recorded when test was initially stopped. Then the test was restarted.

IV. TENSILE TESTING

A. Specimen Configuration

The same specimen design, shown in Figure 1 for LCF testing, was used for tensile testing. Specimen manufacture was also done in the same way.

B. Machine Description

Mechanical testing was performed on an Instron Tensile Testing Machine, Model TT-C. The cross-head was moved at a constant speed utilizing an amplidyne drive and selsyn control elements. A Leeds and Northrup chart recorder (1.5 seconds full scale response time) was driven by the output from the extensometer LVDT. Load was measured by an Instron Load Cell. The chart was operated at 100 lbs full scale to provide good sensitivity of the load-displacement curve. The load cell and the LVDT gain control were calibrated prior to each test. The load train and furnace assembly were essentially the same as shown in Figure 3 for the LCF testing.

C. Computation of Stress and Strain

Stress was simply computed by dividing the load by the cross-sectional area of the specimen. The strain was computed in an analogous manner to that for the LCF data. Thus, a relationship was required to convert displacement to strain. It is certainly true that

$$\varepsilon_t = \varepsilon_e + \varepsilon_p \tag{6}$$

where ε_t is total strain, ε_e is elastic strain, and ε_p is plastic strain. But

$$\varepsilon_e = \frac{\sigma}{E} = \frac{u_e}{L^e_{eff}} \tag{7a}$$

and

$$\varepsilon_p = \frac{u_p}{L^p_{eff}} = \frac{u_t - u_e}{L^p_{eff}} \tag{7b}$$

where σ is the stress (in psi), E is Young's Modulus (in ksi), u_p is the plastic displacement of the gauge section (in inches), u_t is the total displacement of the gauge section (in inches), u_e is the elastic displacement of the gauge section (in inches), L^e_{eff} is the effective gauge length in the elastic regime (in inches), and L^p_{eff} is the effective gauge length in the plastic regime (in inches). Thus, it is apparent that:

$$\varepsilon_t = \frac{\sigma}{E} + \frac{u_t - \frac{\sigma \cdot L^e_{eff}}{E}}{L^p_{eff}} \tag{8}$$

So, Equation 8 is the desired relationship.

V. REJUVENATION TREATMENTS

A. Thermal Treatments

The only thermal rejuvenation treatment which was investigated was STA 3A which is defined in Table 4. It was necessary to suspend the specimen vertically in the furnace in order to minimize creep effects which could warp the specimen. A heat treating fixture, shown in Figure 8(a) and Figure 8(b), was designed to support the specimens in the center of the furnace hot zone. This fixture minimized the

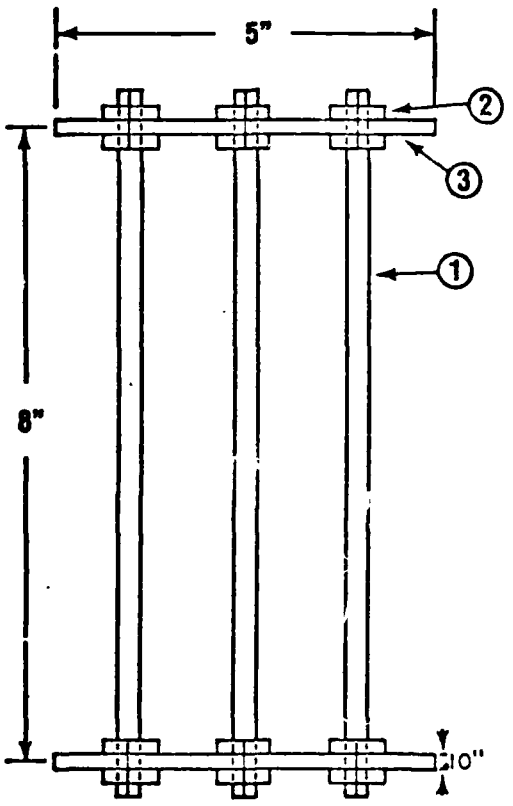

SIDE VIEW

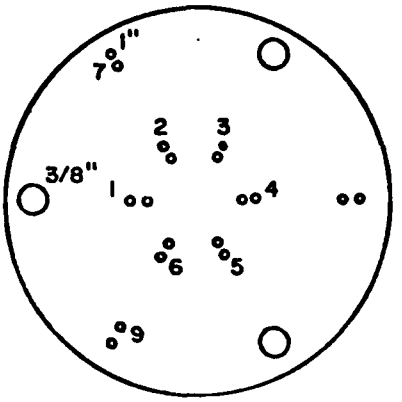

TOP PLATE

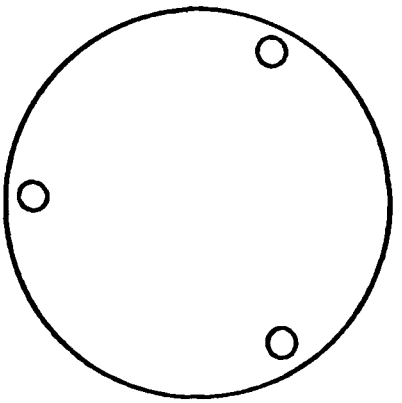

BOTTOM PLATE

LEGEND

① THREADED ROD, 5/16" DIAM

② HEX HEAD NUT

③ STEEL PLATE, .10" THICK

SCALE: 1"= 2"

Figure 8a. Heat Treatment Fixture Design

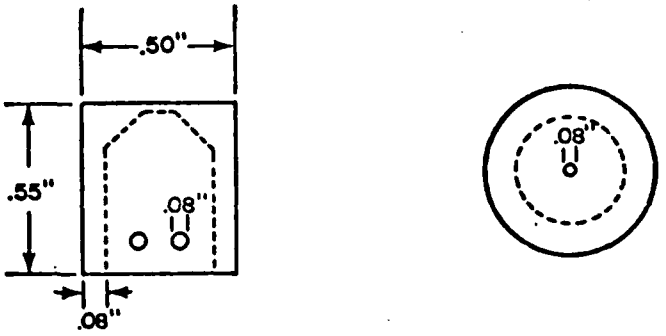

Figure 8b. Button Head Cap Design

possibility of specimen distortion, did not adversely affect critical machined surfaces, and was fairly simple to use. It held nine specimens. The cap, depicted in Figure 8(b), fit over the LCF specimen button head. Fine Nichrome wire was threaded into the two holes on each side of the cap, and thus the specimen was supported on the surface under the button head. Chromel wire, with a bead on one end, was threaded through the hole at the top of the cap. This wire was then pulled through a hole on the top plate of the fixture shown in Figure 8(a). The material used to manufacture the fixture and cap was AISI 1020 steel.

B. Hot Isostatic Pressing (HIP) Treatments

The HIP processing was conducted in a small, high-pressure, 7-in. i.d. × 14-in. long, HIP unit at Kelsey-Hayes, Detroit, Michigan. The chamber was designed by Autoclave Engineering, Erie, Pennsylvania. The heating elements were Kanthal wound, supplied by Conway Pressure Systems, Columbus, Ohio.

The fatigue specimens were vertically supported in a special fixture, shown in Figure 9. The same button head cap design, depicted in Figure 8(b) was used.

The temperature and pressure profiles for the HIP run are shown in Figures 10 and 11. The autoclave gas used was commercially pure argon.

A summary of the HIP run is as follows: The specimens mounted in the fixture were loaded into the HIP chamber, The system was flushed with argon gas until the atmosphere was primarily argon, The unit was slowly heated to 2050°F and the pressure was raied to 15 ksi. The 2050°F temperature was maintained for one hour, then the temperature

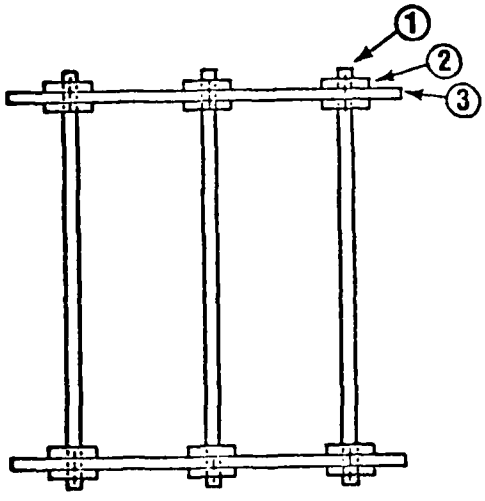

SIDE VIEW

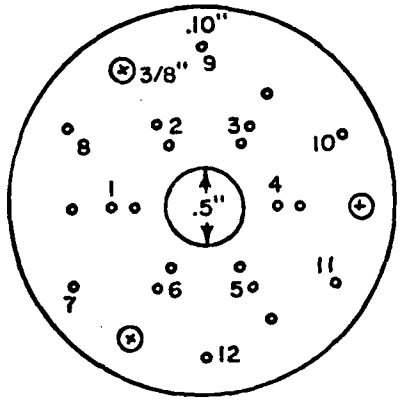

TOP PLATE

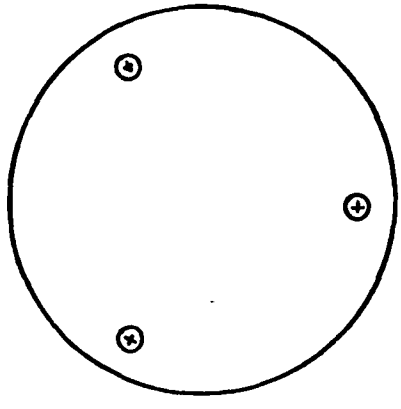

BOTTOM PLATE

LEGEND

① THEADED ROD, 5/16" DIAM

② HEX HEAD NUT

③ STEEL PLATE, .10" THICK

SCALE: 1" = 2"

Figure 9. HIP Fixture Design

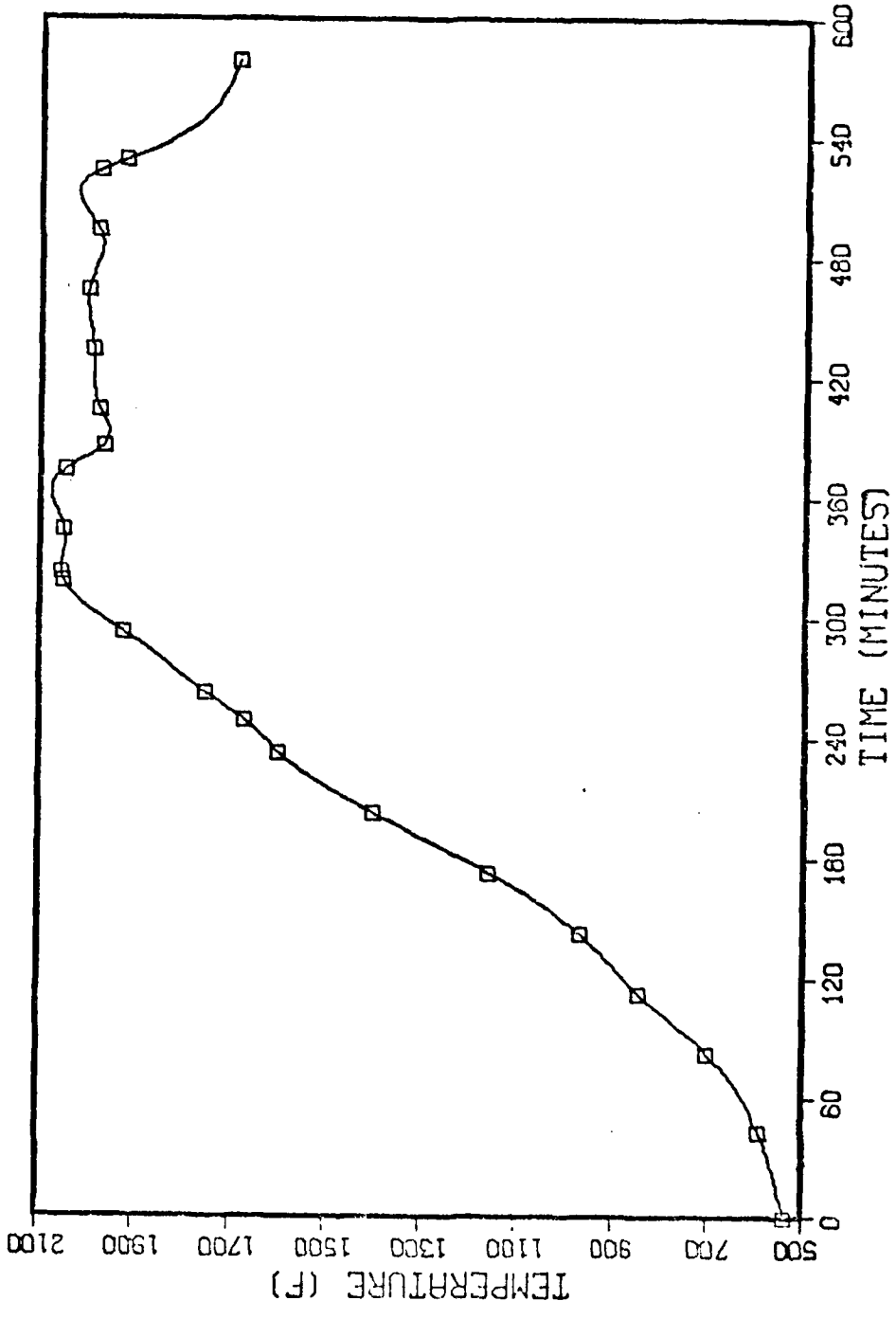

Figure 10. Plot of Temperature vs Time for HIP Run

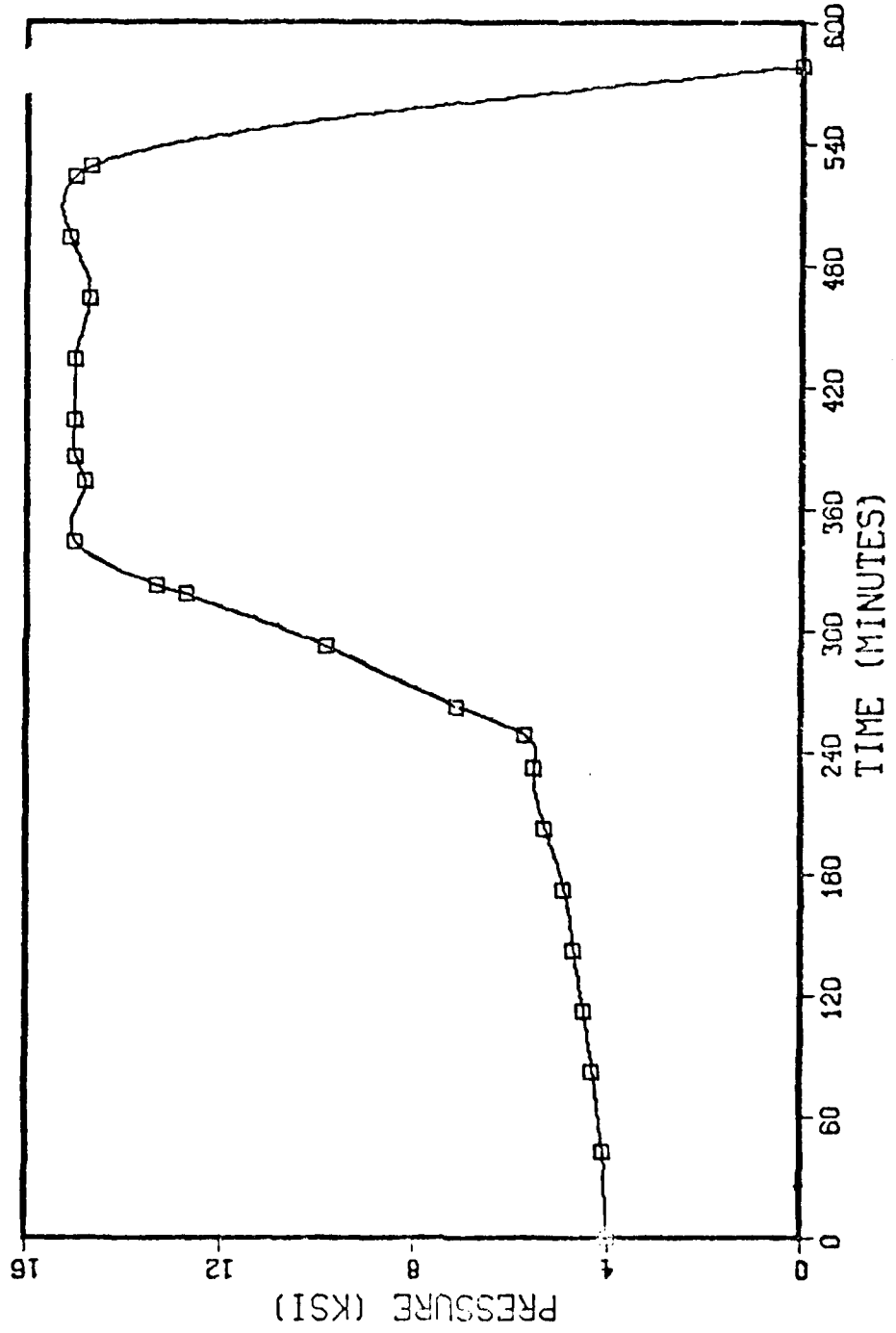

Figure 11. Plot of Pressure vs Time for HIP Run

was lowered to 1975°F while maintaining 15 ksi. After two hours at 1975°F, the pressure was released and the heating elements were turned off. When the chamber temperature reached 1700°F, the unit was opened, and the fixture removed. It was then placed in an argon gas stream until it reached ambient temperature.

VI. SONIC MODULUS TESTING

Moduli of elasticity were measured at room temperature using a Magnaflux FM-500 Elastomat. A right cylindrical rod was centerless ground to a uniform diameter of 0,4983 inches. The rod was 4.483 inches long and weighed 117.625 g.

The test rod was suspended at its nodal points by adjustable cross wires. Mechanical vibration was transmitted to the sample by a piezoelectric transducer by means of a 0.004-inch Nichrome wire spot wleded to the rod about 0.010 inch from the circumference. Another transducer, similarly connected on the other side of the rod, received the mechanical vibration from the specimen. The rod was excited by means of a variable frequency oscillator which contained a digital counter. The resonant frequency was determined by the appearance of a circular Lissajou figure on an oscilloscope. The oscilloscope had the voltage output of one transducer connected to the x-axis and the voltage output of the other transducer connected to the y-axis. In such a manner, the resonant frequencies for the longitudinal (Young's) modulus, transverse modulus, and shear modulus were measured. The following equations were then used to compute the moduli:

Longitudinal (Young's) Modulus (39):

$$E = \frac{4.00 \times 10^{-4}\ \rho\ \ell^2\ f_L^2}{6.895} \tag{9}$$

Shear Modulus (39):

$$G = \frac{4.00 \times 10^{-4}\ \rho\ \ell^2\ f_G^2}{6.895} \tag{10}$$

Transverse Modulus (40):

$$E_T = \frac{1.261886 \times 10^{-4}}{6.895}\ \frac{\rho\ \ell^2\ f_T^2\ T_1}{d^2} \tag{11}$$

Shape Correction Factor, T_1 (41):

$$T_1 = 1 + 4.88669 \left[\frac{1 + 1.26225\ \nu + 0.2098\ \nu^2}{1 + \nu}\right] \left(\frac{d}{\ell}\right)^2 \tag{12}$$

where ρ is density (in g/cc); ℓ is length (in cm); d is diameter (in cm); f_L, f_G, and f_T are the resonant frequencies; E, G, and E_T are the elastic modulii (in psi); and ν is Poisson's ratio.

Chapter 3

RESULTS AND DISCUSSION

I. AGING RESPONSE OF INCOLOY 901

A. Characterization of As-Received Microstructure

The microstructure of the Incoloy 901 forging was examined using a metallograph, a transmission electron microscope, and an electron microprobe.

Figure 12 shows a typical microstructure. Using the ASTM Linear Intercept Method to measure grain size (42), the grain size was determined to be 90 μm or ASTM Equivalent Grain Size 3.5. Particularly evident in Figure 12(a) are the inclusion stringers which parallel the forging direction. Figures 12(b) and 12(c) are higher magnification photographs of these inclusions. It is evident that these particles act as obstacles to grain boundary migration and thus assist in controlling the grain size during processing and thermal treatment. Figures 12(a) and 12(c) contain several annealing twins. These twins were commonly observed in the as-received material. Also evident in Figures 12(b) and 12(c) are much smaller particles.

Figure 13 is an electron image produced in a microprobe of a lightly etched sample. This clearly shows that there are two different particle morphologies.

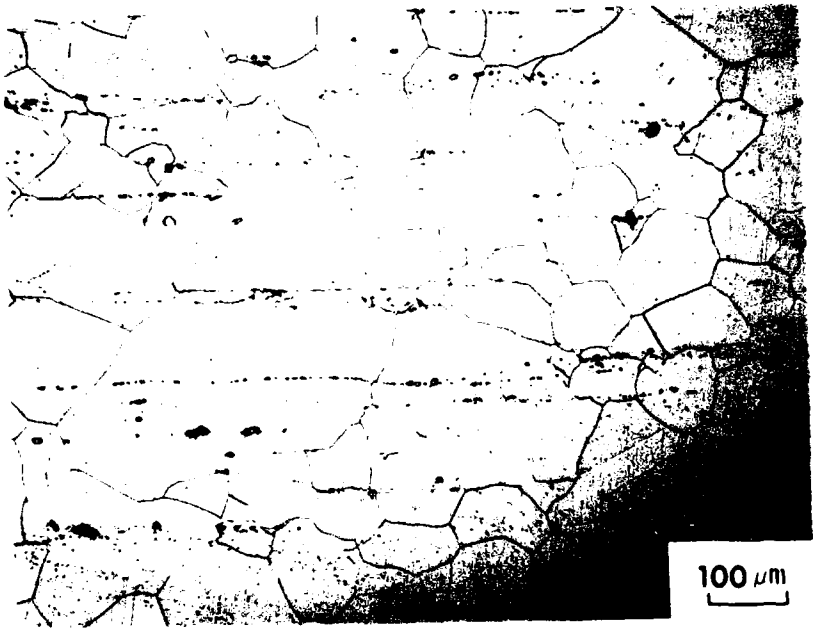

a. General Microstructure

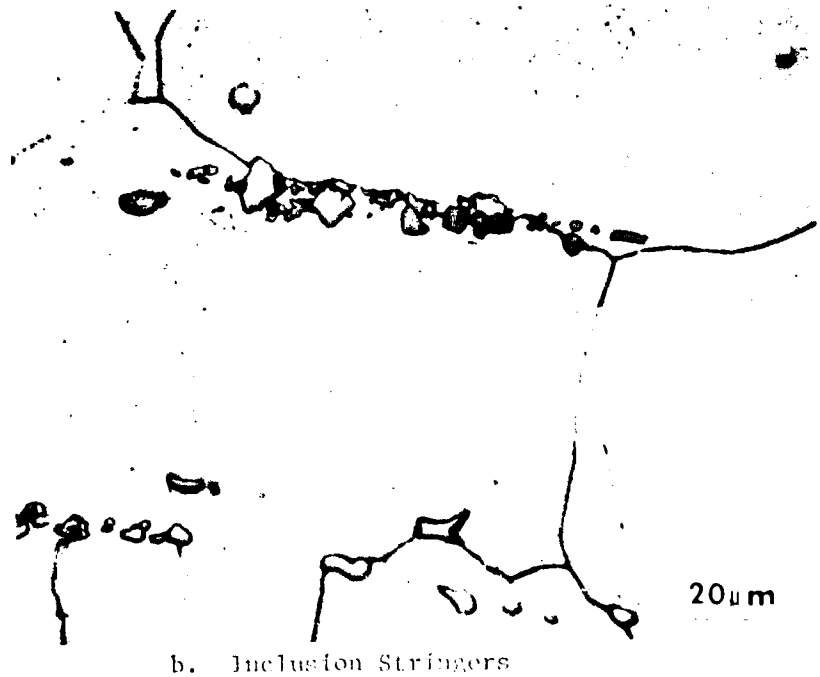

b. Inclusion Stringers

Figure 12. Micrograph of As-Received Material

Figure 12 (continued)

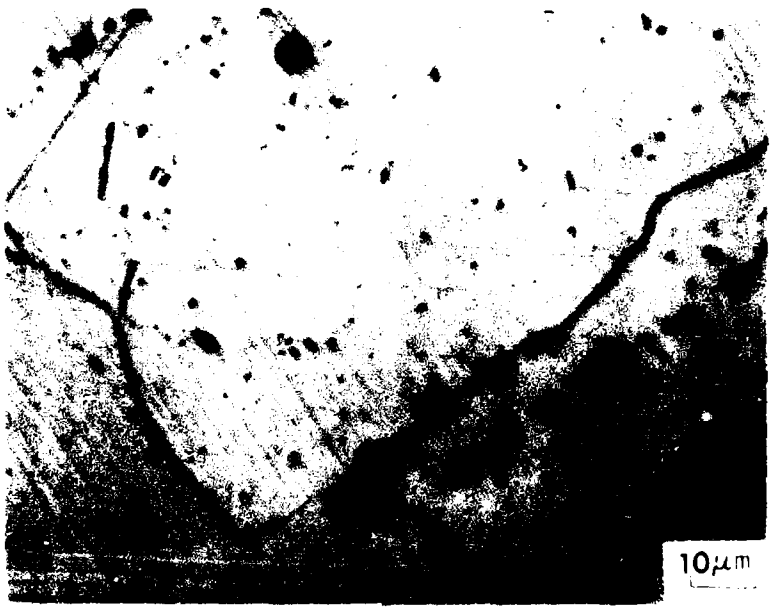

c. Inclusion Stringers

Figure 13. Electron Micrograph of Inclusion

Qualitative electron probe analysis, shown in Figure 14, clearly identifies the large, blocky phase as a titanium/molybdenum carbide. Quantitative analysis indicates that these are MC-type carbides with slightly varying proportions of titanium and molybdenum. A typical carbide had the composition $Ti_{0.8}Mo_{0.2}C$. The sizes of these primary carbides typically ranged from 2-15 μm.

The small symmetrical particles in Figures 13 and 14 were approximately 1 μm in size and thus were difficult to quantitatively analyze. However, the results from an electron microprobe quantitative analysis indicated the following composition in weight percent: Ti-9.88, Co-13.52, Fe-8.55, Ni-3.42, Mo-52.23; difference from 100% is 12.40. Although boron could not be analyzed for in the microprobe, this analysis is consistent with the hypothesis that these particles are M_3B_2 borides. Furthermore, Beattie electrolytically extracted similar particles from Incoloy 901 and analyzed them chemically and by x-ray diffraction (69). His conclusion was that these particles were M_3B_2 borides.

Transmission electron microscopy was used to characterize the small γ' precipitates and the grain boundary precipitates. Figure 15 shows γ' in dark field. The particles have a spherical morphology and an average diameter of 300 Å units. Figure 16 shows the grain boundary precipitates. These are MC carbides of the type (Ti,Mo)C rather than $M_{23}C_6$ carbides (70). It should be noted that some grain boundaries, as indicated in Figure 17, were relatively free of precipitates.

B. Development of Standard Solution and Double-Aged Treatment

Since the LCF test specimens were cut from different portions of a shaft forging, it was desired to subject them all to a standard,

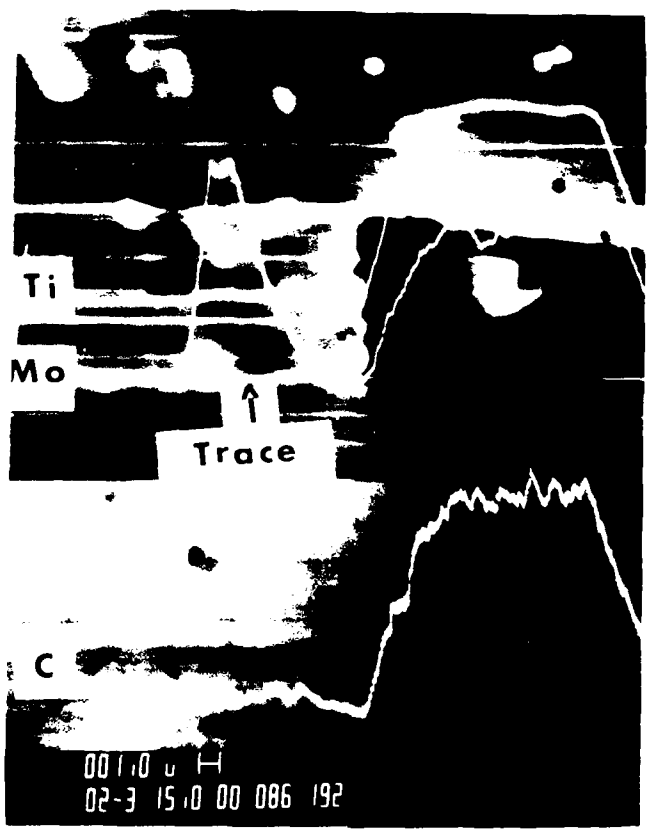

Figure 14. Electron Microprobe Image of Carbide Inclusion

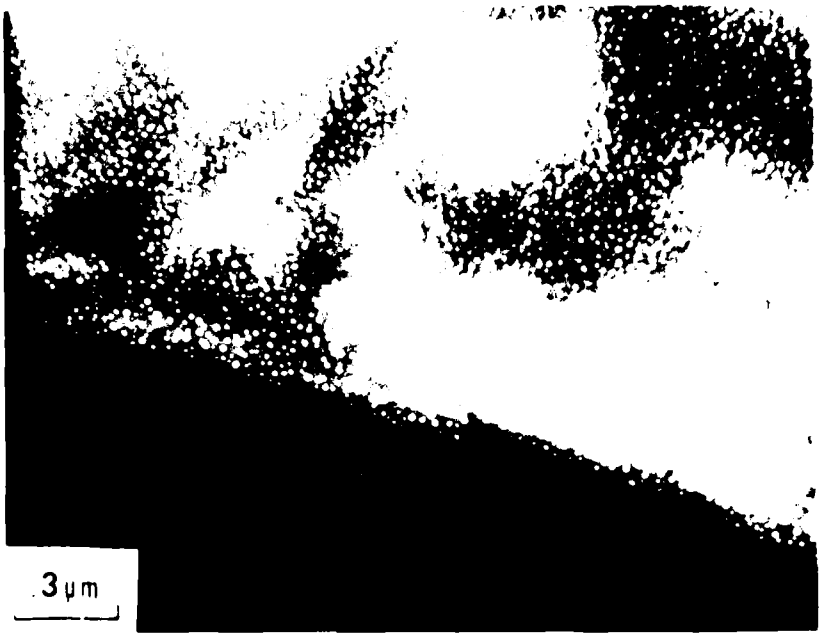

Figure 15. TEM Micrograph of γ'

a. Typical Grain Boundary MC Precipitates

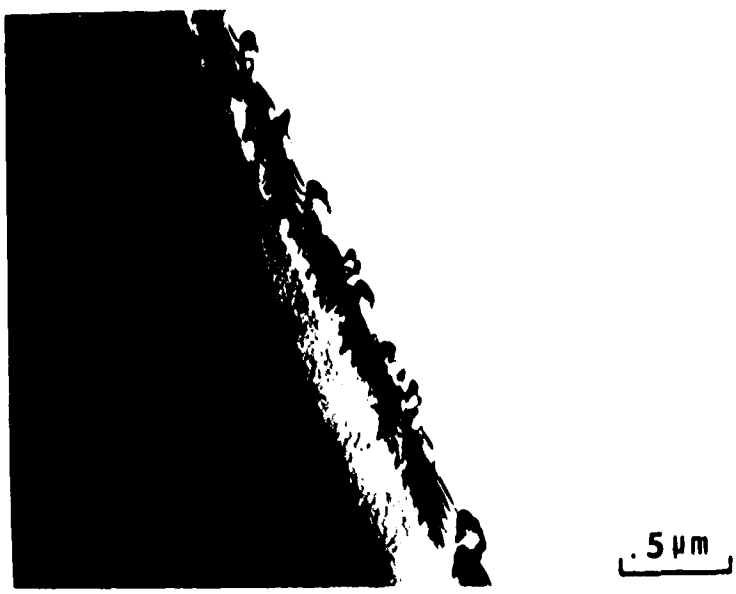

b. Typical Grain Boundary MC Precipitates

Figure 16. TEM Micrograph of Grain Boundary MC Carbides

Figure 17. TEM Micrograph of Precipitate-Free Grain Boundary

known heat treatment prior to testing. Also, this standard heat treatment could be used for thermal rejuvenation and to restore the microstructure of hot isostatically pressed specimens. Table 2 contains the specification for the commercial heat treatment. Since the minimization of grain growth was an important consideration in developing the standard heat treatment, the lowest portion of the time and temperature ranges were selected for the solutioning treatment. The drop furnace was used to rapidly quench a piece of material which was subsequently examined by transmission electron microscopy. It was determined that 2 hours at 1975^{o}F was sufficient to dissolve all phases except for the primary MC carbides.

All heat treatments were done in a vacuum furnace to minimize surface contamination. However, it was necessary to backfill the furnace with helium gas in order to obtain a high enough cooling rate to prevent the nucleation and growth of undesirable precipitates and precipitate morphologies. Such undesirable grain boundary morphologies are shown in Figure 18. Figure 18(a) shows needles of a η phase growing out from a grain boundary MC precipitate in a platelet morphology, and Figure 18(b) is a dark field view of the MC platelets growing out from a grain boundary. These precipitates were formed during vacuum cooling from the solutioning temperature because the cooling rate was too slow. It was found that backfilling the furnace to 640 torr of helium gas produced the proper grain boundary morphology. The standard heat treatment, designated as STA 3A, is presented in Table 4.

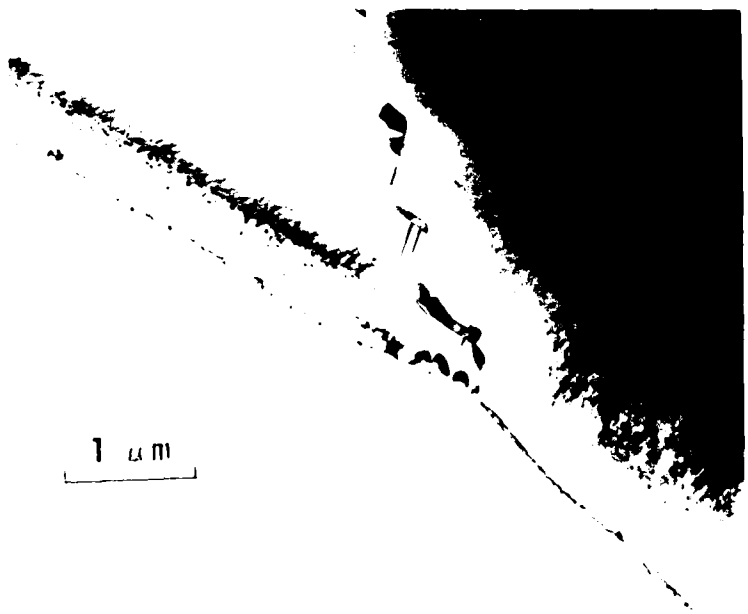

a. Needle-Shaped η Phase and MC Platelets

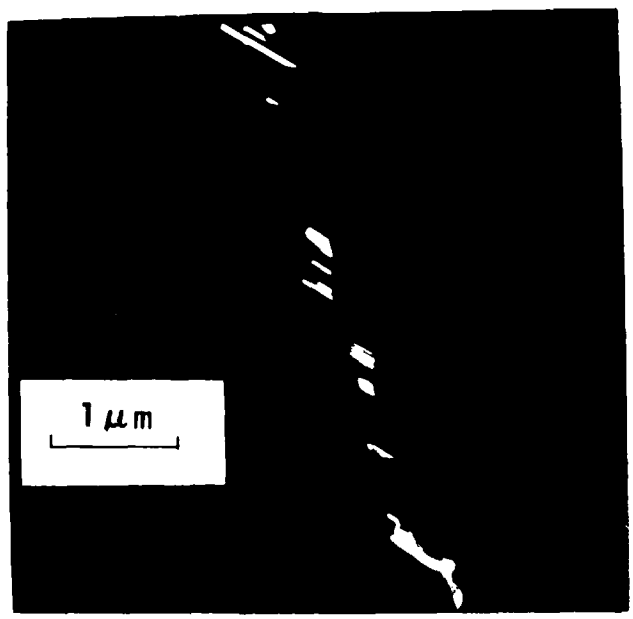

b. MC Platelets (Dark Field)

Figure 15. TEM Micrograph of Undissolvable Grain Boundary Precipitate Morphology

The effect of STA 3A on grain size was measured. The average grain size was increased to 120 μm (ASTM Equivalent Grain Size 3), but remained fairly stable at this size with subsequent heat treatments. The matrix was not dislocation-free, but the dislocations were randomly oriented.

C. Microstructure Response at Elevated Temperatures

In order to better understand the physical metallurgy of Incoloy 901, the microstructure which developed at 1500°F and 1700°F was studied using a drop furnace. After 6 hours at 1500°F, no change in the grain size occurred. The fine γ' coarsened appreciably, approximately doubling in size to 600 Å units. The grain boundary carbides developed a blocky morphology.

After 6 hours at 1700°F, no change in the grain size occurred. The change in precipitates was dramatic. No γ' was seen, although the solvus temperature is assumed to be 1725°F (17). The platelet morphology of the η phase is evident from the transmission electron micrographs in Figure 19. Figure 20 shows these η platelets at lower magnification as seen in a metallograph.

D. Microstructure Resulting from Hot Isostatic Pressing (HIP)

Hot isostatic pressing of superalloys is normally accomplished at very high temperatures; i.e., above the 1975°F solutioning temperature of Incoloy 901. In an attempt to measure the effect on grain growth of these high HIP temperatures, one piece of material was heated in a vacuum furnace to 2100°F for five hours and another piece was heated to 2050°F for three hours. The average grain size after the 2100°F

a. Nucleation of η at Grain Boundary

b. Matrix Nucleation of η

Figure 19. TEM Micrograph of η Platelets

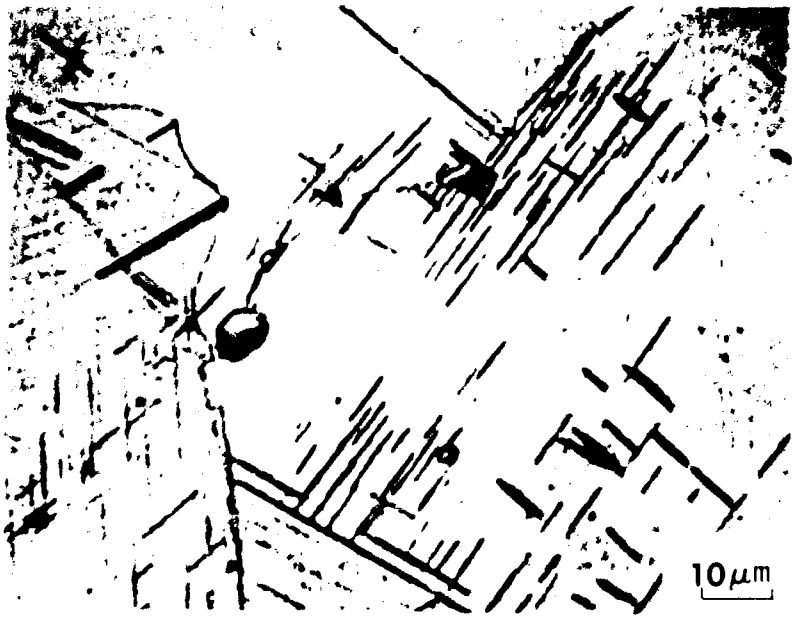

a. Typical η Platelets

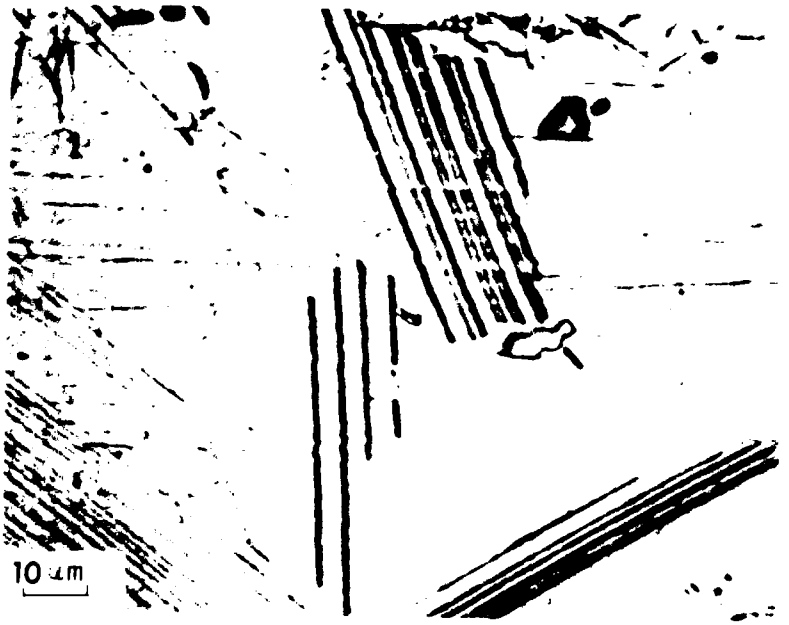

b. Typical η Platelets

Figure 20. Micrographs of η Platelets

heat treatment was 237 μm (ASTM Equivalent Grain Size 1). The average grain size which resulted from the 2050°F heat treatment was 181 μm (ASTM Equivalent Grain Size 1.5).

Figure 21 shows photomicrographs of as-HIPed material (15 ksi pressure, 1 hour at 2050°F, 2 hours at 1975°F). Note that the primary carbides helped to control grain growth. There also appears to be some η-phase precipitation which occurred during cooling. Except for the primary carbides and η platelets, transmission electron microscopy did not reveal any other precipitates. The grain size was about 150 μm, or ASTM Equivalent Grain Size 2.

When the as-HIPed material was given the standard STA 3A heat treatment, the desirable morphology and distribution of precipitates was restored.

II. MECHANICAL PROPERTIES

A. Tensile Properties

The measured tensile properties of the Incoloy 901 test specimens, after STA 3A, are summarized in Table 7. These properties (at room temperature) are well above the specified minimums of 100 ksi yield strength and 150 ksi ultimate tensile strength (43).

B. Elastic Constants

The elastic moduli were measured at room temperature using an Elastomat Sonic Modulus Tester. Young's Modulus was determined to be 30.2×10^6 psi; the corrected transverse modulus was 30.3×10^6 psi; the shear modulus was 11.2×10^6 psi; and Poisson's ratio was 0.35. Young's Modulus of 29.9×10^6 psi at room temperature and 27.51×10^6 psi at 500°F have been reported from mechanical test data (44).

TABLE 7

INCOLOY 901 TENSILE DATA

Specimen	Test Temperature (°F)	Yield Stress (ksi)	Tensile Stress (ksi)	Fracture Stress (ksi)	Reduction in Area (%)	Strain Rate (in./in./min.)
B2	70	135.3	178.3	207.6	14.3	2×10^{-2}
B1	500	119.4	155.4	175.4	12.6	2×10^{-2}
B3	500	123.3	165.7	194.3	14.9	2×10^{-2}
B4	500	123.7	161.3	189.0	15.1	2×10^{-3}

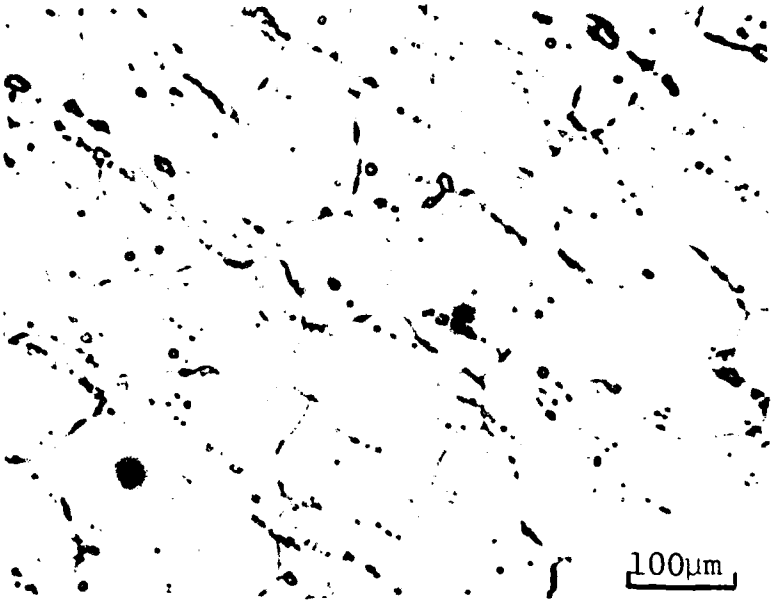

a. Typical Microstructure

b. Grain Boundary Region

Figure 21. Micrographs of As-HIP'd Material

III. LOW-CYCLE FATIGUE BASELINE TESTING

A. Determination of Effective Gauge Length

The low-cycle fatigue specimen design (Figure 1) requires the use of an effective gauge length in order to compute a strain from the measured displacement between the flanges. A plot of Stress vs Displacement at room temperature is shown in Figure 22, and Figure 23 shows Stress vs Displacement at 500°F. The slope of the linear portions of these curves is an effective modulus, $\Delta\sigma/\Delta u$ (recall Equation 4). Thus, Equation 4 allows computation of the effective elastic gauge length, L^e_{eff}, once the effective modulus, $\Delta\sigma/\Delta u$, is known. Using a linear least square error curve fit to the linear portion of the data in Figures 22 and 23, the effective modulus at 70°F was found to be 58.76×10^6 psi/in. with a correlation coefficient of 0.9999. At 500°F, the effective modulus was found to be 54.89×10^6 psi/in. with a correlation coefficient of 0.999. The results are summarized in Table 8. Strain was then computed using Equations 2 and 8.

Table 8

EFFECTIVE ELASTIC GAUGE LENGTH

Temperature (°F)	Young's Modulus ($\times 10^{-6}$ psi)	Effective Modulus ($\times 10^{-6}$ psi/in.)	Effective Elastic Gauge Length (in.)
70	30.2	58.76	0.51
500	27.5	54.89	0.50

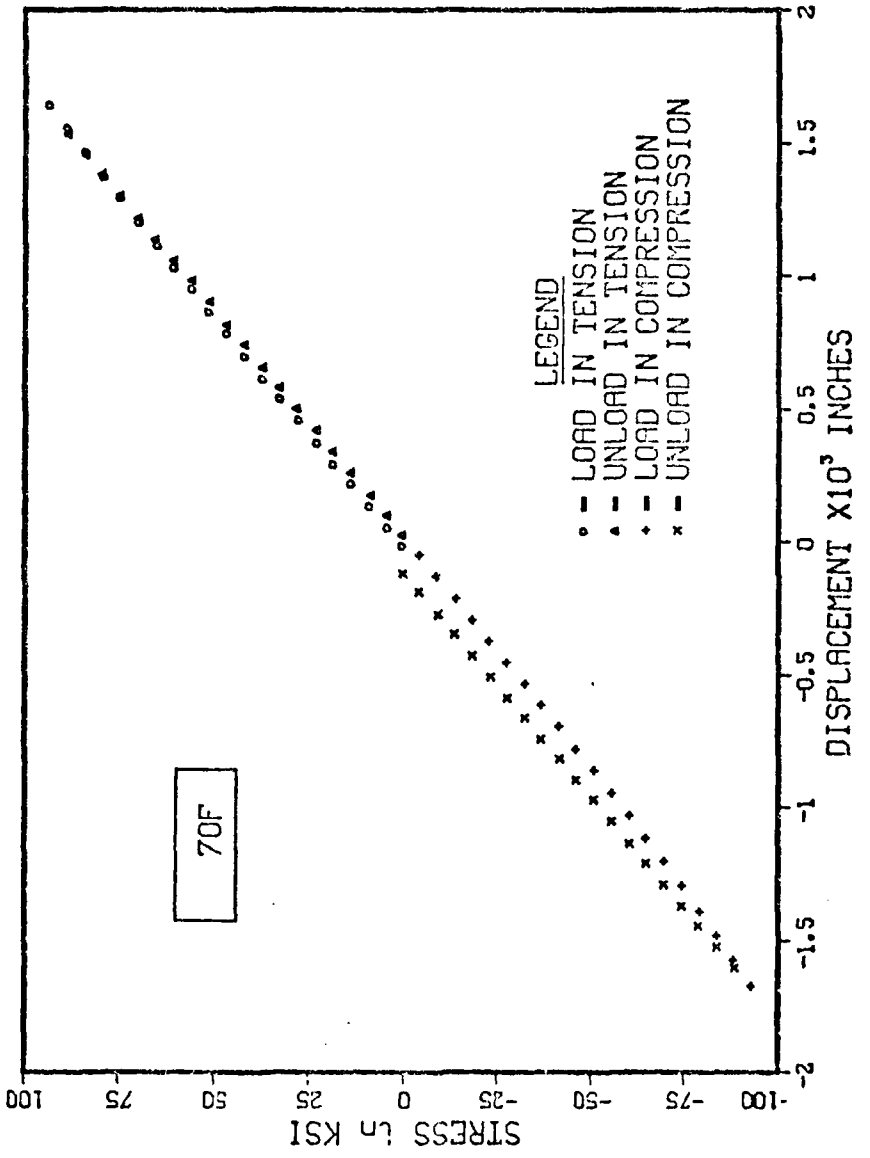

Figure 22. Plot of Stress vs Displacement at 70°F

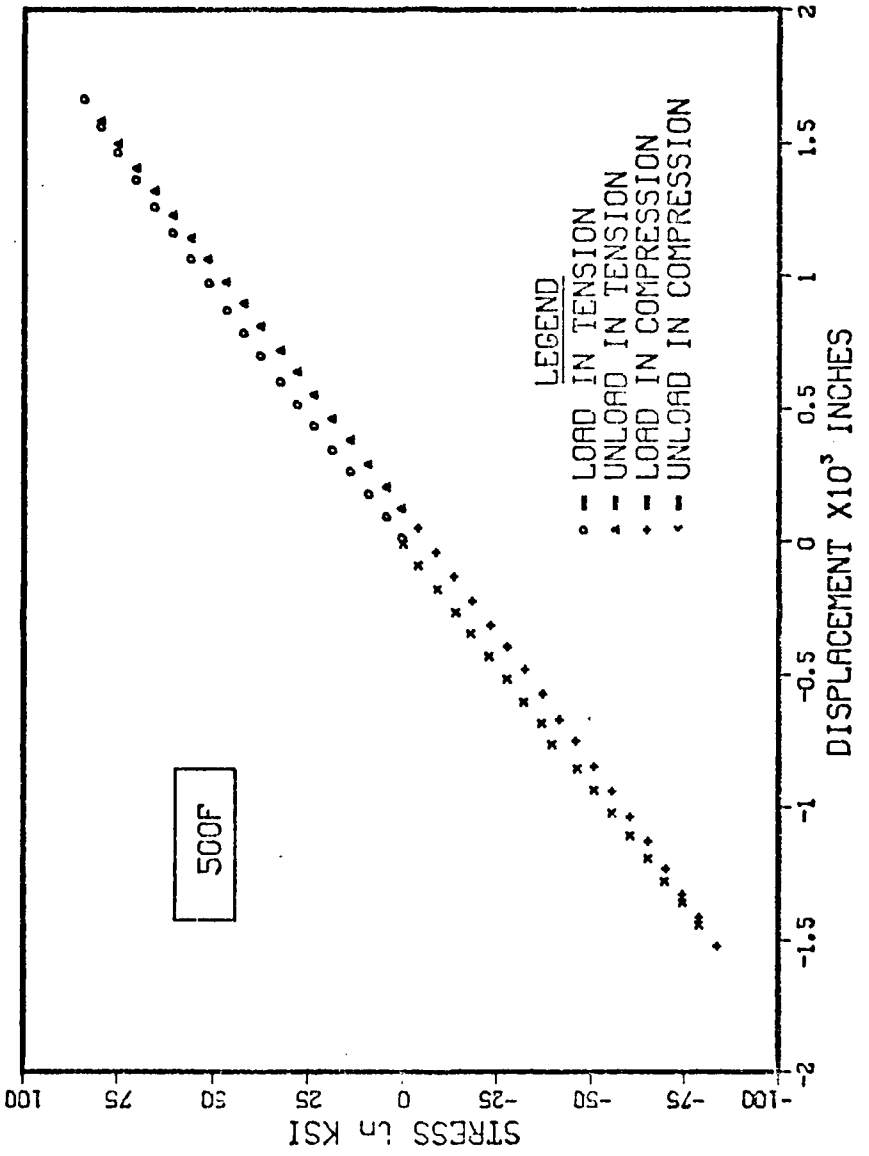

Figure 23. Plot of Stress vs Displacement at 500°F

B. Cyclic Stress-Strain Curve

Using the methodology described by Manson (3), a comparison of a 500°F static stress-strain curve with the 500°F cyclic stress-strain curve was made. For experimental ease, the tensile data used was measured at a strain rate of 2×10^{-2} in./in./min., while the cyclic data was obtained at a higher strain rate of 3.3×10^{-1} in./in./min. The tensile data presented in Table 7 shows that the mechanical properties of this alloy at 500°F are not very sensitive to strain rate within the range studied; thus, this comparison is not expected to be in significant error.

Figure 24 is the cyclic stress-strain curve compared to the static curve. At the lower strain ranges, the alloy cyclically softens; and, at the higher strain ranges, it cyclically hardens. For total strain ranges greater than 2.0%, Merrick observed rapid strain hardening of Incoloy 901 at room temperature and at 1000°F (16). The strain rate was not specified. Hardening peaked at about 10 cycles, then gradual softening occurred. Very rapid strain hardening was observed in this work also. The strain softening which occurred happened very gradually.

Cyclic strain hardening has been explained phenomenologically as being caused by dispersal of slip onto neighboring slip planes, and analogous to unidirectional hardening (4,66,67). The cyclic softening is due to the concentration of cyclic slip in the active slip bands (4,64,65,68). Thus, the shape of the cyclic stress-strain curve can be explained as follows: At the higher strain ranges, strain hardening has occurred but since the lifetimes at these high ranges is short, there was insufficient time for appreciable strain softening to

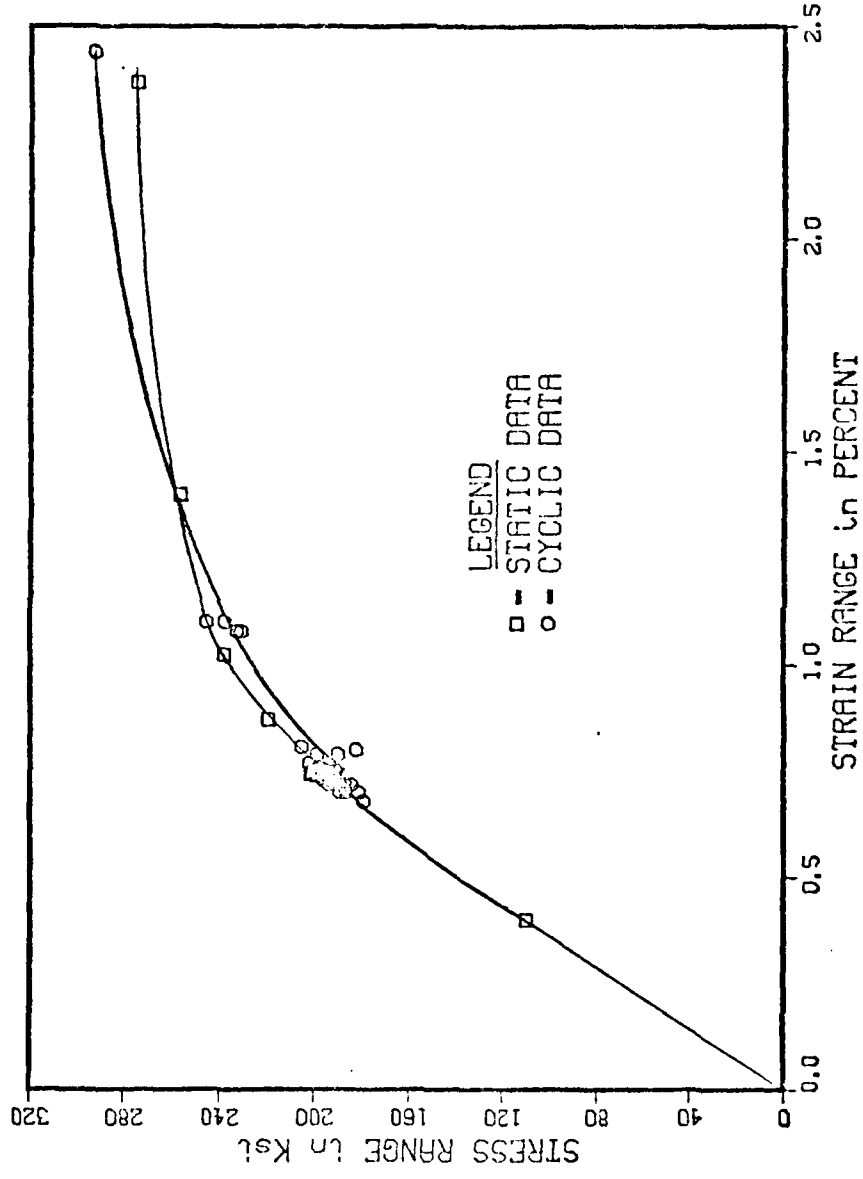

Figure 24. Plot of Cyclic Stress-Strain Curve

occur. At the lower strain ranges, the lifetimes are relatively long and hence there was time for softening to occur.

C. Characterization of Fatigue Damage

1. Baseline Data

A summary of the baseline data is presented in Table 9. The stress range reported is the stabilized range. The initiation cycle, N_i, was determined by extrapolating the asymmetric load drop back to the stable stress range on a plot of expanded Stress Range vs Cycles (2). A typical plot of this type is shown in Figure 25. The transition to the rapid load decrease, N_i', was determined by the point at which the load drop-off was no longer linear. The cycles to failure, N_f, was determined when the maximum tensile stress was 20 ksi. Figure 26 is a log-log plot of Strain Range vs Cycles. Table 10 contains the constants for the linear least square fit lines of Figure 26. Using the data in Table 10, the following Coffin-Manson type equations can be derived:

$$\Delta\varepsilon_t = 8.15\ N^{-0.295} \tag{13a}$$

$$\Delta\varepsilon_e = 1.75\ N^{-0.114} \tag{13b}$$

$$\Delta\varepsilon_p = 71.29\ N^{-0.898} \tag{13c}$$

The data estimated from Merrick (16) was obtained by merely averaging his room temperature and 1000°F data. Figure 27 compares the trend line for Cycles to Initiation with Cycles to Failure.

Plots of Stress Range vs Cycles for the baseline specimens listed in Table 9 are contained in Figures 28-38, respectively. Note that these plots, in general, contain data obtained by measurement of hysteresis loops and by output from the Instron Minicomputer. The computer data

TABLE 9

SUMMARY OF BASELINE LCF PROPERTIES

Specimen	Strain Range (%)			Stress Range (ksi)	Cycles				
	$\Delta\varepsilon_t$	$\Delta\varepsilon_p$	$\Delta\varepsilon_e$		N_i	N_i'	N_f	N_i/N_f	N_i'/N_f
2	1.08	0.25	0.83	232	780	-	1139	0.68	-
3	2.44	1.37	1.07	292	-	-	58	-	-
5	1.10	0.27	0.83	237	480	760	852	0.56	0.89
6	0.71	0.07	0.64	187	1400	2610	3263	0.43	0.80
7	0.72	0.05	0.67	191	1600	3200	3752	0.43	0.85
8	0.72	0.05	0.67	184	1200	3300	3820	0.31	0.82
11	0.70	0.05	0.65	181	2350	3800	4025	0.58	0.94
12	0.79	0.04	0.75	190	1300	2550	3398	0.38	0.75
32	0.70	0.04	0.66	189	1350	2900	4059	0.33	0.71
33	0.76	0.05	0.71	196	1000	2300	2965	0.34	0.78
53*	0.72	0.03	0.69	191	900	2600	3264	0.28	0.80

*Electropolished before test

TABLE 10

LINE CONSTANTS FOR log $\Delta\varepsilon$ vs log N CURVES

	b*	m*
$\Delta\varepsilon_t$	0.911	-0.295
$\Delta\varepsilon_p$	1.853	-0.898
$\Delta\varepsilon_e$	0.242	-0.114

*Equation is of the form:

$$\log \Delta\varepsilon = m \log N + b$$

where $\Delta\varepsilon$ is strain range (%)

N is number of cycles

m is slope of the line

b is the y-intercept

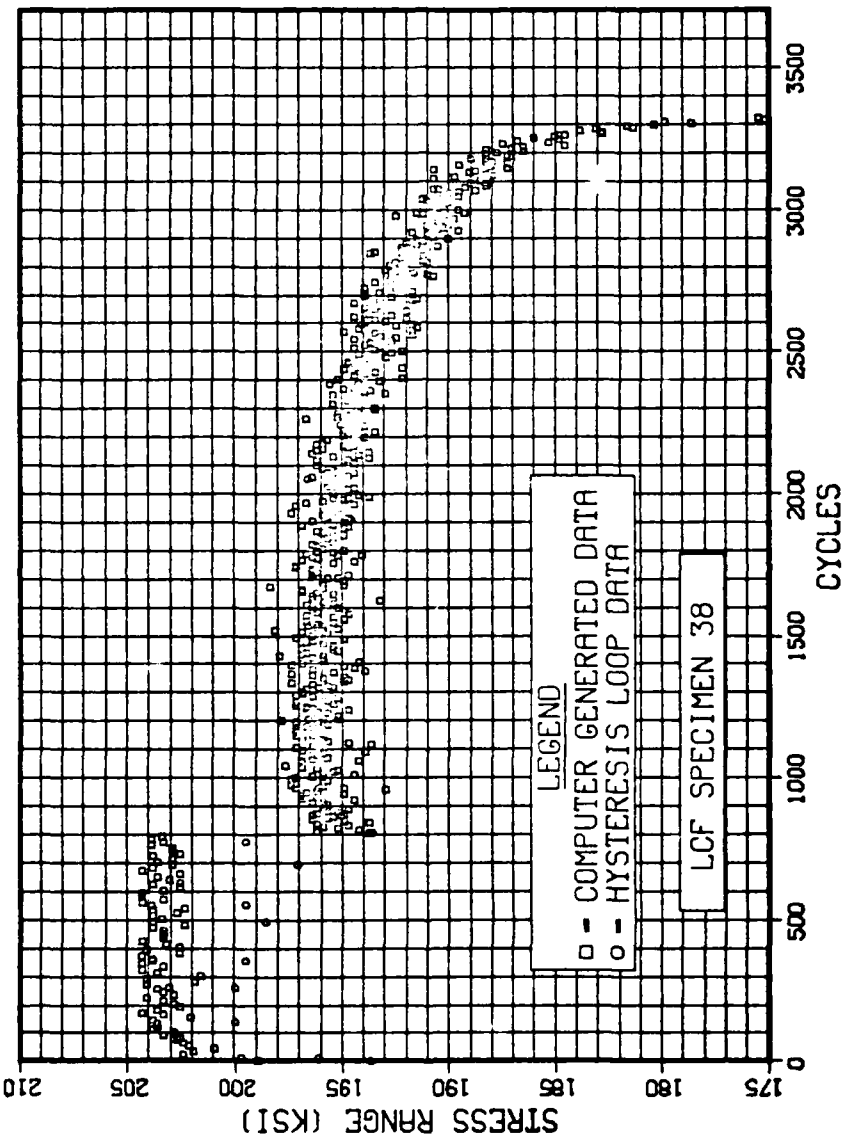

Figure 25. Plot of Stress Range vs Cycles - Expanded Scale

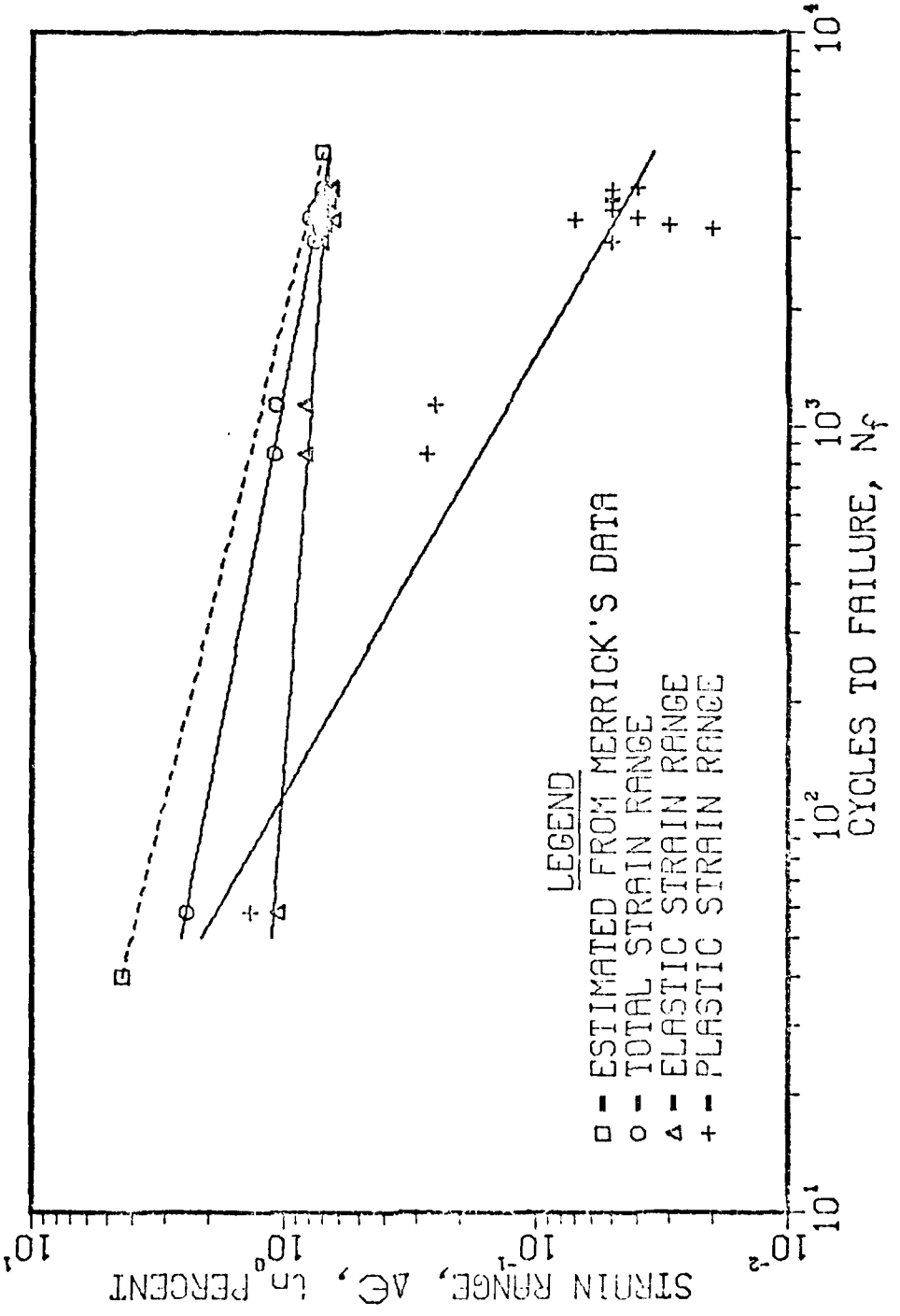

Figure 26. Plot of Baseline Strain Range vs Cycles to Failure

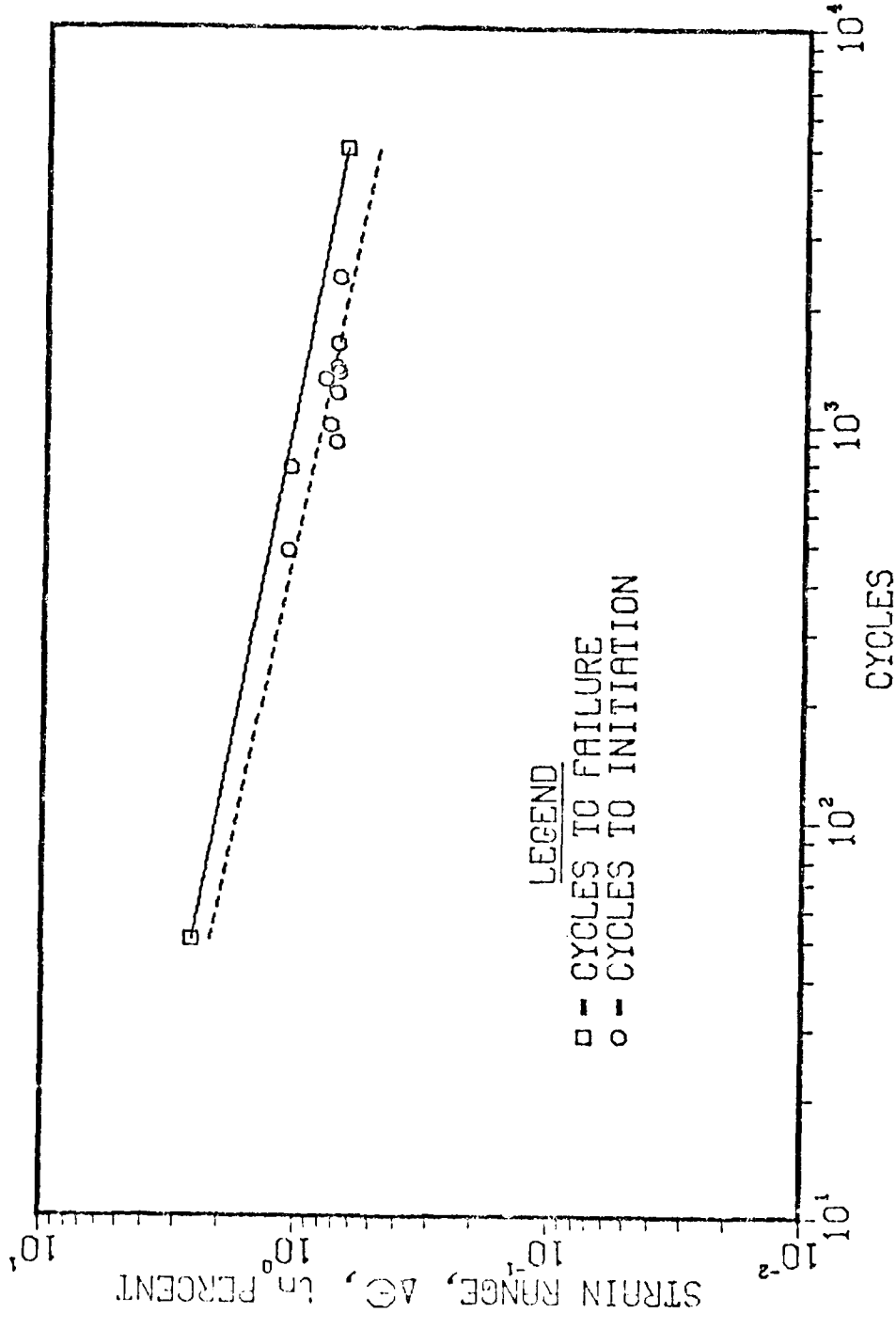

Figure 27. Plot of Baseline Strain Range vs Cycles to Initiation

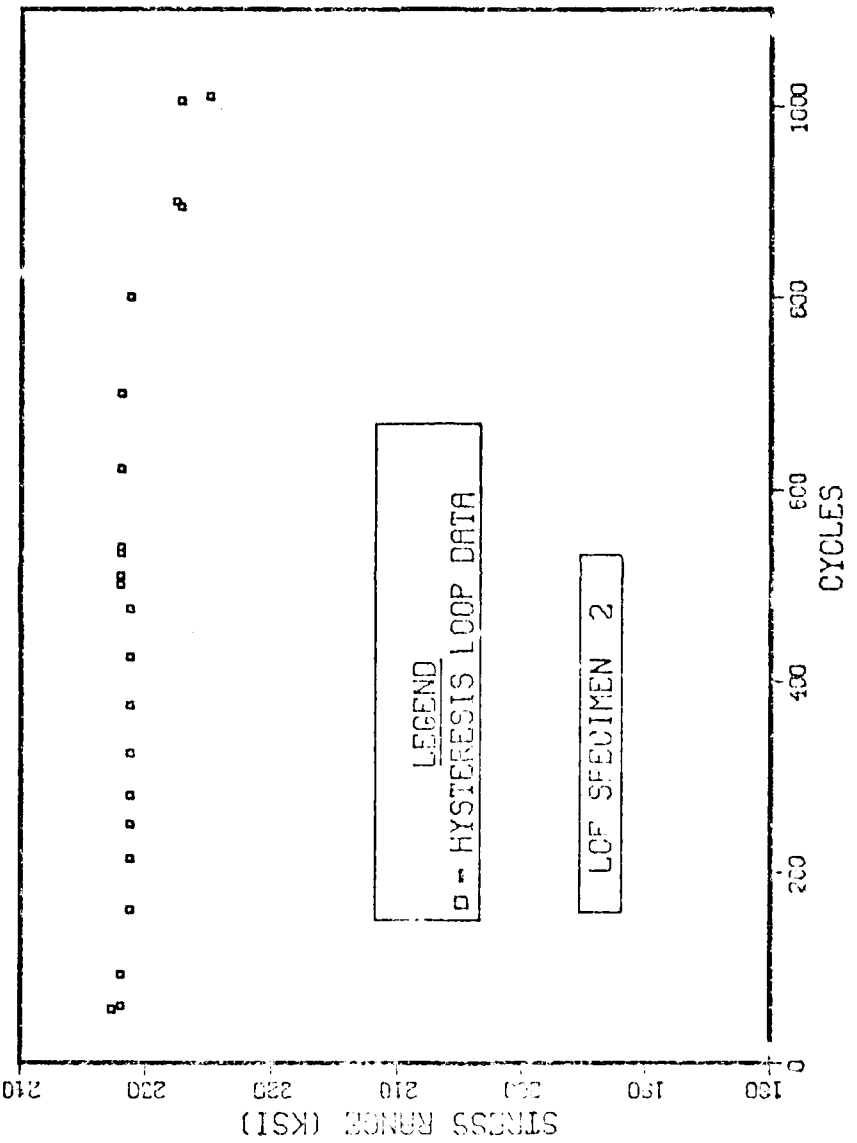

Figure 28. Plot of Stress Range vs Cycles - LCF Specimen 2

AD-A107 255 AIR FORCE INST OF TECH WRIGHT-PATTERSON AFB OH F/G 11/6
MECHANISMS OF RECOVERING LOW CYCLE FATIGUE DAMAGE IN INCOLOY 90--ETC(U)
1979 R E SCHAFRIK
UNCLASSIFIED AFIT-CI-79-212D NL

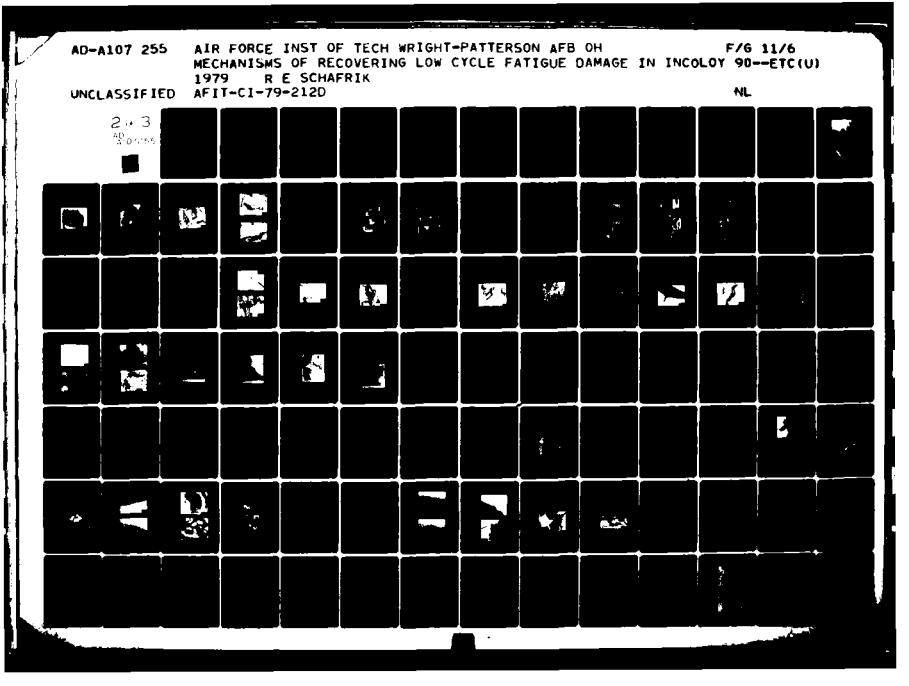

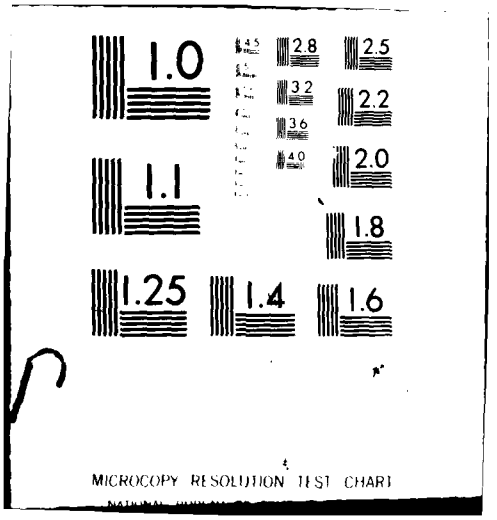
1.0
1.1
1.25
1.4
1.6
1.8
2.0
2.2
2.5
2.8
3.2
3.6
4.0
4.5
MICROCOPY RESOLUTION TEST CHART

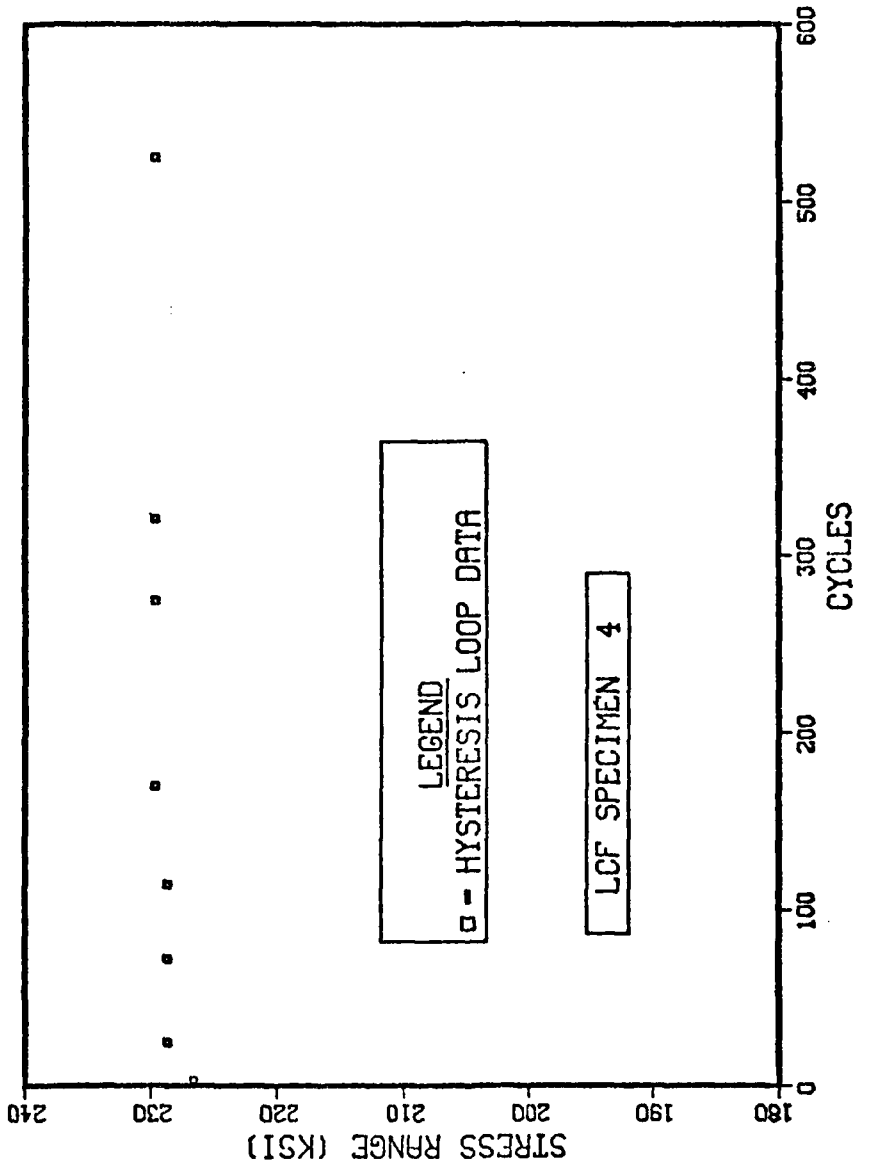

Figure 29. Plot of Stress Range vs Cycles - LCF Specimen 4

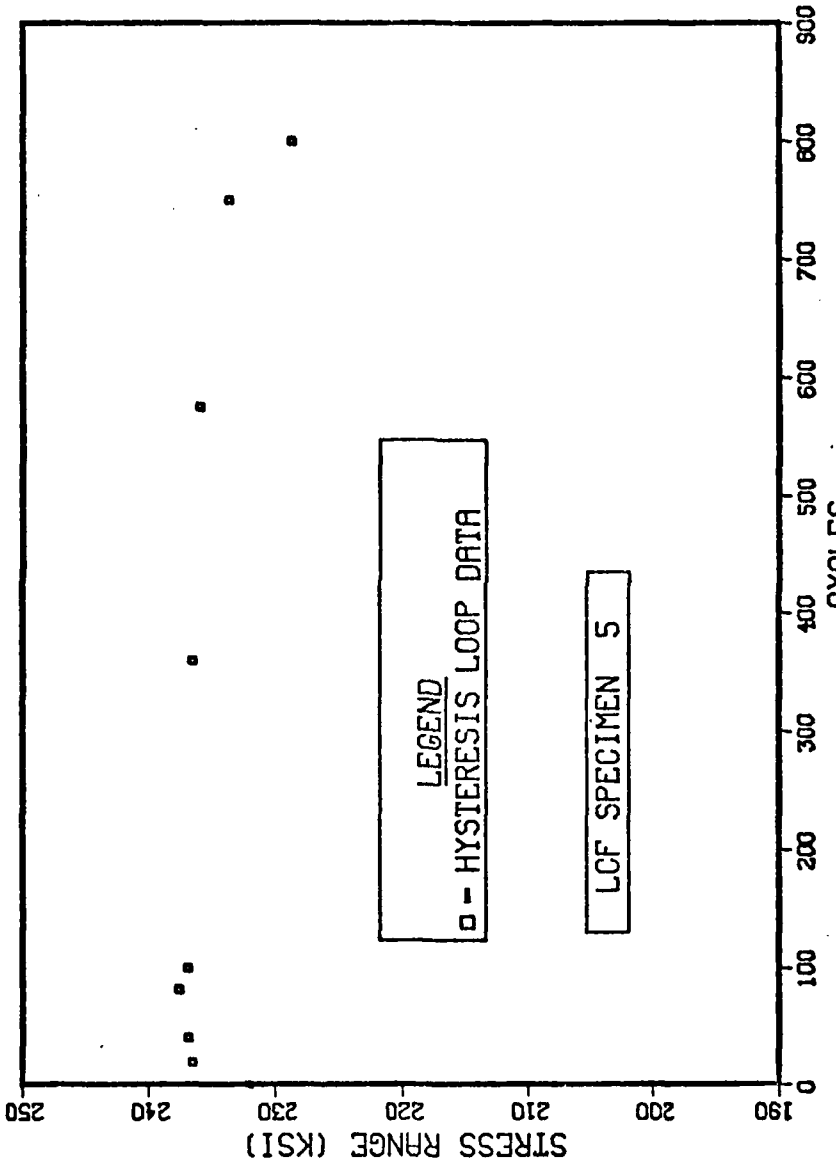

Figure 30. Plot of Stress Range vs Cycles - LCF Specimen 5

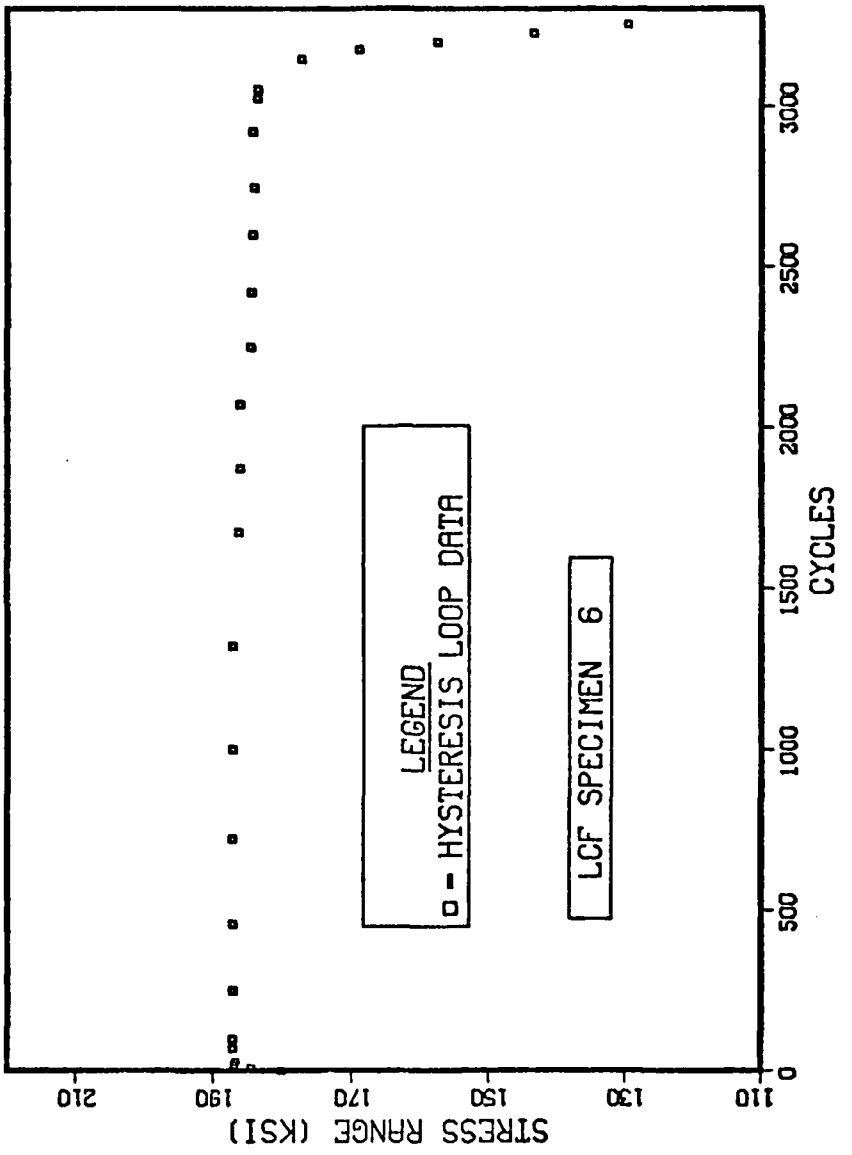

Figure 31. Plot of Stress Range vs Cycles - LCF Specimen 6

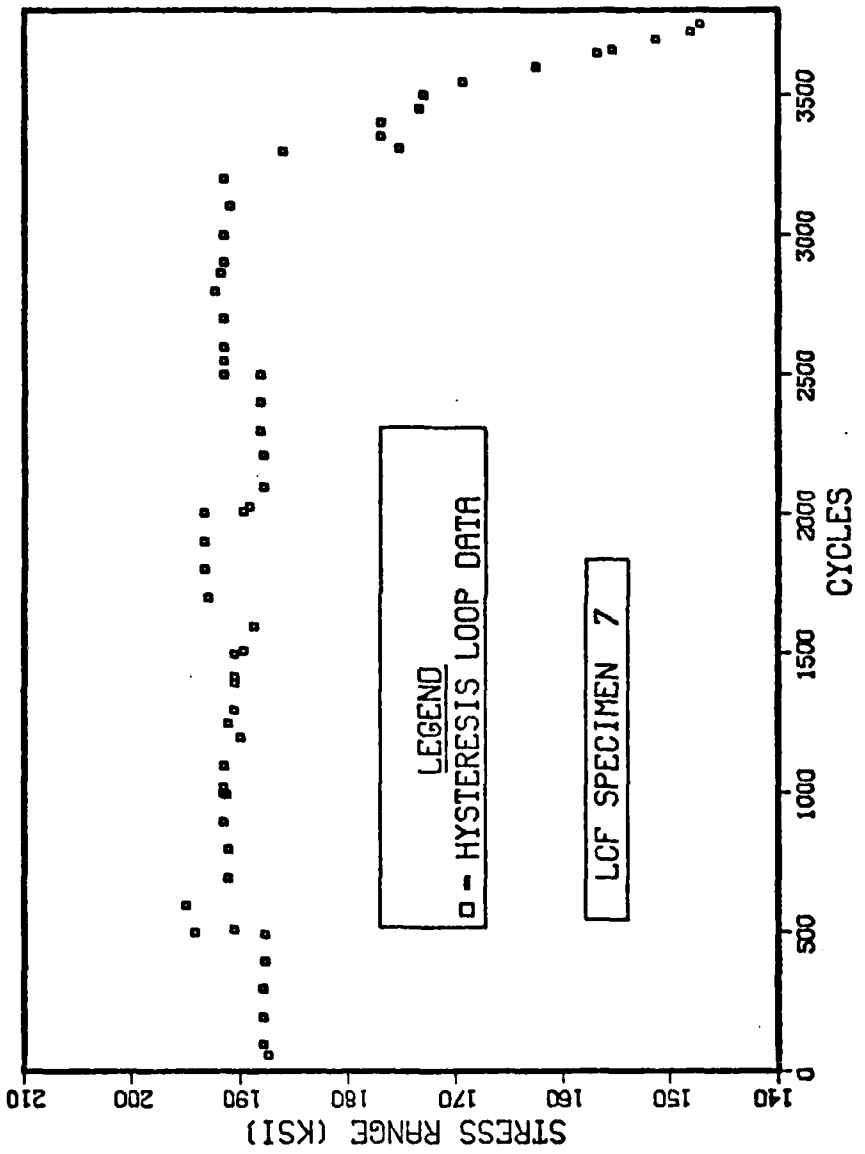

Figure 32. Plot of Stress Range vs Cycles - LCF Specimen 7

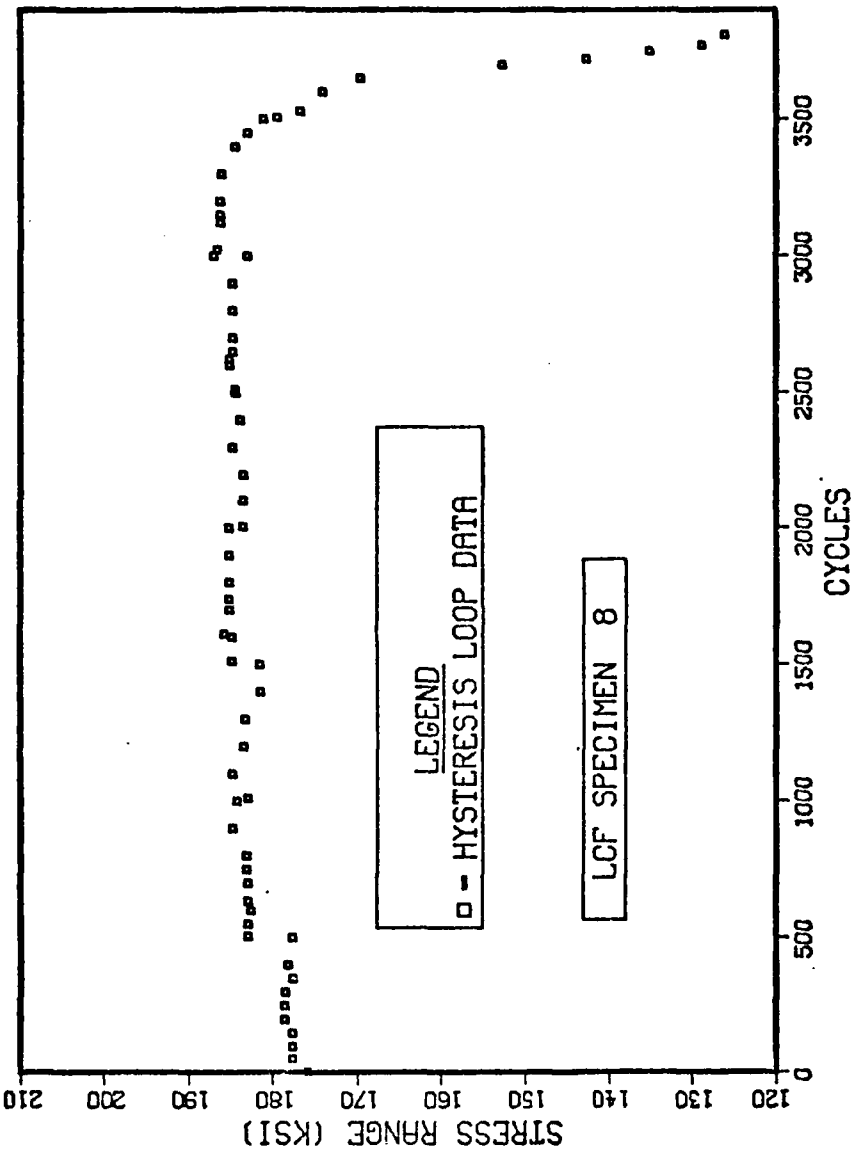

Figure 33. Plot of Stress Range vs Cycles - LCF Specimen 8

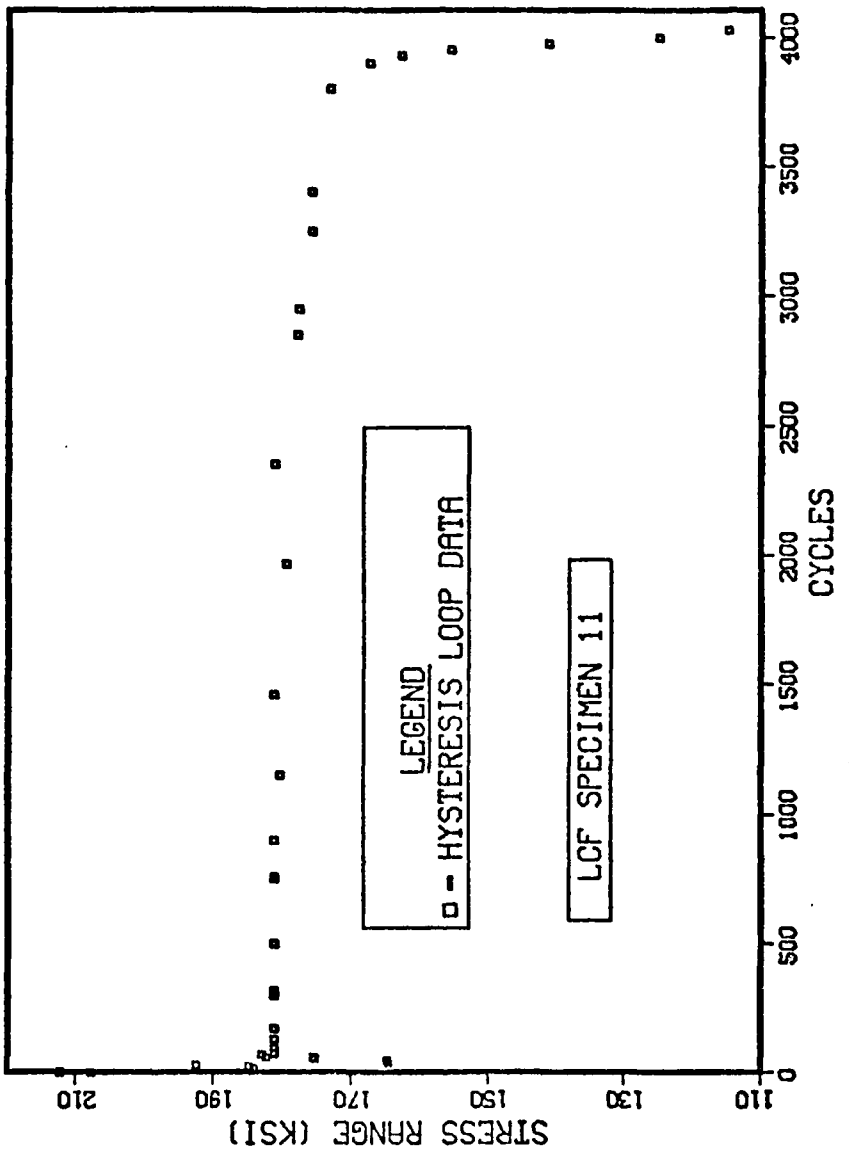

Figure 34. Plot of Stress Range vs Cycles - LCF Specimen 11

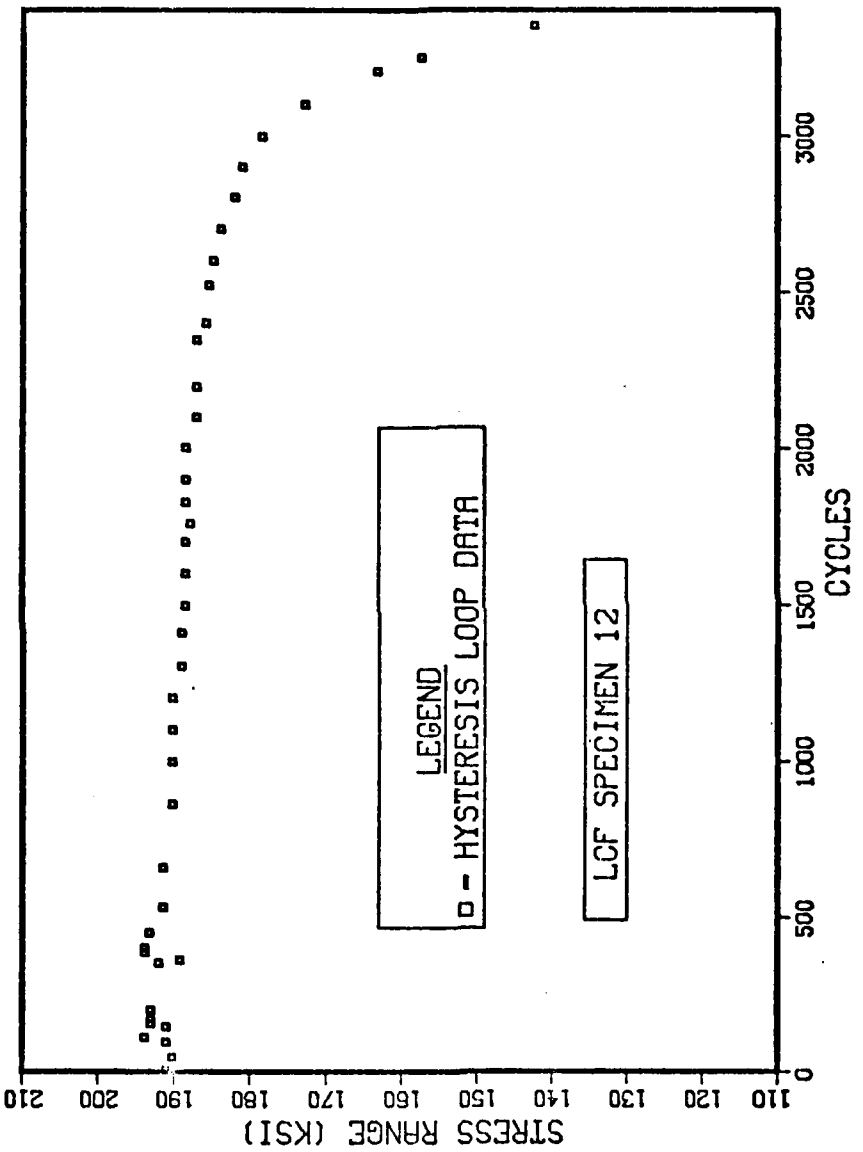

Figure 35. Plot of Stress Range vs Cycles - LCF Specimen 12

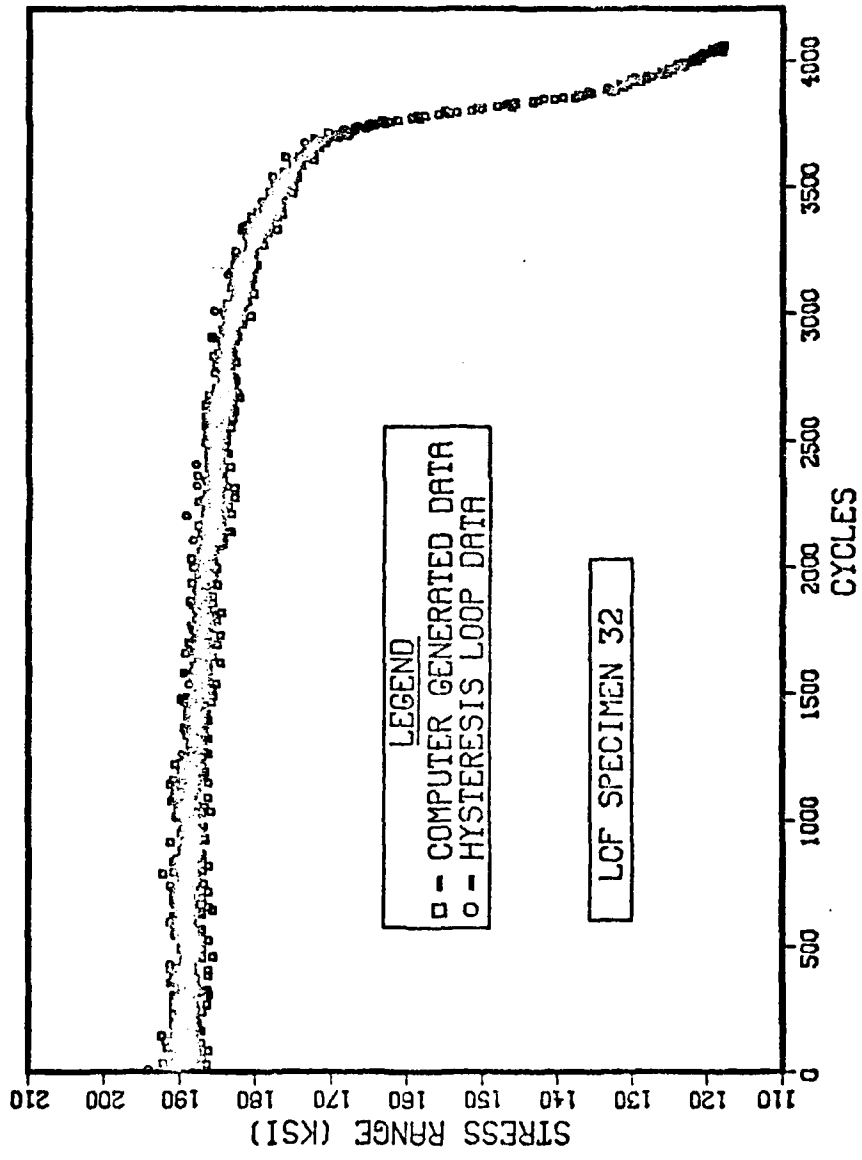

Figure 36. Plot of Stress Range vs Cycles - LCF Specimen 32

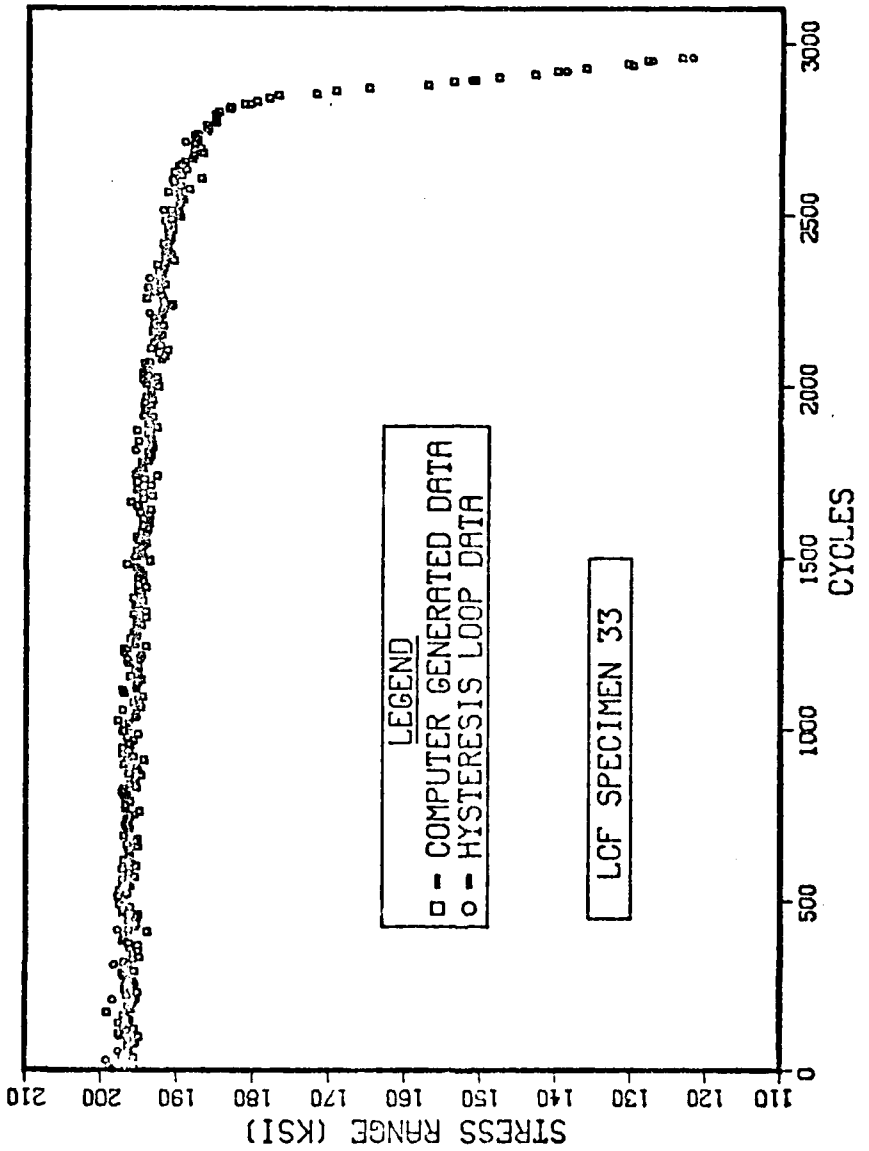

Figure 37. Plot of Stress Range vs Cycles - LCF Specimen 33

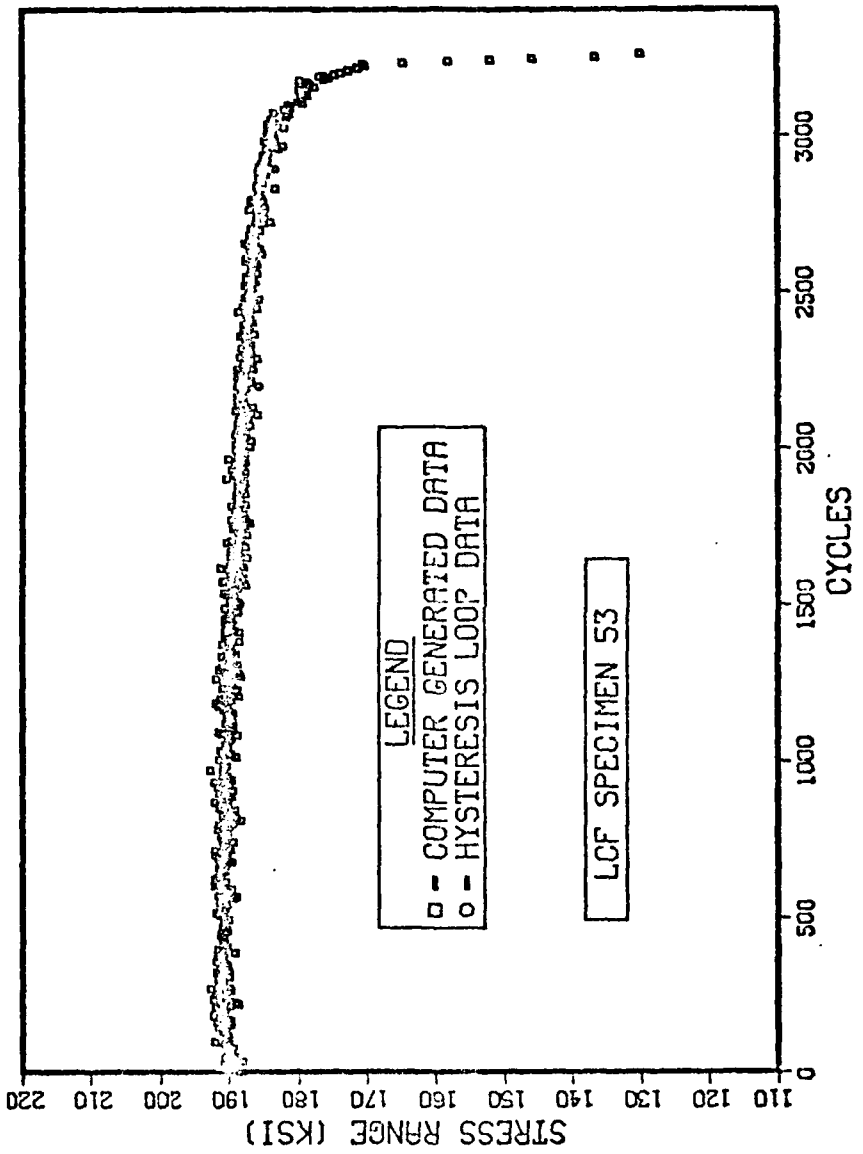

Figure 38. Plot of Stress Range vs Cycles - LCF Specimen 53

was obtained, in general, at every fifth cycle. The hysteresis loop data was usually obtained every 100 cycles. The effect of rejuvenation efforts will be discussed with respect to this baseline data.

ii. Dislocation Substructure

A typical dislocation substructure after a test is shown in Figure 39. The dislocations are aligned in bands, giving rise to the planar slip characteristics of this alloy. The dislocations are bowed around and looped around γ' precipitates, although cutting of the precipitates cannot be ruled out. Stacking fault contrast was observed in some precipitates, leading to the conclusion that they had been sheared. Using surface replication techniques, others have observed sheared γ' on the surface (16). Not every foil showed the concentration of slip bands depicted in Figure 39. Thus, deformation even at these higher strain ranges, is still somewhat localized.

iii. Fractography

Extensive fractography was carried out on samples which were removed unbroken from the fatigue machine and subsequently broken in tension. This procedure preserved the character of the fracture surface. The fractures were mixed mode, with both intergranular and transgranular regions. This behavior has been observed by others (16,45). A typical fractograph for LCF Specimen 33 is shown in Figure 40. Figure 41 is a higher magnification view of a likely crack initiation area. This was determined by following fatigue striations back to the edge. Typical fatigue striations are shown in Figure 42. Striations were seen close to the edge. Figures 43(a) and 43(b) demonstrate the cracking of carbides which lie on the fracture surface. The morphology of the

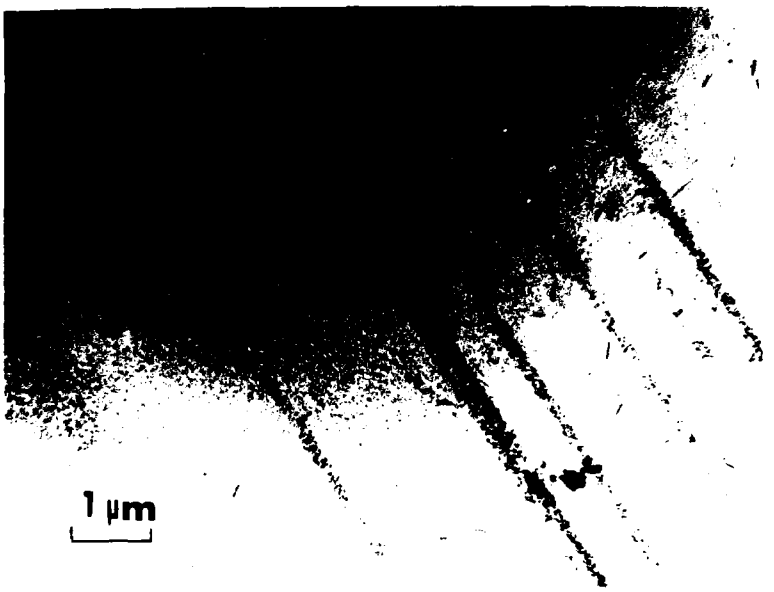

a. Planar Dislocations

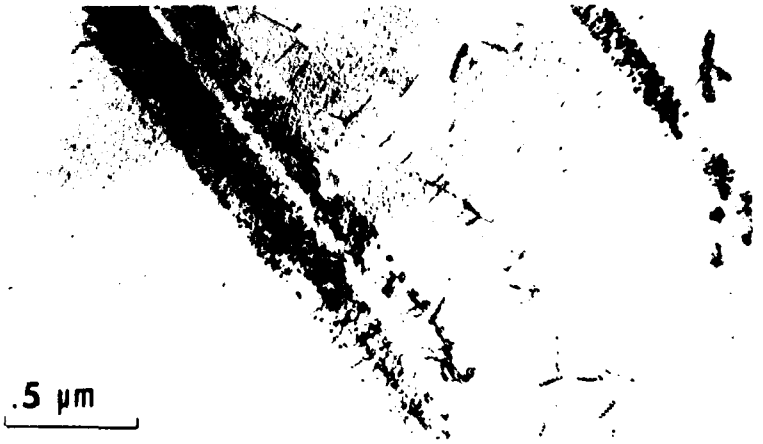

b. Planar Dislocations

Figure 39. TEM Micrograph of Fatigued Specimens with Planar Dislocations

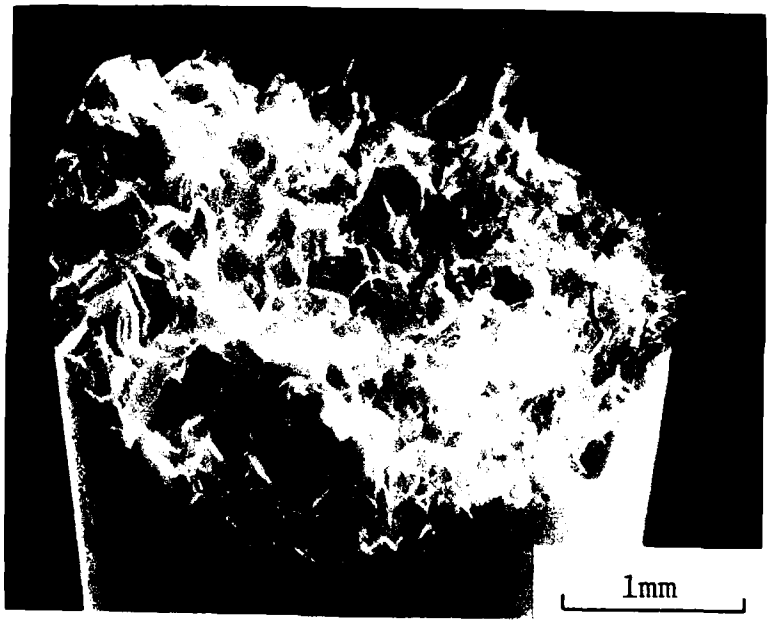

Figure 40. SEM Fractograph - LCF Specimen 33

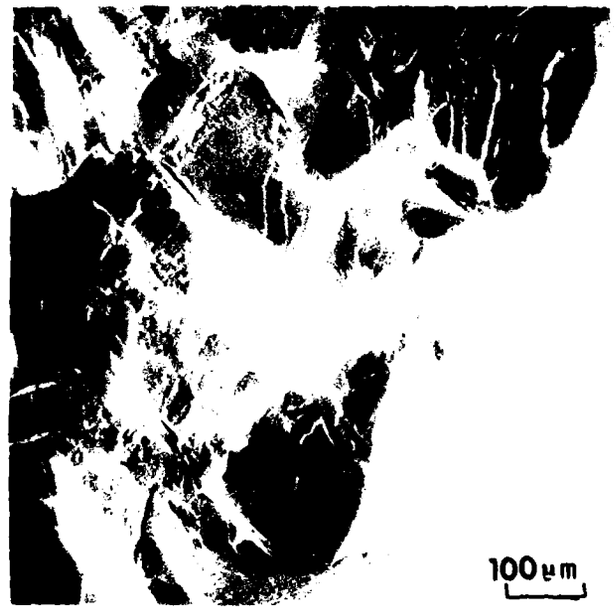

Figure 41. SEM Fractograph, Initiation Site - LCF Specimen 33

Figure 42. SEM Fractograph, Fatigue Striations - LCF Specimen 33

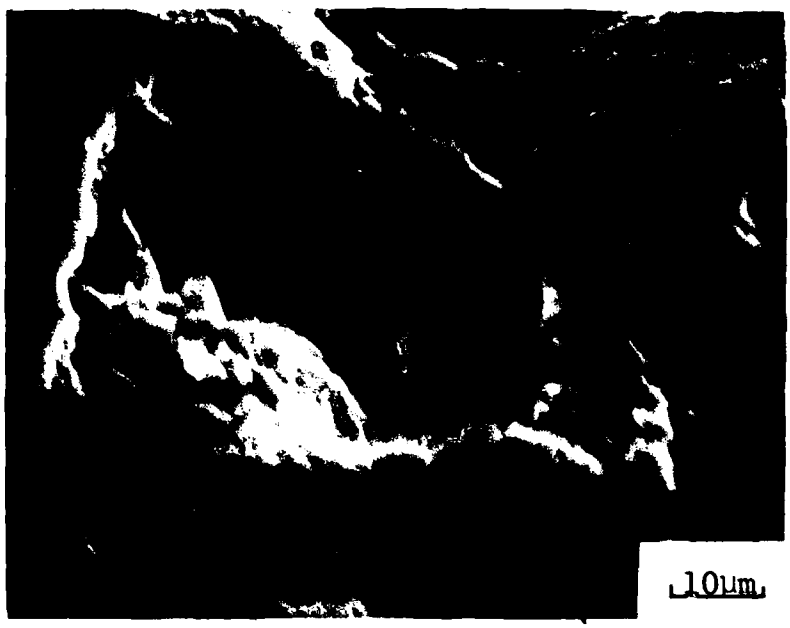

a. Cracked Titanium Carbide Particle

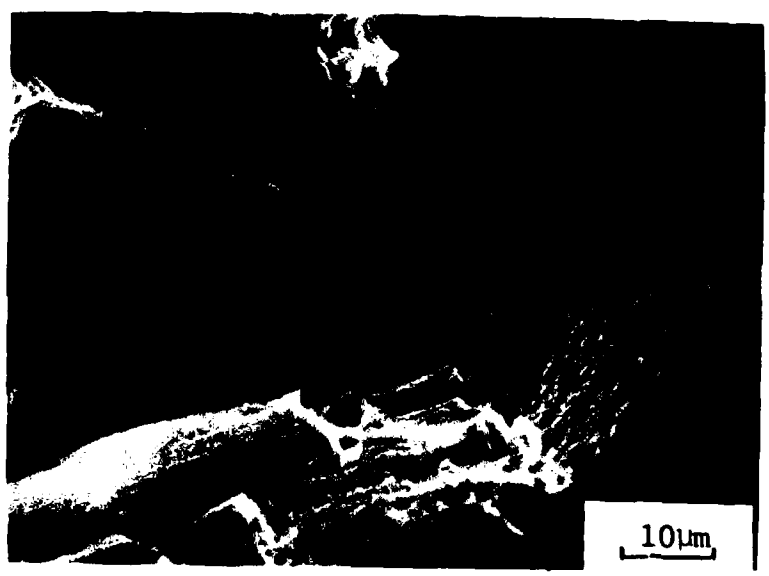

b. Cracked and Pull-Out Titanium Carbide Particles

Figure 43. SEM Fractograph, Cracked Carbides

carbide shown in Figure 43(a) suggests it may be a carbo-sulfide. The presence of these carbides may contribute to the large amount of longitudinal cracking which has been observed in this alloy (9).

D. Crack Initiation Mechanisms

i. Surface Replication

Surface replication during the course of fatigue testing was done in order to find the fraction of life at which crack initiation at 500°F occurred for total strain range of 0.75%. Two specimens, LCF Specimen 7 and LCF Specimen 8, were replicated at 500-cycle intervals. A composite of the replicas' photomicrographs are presented in Figures 44 and 46. Figure 44(a) shows the replication after 500 cycles of the area where the crack will initiate in LCF Specimen 7. At this magnification, there is no apparent crack, but persistent slip lines are evident. Figure 44(b), after 1000 cycles, still does not show a microcrack, but more intense deformation concentrated in the slip bands and grain boundaries is evident. Figure 44(c), after 1500 cycles, shows the first indication of microcracking. In Figure 44(d), after 2000 cycles, the cracking has extended into a persistent slip band. In Figure 44(e), after 2500 cycles, another microcrack becomes evident on the left-hand side. By Figure 44(f), after 3305 cycles, the two cracks have lined up and further extended. In the final series, Figure 44(g), after 3752 cycles (the last cycle), substantial crack propagation had occurred. A plot of Crack Length vs Cycles for LCF Specimen 7 is shown in Figure 45. When the crack length is extrapolated to zero length, the x-ordinate is intercepted at approximately 1500 cycles. The transition to rapid crack growth, N_i', occurred at approximately 3400 cycles.

Figure 44. Micrographs of Replicas, Cracks - LCF Specimen 7

Figure 44 (continued)

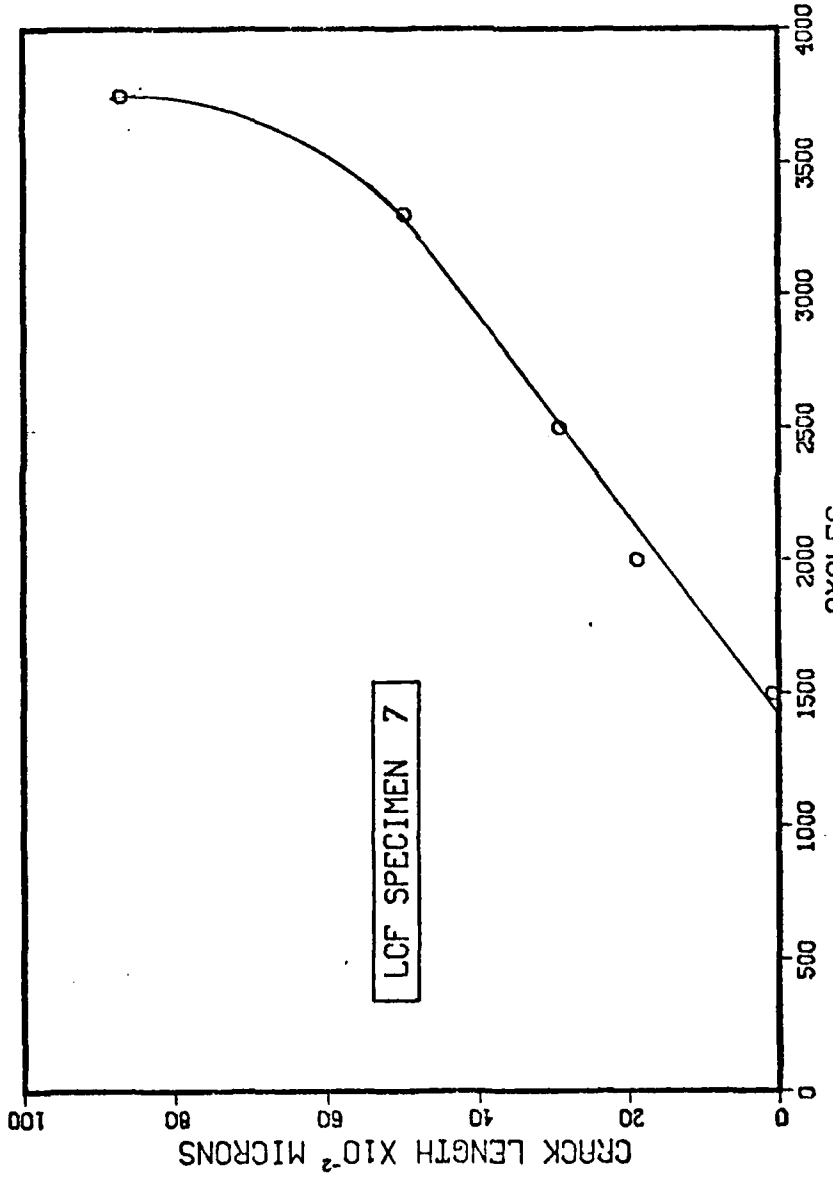

Figure 45. Plot of Crack Length vs Cycles - LCF Specimen 7

A composite of the photomicrographs of the surface replicas for LCF Specimen 8 is contained in Figure 46. In this specimen, three separate cracks form. Figure 46(a), taken after 500 cycles, shows the development of slip lines but no cracks are apparent. In Figure 46(b), after 1000 cycles, there is a persistent slip band evident in the upper right-hand portion of the collage which eventually becomes the upper crack. In Figure 46(c), after 1500 cycles, the V-shaped beginning of the middle crack is apparent. At 2000 cycles, Figure 46(d), the lower crack is evident as is a portion of the upper crack. Unfortunately, the middle crack is obscured by artifacts in the replica. In Figure 46(e), after 2500 cycles, all three cracks are clearly visible and several microcracks at either end of the middle crack are visible. By 3000 cycles, shown in Figure 46(f), the microcracks of the middle crack have linked up. Further crack extension by 3500 cycles, Figure 46(g), is readily apparent. A plot of Crack Lengths vs Cycles for LCF Specimen 8 is contained in Figure 47. The crack lengths plotted are the sum of the individual lengths. Since the measured crack lengths entailed some judgment, the scatter is not unreasonable. At the early cycles, it is especially difficult to ascertain if a crack exists and to measure its extent. Extrapolating the data back to zero crack length, it appears that crack initiation occurred at approximately 1300 cycles.

If the Stress Range vs Cycles plot for Specimens 7 and 8, contained in Figures 32 and 33, are closely examined, the asymmetric stress drop-off for LCF Specimen 7 occurs at about 1500 cycles and at about 1300 cycles for Specimen 8. These cycles correlate reasonably well with those determined from the crack length measurements. Therefore, the

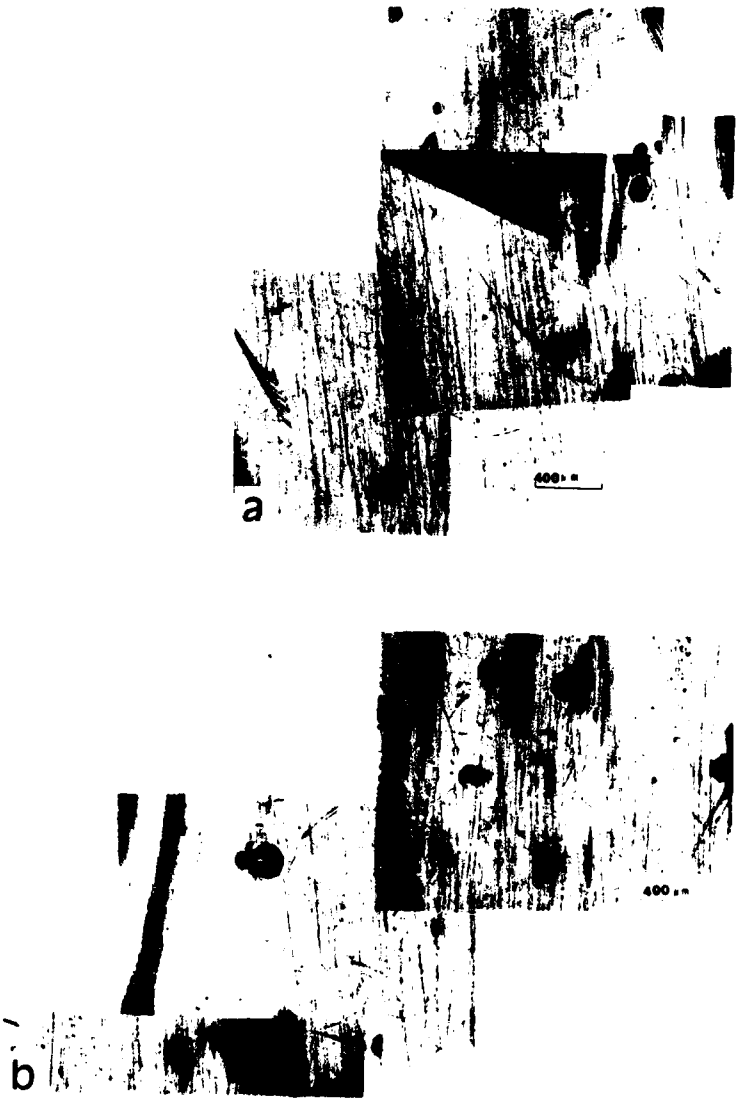

Figure 46. Micrographs of Replicas, Crack - LCF Specimen 8

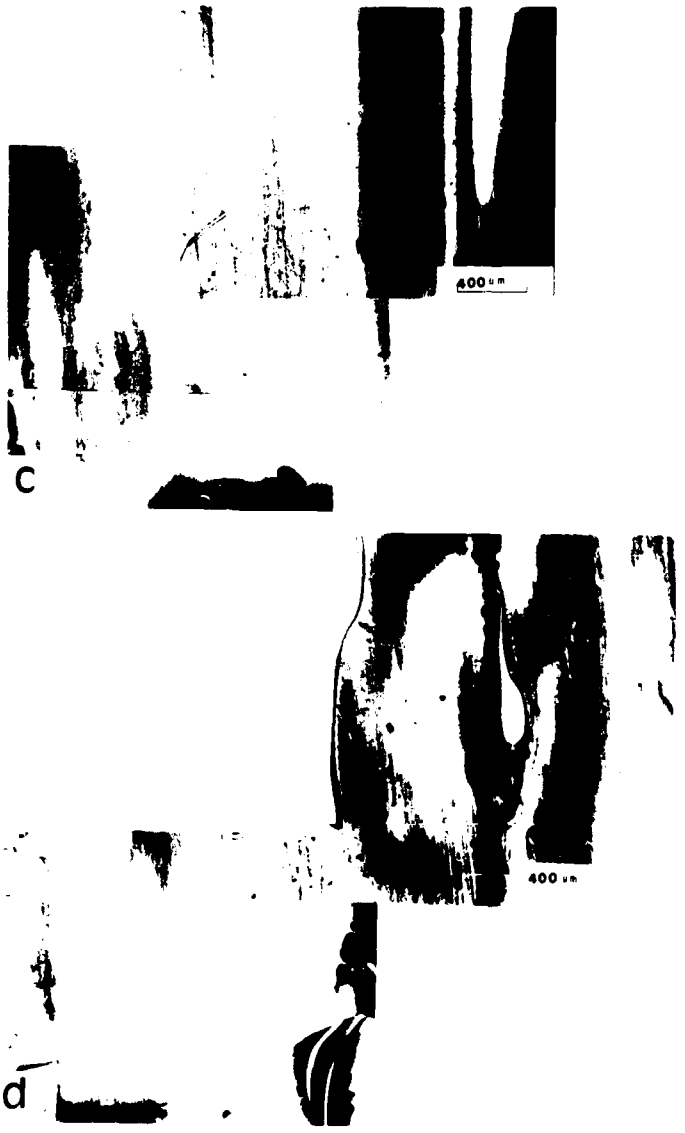
400 µm
c
400 µm
d


e
f
g

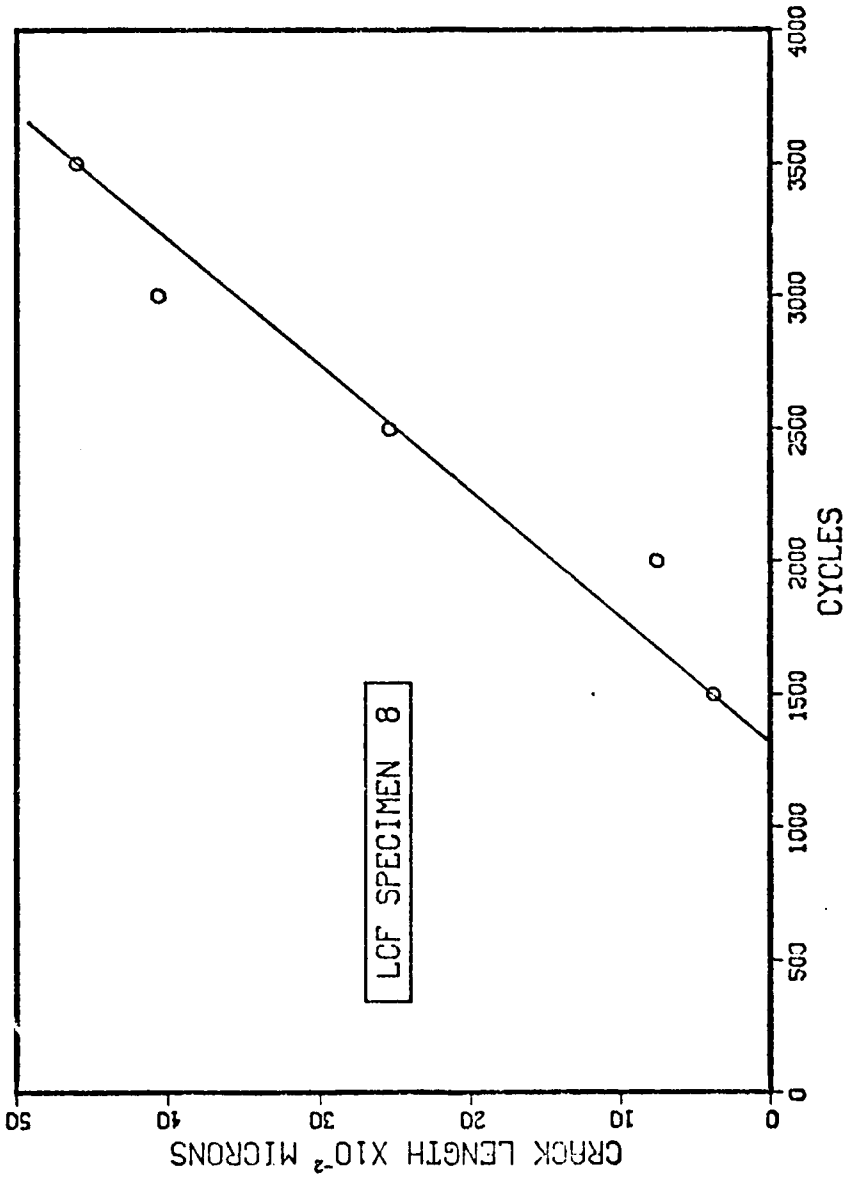

Figure 47. Plot of Crack Length vs Cycles - LCF Specimen 8

asymmetric load drop-off is used in the remainder of this dissertation as evidence that a definite crack exists. In Table 9, N_i is thus a measure of the crack initiation cycle. Furthermore, a damage level of 800 cycles was selected for rejuvenation efforts since it seemed well below the actual crack initiation point.

The slope of the lines in Figures 45 and 47 yields a crack growth rate, da/dN, of 0.27 μm/cycle or 1.07×10^{-4} in./cycle. Macha has determined crack growth rates as a function of ΔK at 400°F and 600°F (62). At 400°F he found that:

$$\frac{da}{dN} = 0.15 \times 10^{-9} (\Delta K)^{2.9} \qquad (14)$$

where da/dN is crack growth rate in in./cycle, and ΔK is stress intensity range in ksi $\sqrt{\text{in.}}$. At 600°F, he found:

$$\frac{da}{dN} = 0.10 \times 10^{-9} (\Delta K)^{3.2} \qquad (15)$$

Since these expressions have the form:

$$\frac{da}{dN} = C (\Delta K)^{m} \qquad (16)$$

C and m can be estimated to be 0.125 and 3.05, respectively, at 500°F, by simple averaging. Thus, at 500°F it is estimated that:

$$\frac{da}{dN} = 0.125 \times 10^{-9} (\Delta K)^{3.05} \qquad (17)$$

By finding ΔK for a fatigue crack in the LCF test specimen, Equation 17 can be used to verify the replication-derived crack growth rate. Irwin's methodology for a semi-elliptical crack, correcting for the plane strain plastic zone in a finite body, was used (63). It is only an approximation for the geometry of the LCF specimen. The details of the calculation are presented in Table 11. The computed value of

TABLE 11

CALCULATION OF CRACK GROWTH RATE FROM FRACTURE MECHANICS

Assumptions:

1. Initial flaw size, 2c, of 0.118 in. (3000 μm)
2. Crack aspect ratio, a/2c, of 0.30
3. Stress range, $\Delta\sigma$, of 190 ksi
4. Ratio $\sigma_{max}/\sigma_{y.s.}$ of 0.75
5. $da/dN = 0.125 \times 10^{-9} (\Delta K)^{3.05}$

Calculation: Irwin's equation of interest is

$$K_I = \frac{1.1\ \sigma\ \sqrt{\pi a}}{\sqrt{Q}}$$

where $Q = \int_0^{\pi/2} [1 - \left(\frac{c^2-a^2}{c^2}\right) \sin^2 \phi]^{1/2} d\phi - 1.12 \left[\frac{\sigma}{\sigma_{y.s.}}\right]^2$

Using the above assumptions, Q = 1.4. Thus $\Delta K = 107.5$ ksi $\sqrt{\text{in.}}$

From Assumption 5,

$$\frac{da}{dN} = 1.96 \times 10^{-4}$$

$da/dN = 1.96 \times 10^{-4}$ in./cycle agrees reasonably well with the measured value.

Higher magnification photographs of the replicas taken for Specimens 7 and 8 revealed evidence of a concentrated deformation zone along grain boundaries. But since these specimens were not lightly etched prior to testing, these observations were inconclusive.

ii. Surface Scanning Electron Microscopy

The above replication procedure was invaluable for finding cracks during a fatigue test, but it was not suitable for defining the crack initiation mechanisms for the following reasons: (1) The sharp radius of curvature of the LCF specimen made the replication process extremely difficult to accomplish without producing artifacts in the replica; and (2) A cycle of cooling the specimen, replicating it, and reheating the specimen for further testing took 3-4 hours with the consequence that a great deal of time was consumed in the testing.

With these difficulties in mind, several different approaches were taken to better determine the crack initiation mechanism: (1) A LCF specimen was lightly etched prior to testing and a search was made for offsets in the longitudinal polishing scratches at grain boundaries; (2) A LCF specimen had two parallel flats machined longitudinally and the specimen was electropolished (one flat was lightly etched), and after 1800 cycles of testing at 500°F at a strain range of 0.75%, the flats were examined in the SEM; (3) A specimen was tested at room temperature and replicated every 300 cycles until the asymmetric load drop-off occurred and a definite microcrack could be seen; (4) A specimen, after complete testing, was placed directly in the SEM for

surface observation; (5) The gauge section of a specimen was examined in the SEM after 800 cycles of testing; and (6) A longitudinal section of a gauge section was made of a specimen tested to 2103 cycles. The results of these metallographical investigations are detailed below, and a proposed mechanism for crack initiation at 500°F at $\Delta\varepsilon_t$ = 0.75% is presented.

LCF Specimen 42 was lightly etched after polishing through 4/0 emergy paper. After testing was completed, the gauge section was placed in the SEM. Using the straight polishing scratches as fiduciary marks, offsets of them along grain boundaries were observed. Figure 48(a) and (b) show typical offsets at grain boundaries. There is an apparent curvature of the scratches in the vicinity of the grain boundary indicating the existence of a band of deformation along the boundary. Also, the offsets along a boundary are not uniform. The formation of grain boundary ledges was not readily apparent, but this experimental technique may not have been sensitive enough to detect them. Figure 48 (c) shows offsets along a persistent slip band. Note that the polishing scratches which pass through a persistent slip band are relatively straight right up to the band, and that the offsets along the length of the band are reasonably uniform.

LCF Specimen F2 had two flats machined which were mechanically polished and then electropolished. One flat was lightly etched before testing. The stabilized stress range was 190.5 ksi, at total strain range of 0.75%. Crack initiation, as determined by the asymmetric load drop-off, occurred at 875 cycles. The fatigue test was halted at 1800 cycles and the flat surfaces examined in the SEM. Figure 49 shows

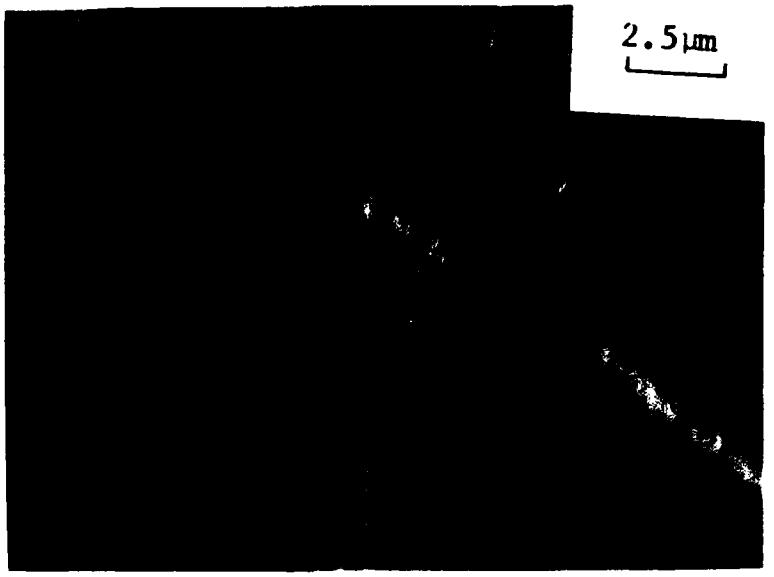

a. Offset of Polishing Scratch at a Grain Boundary

b. Offset of Polishing Scratches at a Grain Boundary

Figure 48. Electron Micrographs Depicting Grain Boundary Offsets

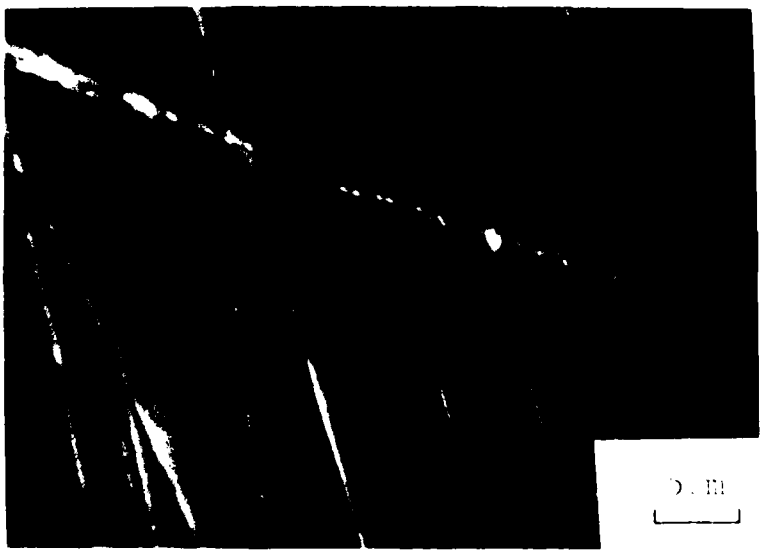

c. Offset of Polishing Scratches at a Persistent Slip Band

Figure 49. SEM Micrograph, Crack at Carbide - LCF Specimen P2

cracks leading away from a large carbide inclusion. Figure 50 graphically shows slip lines and cracks associated with two blocky carbides. The slip lines are at nearly a 45° angle with respect to the longitudinal stress axis.

LCF Specimen 36 was tested at room temperature after light etching. The stress range, after 500 cycles, constantly decreased at the rate of 3.2 psi/cycle. The stabilized stress range was 222 ksi at a total strain range of 0.73%. The test was stopped at 3900 cycles and the specimen broken in liquid nitrogen for fractographic examination. Figure 51 is a 100× view of a replica of a typical area after 3900 cycles. The slip lines within each grain are clearly evident. As the test progressed, there appeared to be a gradual thickening of the grain boundary regions. Using the longitudinal polishing scratches as fiduciary marks, higher magnification definitely revealed offsets along the grain boundaries. Figure 52 shows a typical crack which apparently initiated at a grain boundary carbide. On the fractograph, it was difficult to differentiate the fatigue initiated fracture from the tensile overload fracture.

LCF Specimen 53, which was electropolished before testing, was placed directly in the SEM after testing at 500°F. Table 9 has a summary of its properties. Figure 53 shows a portion of the main crack. Note the grain which pulled out in the center of the photograph. This crack follows a combined transgranular and intergranular path on the surface. Figure 54 shows fatigue striations in an intergranular crack region which are obvious from looking in from the surface. Figure 55

Figure 50. SEM Micrograph, Crack at Carbide - LCF Specimen F2

Figure 51. Micrograph of Replica - LCF Specimen 36

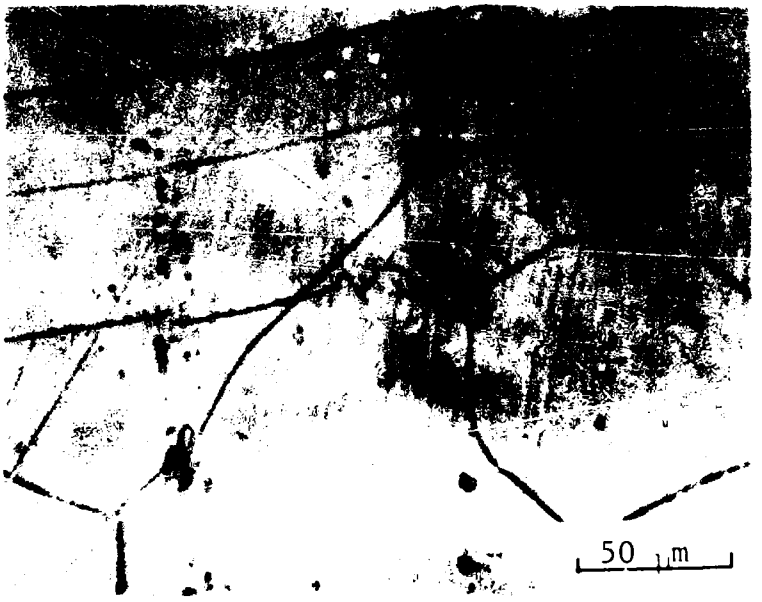

Figure 52. Micrograph of Replica, Crack at Carbide - LCF Specimen 26

Figure 53. SEM Micrograph, Main Crack - 10T Specimen 53

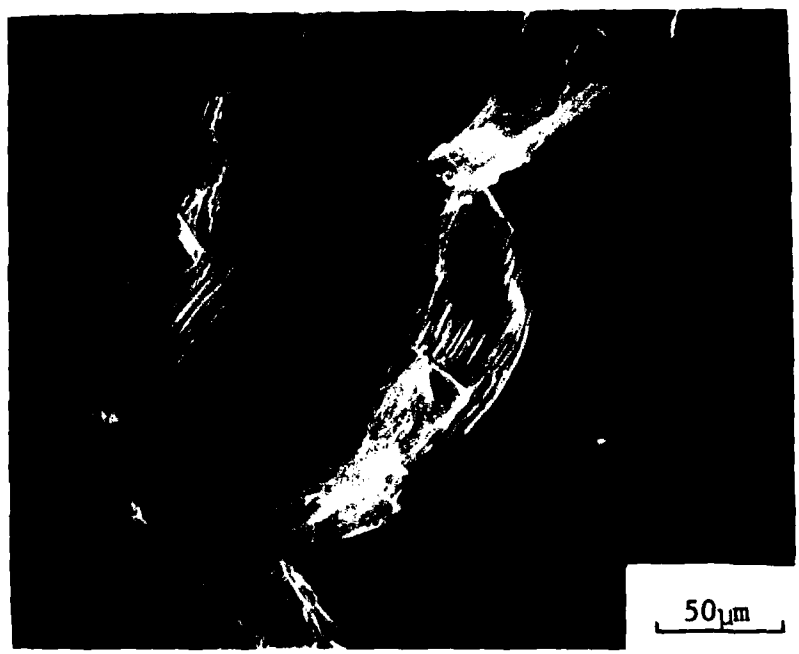

Figure 54. [illegible]

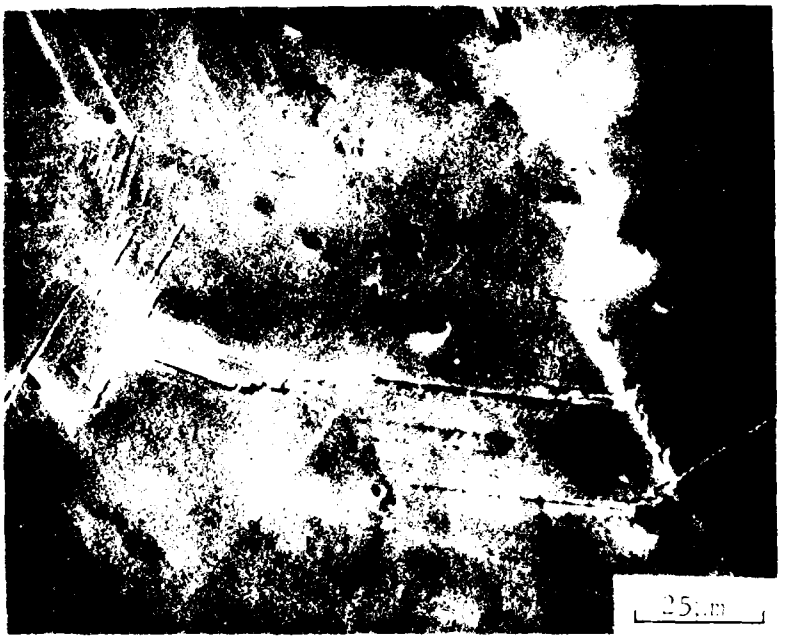

Figure 55. SEM Micrograph, Secondary Cracking - HCF Specimen 53

shows surface cracking which occurred at some distance from the main crack. The crack associated with the carbide is normal to the loading direction.

LCF Specimen 38 was removed from the Instron after 800 cycles at 500°F at a total strain range of 0.77%. It was lightly etched before testing. Figure 56(a) shows the general microstructure as viewed in the SEM. Figure 56(b) is a high magnification view of the slip line in the center of Figure 56(a). At this magnification, the slip line is seen to be an extrusion band. These extrusions were also commonly seen on other fatigue specimens examined in the SEM with greater than 800 cycles of damage. Figure 57(a) shows a blocky carbide in a grain boundary. Figure 57(b) shows that this carbide is beginning to de-cohere. The microstructural damage observed in this specimen at this stage of testing occurred well before the asymmetric load drop-off or the initiation of microcracking.

LCF Specimen 39 was tested at 500°F at a total strain range of 0.77%. The test was stopped after 2103 cycles. Crack initiation, determined by the asymmetric load drop method occurred at 1300 cycles. The specimen was sectioned longitudinally, lightly etched, gold plated, and examined in the SEM. Figure 58 shows the general microstructural appearance. The blocky carbide stringers and the grain boundary Laves phase are clearly evident, as are the small spherical precipitates. Figure 59(a) shows a crack along an apparent slip plane which is oriented 60° with respect to the applied load. Figure 59(b) is a magnified view of the edge of the crack. Figure 59(c) shows a crack running from the edge along a grain boundary oriented at 30° with respect to the applied

a. General Microstructure

b. Extrusion

Figure 56. SEM Micrograph, Extrusion after 800 Cycles - LCF Specimen 38

a. Blocky Carbide

b. Magnified View of Carbide

Figure 57. SEM Micrograph, Decohering Carbide after 800 Cycles - LCF Specimen 38

Figure 56. SEM Fractograph, Longitudinal Section after 2103 Cycles - LCF Specimen 39

a. Crack 1

Figure 59. SEM Micrograph, Cracks in Longitudinal Section after 2103 Cycles - LCF Specimen 39

b. Higher Magnification View of Crack 1

Figure 59 (continued)

c. Crack 2

stress. Note that as predicted by Kim and Laird, the crack is not symmetric with respect to the boundary, but propagates primarily in one grain (48). These cracks, as they progressed into the specimen, followed a path either along another slip plane in a grain or along a grain boundary, but not deviating by more than 15^{o} from a 45^{o} angle with respect to the applied stress. Blocky carbides di[illegible]em to be associated with crack propagation into the thickness.

iii. Proposed Mechanism

At 500^{o}F and within the total strain range 0.7-0.8%, this material can initiate cracks at persistent slip bands or at grain boundaries, whichever is energetically favorable. Generally, cracks initiate at blocky carbide inclusions in those grain boundaries oriented between 30^{o} and 60^{o} with respect to the principle tensile direction. The combination of a deformation zone along a grain boundary, as evidenced by the offsets of polishing scratches across the boundaries, and the tendency to develop grain boundary steps, as developed by Kim and Laird (47,48), results in large compatibility strains between the carbide and the grains which are relieved by the decohering of the carbide. This marks the start of Stage I propagation and is noted by the start of the asymmetric load drop-off. Once the crack begins to propagate along a grain boundary away from the carbide, it either continues growing along the boundary both on the surface and into the material, or it turns and begins to propagate along a favorably oriented persistent slip band which had already formed a crack embryo in the form of instrusions/extrusions. Since the strain range is fairly high, these nucleation events occur at multiple locations. Once these cracks begin to link up, the crack

grows more rapidly, leading to a much larger decrease in stress drop-off per cycle. The point at which this happens corresponds to N_i' in Table 9.

Thus, the carbides play a key role in the crack initiation process, but are not as important during crack propagation. Stage I cracking generally ends when the crack reaches the end of a grain or a grain boundary triple point in terms of through the thickness of the crack dimension.

The material is ductile enough so that Stage II cracking leads to the formation of fatigue striations. It is not surprising that the fracture surface shows both intergranular and transgranular cracking.

It is clear that after 800 cycles, well before the start of Stage I crack growth, substantial microstructural damage in the form of partially de-cohered carbides and persistent slip bands already exists. This information is crucial in evaluating the effects of the rejuvenation treatments.

IV. REJUVENATION EFFECTS

A. Results of HIP Treatments

i. Presentation of Data

The results of the 11 specimens, pre-damaged in LCF to a given number of cycles, hot isostatically pressed and heat treated, and then retested to failure, are summarized in Table 12. The plots of stress range vs cycles are contained in Figures 60-70. Specimen 16 was mechanically polished and electro-polished three times before retesting.

It is apparent from this data, in comparison with the baseline data of Table 9, that no rejuvenation by HIP occurred. The ceramic

TABLE 12

SUMMARY OF HIP REJUVENATION ON LCF PROPERTIES

Specimen	Prior Damage Cycles	Strain Range (%)			Stress Range (ksi)	Cycles			N_i/N_f	N_i'/N_f	Remarks
		$\Delta\varepsilon_t$	$\Delta\varepsilon_p$	$\Delta\varepsilon_e$		N_i	N_i'	N_f			
14	800	0.73	0.02	0.71	196.0	801	1750	2297	0.35	0.76	
16	800	0.73	0.03	0.70	193.0	1350	1800	2134	0.63	0.84	Electro-polished
18	800	0.72	0.03	0.69	189.0	1750	2250	2619	0.67	0.86	
19	800	0.76	0.05	0.71	195.5	1450	1650	1933	0.75	0.85	
20	800	0.73	0.02	0.71	194.8	1750	2350	3147	0.56	0.75	Coated
21	800	0.74	0.02	0.72	200.0	1150	1450	1797	0.64	0.81	Coated
22	800	0.76	0.05	0.71	197.0	1400	1700	2287	0.61	0.74	Coated
23	2100	0.76	0.05	0.71	195.0	2650	2950	3286	0.81	0.90	Coated
24	2100	0.70	0.04	0.66	186.5	801	2900	3862	0.21	0.75	
25	0	0.68	0.03	0.65	179.4	700	950	1573	0.45	0.60	Coated
29	0	0.77	0.04	0.73	202.0	900	1250	1660	0.54	0.75	

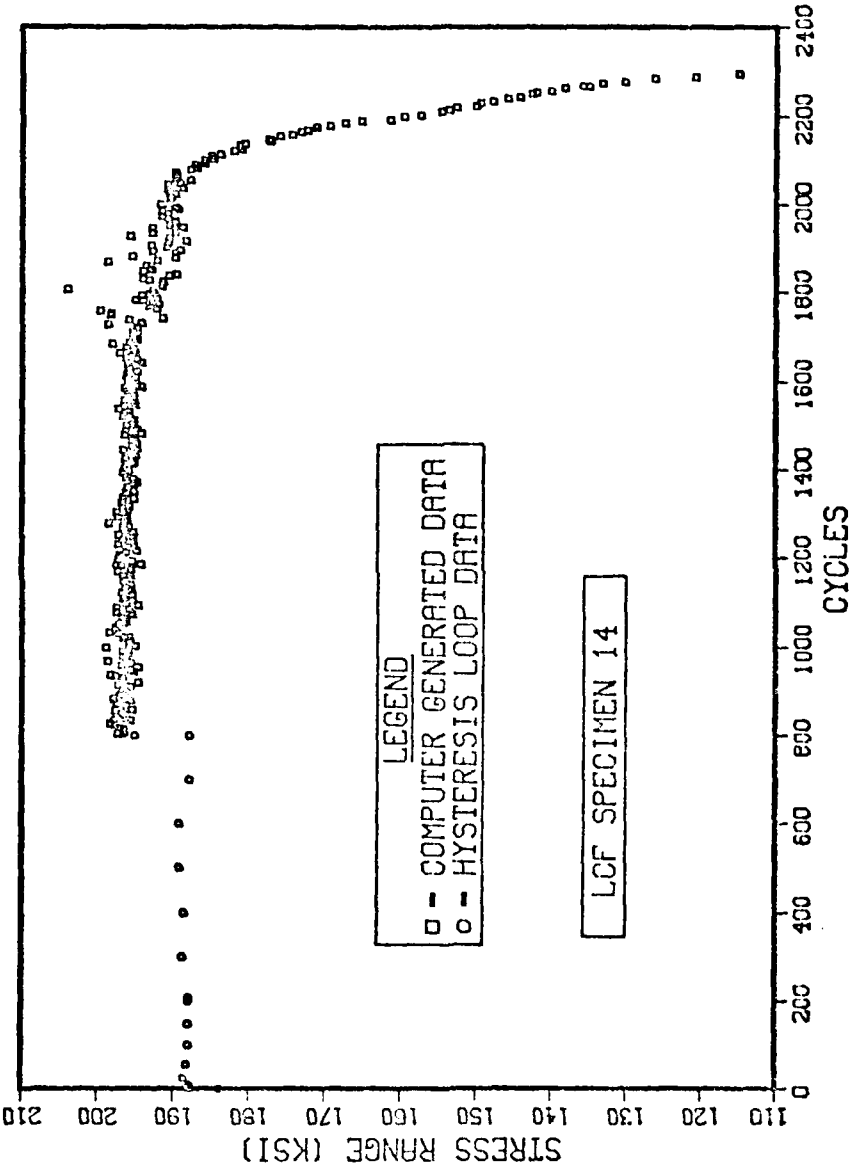

Figure 60. Plot of Stress Range vs Cycles - LCF Specimen 14

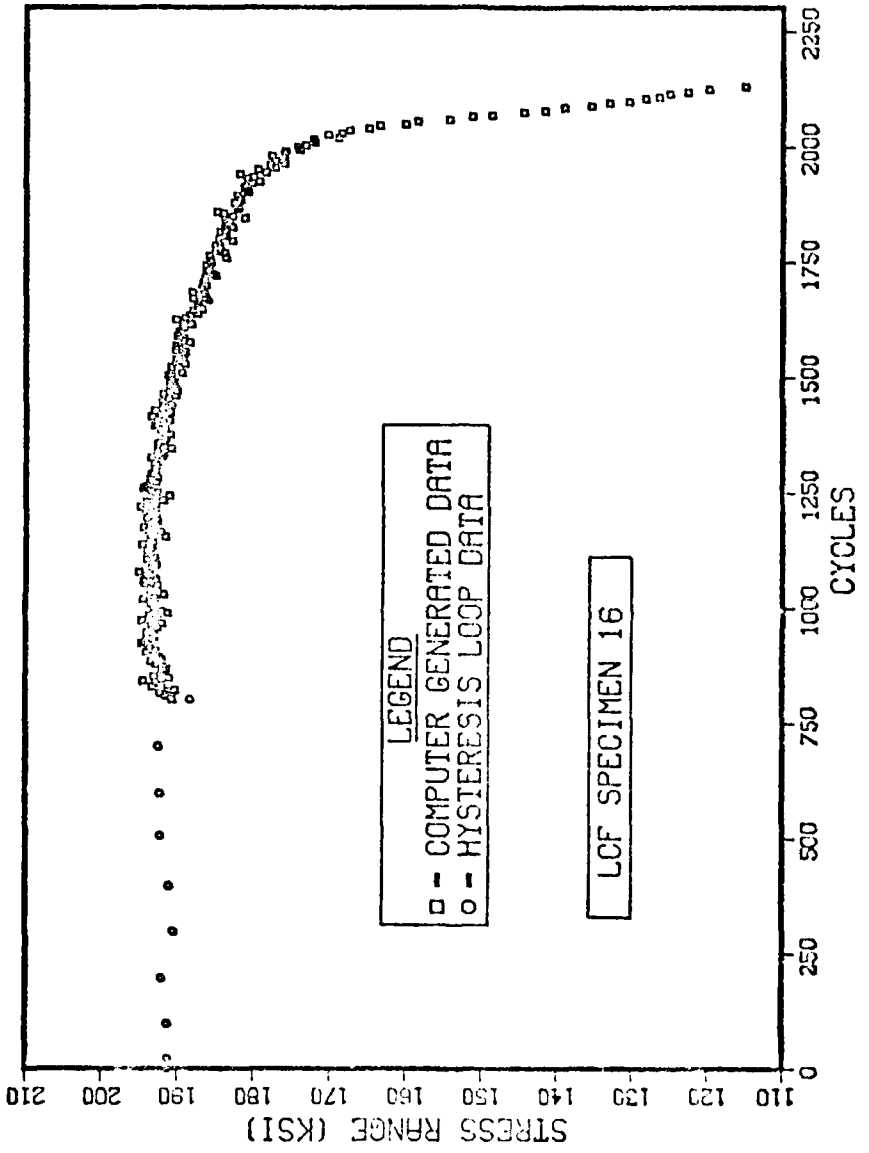

Figure 61. Plot of Stress Range vs Cycles - LCF Specimen 16

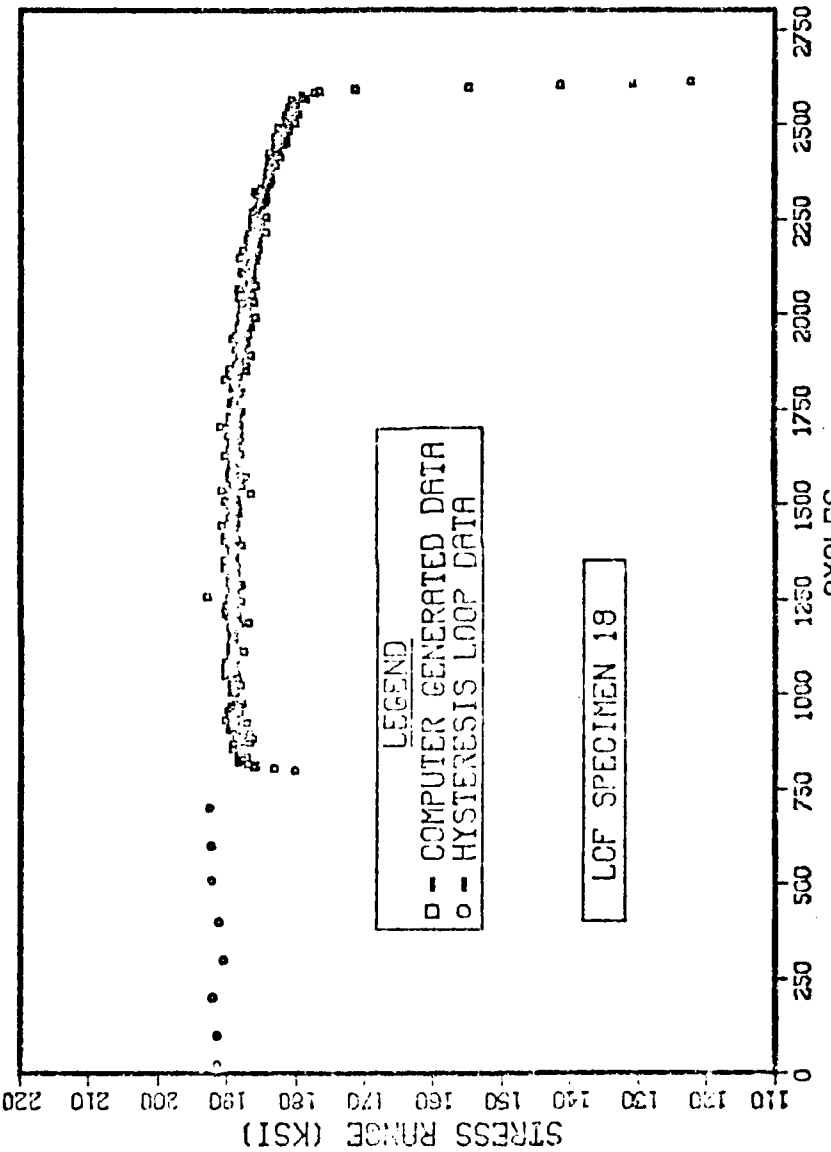

Figure 62. Plot of Stress Range vs Cycles - LCF Specimen 18

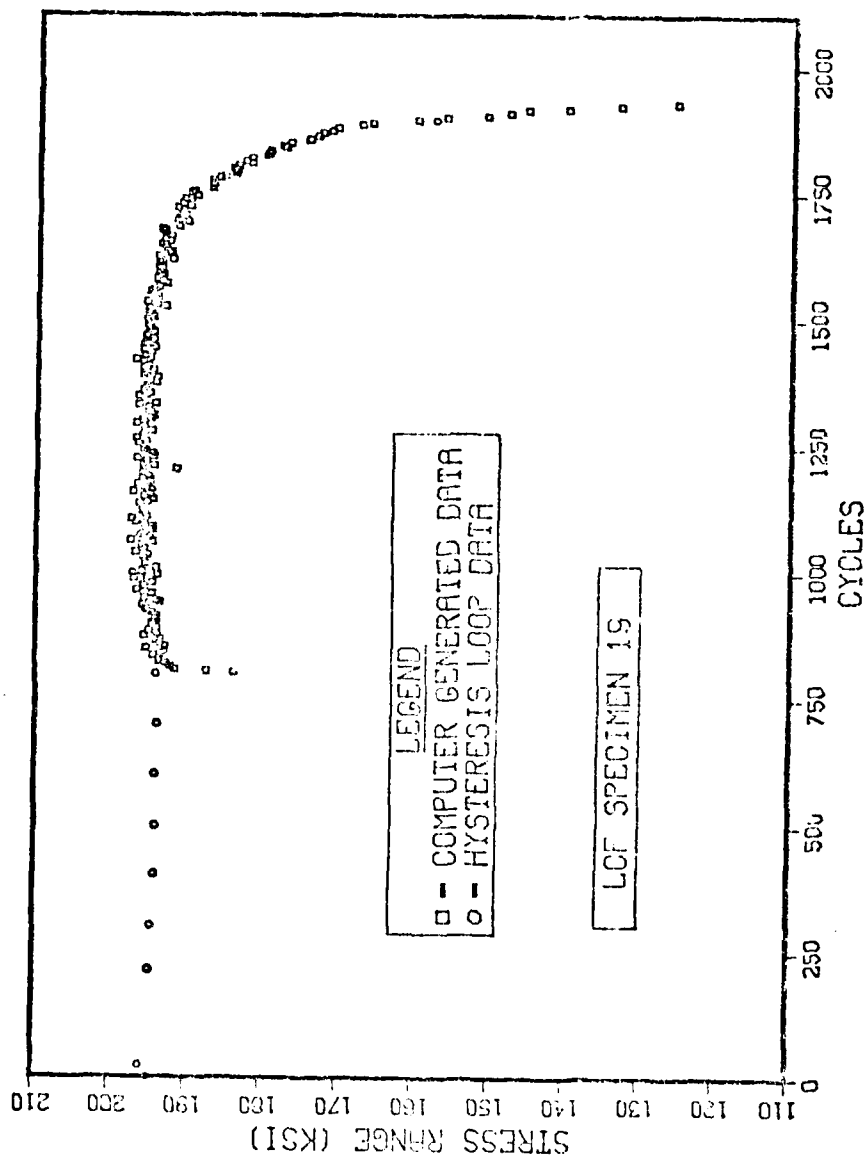

Figure 63. Plot of Stress Range vs Cycles - LCF Specimen 19

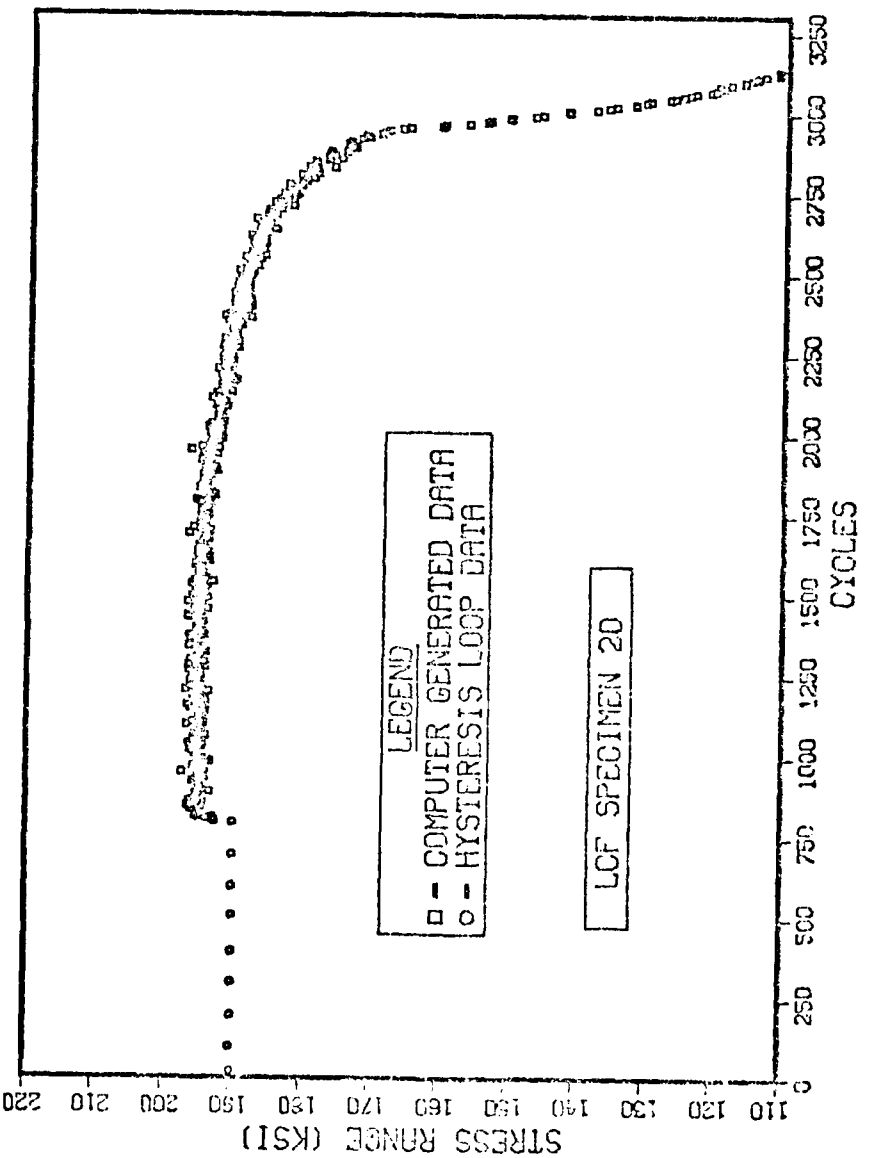

Figure 64. Plot of Stress Range vs Cycles - LCF Specimen 20

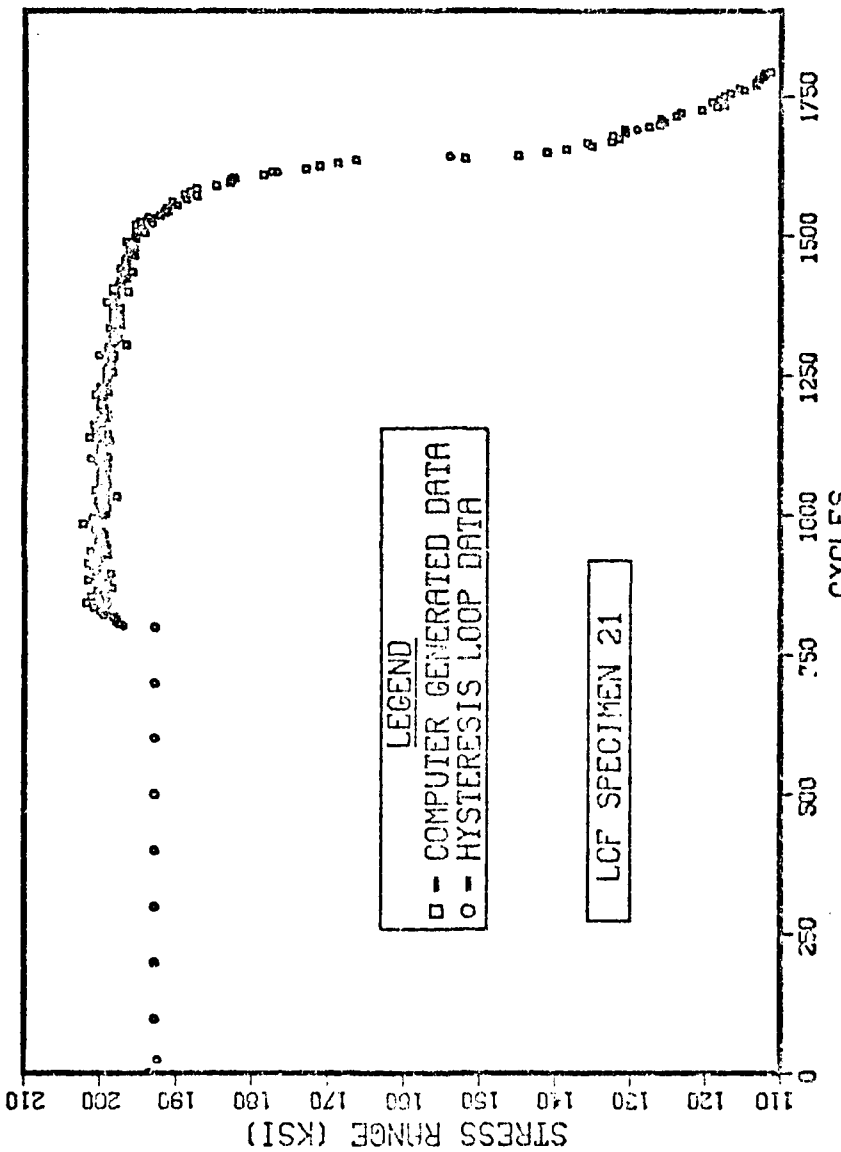

Figure 65. Plot of Stress Range vs Cycles - LCF Specimen 21

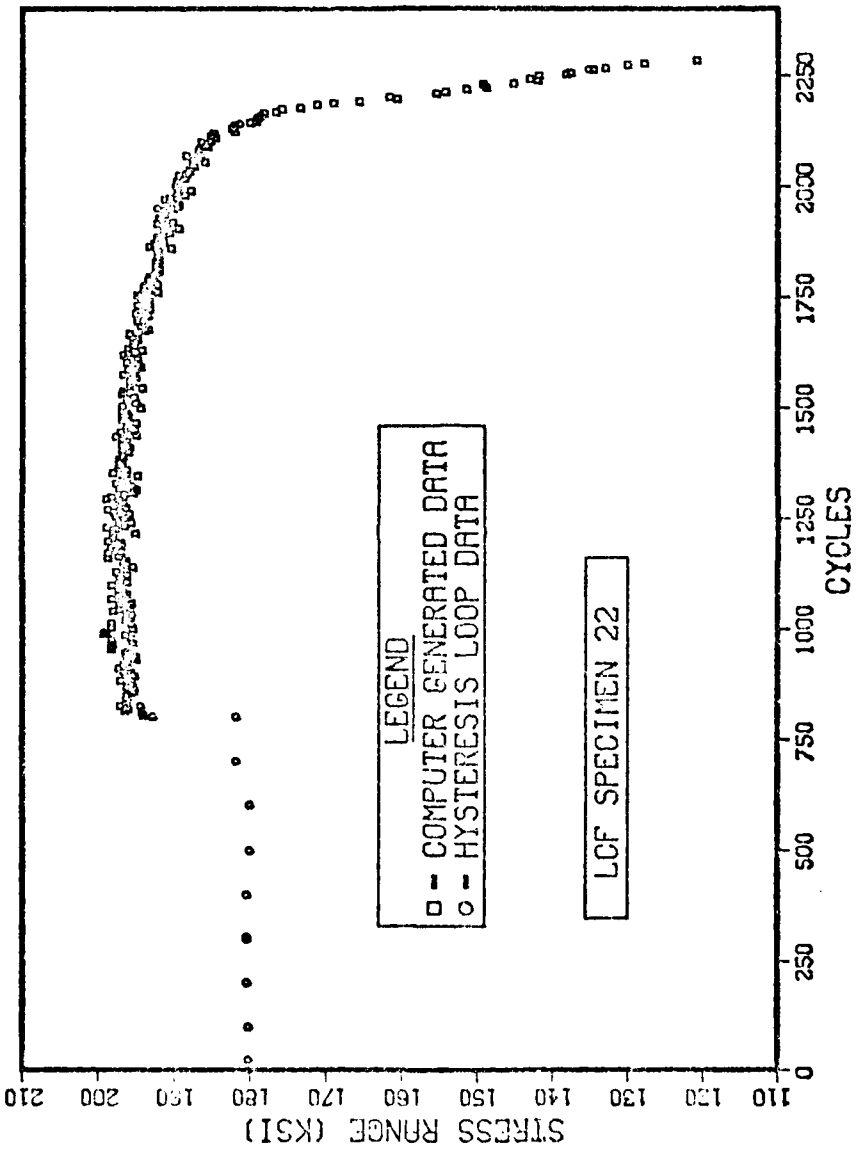

Figure 66. Plot of Stress Range vs Cycles - LCF Specimen 22

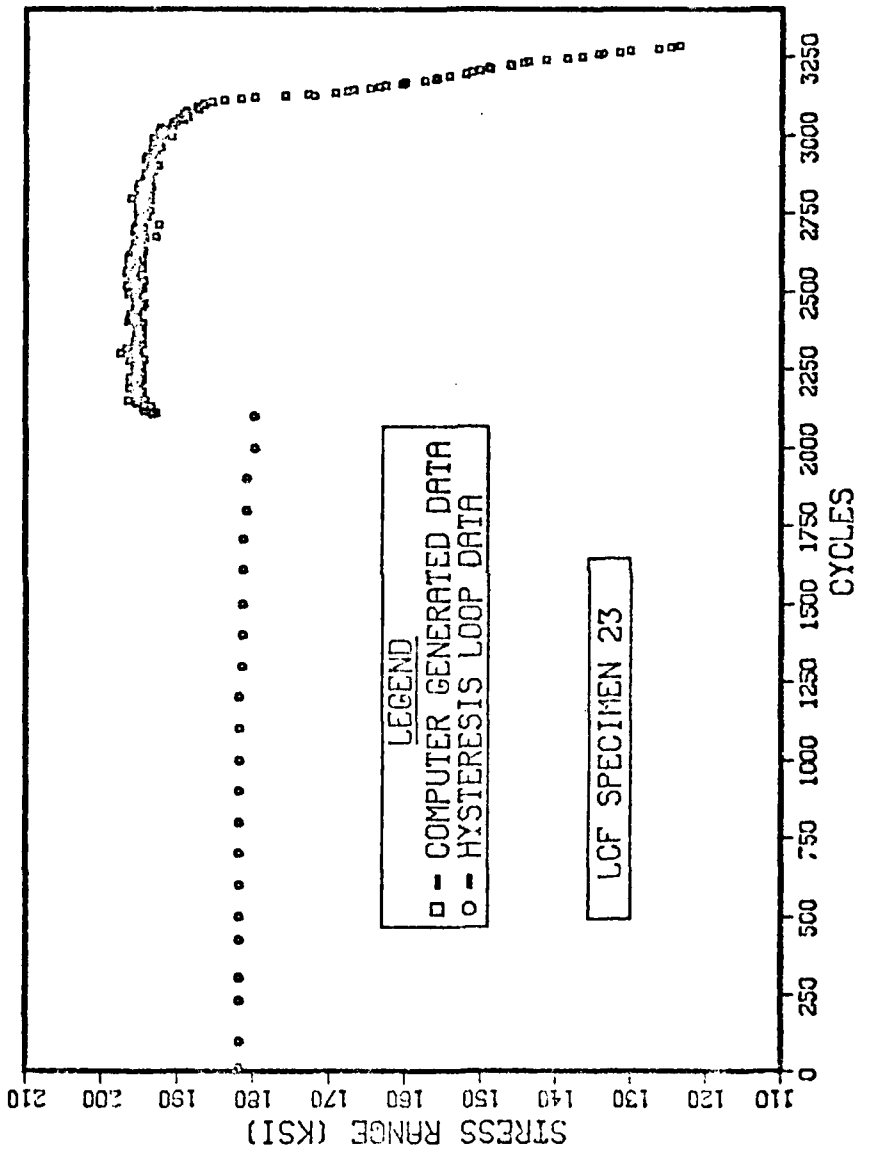

Figure 67. Plot of Stress Range vs Cycles - LCF Specimen 23

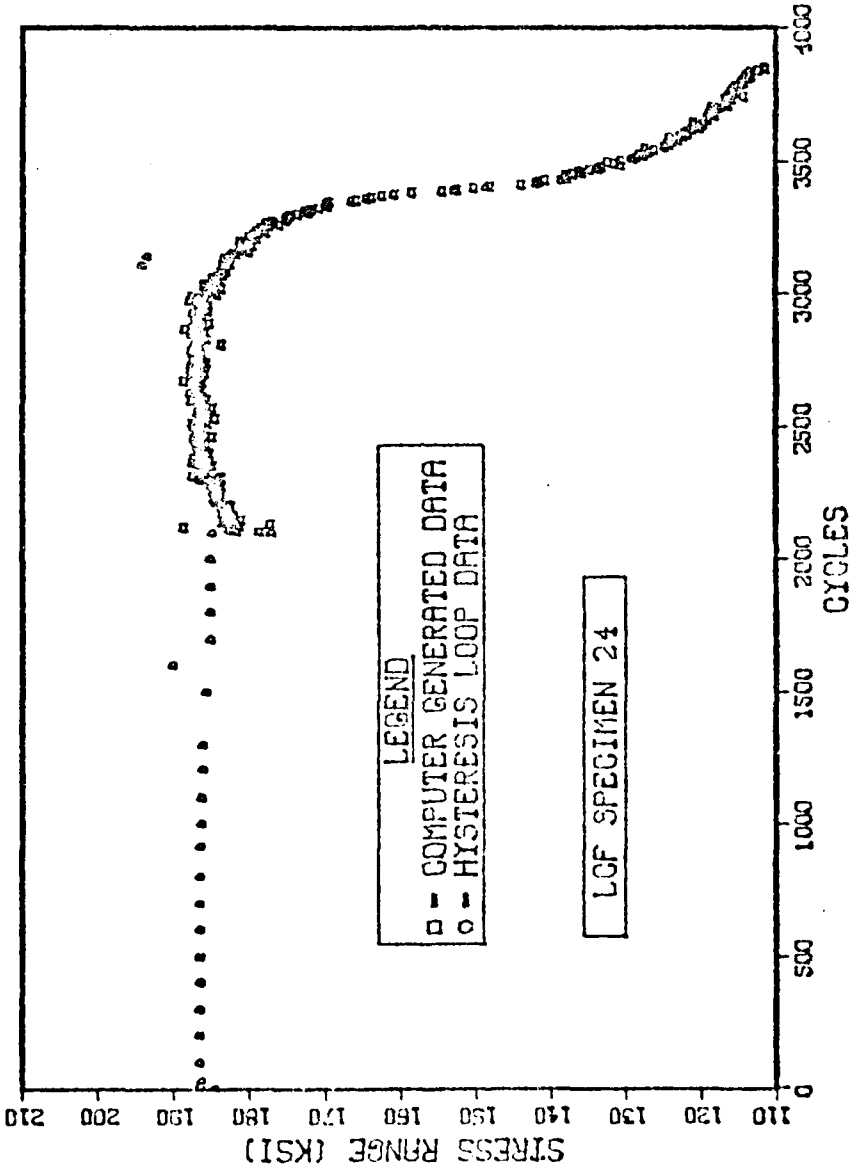

Figure 68. Plot of Stress Range vs Cycles - LCF Specimen 24

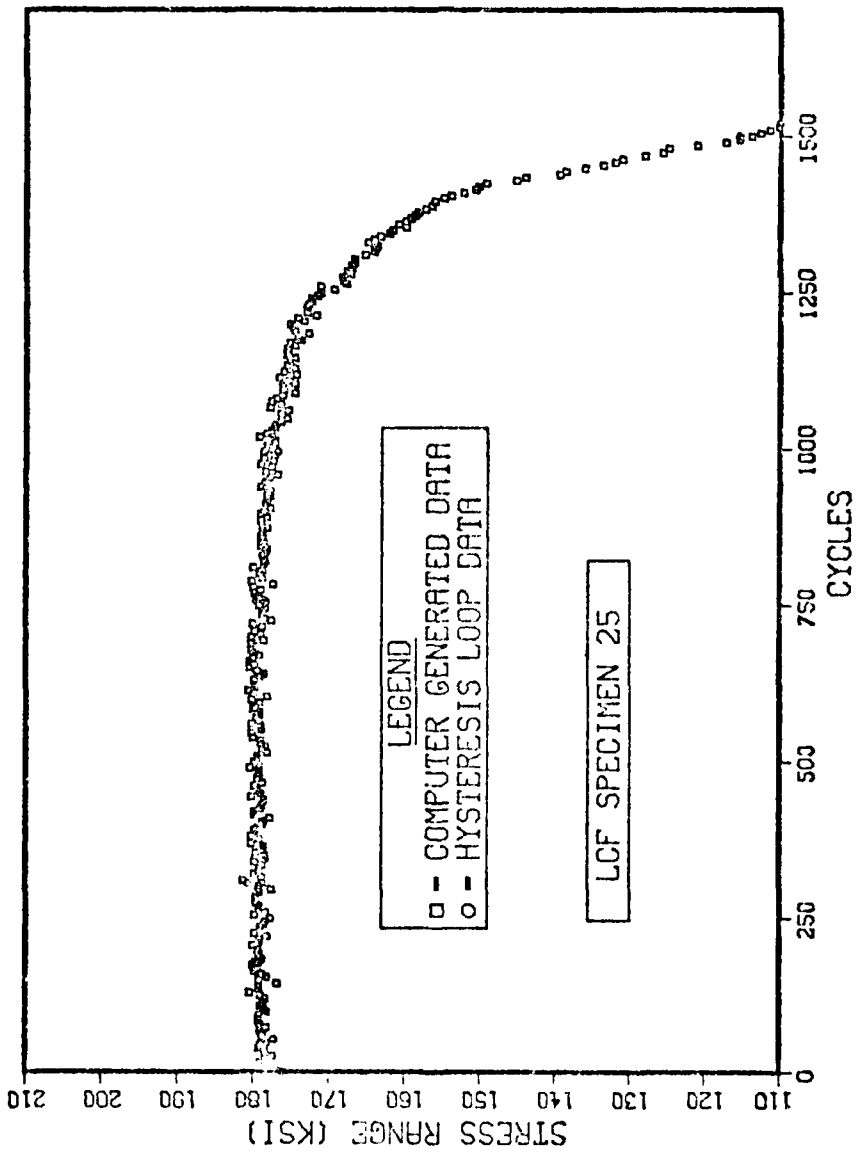

Figure 69. Plot of Stress Range vs Cycles - LCF Specimen 25

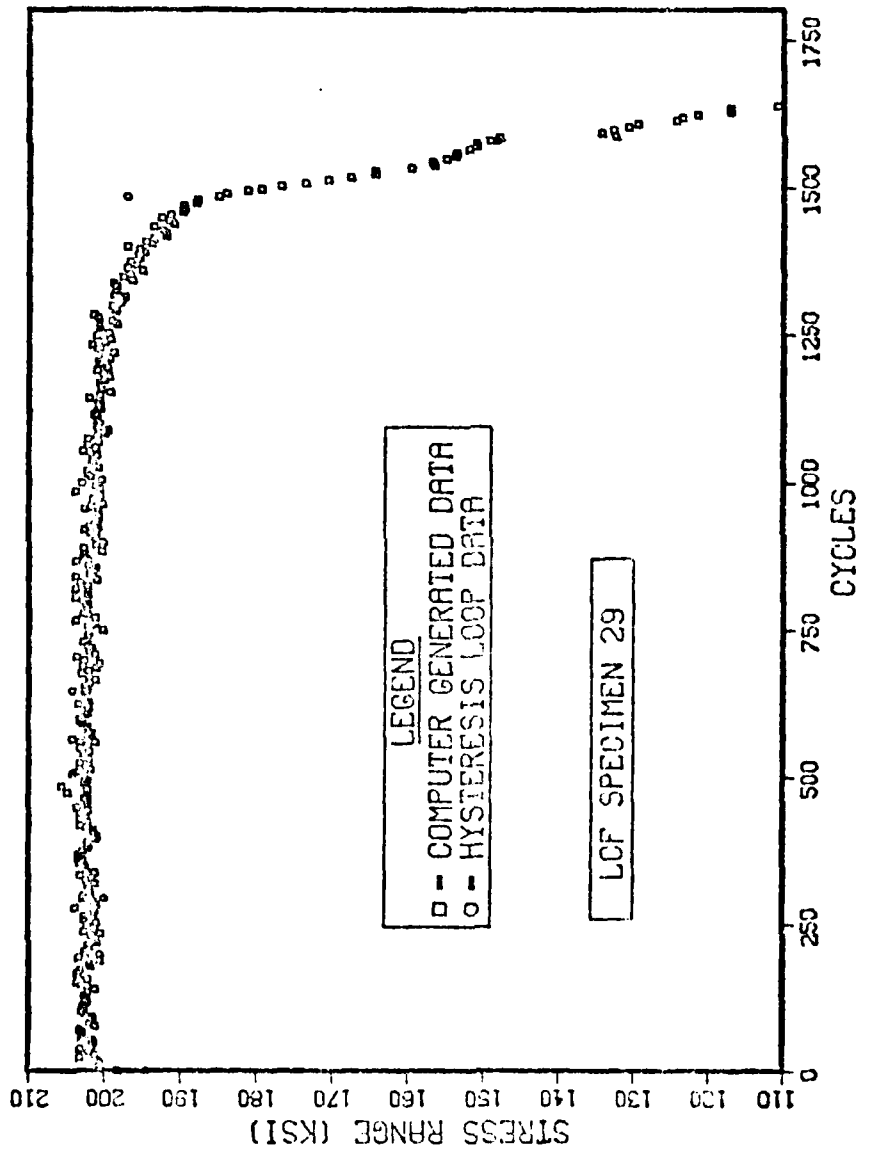

Figure 70. Plot of Stress Range vs Cycles - LCF Specimen 29

coated and the uncoated specimens performed about the same; although Specimen 20, which was coated, performed the best. On the basis of total life, these HIP specimens were clearly inferior to the baseline specimens. Specimens 25 and 29, which were HIP'd without prior damage, failed within the range of about 1600-1700 cycles. The remaining HIP'd specimens with different levels of pre-HIP damage also failed within this range of cycles after retesting commenced, regardless of the level of pre-HIP damage. This includes two specimens which were predamaged to 2100 cycles; crack initiation had already occurred in these specimens prior to the HIP treatment. This is strong evidence that the HIP processing itself adversely damaged the microstructure at the surface of the material.

Those specimens which were to be ceramic coated were first vapor honed to provide a suitable surface for the coating to adhere to. The effect of the vapor honed surface on the LCF properties was investigated. Figure 71 shows a SEM photomicrograph of the as-vapor-honed surface. The surface is fairly rumpled and some inclusions appear to have already decohered from the microstructure. The gauge section of two vapor-honed specimens was repolished and then tested at 500°F. The Stress Range vs Cycles for these specimens, Specimens 27 and 28, are shown in Figures 72 and 73. Table 13 is a summary of the LCF data. It is clear that vapor honing, even after repolishing, was deleterious to the fatigue life. During repolishing, the diameter was reduced from 0.118 in. to about 0.116 in., or by 25 μ (about one-fifth of a grain diameter) along the specimen radius. Specimen 28, after testing, was placed in the SEM. In addition to the main crack, extensive cracking along the gage

TABLE 13

EFFECT OF VAPOR HONING ON LCF PROPERTIES

Specimen	Strain Range (%)			Stress Range (ksi)	Cycles				
	$\Delta\varepsilon_t$	$\Delta\varepsilon_p$	$\Delta\varepsilon_e$		N_i	N_i'	N_f	N_i/N_f	N_i'/N_f
27	0.81	0.06	0.75	205.0	900	1200	1505	0.60	0.80
28	0.76	0.04	0.72	198.0	1100	1850	1995	0.55	0.93

Figure 71. SEM Micrograph, As-Vapor-Honed Surface - LCF Specimen 55

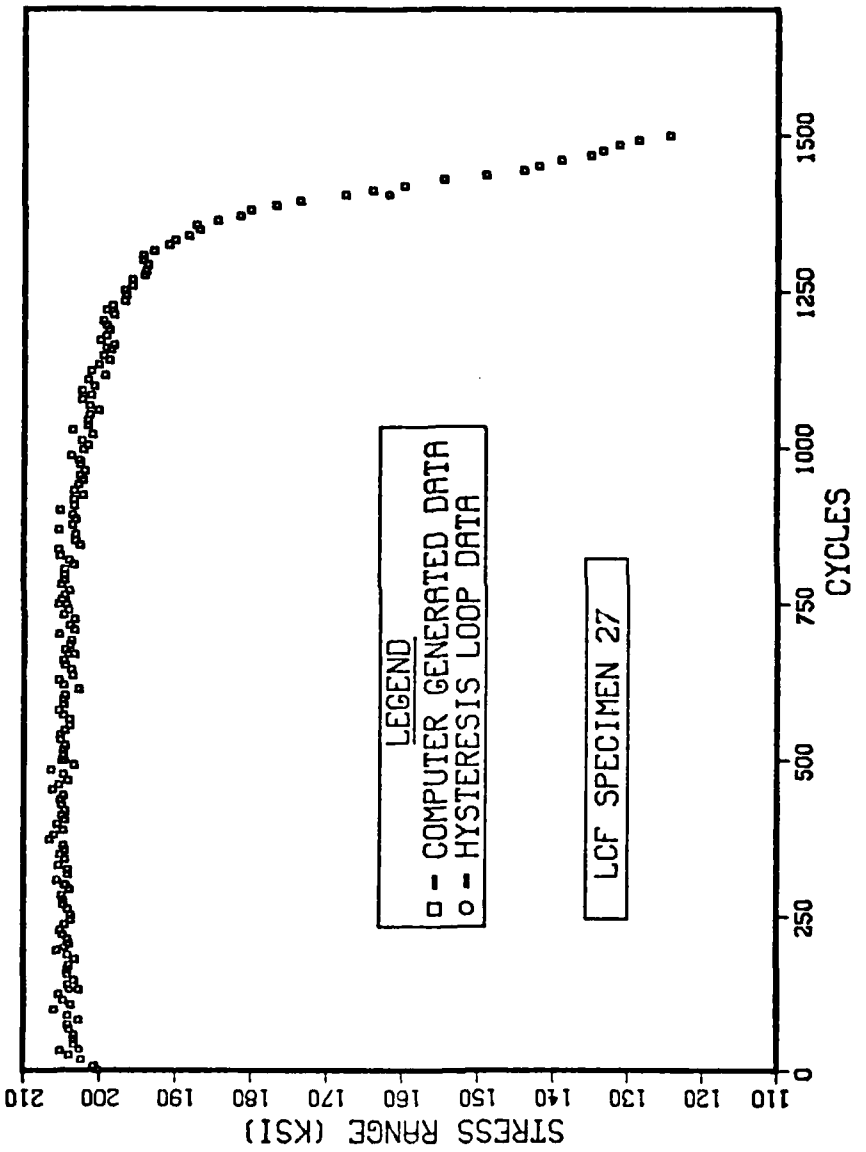

Figure 72. Plot of Stress Range vs Cycles - LCF Specimen 27

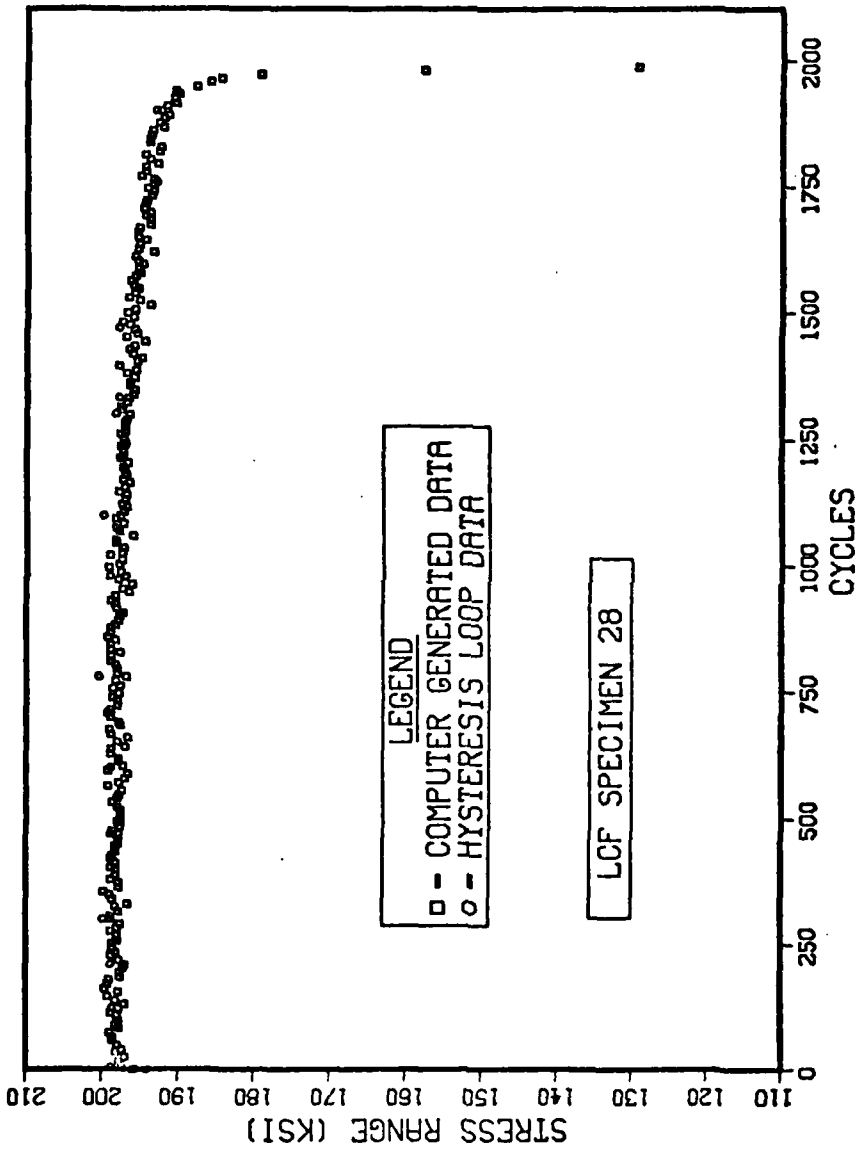

Figure 73. Plot of Stress Range vs Cycles - LCF Specimen 28

length was observed. Typical examples of secondary cracks are shown in Figures 74, 75, and 76. All three of these cracks seem to be associated with inclusions which have decohered, cracked, or fallen out.

There was a reaction between the ceramic coating and the base material during HIPing. Figure 77 shows a typical reaction zone from LCF Specimen 20. This reaction was observed in the shank region, above the extensometer flange. It is assumed a similar reaction occurred in the gauge section. The apparent penetration depth of the reaction zone was at least 5 μ. This zone should have been removed during the polishing operation prior to retesting. However, the grain boundaries may have been damaged to much greater penetration depths by alloy depletion. Greater material removal than that accomplished by repolishing was deemed unwise due to the already small specimen diameter.

Figure 78 shows some fractographs taken of ceramic-coated LCF Specimen 25. The fracture appears much more intergranular in nature than for the baseline specimens.

Crack growth rate in another ceramic-coated specimen, LCF Specimen 21, was also measured by the surface replication technique. Photomicrographs of the replicas are shown in Figure 79. The plot of Crack Length vs Cycles is contained in Figure 80. Extrapolation of the crack length to zero shows that initiation occurred between 1100 and 1200 cycles. This agrees with the asymmetric load drop-off point, N_1, in Table 12 of 1150 cycles. Note that the slope of this curve is about 1.5 μm/cycle. This is 5.5 times the slope of the two baseline specimens plotted in Figures 45 and 47. Thus, the crack growth rate was greatly accelerated in the HIP rejuvenated specimen.

a. Low Magnification View of Crack

b. High Magnification View of Crack

Figure 74. SEM Micrograph, Secondary Cracking - LCF Specimen 28

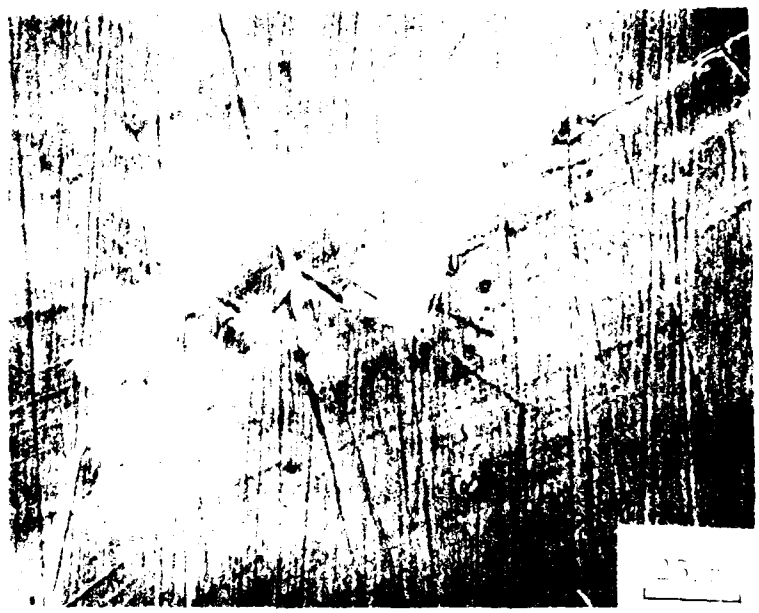

a. General Crack

b. Higher Magnification View of Crack

Figure 75. SEM Micrograph, Secondary Cracking - LCF Specimen 28

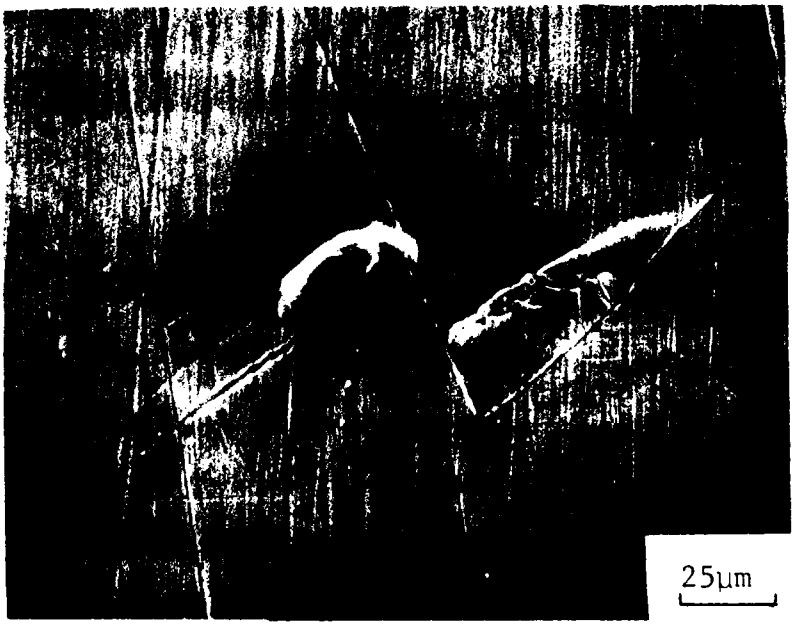

Figure 76. SEM Micrograph, Secondary Cracking - LCF Specimen 28

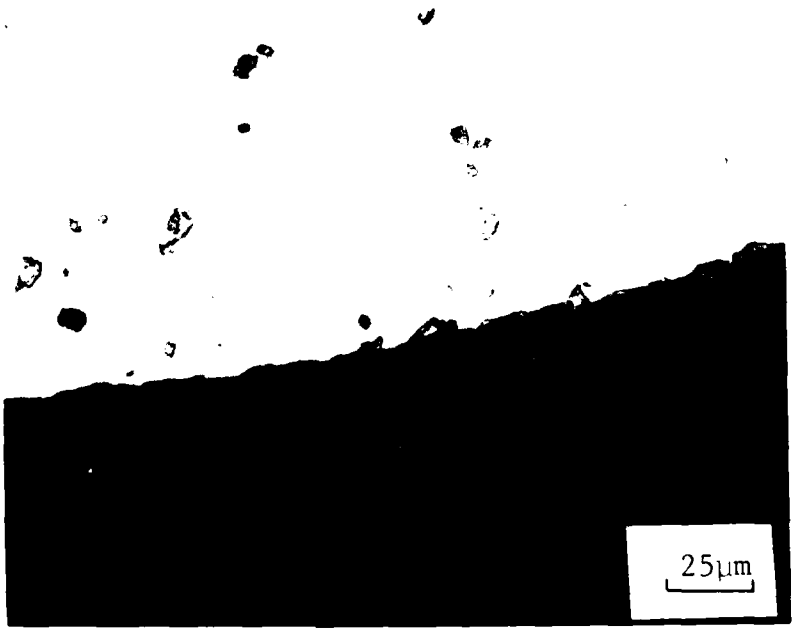

a. General Area

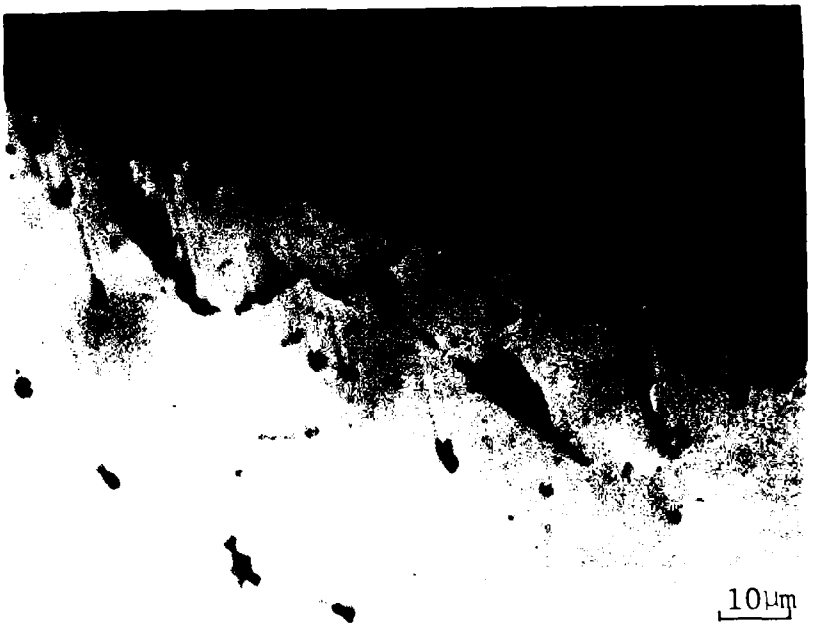

b. Higher Magnification of Reaction Zone

Figure 77. Micrograph, Coating Reaction

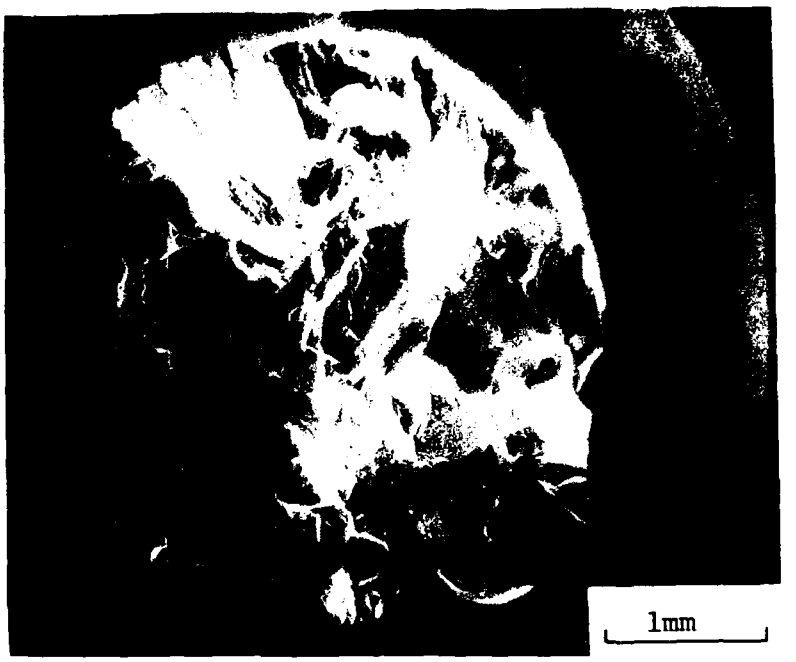

a. Fractograph

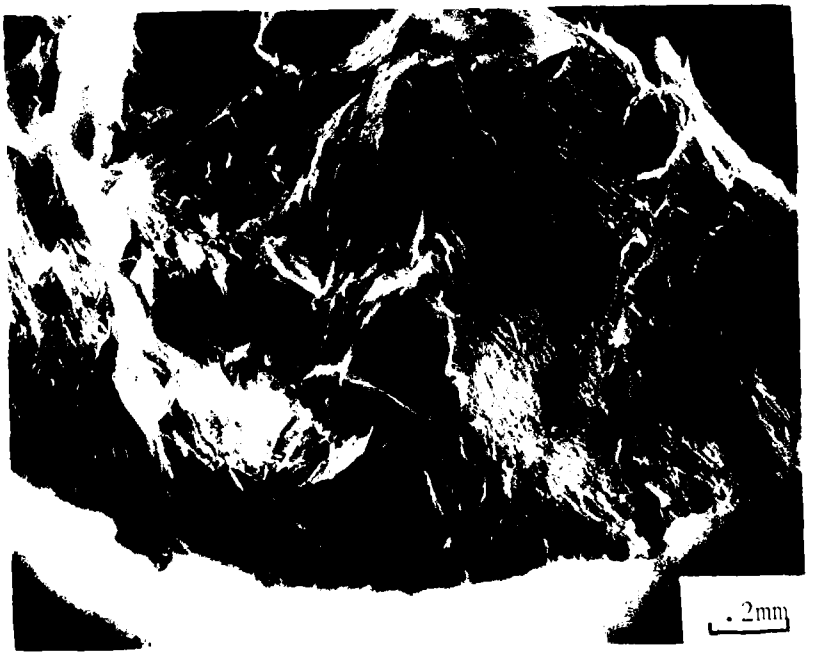

b. Possible Crack Initiation Area

Figure 78. SEM Fractography - LCF Specimen 25

Figure 79. Micrographs of Replicas, Cracks - LCF Specimen 21

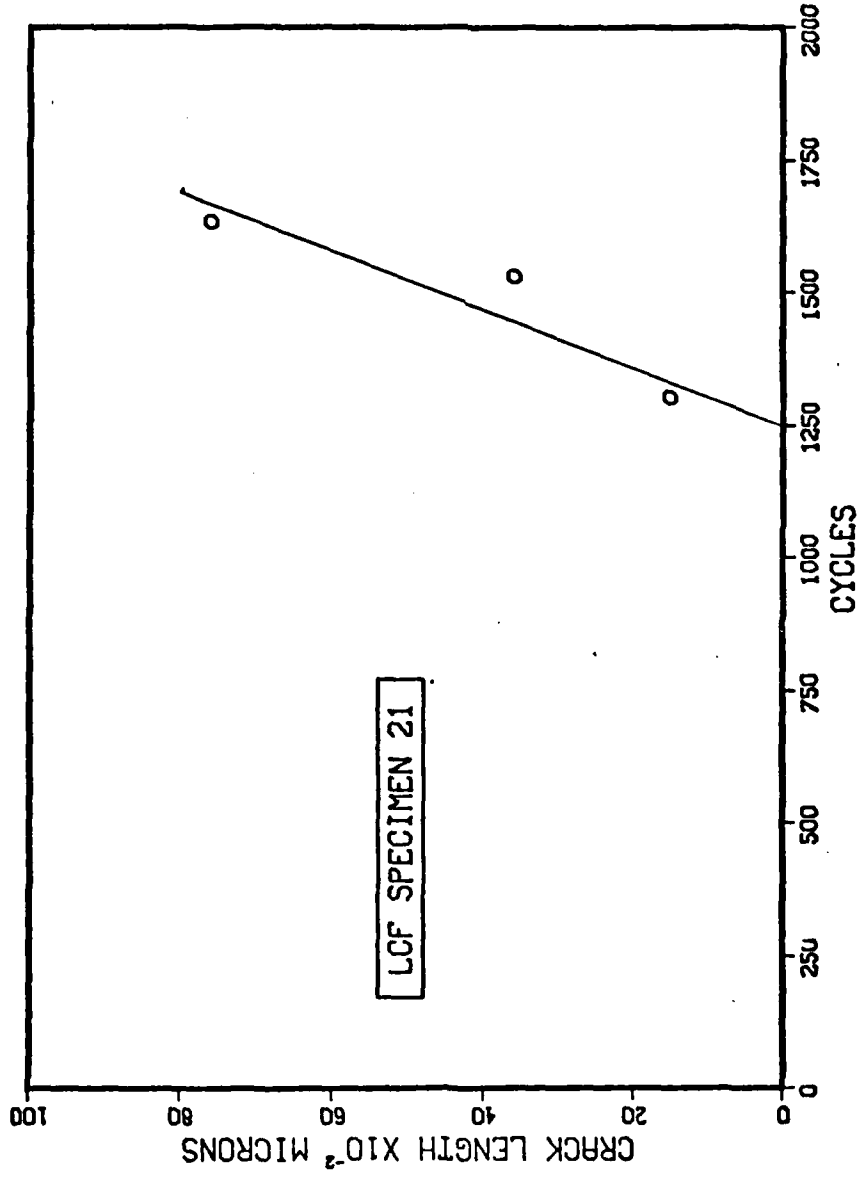

Figure 80. Plot of Crack Length vs Cycles - LCF Specimen 21

The uncoated specimens were badly contaminated after HIP processing. Figure 81 shows the reaction zone for LCF Specimen 26. The apparent reaction zone is 5-10 μ in depth. After HIP processing, alloy depletion along the grain boundaries to much greater depths has been observed in IN-713 (54). Thus, even after repolishing, the grain boundaries were still substantially weakened compared to the baseline. Figure 82 contains SEM photomicrographs of the primary crack in LCF Specimen 16. This crack had progressed completely around the circumference of the specimen. No baseline specimen had a complete circumferential crack, but it was not unusual for the HIP processed specimens (both coated and bare) to have one. Note that the crack in Figure 82(a) is both intergranular and transgranular. The role of a fractured blocky carbide in promoting cracking is graphically shown in Figures 82(b) and (c). Cracking throughout the gauge length was extensive. Figure 83 shows a typical intergranular crack located at some distance from the main crack. The fracture appearance for the uncoated specimens was very similar to that of the coated specimens.

HIP processing increased the material grain size from 120 μm to 150 μm. It is known that LCF life is usually sensitive to grain size. Merrick found an inverse relationship between grain size and fracture life for two different grain sizes at room temperature and at 1000°F (16). Handbook data at room temperature for three grain sizes also shows an inverse relationship with fracture life for stress-controlled tests (43). When this data is plotted, it is apparent that the relationship follows a Hall-Petch dependency:

$$N_f \propto \frac{1}{\sqrt{g.s.}} \qquad (18)$$

a. Surface Contamination, Area 1

b. Surface Contamination, Area 2

Figure 81. Micrograph, Surface Oxidation - LCF Specimen 26

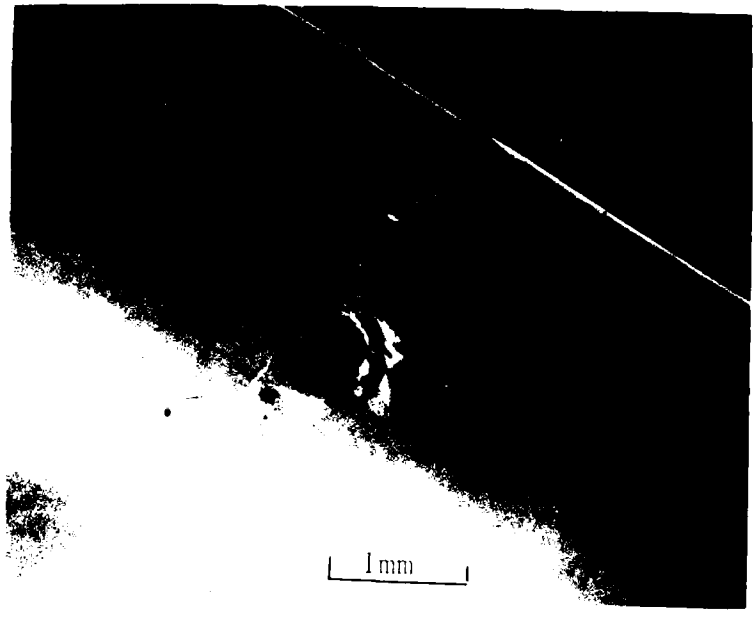

a. Main Crack

b. Magnification of Center Portion of Crack

Figure 82. SEM Micrographs, Main Crack - LCF Specimen 16

Figure 82 (continued)

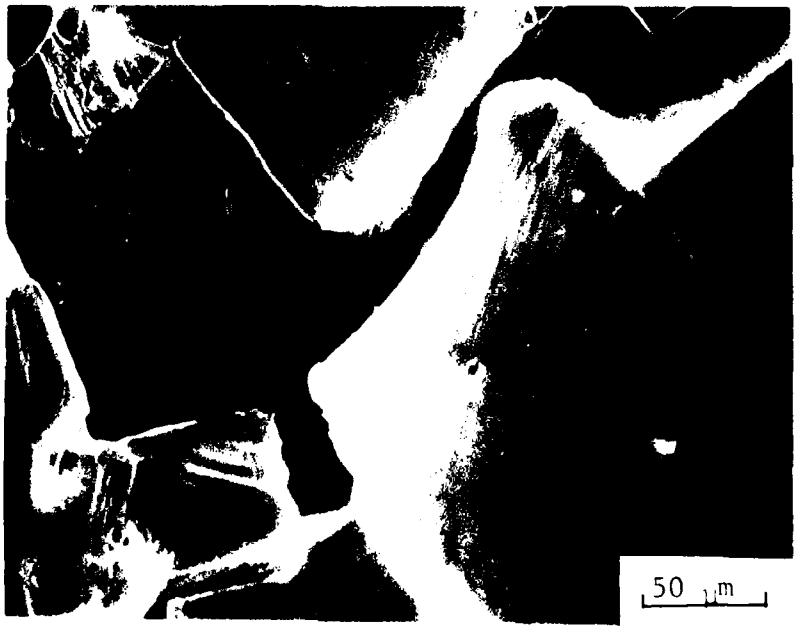

c. Possible Carbide Pullout

Figure 83. SEM Micrographs, Secondary Cracking - LCF Specimen 16

where N_f is the cycles to failure, and g.s. is the grain size. Thus, the effect of increased grain size from the rejuvenation processing on the cycles to failure can be estimated:

$$N_{f_2} = N_{f_1} \times \frac{\overline{g.s._1}}{g.s._2} \tag{19}$$

Using Equation 18, a decrease in cycles to failure of 12% can be estimated to be due to the grain size changes alone.

iii. Mechanisms

Considering the data presented in Tables 12 and 13, the fatigue behavior for the HIP'd specimens (both coated and uncoated) and the vapor-honed specimens is similar. But the mechanisms of crack nucleation and growth are most likely not the same. Recall that the previous section demonstrated that the critical step for crack initiation in the baseline specimens was the decohering of a grain boundary carbide. Clearly, vapor honing, even with repolishing, can decohere or fracture carbides. This not only would greatly shorten the initiation time, but would provide many crack initiation sites. Thus, once crack growth began, it would progress very rapidly due to microcrack linkup. This is what was observed for the vapor-honed specimens,

The ceramic coating reacts with the matrix during HIP processing. Even though optical microscopy showed that the reaction depth was such that it should be removed by repolishing, localized contamination along the grain boundaries and existing persistent slip bands can be substantially greater. This would promote the early intergranular failure as was observed. This investigation is inconclusive, however,

in differentiating between the damage due to vapor honing and the damage due to contamination by the ceramic coating.

The uncoated specimens had contaminated grain boundaries which were relatively weak. Thus, the carbides readily decohered and crack propagation was fairly rapid.

B. Results of Thermal Treatments

1. Presentation of Data

The results of seven thermally rejuvenated specimens are contained in Table 14. A comparison of this data with the baseline data (Table 9) and the HIP rejuvenated data (Table 12) reveals that some rejuvenation definitely occurred as a result of the thermal treatment. The plots of Stress Range vs Cycles are contained in Figures 84-90. Note that LCF Specimen 13 was heat treated in a poor vacuum and, as a result, the surface was badly oxidized. It was tested without repolishing. The remaining specimens, except for LCF Specimen 54, were all repolished after thermal treatment.

An investigation was made to determine the effect of repolishing alone on enhancing the fatigue properties. A summary of the data is contained in Table 15. The plots of Stress Range vs Cycles are shown in Figures 91 and 92. These data are essentially no different than the baseline properties. Also, since LCF Specimen 54 was not repolished after the thermal treatment and yet was clearly rejuvenated, it can be concluded that repolishing alone does not recover LCF damage for the conditions studied in this investigation.

Table 14 indicates that complete recovery of LCF damage was not accomplished. But, it was previously shown that after 800 cycles,

Specimen	Heat Treatment (°C)	Strain Range (%)			Stress Range (ksi)	Cycles				
		$\Delta\varepsilon_t$	$\Delta\varepsilon_p$	$\Delta\varepsilon_e$		N_i	N_i'	N_f	N_i/N_f	N_i'/N_f
13*	800	0.79	0.07	0.72	198.0	1650	2100	2504	0.66	0.84
34	400	0.75	0.05	0.70	194.5	1800	2700	3333	0.54	0.81
35	800	0.74	0.03	0.71	194.0	1800	3900	5384	0.33	0.72
42	803	0.74	0.02	0.72	197.6	1800	3300	4134	0.44	0.80
43	803	0.75	0.02	0.73	200.5	2000	2650	2890	0.69	0.92
51	803	0.72	0.02	0.70	194.0	1700	3700	4475	0.38	0.83
54**	803	0.75	0.04	0.71	194.2	1900	3200	4106	0.46	0.78

*Heat treated in a poor vacuum

**Retested without repolishing

TABLE 15

SUMMARY OF REPOLISHING ON LCF PROPERTIES

Specimen	Prior Damage Cycles	Strain Range (%)			Stress Range (ksi)	Cycles				
		$\Delta\varepsilon_t$	$\Delta\varepsilon_p$	$\Delta\varepsilon_e$		N_i	N_i'	N_f	N_i/N_f	N_i'/N_f
38	803	0.76	0.05	0.71	196.0	1575	2700	3562	0.44	0.76
40	803	0.73	0.02	0.71	194.5	1300	2800	3206	0.41	0.87

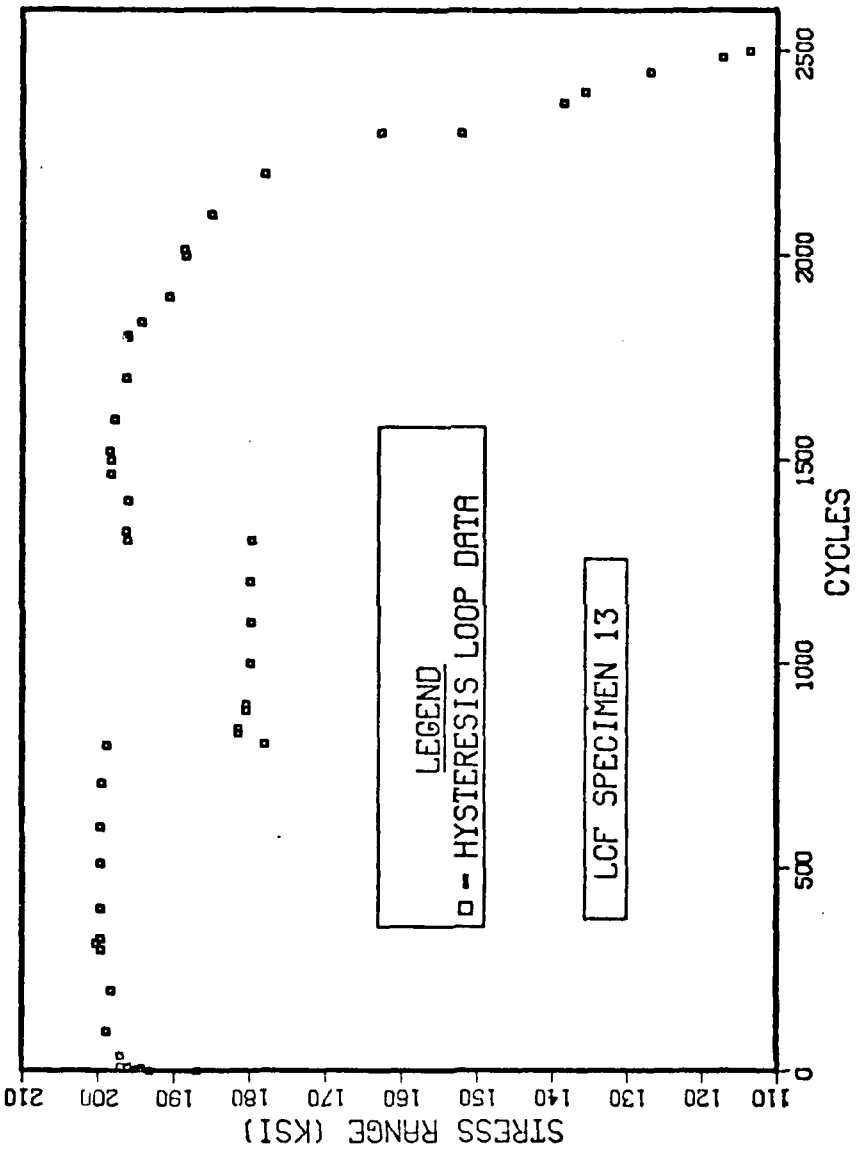

Figure 84. Plot of Stress Range vs Cycles - LCF Specimen 13

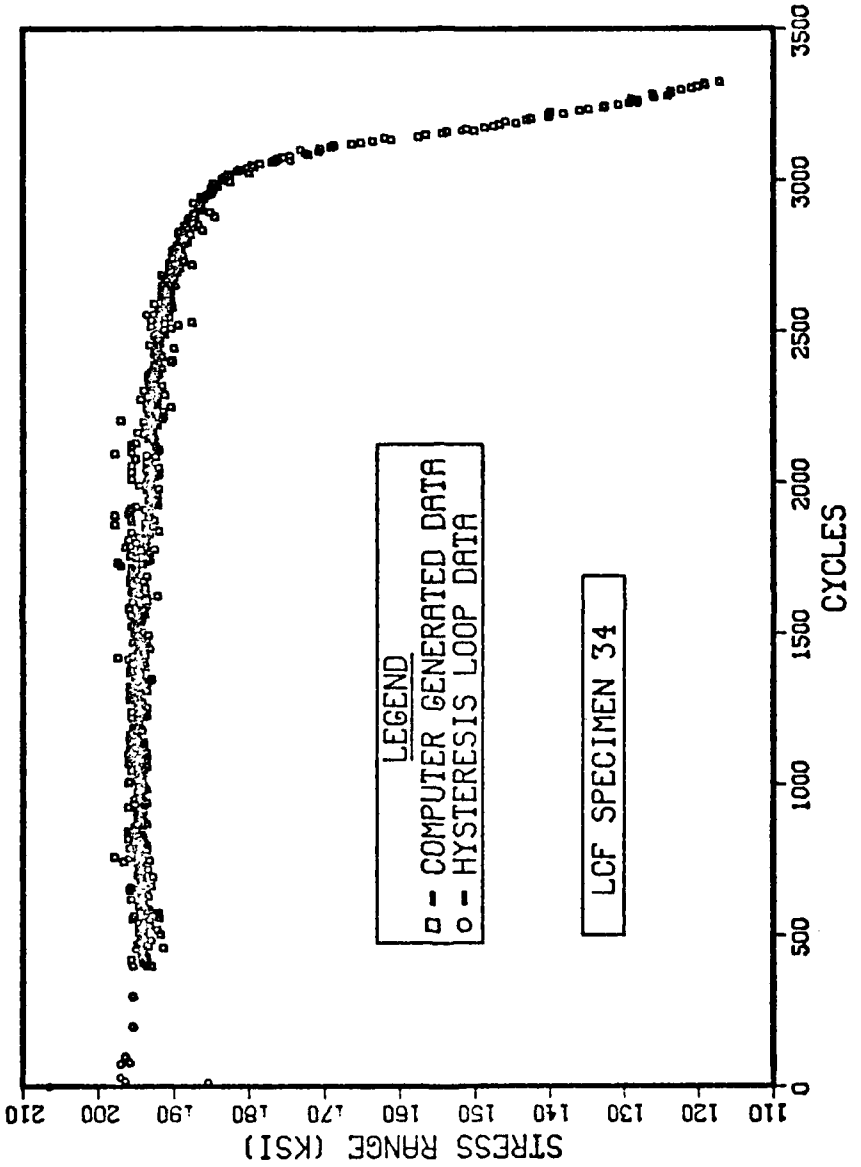

Figure 85. Plot of Stress Range vs Cycles - LCF Specimen 34

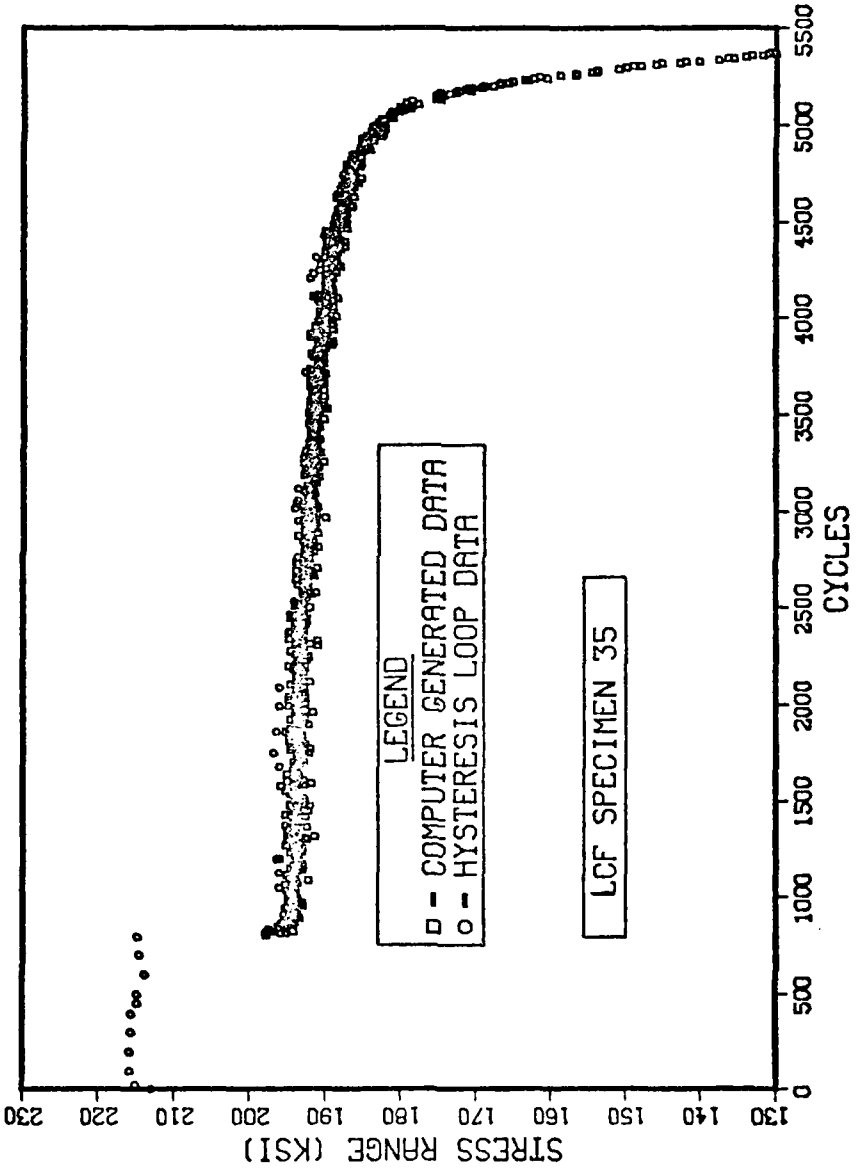

Figure 86. Plot of Stress Range vs Cycles - LCF Specimen 35

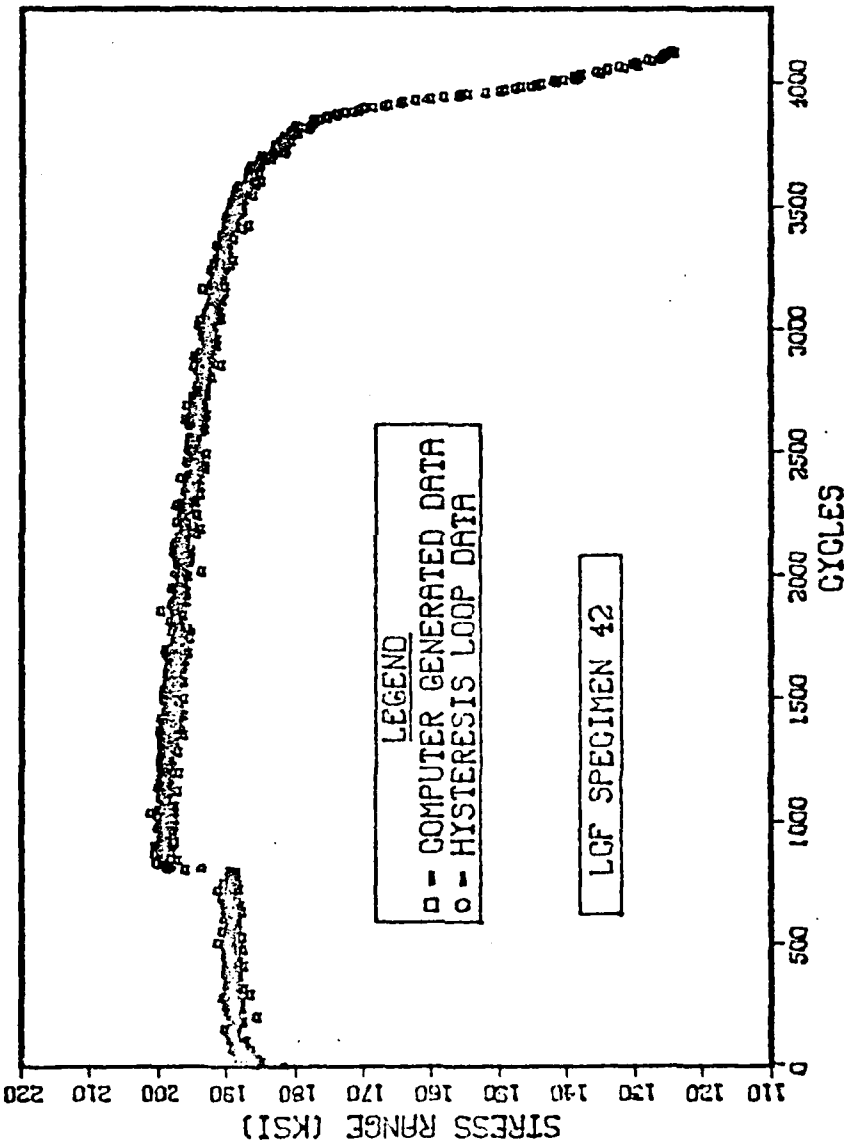

Figure 87. Plot of Stress Range vs Cycles - LCF Specimen 42

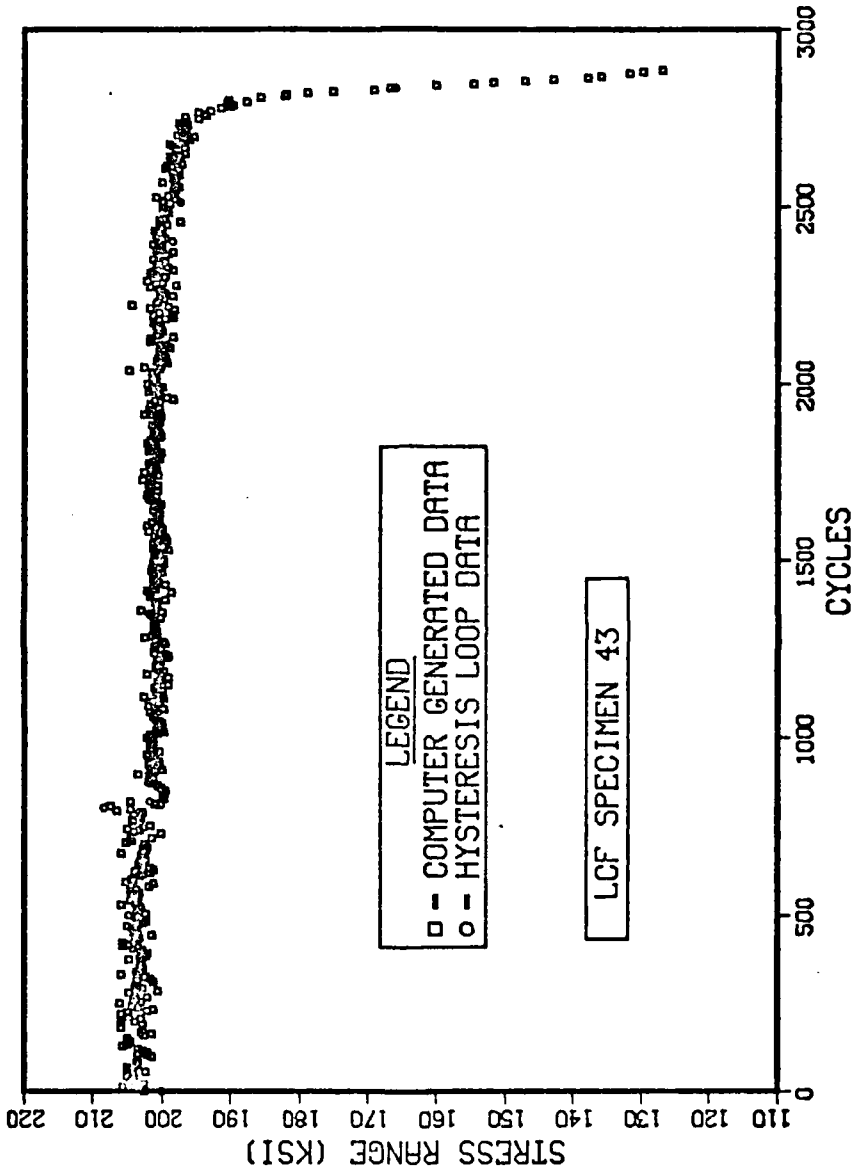

Figure 88. Plot of Stress Range vs Cycles - LCF Specimen 43

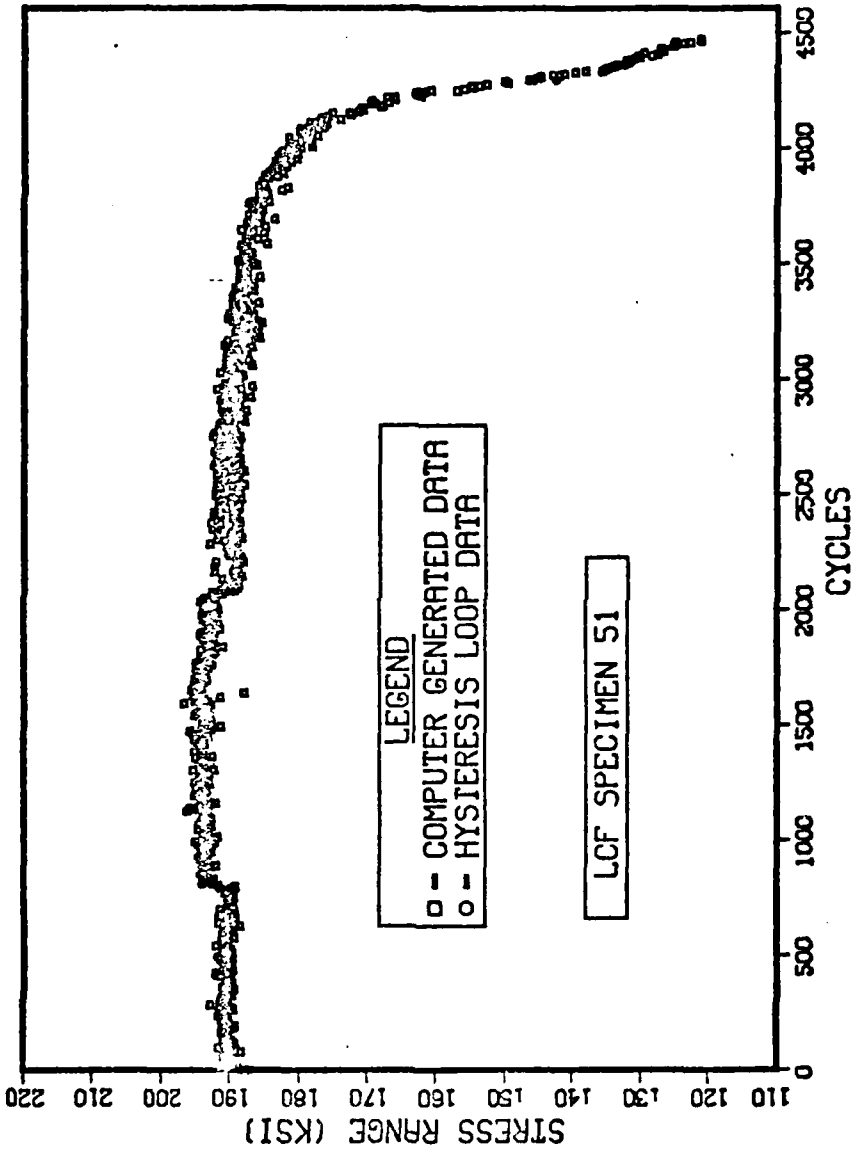

Figure 89. Plot of Stress Range vs Cycles - LCF Specimen 51

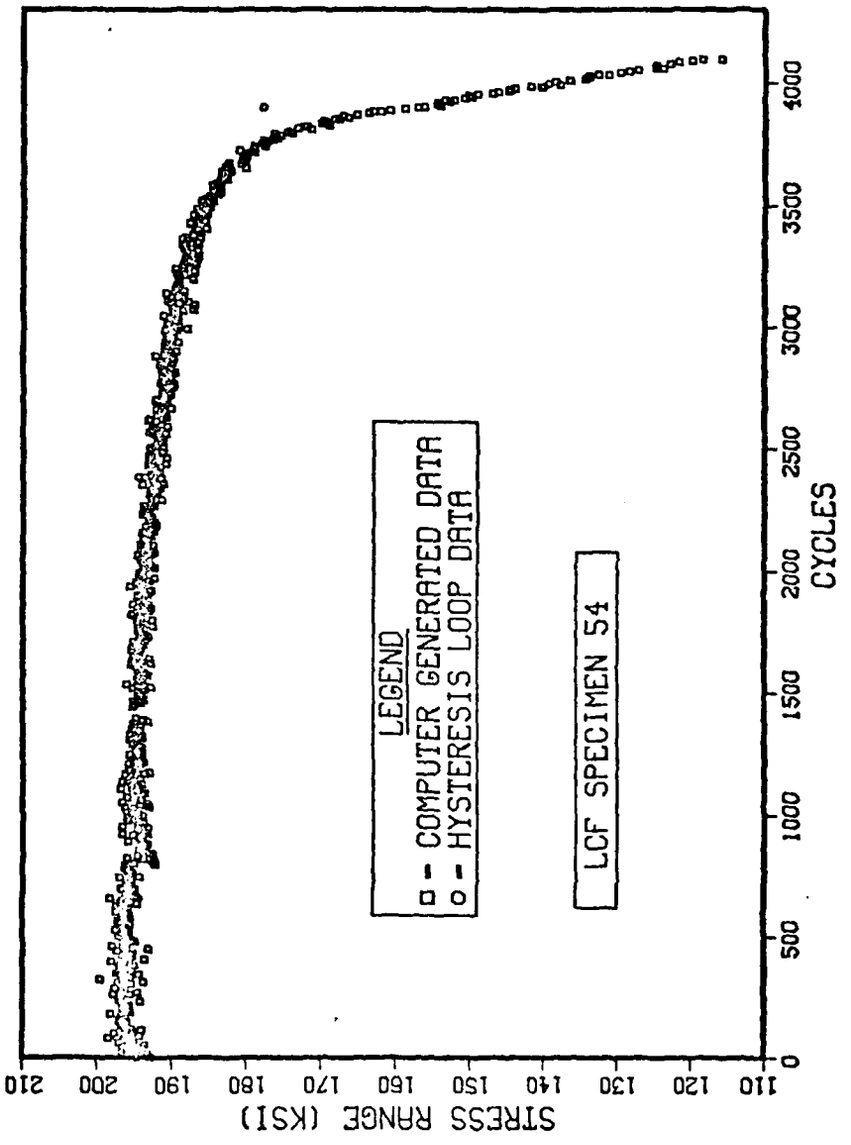

Figure 90. Plot of Stress Range vs Cycles - LCF Specimen 54

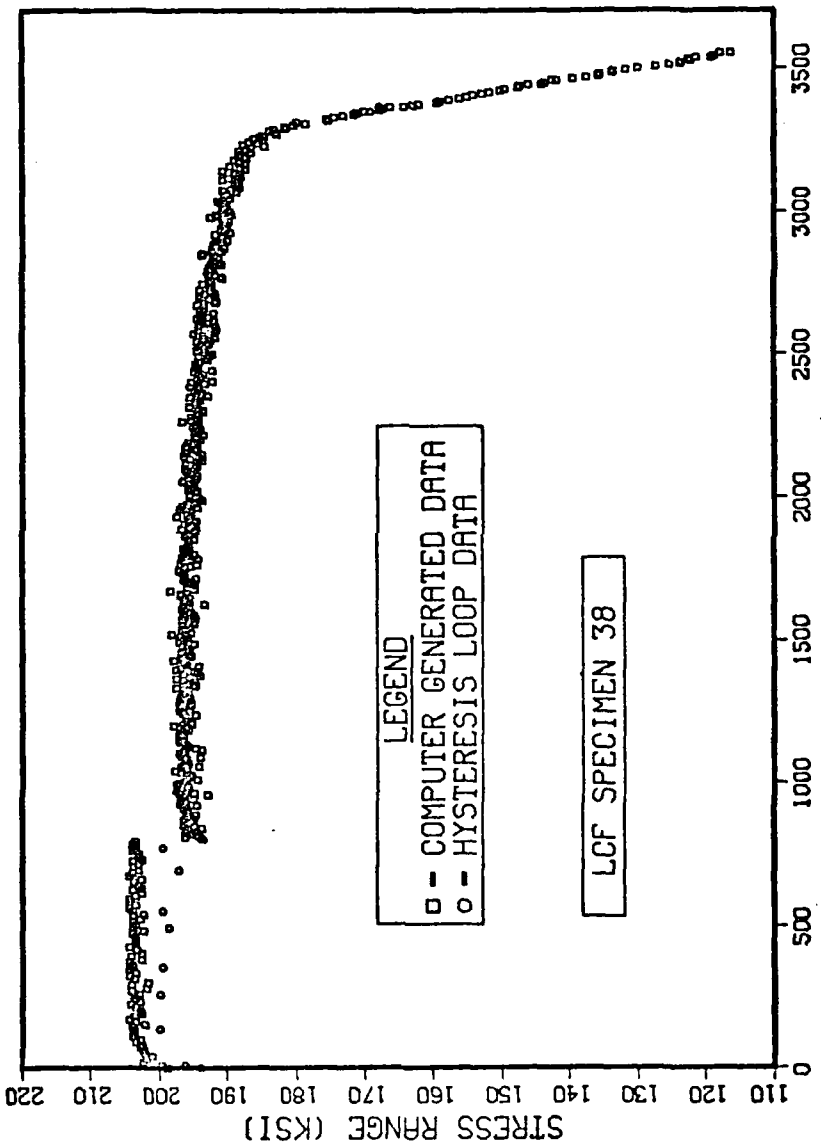

Figure 91. Plot of Stress Range vs Cycles - LCF Specimen 38

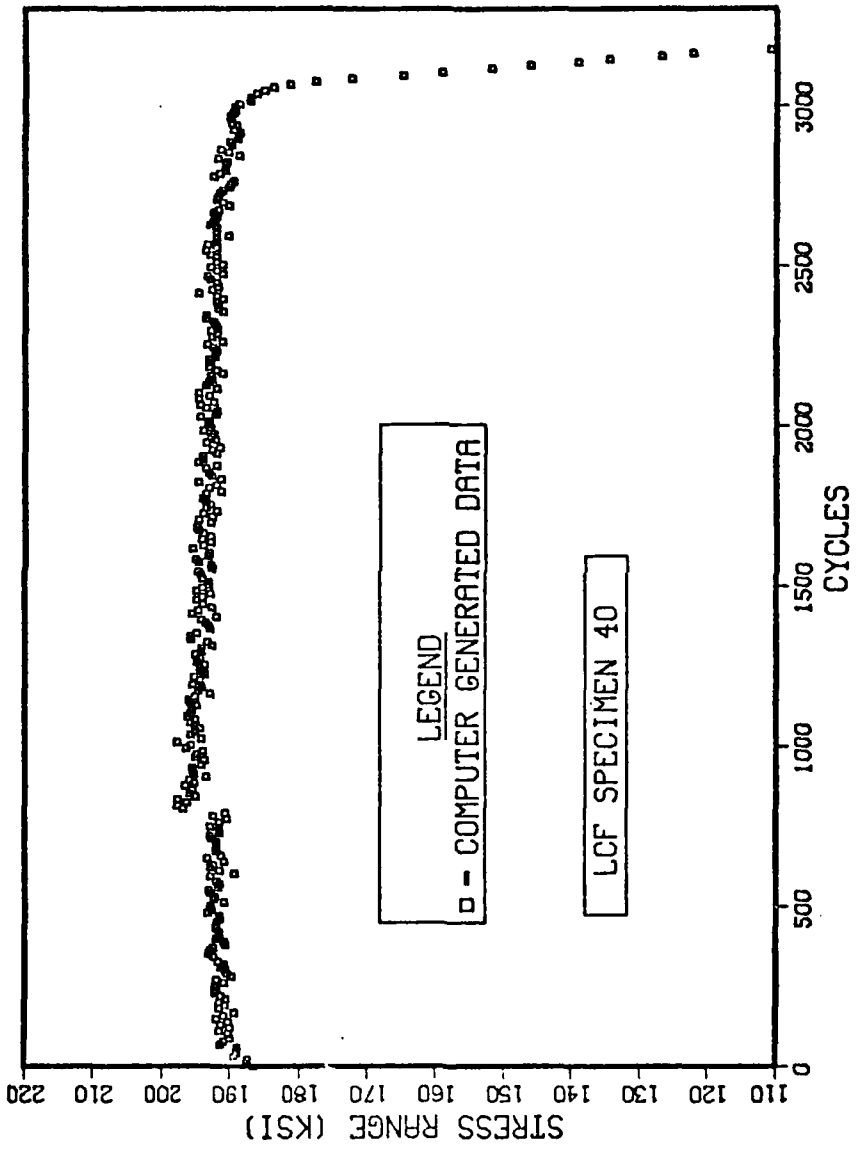

Figure 92. Plot of Stress Range vs Cycles - LCF Specimen 40

blocky carbides in the grain boundary began to decohere (Figure 51), and extrusions at persistent slip bands occurred (Figure 50). This is not the type of damage that thermal treatment can remove.

SEM photomicrographs of the gauge section of the thermally rejuvenated specimens after N_f revealed extensive cracking and decohering of inclusions. A typical example is shown in Fig. 93 from LCF Specimen 42.

LCF Specimen 31 was damaged in LCF at 500°F at a total strain range of 0.75% (stabilized stress range was 191 ksi). The gauge section was cut in two. Foils were made from one half for TEM investigation. The other half was given the thermal rejuvenation treatment, and the foils were prepared for TEM investigation. Figure 94 shows a network of dislocations beginning to form after 800 cycles. Figure 95, after the thermal treatment, shows that most of the dislocations have been annealed out.

The previous results were for a single rejuvenation treatment. In an attempt to determine the effect of multiple rejuvenations, LCF Specimen 41 was subjected to multiple blocks of 803 cycl of LCF damage plus thermal rejuvenation. The plot of Stress Range vs Cycles is contained in Figure 96. Table 16 summarizes the LCF data. Note that the thermal rejuvenation treatments seemed to have forestalled the onset of crack initiation as determined by the asymmetric load dropoff, but once the dropoff occurred, the crack progressed very rapidly. The surface of this specimen was examined in the SEM after the second block of 803 cycles (i.e., after 1606 cycles) and after failure. Figure 97 shows photomicrographs taken after 1606 cycles. Figure 97(a) shows the development of persistent slip bands

TABLE 16

SUMMARY OF LCF DATA FOR MULTIPLE THERMAL REJUVENATION - LCF SPECIMEN 41

Prior Damage Cycles	Strain Range (%)			Stress Range (ksi)	Cycles				
	$\Delta\varepsilon_t$	$\Delta\varepsilon_p$	$\Delta\varepsilon_e$		N_i	N_i'	N_f	N_i/N_f	N_i'/N_f
0	0.76	0.05	0.71	197.0	-	-	-	-	-
803	0.77	0.07	0.70	201.0	-	-	-	-	-
1606	0.77	0.06	0.71	193.0	-	-	-	-	-
2409	-	-	-	195.5	2500	2700	3134	0.80	0.86

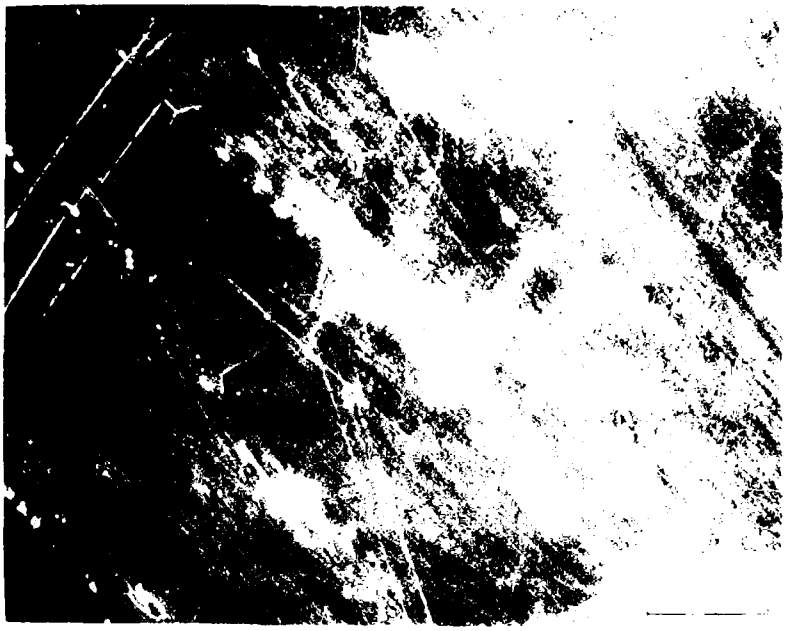

a. General Appearance of Cracking

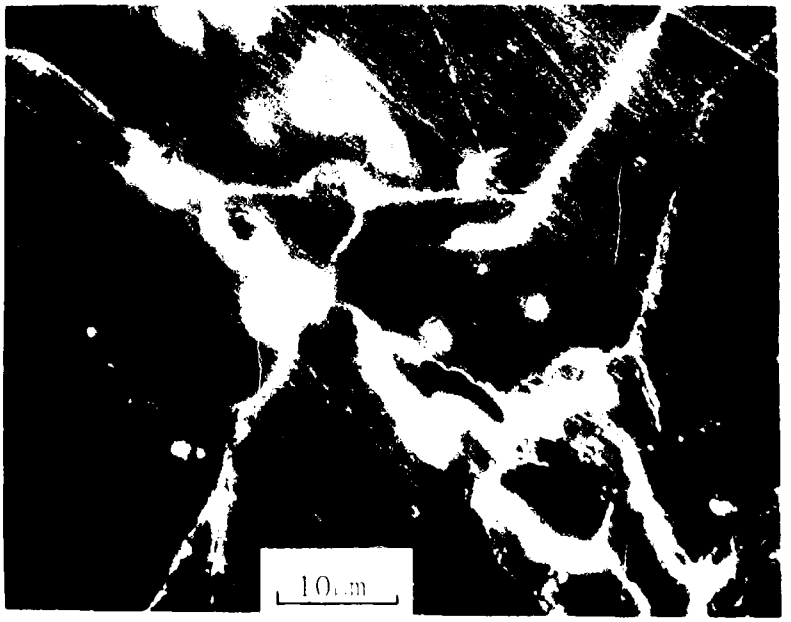

b. Decohered Inclusions and Cracking

Figure 93. SEM Micrograph, Cracking at Inclusions - LCF Specimen 42

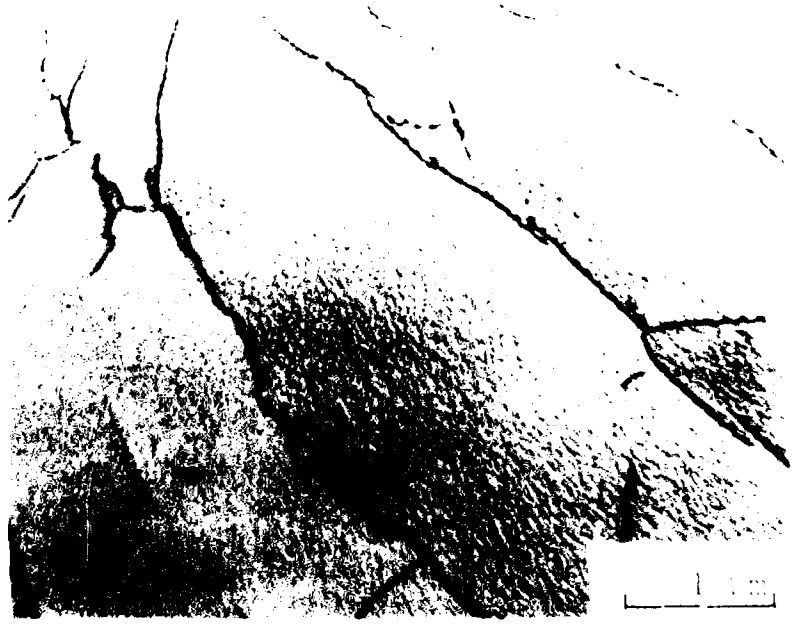

Figure 94. TEM Micrograph, Dislocation Network after 800 Cycles - LCF Specimen 31

Figure 95. TEM Micrograph, Annealed Dislocation Network - LCF Specimen 31

AD-A107 255 AIR FORCE INST OF TECH WRIGHT-PATTERSON AFB OH F/G 11/6
MECHANISMS OF RECOVERING LOW CYCLE FATIGUE DAMAGE IN INCOLOY 90--ETC(U)
1979 R E SCHAFRIK
UNCLASSIFIED AFIT-CI-79-212D NL

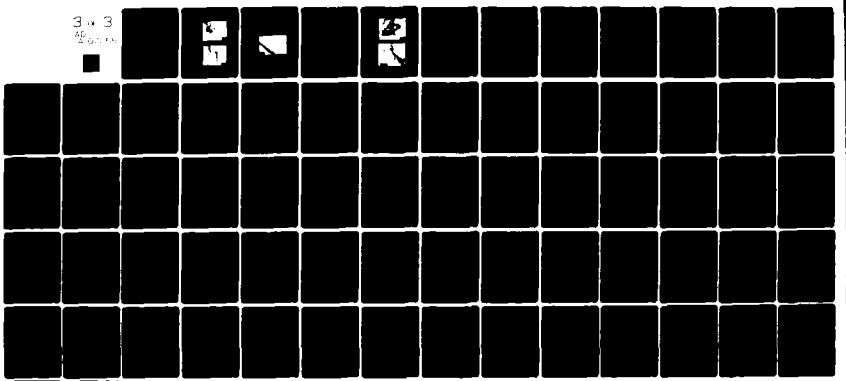

END
DATE FILMED
12-81
DTIC

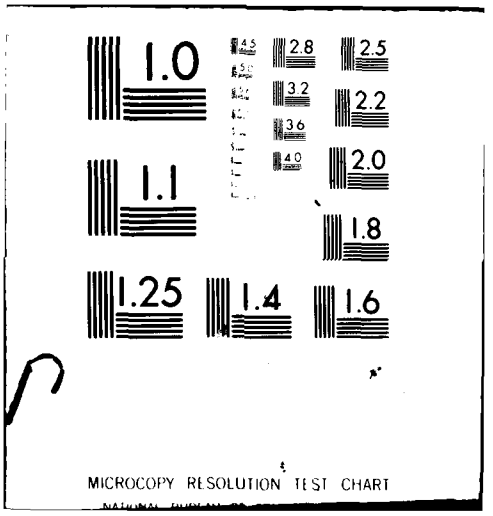
1.0
1.1
1.25
1.4
1.6
1.8
2.0
2.2
2.5
2.8
3.2
3.6
4.0
MICROCOPY RESOLUTION TEST CHART

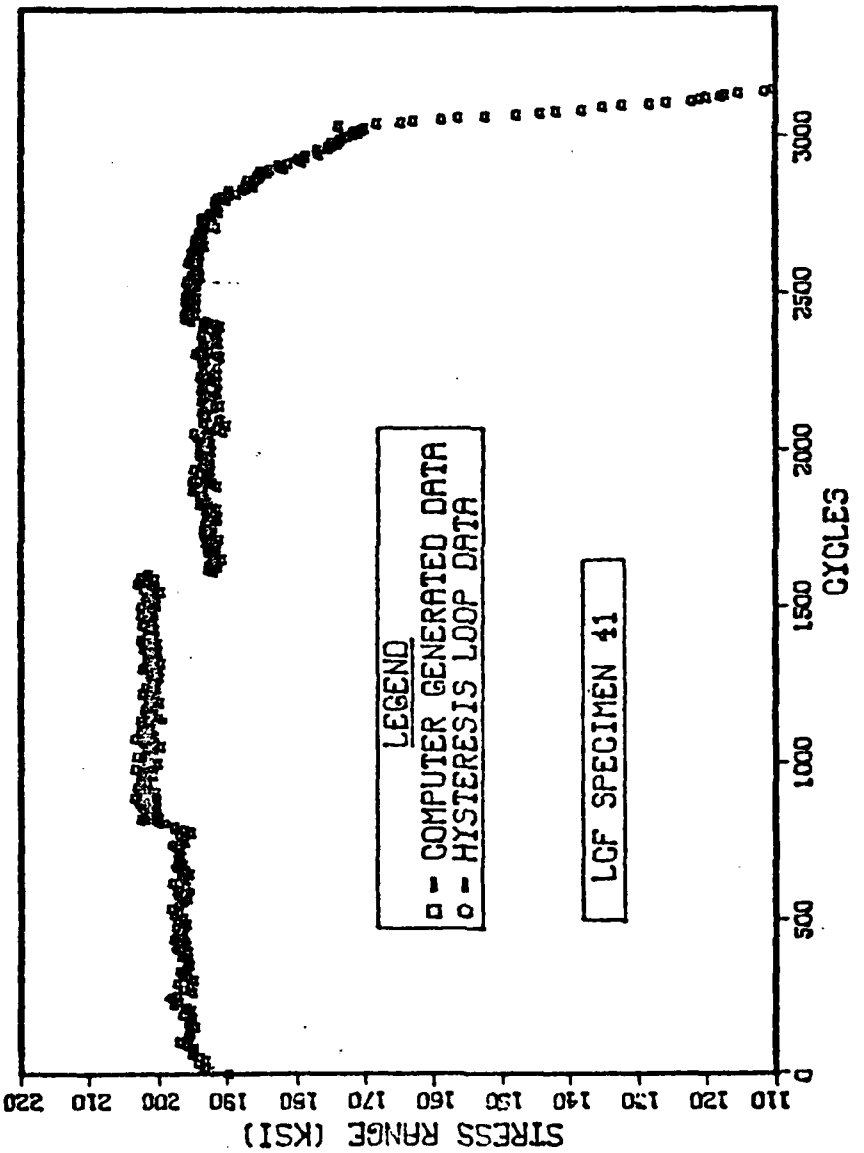

Figure 96. Plot of Stress Range vs Cycles - LCF Specimen 41

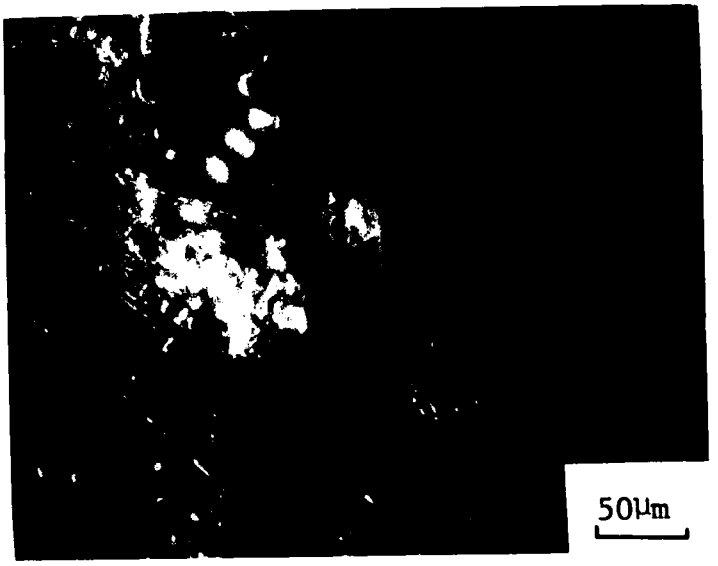

a. General Appearance of Cracking

b. Decohered Inclusion

Figure 97. SEM Micrograph, Surface Cracking after 1606 Cycles - LCF Specimen 41

c. Possible Cracked Grain Boundary

and the effect of polishing a group of carbides. Figure 97(b) shows a blocky grain boundary carbide in the process of decohering. Figure 97 (c) shows a grain boundary beginning to crack or form a ledge. Figure 98 are photomicrographs taken after failure. Figure 98(a) shows extensive deformation and cracking in a region near the principle crack. Figure 98(b) is a typical area located at some distance from the main crack. The grain boundary cracking and persistent slip bands are readily apparent. Note that the total life for LCF Specimen 41 was the same as could be expected for a baseline specimen. Thus, no overall rejuvenation was accomplished although the onset of gross microcracking may have been significantly retarded.

ii. Mechanisms

The rejuvenation effect of the thermal treatment was primarily due to the recovery of dislocations in the persistent slip bands and the deformation zone along the grain boundary. The fact that dislocation recovery can occur at elevated temperatures is well established, and several mechanisms have been postulated (55,56,57). Thus, after thermal rejuvenation and during subsequent testing, the planar dislocation arrays must re-form the persistent slip bands and the deformation zone along the grain boundary must be re-established. Also, the γ' precipitates which were sheared and possibly disordered are restored to their original distribution and morphology (65). The result is that the processes which lead to the decohering of the blocky grain boundary carbides are retarded. However, the decohering itself is not repaired by thermal treatment. Nor are the voids healed on the interior of a persistent slip band which developed intrusions and extrusions.

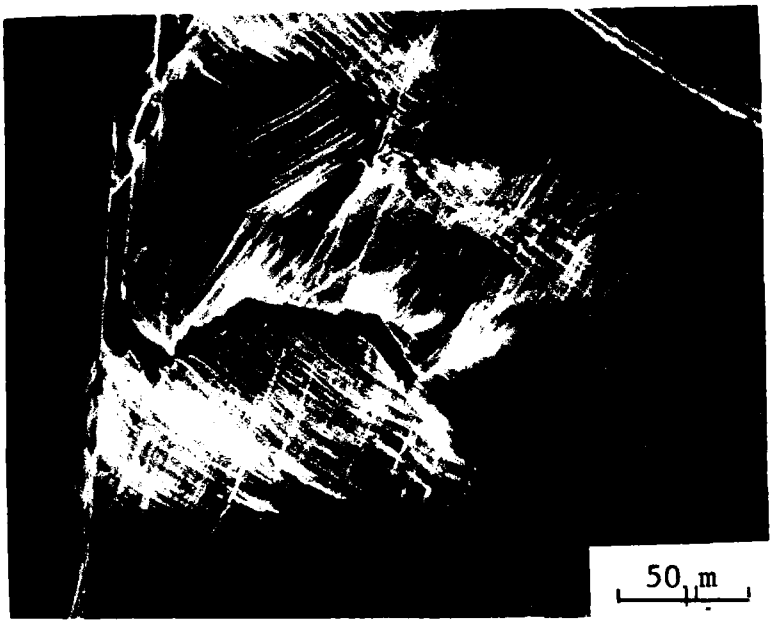

a. Surface Deformation Near Crack

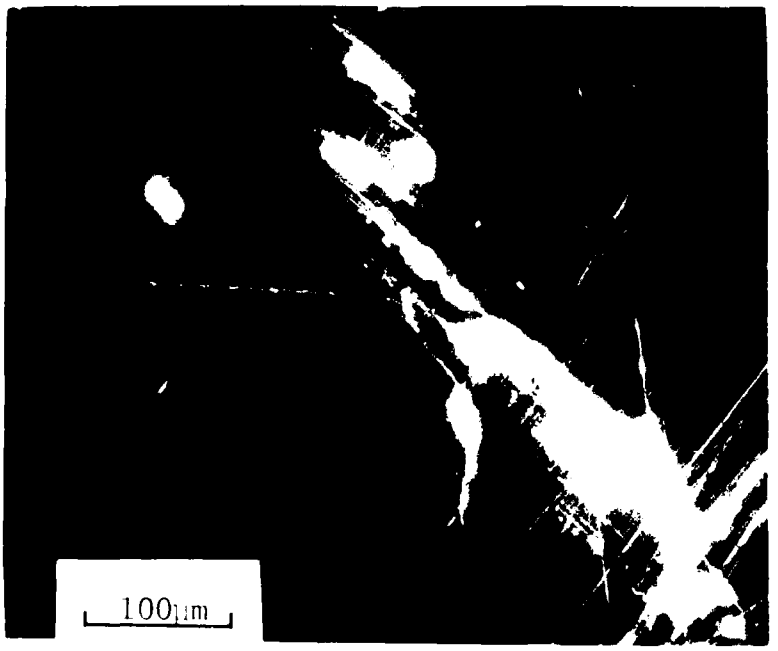

b. General Cracking

Figure 98. SEM Micrograph, Cracking after Failure - LCF Specimen 41

Also, the rejuvenation process acts to disperse slip throughout the gauge section, leading to a greater number of decohering carbides. Thus, when microcracks begin to propagate, they readily link up, leading to an accelerated crack growth rate. If the grain boundaries are simultaneously weakened during the thermal rejuvenation processing, such as by contamination from a poor vacuum, crack growth is accelerated even more.

C. Conclusions

Table 17 summarizes the cycles to crack initiation as a function of the processing, and Table 18 similarly summarizes the cycles to failure. It is evident that the data for the repolishing treatment alone belongs to the same population as the baseline data. The vapor-honed plus repolished data indicates crack initiation at about 400 cycles earlier than the baseline data, and less than half the total lifetime to failure. The HIP samples did not show any rejuvenation of LCF properties. The uncoated HIP specimens performed slightly worse than the coated HIP specimens. Crack initiation for the HIP samples (with 800 cycles of pre-HIP damage) occurred at about the same point as for the baseline specimens. But failure occurred 1300-1500 cycles earlier than the baseline data. Also, the data indicates that failure occurred within about 1600 cycles after HIP processing regardless of the level of initial damage (Table 12). The conclusion is that vapor honing and HIP processing damaged the surface of the test specimens. Vapor honing caused fracturing and decohering of blocky grain boundary carbides. Ceramic-coated plus HIP specimens not only had the deleterious effects of the vapor-honing induced damage, but also contamination due to reaction

TABLE 17

SUMMARY OF CYCLES TO CRACK INITIATION

0.70-0.80 TOTAL STRAIN RANGE

500 F TEST TEMPERATURE

		Treatment					
	Baseline	Repolish	Vapor Honed	HIP-Bare	HIP-Coated	Thermal	Thermal
Prior Damage (cycles)	0	803	0	800	800	800-803	400
No. of Data Points	8	2	2	4	3	5*	1
Mean	1388	1438	1000	1338	1433	1840	1800
Standard Deviation	448	194	141	396	301	114	-

*Excludes LCF Specimen 13

TABLE 18

SUMMARY OF CYCLES TO FAILURE

0.70-0.80 TOTAL STRAIN RANGE

500 F TEST TEMPERATURE

		Treatment					
	Baseline	Repolish	Vapor Honed	HIP-Bare	HIP-Coated	Thermal	Thermal
Prior Damage (cycles)	0	803	0	800	800	800-803	400
No. of Data Points	8	2	2	4	3	5*	1
Mean	3568	3384	1750	2246	2410	4198	3333
Standard Deviation	401	252	346	290	683	895	-

*Excludes LCF Specimen 13

between the ceramic coating and the superalloy. The uncoated HIP specimens were badly contaminated from impure argon in the HIP unit.

The thermally rejuvenated specimens definitely showed some rejuvenation. Those specimens damaged to 800 cycles before rejuvenation increased their initiation time by about 450 cycles and their total lifetime by about 630 cycles on the average (but note the high standard deviation in Table 18). The specimen predamaged 400 cycles before rejuvenation increased its initiation time by 400 cycles, but no increase in total lifetime was obtained. The experience with multiple rejuvenation (Table 16) indicates that damage accumulation in the form of decohering carbides, which are not affected by thermal treatments, leads to eventual very rapid crack extensions.

Chapter 4

SUMMARY

The mechanisms of crack initiation and growth in strain-controlled low cycle fatigue (LCF) damage were determined for the iron-nickel superalloy, Incoloy 901. Testing was done in air at a temperature of 500°F (260°C) and total strain range of 0.75%. The effect of hot isostatic pressing (HIP) and thermal treatment in reducing LCF damage was investigated.

The LCF specimens were manufactured using a low stress grinding method to maintain surface quality. Specimens were hand polished along the axial direction through 4/0 emery paper. Prior to testing, all specimens were given a standard solution treatment and double age, referred to as STA 3A (Table 4), to insure the uniform precipitate morphology and distribution from specimen to specimen. The as-received grain size was 90 μm. After STA 3A, the grain size was increased to 120 μm, but remained stable after subsequent heating to the solutioning temperature. The 0.2% offset yield stress at 500°F was 122 ksi.

Initial LCF testing was conducted over the total strain range of 0.70% to 2.44%. The Cyclic Stress-Strain Curve (Figure 24) exhibited cyclic hardening at the high strain ranges and cyclic softening at the lower ranges. A log-log plot of Total Strain Range vs Cycles (Figure 26) exhibits a linear curve with a negative slope.

Crack initiation in the baseline specimens was due to the decohering of blocky grain boundary carbides. Pre-crack initiation damage consisted of planar dislocation arrays forming persistent slip bands and an intense deformation region adjacent to favorably oriented grain boundaries. The persistent slip bands formed intrusions and extrusions at a total strain range of 0.75% by 800 cycles (about 60% of crack initiation time). Stage I crack propagation occurred along the grain boundary or along a favorably oriented persistent slip band. Substantial Stage II crack propagation occurred, as evidenced by the formation of fatigue striations. Fractography revealed a mixed fracture mode, consisting of both intergranular and transgranular fracture.

The HIP-processed specimens were subjected to a HIP cycle of 2025°F for one hour and 1975°F for two hours at 15 ksi of argon (Figures 10 and 11). Both uncoated and ceramic-coated specimens were HIP'd. Specimens had pre-HIP LCF damage of 0 cycles, 800 cycles, and 2100 cycles. The HIP processing increased the grain size by 25%. The specimens were subjected to STA 3A to restore the original morphology and distribution of the precipitates. No rejuvenation occurred. In fact, the fatigue properties were worse than the baseline properties by a substantial amount. Even correcting for the grain size change utilizing a Hall-Petch-type equation, it is clear that the HIP processing itself produced surface-related damage in the microstructure. In fact, the HIP processing caused more damage than the LCF pre-HIP damage levels.

In the case of the ceramic-coated specimens, damage resulted from at least two sources: (1) vapor honing the specimen surface to provide

a matte finish for the coating to adhere to, damaged the blocky carbides by decohering and cracking them; and (2) the ceramic coating reacted with the superalloy. As a consequence, intergranular cracking was promoted, and crack growth rates were greater than five times the rate in the baseline specimens.

The uncoated HIP specimens were damaged by contamination from the HIP atmosphere. Preferential formation of oxides and nitrides along the grain boundaries led to weakening of the boundaries. This promoted intergranular cracking, accelerated crack growth rates, and early failures. Overall, there was not much apparent difference between the behavior of the coated and uncoated specimens, although the coated ones were slightly superior.

Figure 99 plots the rejuvenation data and the trend line for the baseline data on a log-log plot of Total Strain Range vs Cycles to Failure.

The thermally rejuvenated specimens were given STA 3A after 800 cycles of damage. As long as the heat treating was done in a good vacuum so that surface contamination did not occur, partial rejuvenation was accomplished. Initiation life was increased by 400 cycles and the failure cycle was increased by 600 cycles. Complete rejuvenation was not attained because the grain boundary carbides had already begun to decohere after 800 cycles and persistent slip bands had formed intrusions and extrusions. When a specimen was rejuvenated three times after blocks of 803 cycles of damage, it failed catastrophically due to rapid crack extension. Thus, the unrecovered microstructural damage can adversely affect the fatigue life.

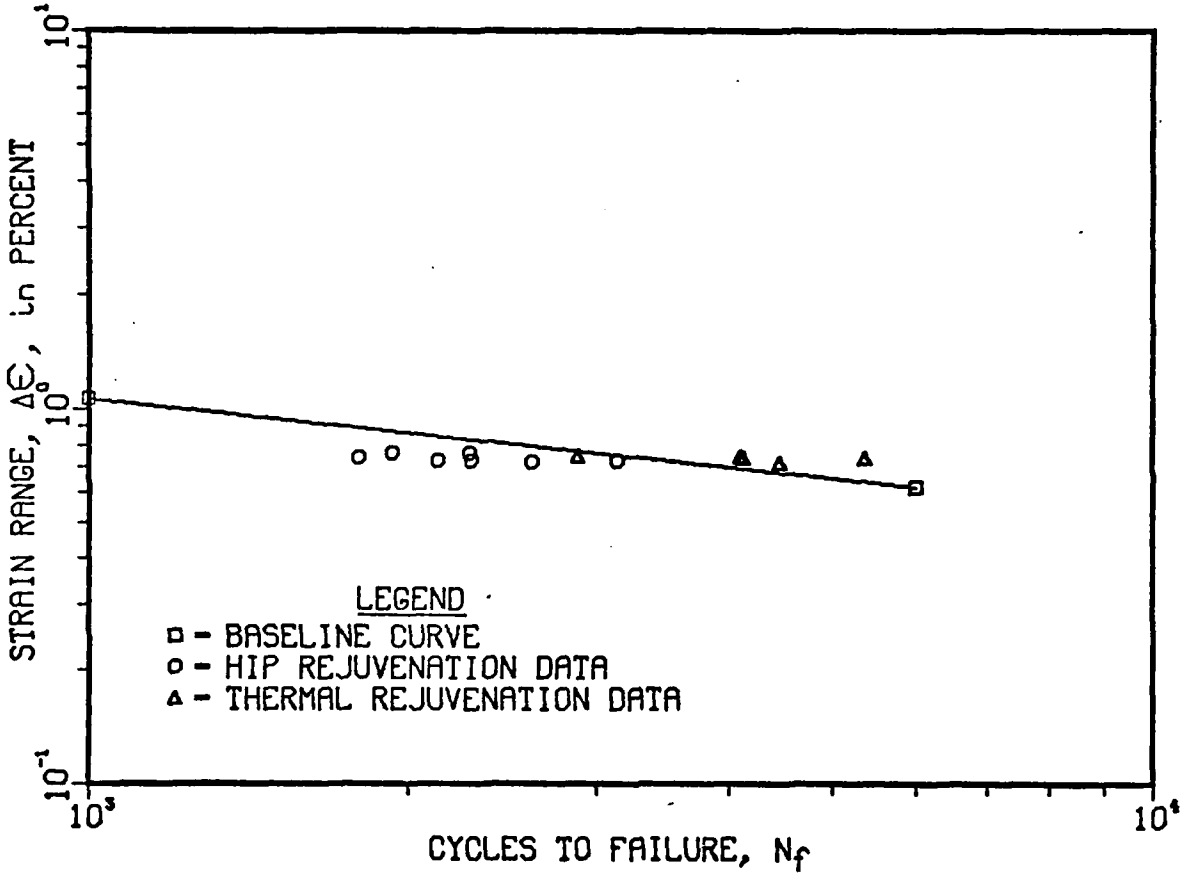

Figure 99. Plot of Strain Range vs Cycles to Failure with Baseline Trend Line and Rejuvenation Data

APPENDIX

LISTING OF COMPUTER PROGRAMS

APPENDIX I

SOURCE LISTING OF MODIFIED INSTRON LOW CYCLE FATIGUE APPLICATION PROGRAM APP-900-A3A8

```
PAGE  0001

0001              ************************************
0002              *
0003              *
0004              *      LOW CYCLE FATIGUE
0005              *
0006              *      APP-900-A3A8+M10D2
0007              *
0008              *      04/04/75
0009              *
0010              *
0011              ************************************
0012              *
0013              *      COPYRIGHT INSTRON CORPORATION
0014              *       DECEMBER  1974
0015              *
0016              *      MODIFIED BY STEVE LEFFLER &
0017              *                BOB SCHAFRIK
0018              *
0019              *           4/13/79
0020              *
0021              ************************************
```

```
PAGE  0003                        LOW CYCLE FATIGUE

0039                        *
0040                        ****** BEGIN SECTION ******
0041                        *
0042  001B  F98E  BEGIN   ITBL TABLE1,33
      001C  0468
      001D  0021
0043  001E  F98E          ITBL TABLE2,33
      001F  0489
      0020  0021
0044  0021  F98E          ITBL TABLE3,23
      0022  04AA
      0023  0017
0045  0024  F98E          ITBL TABLE4,33
      0025  04C1
      0026  0021
0046  0027  F95E          INID BUFFID
      0028  053E
0047  0029  F947          FMOV F0,AUGSTN
      002A  006E
      002B  0450
0048  002C  F947          FMOV F0,DATPX AND DATPY
      002D  006E
      002E  0178
0049  002F  F997          JST  *GETSTA
0050  0030  EA8C          STX  INDEX1
0051  0031  9900          STA  INDEX     ALSO XB
            0172
0052  0032  C2B1          AXI  '1'
0053  0033  0E00          SBM
0054  0034  EB8D          STXB *CURSTP
0055  0035  0F00          SWM
0056  0036  F947          FMOV F1,FCYCLE
      0037  045E
      0038  043A
0057  0039  FA71          JST  INITCY
0058  003A  F90F          CRLF
0059  003B  F909          TYPE MAREA     ASK AREA DIMS.
      003C  04F7
0060  003D  F93D          IFLT FTHICK    GET THICKNESS
      003E  043C
0061  003F  F93D          IFLT FWIDTH    GET WIDTH
      0040  043E
0062  0041  F90F          CRLF
0063  0042  F948          FCMP FWIDTH,F0
      0043  043E
      0044  006E
0064  0045  2105          JAZ  ROUND     ZERO = ROUND
0065  0046  F943          FMPL FTHICK,FWIDTH,FAREA
      0047  043C
      0048  043E
      0049  0442
0066  004A  F20C          JMP  CLEAR1
0067  004B  F944  ROUND   FDVD FTHICK,F2,FAC:1
```

```
PAGE  0002                        LOW CYCLE FATIGUE

0023  0000                  REL  0
0024                        *
0025                        ****** SSP-LINKAGE ******
0026                        *
0027  0000  0007          DATA NAME
0028  0001  001B          DATA BEGIN
0029  0002  00D6          DATA RESTRT
0030  0003  017A          DATA UPDATE
0031  0004  027A          DATA FINAL
0032  0005  0266          DATA STAT;A
0033  0006  0269          DATA STAT;B
0034                        *
0035  0007  C1D0  NAME    TEXT 'APP-900-A3'
      0008  D0AD
      0009  B9B0
      000A  B0AD
      000B  C1B3
0036  000C  C1B8          TEXT 'A8+MOD2'
      000D  ABCD
      000E  CFC4
      000F  B2A0
0037  0010  A0A0          TEXT '  LOW CYCLE FATIGUE0'
      0011  A0CC
      0012  CFD7
      0013  A0C3
      0014  D9C3
      0015  CCC5
      0016  A0C6
      0017  C1D4
      0018  C9C7
      0019  D5C5
      001A  C0A0
```

```
PAGE  0004                        LOW CYCLE FATIGUE

      004C  043C
      004D  0070
      004E  0426
0068  004F  F943        FMPL FAC:1,FAC:1,FAC:1
      0050  0426
      0051  0426
      0052  0426
0069  0053  F943        FMPL FAC:1,F:PI,FAREA
      0054  0426
      0055  007A
      0056  0442
0070  0057  F909  CLEAR1 TYPE MSTRLM   ASK STRAIN LIMITS
      0058  050D
0071  0059  F93D        IFLT MAXLIM   MAX. LIMIT
      005A  0446
0072  005B  F93D        IFLT MINLIM   MIN. LIMIT
      005C  0448
0073  005D  E100        LDX  XABC
            0170
0074  005E  F944        FDVD MAXLIM,*STVALP,HLIMIT
      005F  0446
      0060  80B4
      0061  00BE
0075  0062  F944        FDVD MINLIM,*STVALP,LLIMIT
      0063  0448
      0064  80B4
      0065  00C0
0076                    ***
0077  0066  F90F        CRLF
0078  0067  F909        TYPE RNDMES   RANDOM LIMITS?
      0068  0518
0079  0069  F90B        IKB
0080  006A  C0AC        CAI  ','      LEAVE AS IS?
0081  006B  F20A        JMP  CLEAR2   YES
0082  006C  C0D9        CAI  'Y'
0083  006D  F202        JMP  RNDMLT
0084  006E  0110        ZAR           RQSTD/ASSMD NO
0085  006F  F201        JMP  $+2
0086  0070  0350  RNDMLT APP           SET RANDOM FLAG
0087  0071  9900        STA  RNDFLG   -
            0175
0088  0072  F90B  WTCLR IKB           TERMINATION CHAR?
0089  0073  C0AC        CAI  ','
0090  0074  F201        JMP  CLEAR2
0091  0075  F6C3        JMP  WTCLR    NO
0092                    ***
0093  0076  B2FE  CLEAR2 LDA  RNDFLG
0094  0077  3105        JAN  CLR2
0095  0078  F90F        CRLF
0096  0079  F909        TYPE MNSTRS   ASK MIN. STRESS
      007A  0503
0097  007B  F93D        IFLT STRSLM   GET STRESS LIMIT
      007C  0444
```

```
PAGE  0005                          LOW CYCLE FATIGUE

0098  007D  F944  CLR2    FDVD HLIMIT,F32767,HRNGE
      007E  00BE
      007F  0074
      0080  0452
0099  0081  F944          FDVD LLIMIT,F32767,LRNGE
      0082  00C0
      0083  0074
      0084  0454
0100  0085  F945          FIX  HLIMIT,HLIMIT
      0086  00BE
      0087  00BE
0101  0088  F945          FIX  LLIMIT,LLIMIT
      0089  00C0
      008A  00C0
0102  008B  F947          FMOV F1,NN
      008C  045E
      008D  0458
0103  008E  F947          FMOV F0,XX     CALC. MD AFTER
      008F  006E
      0090  045A
0104                * GET CYCLE #'S & INCREMENTS
0105  0091  F90F          CRLF
0106  0092  F909          TYPE NMMESS
      0093  00CC
0107  0094  F93D          IFLT FNM1
      0095  00C4
0108  0096  F93D          IFLT FNM2
      0097  00C6
0109  0098  F93D          IFLT FNM3
      0099  00C8
0110  009A  F90F          CRLF
0111  009B  0010          ARM            1 PASS INITIALLY
0112  009C  9ADA          STA  CNT
0113  009D  9AD5          STA  XC        NEEDED FOR FINAL
0114  009E  C70A          LAM  10
0115  009F  9AC9          STA  CNTN1     INITIALIZE
0116  00A0  B0CA          LDA  NUM1      SLOPE ROUTINE
0117  00A1  9ACA          STA  NUM
0118  00A2  9A95          STA  DLTLD
0119  00A3  8A97          ADD  I300
0120  00A4  9A97          STA  LOAD2
0121  00A5  0110          ZAR
0122  00A6  9900          STA  BRANCH
                01C7
0123  00A7  9AD0          STA  DATPX
0124  00A8  9AD0          STA  DATPY
0125  00A9  9AC3          STA  MDFLG
0126  00AA  F22B          JMP  RESTRT
```

```
PAGE  0006                          LOW CYCLE FATIGUE

0128  00AB  0350  INITCY EIT
0129  00AC  0350        ARP
0130  00AD  9AC3        STA  XBPT     OR XA
0131  00AE  F947        FMOV F1,CMPTBL
      00AF  045E
      00B0  058A
0132  00B1  F947        FMOV F2,CMPTBL+2
      00B2  0070
      00B3  058C
0133  00B4  F941        FADD F1,F2,F3
      00B5  045E
      00B6  0070
      00B7  00CA
0134  00B8  F947        FMOV F3,CMPTBL+4
      00B9  00CA
      00BA  058E
0135  00BB  DABC        IMS  DATPX    PRINT FIRST CYCLE
0136  00BC  F711        RTN  INITCY
0137                    *
0138                    *
0139                    *
0140  00BD  0000  INDEX1 DATA 0
0141  00BE  0000  HLIMIT RES  2,0
0142  00C0  0000  LLIMIT RES  2,0
0143  00C2  0000  CURSTP BAC  STANUM+9

0144  00C3  00D9  RNDM   DATA 'Y'
0145  00C4  0000  FNM1   RES  2,0      CUT-OFF CYCLE 1 INC
0146  00C6  0000  FNM2   RES  2,0      INCREMENT TWO
0147  00C8  0000  FNM3   RES  2,0      LAST CYCLE
0148  00CA  0000  F3     RES  2,0
0149  00CC  C5CE  NMMESS TEXT 'ENTER NM1,NM2,NM3:0'
      00CD  D4C5
      00CE  D2A0
      00CF  CECD
      00D0  B1AC
      00D1  CECD
      00D2  B2AC
      00D3  CECD
      00D4  B3BA
      00D5  C0A0
```

```
PAGE  0007                        LOW CYCLE FATIGUE

0151                    *
0152                    ****** RESTART SECTION ******
0153                    *
0154  00D6  F93D  RESTPT STOP
0155  00D7  B29D        LDA  RNDFLG    RANDOM LIMITS
0156  00D8  2114        JAZ  RSTEX     NO
0157  00D9  F90F        CRLF
0158  00DA  F909        TYPE RESETM    RESET RANDOM SEQUENCE
      00DB  0531
0159  00DC  F90B        IKB
0160  00DD  0048        TAX
0161  00DE  C0AC        CAI  ','       DO THE SAME AS LAST TIME?
0162  00DF  F20B        JMP  SAME2     YES
0163  00E0  EE1D        STX  RNDM
0164  00E1  C0CE  RESET1 CAI  'N'       RESET SEQUENCE?
0165  00E2  F202        JMP  RSTRT0    NO
0166  00E3  C603        LAP  3         YES
0167  00E4  9B3F        STA  *RN1PTR
0168  00E5  C1AC  RSTRT0 CXI  ','       SAME AS LAST TIME?
0169  00E6  F206        JMP  RSTEX     YES
0170  00E7  F93B        IKB            INPUT TERMINATION?
0171  00E8  C0AC        CAI  ','
0172  00E9  F203        JMP  RSTEX
0173  00EA  F625        JMP  RSTRT0    NO, KEEP WAITING
0174  00EB  9628  SAME2  LDA  RNDM
0175  00EC  F60B        JMP  RESET1
0176                    *
0177  00ED  F90F  RSTEX  CRLF
0178  00EE  F909        TYPE MRATE
      00EF  0522
0179  00F0  F93D        IFLT SRRATE
      00F1  044A
0180  00F2  F90F        CRLF
0181  00F3  E27C        LDX  XABC
0182  00F4  F944        FDVD SRRATE,*STVALP,CLKRT
      00F5  044A
      00F6  80B4
      00F7  044C
0183  00F8  F90F        CRLF
0184  00F9  F913        RATE CLKRT     SET TIME VALUE
      00FA  044C
0185  00FB  E274        LDX  XABC      FORCE INDEX IN XA
0186  00FC  0109        IXR
0187  00FD  F944        FDVD *LDVALP,FAREA,STRESV
      00FE  80A9
      00FF  0442
      0100  044E
0188  0101  F944        FDVD STRSLM,STRESV,STPESS
      0102  0444
      0103  044E
      0104  0272
0189  0105  F945        FIX  STRESS,STRESS
      0106  0272
```

```
PAGE  0008                        LOW CYCLE FATIGUE

      0107  0272
0190  0108  F912          MODE STROKE
      0109  0001
0191  010A  F90F          CRLF
0192  010B  F909          TYPE MEXEC     PRINT EXECUTE
      010C  052D
0193  010D  F90F          CRLF
0194  010E  F909          TYPE MHEAD
      010F  0553
0195  0110  F90F          CRLF
0196  0111  F951          CLOS
0197                  *
0198  0112  0800  SETTBL  ENT
0199  0113  DA64          IMS  DATPX     PRINT ALL TRIGGER CYCLES
0200                  * STORE CURRENT CYCLE - END OF TEST?
0201  0114  F947          FMOV FCYCLE,FTCYC
      0115  043A
      0116  013F
0202  0117  F948          FCMP FNM3,F0  SEE IF DEFAULT
      0118  00C8
      0119  006E
0203  011A  2104          JAZ  SETTB2
0204  011B  F948          FCMP FTCYC,FNM3 LAST CYCLE?
      011C  013F
      011D  00C8
0205  011E  3095          JAP  INCDNE
0206  011F  B251  SETTB2  LDA  XBPT
0207  0120  0150          IAR
0208  0121  C004          CAI  4
0209  0122  F202          JMP  INCTBL
0210  0123  9A4D          STA  XBPT
0211  0124  F712          RTN  SETTBL
0212  0125  0350  INCTBL  ARP
0213  0126  9A4A          STA  XBPT
0214  0127  FA19  INCTB2  JST  CYADJ
0215  0128  F947          FMOV FTCYC,CMPTBL
      0129  013F
      012A  058A
0216  012B  FA15          JST  CYADJ
0217  012C  F947          FMOV FTCYC,CMPTBL+2
      012D  013F
      012E  058C
0218  012F  FA11          JST  CYADJ
0219  0130  F947          FMOV FTCYC,CMPTBL+4
      0131  013F
      0132  058E
0220  0133  F721          RTN  SETTBL
0221  0134  0010  INCDNE  APM
0222  0135  9A91          STA  BPANCH    FINI
0223  0136  F956          EXIT
0224                  *
0225  0137  0000  OLDLD   DATA 0
0226  0138  0000  DLTLD   DATA 0
```

```
PAGE  0009                          LOW CYCLE FATIGUE

0227  0139  0000  DLTSTN DATA 0,0
      013A  0000
0228  013B  012C  I300   DATA 300
0229  013C  0000  LOAD2  DATA 0
0230  013D  0000  CUPLD  DATA 0
0231  013E  0020  CUPSTN DATA 0
0232  013F  0000  FTCYC  RES  2,0      CYCLE VALUE
0233              *
0234              * ADJUST CYCLE TRIGGER VALUE
0235  0141  0800  CYADJ  ENT
0236  0142  F948        FCMP FTCYC,FNM1 SEE IF INC BY 1
      0143  013F
      0144  00C4
0237  0145  3085        JAP  CYAD2    INC BY MORE
0238  0146  F941        FADD F1,FTCYC,FTCYC
      0147  045E
      0148  013F
      0149  013F
0239  014A  F204        JMP  CYAD3
0240  014B  F941  CYAD2 FADD FNM2,FTCYC,FTCYC INC BY FNM2
      014C  00C6
      014D  013F
      014E  013F
0241  014F  F70E  CYAD3 RTN  CYADJ
0242              *
0243              *
```

```
PAGE  0010                        LOW CYCLE FATIGUE

0245                    *
0246  0150  B218  N1      LDA   CNTN1
0247  0151  21C3        JAZ   NIX
0248  0152  B219        LDA   NUM
0249  0153  9616        SUB   CURLD     SAVE POINTS
0250  0154  2C31        JAM   DATN1
0251  0155  F236  NIX     JMP   NOT1
0252  0156  B214  DATN1   LDA   NUM1     OF LOAD
0253  0157  8A14        ADD   NUM
0254  0158  9A13        STA   NUM       AND STRAIN
0255  0159  B61C        LDA   CURLD
0256  015A  F991        GIVE  TABLE3
      015B  04AA
0257  015C  F206        JMP   FULLN1
0258  015D  B61F        LDA   CURSTN    IN 5%
0259  015E  F991        GIVE  TABLE3
      015F  04AA
0260  0160  F202        JMP   FULLN1
0261  0161  DA27        IMS   CNTN1
0262  0162  F279        JMP   NOT1
0263  0163  0110  FULLN1 ZAP
0264  0164  9A04        STA   CNTN1     SLOPE
0265  0165  F957        CUE   SLOPE:,1000
      0166  0339
      0167  03E8
0266  0168  F273        JMP   NOT1
0267                    *
0268  0169  0000  CNTN1   DATA  0         CALCULATION
0269  016A  0190  SPEAK   DATA  400       20% FS
0270  016B  0004  NUM1    DATA  100
0271  016C  0000  NUM     DATA  0
0272  016D  0000  MDFLG   DATA  0
0273  016E  0000  UTEMP1  DATA  0
0274  016F  0000  UTEMP2  DATA  0
0275  0170  0171  XABC    DATA  $+1
0276  0171  0000  XBPT    DATA  0         OR XA
0277  0172  0000  INDEX   DATA  0         OR XB
0278  0173  0000  XC      DATA  0
0279        0004  VALPTR  EQU   :4
0280  0174  0395  PNIPTR  DATA  PN1
0281  0175  0000  PNDFLG  DATA  0
0282  0176  0368  GETNUM  DATA  RANDOM
0283  0177  0000  CNT     DATA  0
0284  0178  0000  DATPX   DATA  0
0285  0179  0000  DATPY   DATA  0
```

```
PAGE  0011                        LOW CYCLE FATIGUE

0287                *

PAUSE
0288                *
0289                ****** UPDATE SECTION ******
0290                *
0291  017A  F910   UPDATE READ LOAD,CUPLD
      017B  0000
      017C  013D
0292  017D  F910         READ STROKE,CURSTN
      017E  0001
      017F  013E
0293  0180  B246         LDA  BRANCH
0294  0181  3081         JAP  $+2        IF < 0 THEN
0295  0182  F95F         DONE            REQUESTED DONE
0296  0183  3181         JAG  $+2
0297  0184  F243         JMP  UP:
0298  0185  E6C8         LDX  INDEX1
0299  0186  B648         LDA  CURSTN
0300  0187  9504         SUB  @*VALPTR
0301  0188  D61E         CMS  BREAK
0302  0189  F202         JMP  $+3
0303  018A  0000         NOP
0304  018B  F95F         DONE
0305  018C  B64E         LDA  CURSTN
0306  018D  D6CD         CMS  LLIMIT
0307  018E  F2C6         JMP  REVUP
0308  018F  0000         NOP
0309  0190  B653         LDA  CUPLD
0310  0191  9E5A         STA  OLDLD
0311  0192  F911         RAMP DOWN
      0193  8000
0312  0194  F956         EXIT
0313                *
0314  0195  B61C   REVUP  LDA  DATPY
0315  0196  210A         JAZ  XX3
0316  0197  B659         LDA  CURSTN
0317  0198  BE29         EMA  UTEMP2
0318  0199  0048         TAX
0319  019A  B65D         LDA  CUPLD
0320  019B  BE2D         EMA  UTEMP1
0321  019C  F957         CUE  PRINT,2900
      019D  02F6
      019E  0B54
0322  019F  0110         ZAR
0323  01A0  9E27         STA  DATPY
0324  01A1  E631   XX3   LDX  XABC
0325  01A2  F948         FCMP *CMPTRL,FCYCLE
      01A3  858A
      01A4  C43A
0326  01A5  3189         JAG  DATA01     FILL TABLE UNLESS CYCLE <
0327  01A6  B669         LDA  CUPLD      VALUE SOUGHT
0328  01A7  0000         NOP
0329  01A8  0000         NOP
0330  01A9  0000         NOP
```

```
PAGE  0012                          LOW CYCLE FATIGUE

0331  01AA  B66C          LDA  CURSTN
0332  01AB  0000          NOP
0333  01AC  0000          NOP
0334  01AD  0000          NOP
0335  01AE  FE9C          JST  SETTBL
0336  01AF  F941  DATA01  FADD F1,FCYCLE,FCYCLE
      01B0  045E
      01B1  043A
      01B2  043A
0337  01B3  B67C          LDA  OLDLD
0338  01B4  8E49          ADD  NUM1
0339  01B5  9E7D          STA  DLTLD
0340  01B6  8E7B          ADD  1300
0341  01B7  9E7B          STA  LOAD2
0342  01B8  F911          RAMP UP
      01B9  0000
0343  01BA  B645          LDA  PNDFLG
0344  01BB  2108          JAZ  PMPUP
0345  01BC  FF46          JST  *GETNUM
0346  01BD  F943          FMPL HRNGE,PNDTMP,HLIMIT
      01BE  0452
      01BF  0456
      01C0  00BE
0347  01C1  F945          FIX  HLIMIT,HLIMIT
      01C2  00BE
      01C3  00BE
0348  01C4  0110  PMPUP   ZAR
0349  01C5  9A01          STA  BRANCH
0350  01C6  F956          EXIT
0351                *
0352  01C7  0000  BRANCH  DATA 0
0353                *
0354  01C8  E100  UP:     LDX  INDEX1
                00BD
0355  01C9  B504          LDA  @*VALPTR
0356  01CA  968C          SUB  CURSTN
0357  01CB  D661          CMS  BREAK
0358  01CC  F202          JMP  $+3
0359  01CD  0000          NOP
0360  01CE  F95F          DONE
0361  01CF  B100          LDA  HLIMIT
                00BE
0362  01D0  D692          CMS  CURSTN
0363  01D1  F24C          JMP  REVDWN
0364  01D2  0000          NOP
0365  01D3  D696          LDA  CURLD
0366  01D4  9E9D          STA  OLDLD
0367  01D5  F911          RAMP UP
      01D6  0000
0368  01D7  F948          FCMP FCYCLE,F1
      01D8  043A
      01D9  045E
0369  01DA  3101          JAN  NOT1
```

```
PAGE  0013                          LOW CYCLE FATIGUE

0370  01DB  F69B          JMP  NI        RETURNS TO NOT1
0371  01DC  B66F  NOT1    LDA  MDFLG
0372  01DD  20DF          JAM  UPEXIT
0373  01DE  3189          JAG  MD2ND
0374  01DF  B6A2          LDA  CUPLD     AT 1ST SMPL PT?
0375  01E0  D6A8          CMS  DLTLD
0376  01E1  F23B          JMP  UPEXIT    NO
0377  01E2  0000          NOP
0378  01E3  9EAB          STA  DLTLD     YES, STORE DATA
0379  01E4  B6A6          LDA  CURSTN
0380  01E5  9EAC          STA  DLTSTN
0381  01E6  DE79          IMS  MDFLG
0382  01E7  F235          JMP  UPEXIT
0383  01E8  B6AB  MD2ND   LDA  CUPLD     AT 2ND SMPL PT?
0384  01E9  D6AD          CMS  LOAD2
0385  01EA  F232          JMP  UPEXIT
0386  01EB  0000          NOP
0387  01EC  B6AF          LDA  CUPLD     YES, CALC. MD
0388  01ED  96B5          SUB  DLTLD
0389  01EE  9EB6          STA  DLTLD
0390  01EF  B6B1          LDA  CURSTN
0391  01F0  96B7          SUB  DLTSTN
0392  01F1  9EB3          STA  DLTSTN
0393  01F2  F946          FLT  DLTLD,MOD
      01F3  0138
      01F4  045C
0394  01F5  F943          FMPL MOD,STPESV,MOD
      01F6  045C
      01F7  044E
      01F8  045C
0395  01F9  F946          FLT  DLTSTN,DLTSTN
      01FA  0139
      01FB  0139
0396  01FC  E68C          LDX  XABC      XR=INDEX
0397  01FD  F943          FMPL DLTSTN,*STVALP,DLTSTN
      01FE  0139
      01FF  80B4
      0200  0139
0398  0201  F944          FDVD MOD,DLTSTN,MOD
      0202  045C
      0203  0139
      0204  045C
0399  0205  F943          FMPL MOD,F1000,MOD
      0206  045C
      0207  0466
      0208  045C
0400  0209  F941          FADD MOD,XX,XX CALC. NEW
      020A  045C
      020B  045A
      020C  045A
0401  020D  DE96          IMS  CNT       MODULUS
0402  020E  F20C          JMP  XIT       EVERY 4TH
0403  020F  F944          FDVD XX,NN,MD  CYCLE
```

```
PAGE  0014                          LOW CYCLE FATIGUE

      0210  045A
      0211  0458
      0212  0274
0404  0213  C704          LAM  4          AVERAGE OVER
0405  0214  9E9D          STA  CNT        4 CYCLES
0406  0215  F947          FMOV F0,XX
      0216  006E
      0217  045A
0407  0218  F947          FMOV F4,NN
      0219  0460
      021A  0458
0408  021B  0010  XIT     APM             RESET FLAG
0409  021C  9EAF          STA  MDFLG
0410  021D  F956  UPEXIT  EXIT
0411                      *
0412  021E  B6A9  REVDUN  LDA  RNDFLG     NO STRESS TEST
0413  021F  3104          JAN  RVDN       WITH RANDOM OPTION
0414  0220  B251          LDA  STRESS
0415  0221  96E4          SUB  CUPLD
0416  0222  2031          JAM  $+2
0417  0223  F95F          DONE            END OF TEST
0418  0224  B6AC  RVDN    LDA  DATPX
0419  0225  210D          JAZ  XX2
0420  0226  B6E9          LDA  CUPLD
0421  0227  9EB9          STA  UTEMP1
0422  0228  B6EA          LDA  CURSTN
0423  0229  9E2A          STA  UTEMP2
0424  022A  F947          FMOV FCYCLE,FAC:3
      022B  043A
      022C  0278
0425  022D  F947          FMOV MD,FAC:4
      022E  0274
      022F  02F4
0426  0230  0110          ZAR
0427  0231  9EB9          STA  DATPX
0428  0232  DEB9          IMS  DATPY
0429  0233  F946  XX2     FLT  CURSTN,TEMPAV
      0234  013E
      0235  0438
0430  0236  F941          FADD TEMPAV,AUGSTN,AUGSTN
      0237  0438
      0238  0450
      0239  0450
0431  023A  E6CA          LDX  XABC
0432  023B  F948          FCMP *CMPTBL,FCYCLE
      023C  858A
      023D  043A
0433  023E  3190          JAG  DATA02
0434  023F  B1C0          LDA  CURLD
            013D
0435  0240  0000          NOP
0436  0241  0000          NOP
0437  0242  0000          NOP
```

```
PAGE  0015                          LOW CYCLE FATIGUE

0438  0243  B1C0          LDA  CURSTN
            013E
0439  0244  0000          NOP
0440  0245  0000          NOP
0441  0246  0000          NOP
0442  0247  B22C          LDA  MD
0443  0248  0000          NOP
0444  0249  0000          NOP
0445  024A  0000          NOP
0446  024B  B229          LDA  MD+1
0447  024C  0000          NOP
0448  024D  0000          NOP
0449  024E  0000          NOP
0450  024F  F911  DATA02 RAMP DOWN
      0250  8000
0451  0251  0110          ZAR
0452  0252  9EE5          STA  MDFLG
0453  0253  B6DE          LDA  PNDFLG
0454  0254  2108          JAZ  PMPDN
0455  0255  FFDF          JST  *GETNUM
0456  0256  F943          PMPL LENGE,PNDTMP,LLIMIT
      0257  0454
      0258  0456
      0259  00C0
0457  025A  F945          FIX  LLIMIT,LLIMIT
      025B  00C0
      025C  00C0
0458  025D  0350  PMPDN   ARP
0459  025E  9E97          STA  BRANCH
0460  025F  F956          EXIT
0461                      *
0462  0260  F957  FULL    CUE  WINKER,1005 FLASH STATUS 1
      0261  026D
      0262  03ED
0463  0263  0010          ARM             REQUEST A DONE
0464  0264  9E9D          STA  BRANCH     IN UPDATE
0465  0265  F956          EXIT
0466                      *
0467  0266  0010  STAT:A  ARM             REQUEST A DONE
0468  0267  9EA0          STA  BRANCH     IN UPDATE
0469  0268  F951          CLOS
0470                      *
0471  0269  DEF1  STAT:B  IMS  DATPX
0472  026A  F958          WINK 2
      026B  0002
0473  026C  F951          CLOS
0474                      *
0475  026D  F958  WINKER  WINK 1
      026E  0001
0476  026F  F951          CLOS
0477                      *
0478  0270  00AB  INITCY  DATA INITCY
0479  0271  0112  SETPTR  DATA SETTBL
```

```
PAGE  0016                          LOW CYCLE FATIGUE

0480  0272  0000  STPESS RES  2,0
0481  0274  0000  MD     RES  2,0
0482  0276  0000  FAC:2   RES  2,0
0483  0278  0000  FAC:3   RES  2,0
0484              *

PAUSE
0485              ****** FINAL SECTION ******
0486              *
0487  027A  0110  FINAL  ZAR
0488  027B  9EB4         STA  BRANCH
0489  027C  F90F         CRLF
0490  027D  F90F         CRLF
0491              * TYPE TRAILER
0492  027E  F909         TYPE NULL
      027F  04E2
0493  0280  F909         TYPE NULL
      0281  04E2
0494  0282  0000         NOP
0495  0283  F993         DATE
0496  0284  F90F         CRLF
0497  0285  F909         TYPE BUFFID
      0286  053E
0498  0287  F90F         CRLF
0499  0288  F90F         CRLF
0500  0289  F900         JST  SWAP      SAVE CYCLE
                  0398
0501  028A  B400         LDA  00        DATA IN CASE OF
0502  028B  3181         JAG  LOOP3     START
0503  028C  FF1C         JST  *INITCX
0504  028D  E265  LOOP3  LDX  XABCP
0505  028E  F947         FMOV *CMPTBL,FAC:1
      028F  859A
      0290  0426
0506  0291  F992         GET  TABLE1
      0292  0468
0507  0293  F242         JMP  EMPTY
0508  0294  9E1C         STA  FAC:3
0509  0295  F992         GET  TABLE4
      0296  04C1
0510  0297  F23E         JMP  EMPTY
0511  0298  9E22         STA  FAC:2
0512  0299  F992         GET  TABLE4
      029A  04C1
0513  029B  F23A         JMP  EMPTY
0514  029C  9E25         STA  FAC:2+1
0515              *      TAB 2
0516              *      WDEC FAC:1,9,0 CYCLE #
0517  029D  F94D         WFLT FAC:1
      029E  0426
0518              *      TAB 5
0519              *      WDEC FAC:2,10,0 MODULUS
0520  029F  F94D         WFLT FAC:2
      02A0  0276
0521              *      TAB 6
```

```
PAGE  0017                          LOW CYCLE FATIGUE

0522  02A1  FA0C          JST  PRINTV
0523  02A2  C6A0          LAP  ' '
0524                *     LXP 31
0525  02A3  C41C          LXP  28
0526  02A4  F92E          OTT
0527  02A5  00A8          DXR
0528  02A6  3842          JXN  S-2
0529  02A7  F992          GET  TABLE1
      02A8  0468
0530  02A9  F22C          JMP  EMPTY
0531  02AA  9532          STA  FAC:3
0532  02AB  FA02          JST  PRINTV
0533  02AC  FF3B          JST  *SETPTR
0534  02AD  F620          JMP  LOOP3
0535                *
0536  02AE  0300  PRINTV  ENT
0537  02AF  F946          FLT  FAC:3,FAC:3
      02B0  0278
      02B1  0278
0538  02B2  F943          FMPL FAC:3,STRESV,FAC:3
      02B3  0278
      02B4  044E
      02B5  0278
0539                *     WDEC FAC:3,8,3 STRESS
0540  02B6  F94D          WFLT FAC:3
      02B7  0278
0541                *     TAB 6
0542  02B8  E23A          LDX  XABCP
0543  02B9  F992          GET  TABLE2
      02BA  0489
0544  02BB  F21A          JMP  EMPTY
0545  02BC  9A37          STA  FAC:4
0546  02BD  F946          FLT  FAC:4,FAC:4
      02BE  02F4
      02BF  02F4
0547  02C0  F943          FMPL FAC:4,*STVALP,FAC:4
      02C1  02F4
      02C2  80B4
      02C3  02F4
0548                *     WDEC FAC:4,7,4 STRAIN
0549  02C4  F94D          WFLT FAC:4
      02C5  02F4
0550                *     TAB 7
0551  02C6  F944          FDVD FAC:3,FAC:2,FAC:3
      02C7  0278
      02C8  0276
      02C9  0273
0552  02CA  F943          FMPL FAC:3,F1000,FAC:3
      02CB  0273
      02CC  0466
      02CD  0279
0553  02CE  F942          FSUB FAC:4,FAC:3,FAC:3
      02CF  02F4
```

```
PAGE  0018                          LOW CYCLE FATIGUE

      02D0  0278
      02D1  0278
0554                  *       WDEC FAC:3,9,7 PLASTIC STRAIN
0555  02D2  F94D              WFLT FAC:3
      02D3  0278
0556  02D4  F90F              CRLF
0557  02D5  F727              RTN  PRINTV
0558                  *
0559  02D6  F90F      EMPTY   CRLF
0560  02D7  F90F              CRLF
0561  02D8  F909              TYPE MLAST
      02D9  0575
0562                  *       WDEC FCYCLE,9,0 FINAL CYCLE #
0563  02DA  F94D              WFLT FCYCLE
      02DB  043A
0564  02DC  F90F              CRLF
0565  02DD  F909              TYPE MAVGS
      02DE  057A
0566  02DF  F944              FDVD AUGSTN,FCYCLE,AUGSTN
      02E0  0450
      02E1  043A
      02E2  0450
0567  02E3  520F              LDX  XABCP
0568  02E4  F943              FMPL AUGSTN,*STVALP,FAC:3
      02E5  0450
      02E6  80B4
      02E7  0278
0569                  *       WDEC FAC:3,7,4 PEAK STRAIN
0570  02E8  F94D              WFLT FAC:3
      02E9  0278
0571  02EA  F90F              CRLF
0572  02EB  F909              TYPE MSLOPE
      02EC  0583
0573                  *       WDEC RESULT,10,0 SLOPE
0574  02ED  F94D              WFLT RESULT
      02EE  0436
0575  02EF  FAA8              JST  SWAP
0576  02F0  F90F              CRLF
0577  02F1  F90F              CRLF
0578  02F2  F951              CLOS
0579                  *
0580  02F3  0171      XABCP   DATA XBPT
0581  02F4  0000      FAC:4   RES  2,0
0582                  *
0583  02F6  9900      PRINT   STA  FAC:1
                      0426
0584  02F7  EE81              STX  FAC:2
0585  02F8  F946              FLT  FAC:1,FAC:1
      02F9  0426
      02FA  0426
0586  02FB  F946              FLT  FAC:2,FAC:2
      02FC  0276
      02FD  0276
```

```
PAGE  0019                          LOW CYCLE FATIGUE

0587  02FE  F943        FMPL FAC:1,STRESV,FAC:1
      02FF  0426
      0300  044E
      0301  0426
0588  0302  E60F        LDX  XABCP
0589  0303  F943        FMPL FAC:2,*STVALP,FAC:2
      0304  0276
      0305  80B4
      0306  0276
0590  0307  C606        LAP  6
0591  0308  9900        STA  OUFLEN   FIELD LENGTH = 6
            05EE
0592  0309  FAA5        JST  CRLF2
0593              *     TAB 2
0594              *     WDEC FAC:3,9,0 CYCLE #
0595              * OUTPUT CYCLE #
0596  030A  F947        FMOV F1,OUFLZ / 1.
      030B  045E
      030C  05F2
0597  030D  F947        FMOV FAC:3,OUFLX
      030E  0278
      030F  05F0
0598  0310  F941        FADD F1E14,OUFLX,OUFLX ELIM 13.99
      0311  05F8
      0312  05F0
      0313  05F0
0599  0314  F900        JST  OUFLFX
            0596
0600  0315  FA95        JST  SPACE
0601              * OUTPUT MODULUS
0602  0316  F947        FMOV F1E6,OUFLZ / 1.E6
      0317  05F4
      0318  05F2
0603  0319  F947        FMOV FAC:4,OUFLX
      031A  02F4
      031B  05F0
0604  031C  F900        JST  OUFLFX
            0596
0605  031D  FA8D        JST  SPACE
0606              * OUTPUT MAX STRESS
0607  031E  F947        FMOV FAC:1,OUFLX
      031F  0426
      0320  05F0
0608  0321  F947        FMOV F1,OUFLZ / 1.
      0322  045E
      0323  05F2
0609  0324  F900        JST  OUFLFX   PRINT NUM
            0596
0610  0325  FA85        JST  SPACE
0611              * STORE STRAIN
0612  0326  F947        FMOV FAC:2,OUTMP1
      0327  0276
      0328  03B5
```

```
PAGE  0020                          LOW CYCLE FATIGUE

0613                        *       TAB 7
0614  0329  FA5D                    JST  PRNTSB
0615  032A  F946                    FLT  UTEMP1,FAC:1
      032B  016E
      032C  0426
0616  032D  F946                    FLT  UTEMP2,FAC:2
      032E  016F
      032F  0276
0617  0330  F943                    FMPL FAC:1,STRESV,FAC:1
      0331  0426
      0332  044E
      0333  0426
0618  0334  E641                    LDX  XABCP
0619  0335  F943                    FMPL FAC:2,*STVALP,FAC:2
      0336  0276
      0337  80B4
      0338  0276
0620                        * OUTPUT MIN STRESS
0621  0339  F947                    FMOV FAC:1,OUFLX
      033A  0426
      033B  05F0
0622  033C  F947                    FMOV F1,OUFLZ / 1.0
      033D  045E
      033E  05F2
0623  033F  F900                    JST  OUFLFX
            0596
0624  0340  FA6A                    JST  SPACE
0625                        * OUTPUT MAX STRAIN
0626  0341  F947                    FMOV F1E13,OUFLZ / 1.E-3
      0342  05F6
      0343  05F2
0627  0344  F947                    FMOV OUTMP1,OUFLX
      0345  03B5
      0346  05F0
0628  0347  F900                    JST  OUFLFX
            0596
0629  0348  FA62                    JST  SPACE
0630                        * OUTPUT MIN. STRAIN
0631  0349  F947                    FMOV F1E13,OUFLZ / 1.E-3
      034A  05F6
      034B  05F2
0632  034C  F947                    FMOV FAC:2,OUFLX
      034D  0276
      034E  05F0
0633  034F  F900                    JST  OUFLFX
            0596
0634  0350  FA5A                    JST  SPACE
0635                        *       TAB 7
0636                        * OUTPUT PLASTIC STRAIN MAX.
0637  0351  F947                    FMOV F1E14,OUFLZ / 1.E-4
      0352  05F8
      0353  05F2
0638  0354  F947                    FMOV OUTMP2,OUFLX
```

```
PAGE  0021                        LOW CYCLE FATIGUE

      0355  03B7
      0356  05F0
0639  0357  F900        JST  OUFLFX
            0596
0640  0358  FA52        JST  SPACE
0641  0359  FA2D        JST  PRNTSB
0642                  * OUTPUT MIN PSTRAIN
0643  035A  F947        FMOV F1E14,OUFLZ / 1.E-4
      035B  05F8
      035C  05F2
0644  035D  F947        FMOV OUTMP2,OUFLX
      035E  03D7
      035F  05F0
0645  0360  F900        JST  OUFLFX
            0596
0646  0361  FA49        JST  SPACE
0647  0362  FA4C        JST  CRLF2
0648  0363  F95A        DIM  2
      0364  0002
0649  0365  F95A        DIM  1
      0366  0001
0650  0367  F951        CLOS
0651                  *
0652                  *
0653  0368  0800  RANDOM EXT
0654  0369  5804        DATA :5804    ICA, GET CONSOLE STATUS
0655  036A  9AEB        STA  RNDTMP   SAVE IT
0656  036B  C6AA        LAP  ;AA      IS THIS AN LSI OR ALPHA?
0657  036C  4404        DATA :4404    OCA
0658  036D  5804        DATA :5804    ICA
0659  036E  3107        JAN  LSI      IT'S AN LSI IF NON-ZERO RESPON
0660  036F  E215        LDX  RN1      ELSE, IT'S AN ALPHA
0661  0370  11A8        RPX  1
0662  0371  6803        SIN  2
0663  0372  B213        LDA  RN2
0664  0373  0110        ZAR
0665  0374  19AE        DATA :19AE    MPS 15
0666  0375  F204        JMP  RNDFIN
0667  0376  0110  LSI   ZAR
0668  0377  E20E        LDX  RN2      ASSURE X-REG POSITIVE FOR LSI
0669  0378  1960        DATA :1960,RN1 MPY RN1
      0379  0385
0670  037A  B2DB  RNDFIN LDA  RNDTMP
0671  037B  4404        DATA :4404    OCA, RESTORE CONSOLE STATUS
0672  037C  13A3        LPX  1
0673  037D  3801        JXN  $+2
0674  037E  C403        LXP  3
0675  037F  EAC5        STX  RN1
0676  0380  EAD5        STX  RNDTMP
0677  0381  F246        FLT  RNDTMP,RNDTMP
      0382  0456
      0383  0456
0678  0384  F71C        RTN  RANDOM
```

```
PAGE  0022                        LOW CYCLE FATIGUE

0679  0385  0003  PN1     DATA 3
0680  0386  00FD  PN2     DATA 253
0681                    *
0682  0387  0800  PRNTSB ENT
0683  0388  F944          FDVD FAC:1,FAC:4,FAC:1
      0389  0426
      038A  02F4
      038B  0426
0684  038C  F943          FMPL FAC:1,F100C,FAC:1
      038D  0426
      038E  0466
      038F  0426
0685  0390  F942          FSUB FAC:2,FAC:1,FAC:1
      0391  0276
      0392  0426
      0393  0426
0686                    *       WDEC FAC:1,9,7 PLASTIC STRAIN
0687                    * STORE MAX. PLASTIC STRAIN
0688  0394  F947          FMOV FAC:1,OUTMP2
      0395  0426
      0396  03B7
0689  0397  F710          RTN  PRNTSB
0690                    *
0691  0398  0800  SWAP   ENT
0692  0399  E23B          LDX  ACMPTB   SWAP THE CONTENTS OF
0693  039A  EA97          STX  TEMP1    CMPTBL & TMPTBL
0694  039B  C206          AXI  6
0695  039C  EA97          STX  TEMP2
0696  039D  C706          LAM  6
0697  039E  9AB7          STA  RNDTMP
0698  039F  E6AC          LDX  XABCP
0699  03A0  B402          LDA  @2
0700  03A1  BC00          EMA  @0
0701  03A2  9C02          STA  @2
0702  03A3  B3FE  SWLOOP LDA  *TEMP1
0703  03A4  BBFF          EMA  *TEMP2
0704  03A5  9BBC          STA  *TEMP1
0705  03A6  DA3B          IMS  TEMP1
0706  03A7  DA3C          IMS  TEMP2
0707  03A8  DAAD          IMS  RNDTMP
0708  03A9  F6C6          JMP  SWLOOP
0709  03AA  F712          RTN  SWAP
0710                    * PRINT SPACE
0711  03AB  0800  SPACE  ENT
0712  03AC  C620          LAP  :20
0713  03AD  F9CE          OTT
0714  03AE  F703          RTN  SPACE
0715                    * DO CRLF - NO PARITY BIT
0716  03AF  0800  CRLF2  ENT
0717  03B0  C60D          LAP  :0D      CR
0718  03B1  F9CE          OTT
0719  03B2  C60A          LAP  :0A      LF
0720  03B3  F90E          OTT
```

```
0721  03B4  F725          RTN  CRLF2
0722  03B5  0000  OUTMP1  RES  2,0
0723  03B7  0000  OUTMP2  RES  2,0
```

```
PAGE  0024                          LOW CYCLE FATIGUE

0725                        *
0726                        ****** CALCULATE SLOPE ******
0727                        *
0728  03B9  F947   SLOPE:  FMOV F0,NMBPTS
      03BA  006E
      03BB  0428
0729  03BC  F947           FMOV F0,XSUM
      03BD  006E
      03BE  042A
0730  03BF  F947           FMOV F0,YSUM
      03C0  006E
      03C1  042C
0731  03C2  F947           FMOV F0,XXSUM
      03C3  006E
      03C4  042E
0732  03C5  F947           FMOV F0,XYSUM
      03C6  006E
      03C7  0430
0733  03C8  F992   SLOPE1 GET  TABLE3
      03C9  04AA
0734  03CA  F228           JMP  LAST
0735  03CB  9A66           STA  TEMP1
0736  03CC  F946           FLT  TEMP1,TEMP2
      03CD  0432
      03CE  0434
0737  03CF  F941           FADD TEMP2,YSUM,YSUM
      03D0  0434
      03D1  042C
      03D2  042C
0738  03D3  F992           GET  TABLE3
      03D4  04AA
0739  03D5  F21D           JMP  LAST
0740  03D6  9A5B           STA  TEMP1
0741  03D7  F946           FLT  TEMP1,TEMP1
      03D8  0432
      03D9  0432
0742  03DA  F943           FMPL TEMP1,TEMP2,TEMP2
      03DB  0432
      03DC  0434
      03DD  0434
0743  03DE  F941           FADD TEMP2,XYSUM,XYSUM
      03DF  0434
      03E0  0430
      03E1  0430
0744  03E2  F941           FADD TEMP1,XSUM,XSUM
      03E3  0432
      03E4  042A
      03E5  042A
0745  03E6  F943           FMPL TEMP1,TEMP1,TEMP1
      03E7  0432
      03E8  0432
      03E9  0432
0746  03EA  F941           FADD TEMP1,XXSUM,XXSUM
```

```
PAGE  0025                          LOW CYCLE FATIGUE

      03EB  0432
      03EC  042E
      03ED  042E
0747  03EE  F941        FADD F1,NMBPTS,NMBPTS
      03EF  045E
      03F0  0428
      03F1  0423
0748  03F2  F62A        JMP  SLOPE1
0749                *
0750  03F3  F943  LAST  FMPL XSUM,YSUM,TEMP1
      03F4  042A
      03F5  042C
      03F6  0432
0751  03F7  F943        FMPL NMBPTS,XYSUM,TEMP2
      03F8  0428
      03F9  0430
      03FA  0434
0752  03FB  F942        FSUB TEMP2,TEMP1,TEMP2
      03FC  0434
      03FD  0432
      03FE  0434
0753  03FF  F943        FMPL XSUM,XSUM,TEMP1
      0400  042A
      0401  042A
      0402  0432
0754  0403  F943        FMPL NMBPTS,XXSUM,XXSUM
      0404  0428
      0405  042E
      0406  042E
0755  0407  F942        FSUB XXSUM,TEMP1,TEMP1
      0408  042E
      0409  0432
      040A  0432
0756  040B  F944        FDVD TEMP1,TEMP2,RESULT
      040C  0432
      040D  0434
      040E  0436
0757  040F  E100        LDX  XABCP
            02F3
0758  0410  F944        FDVD F1,RESULT,RESULT
      0411  045E
      0412  0436
      0413  0436
0759  0414  F943        FMPL RESULT,*LDVALP,RESULT
      0415  0436
      0416  80A0
      0417  0436
0760  0418  F944        FDVD RESULT,*STVALP,RESULT
      0419  0436
      041A  80D4
      041B  0436
0761  041C  F944        FDVD RESULT,FAREA,RESULT
      041D  0436
```

```
PAGE  0026                          LOW CYCLE FATIGUE

      041E  0442
      041F  0436
0762  0420  F943        FMPL RESULT,F1000,RESULT
      0421  0436
      0422  0466
      0423  0436
0763  0424  F951        CLOS
0764              *

PAUSE
0765              *
0766              *
0767  0425  058A  ACMPTB DATA CMPTBL
0768  0426  0000  FAC:1  RES  2,0
0769  0428  0000  NMBPTS RES  2,0
0770  042A  0000  XSUM   RES  2,0
0771  042C  0000  YSUM   RES  2,0
0772  042E  0000  XXSUM  RES  2,0
0773  0430  0000  XYSUM  RES  2,0
0774  0432  0000  TEMP1  RES  2,0
0775  0434  0000  TEMP2  RES  2,0
0776  0436  0000  RESULT RES  2,0
0777  0438  0000  TEMPAV RES  2,0
0778  043A  0000  FCYCLE RES  2,0
0779  043C  0000  FTHICK RES  2,0
0780  043E  0000  FWIDTH RES  2,0
0781  0440  0000  WIDTH  RES  2,0
0782  0442  0000  FAREA  RES  2,0
0783  0444  0000  STRSLM RES  2,0
0784  0446  0000  MAXLIM RES  2,0
0785  0448  0000  MINLIM RES  2,0
0786  044A  0000  SPRATE RES  2,0
0787  044C  0000  CLMPT  RES  2,0
0788  044E  0000  STRESS RES  2,0
0789  0450  0000  AUGSTN RES  2,0
0790  0452  0000  HRNGE  RES  2,0
0791  0454  0000  LRNGE  RES  2,0
0792  0456  0000  RNDTRP RES  2,0
0793  0458  0000  NN     RES  2,0
0794  045A  0000  XX     RES  2,0
0795  045C  0000  MOD    RES  2,0
0796  045E  4080  F1     DATA :4080,0
      045F  0000
0797  0460  4180  F4     DATA :4180,0
      0461  0000
0798  0462  41A0  F5     DATA :41A0,0
      0463  0000
0799  0464  4220  F10    DATA :4220,0
      0465  0000
0800  0466  457A  F1000  DATA :457A,0
      0467  0000
0801              *
0802              *
0803              *
0804              *
```

```
PAGE  0027                          LOW CYCLE FATIGUE

0805          0000  LOAD    EQU  0
0806          0001  STROKE  EQU  1
0807          0002  STRAIN  EQU  2
0808                *
0809          0000  UP      EQU  0
0810          8000  DOWN    EQU  :8000
0811                *
0812                *
0813          0074  F32767  EQU  :74
0814          007A  F:PI    EQU  :7A
0815          006E  F0      EQU  :6E
0816          0070  F2      EQU  :70
0817          0097  GETSTA  EQU  :97
0818                *
0819                *
0820          00A0  LDVALP  EQU  :A0
0821          00B4  STVALP  EQU  :B4
0822                *
0823  0469    0000  TABLE1  RES  33,0
0824  0489    0000  TABLE2  RES  33,0
0825  04AA    0000  TABLE3  RES  23,0
0826  04C1    0000  TABLE4  RES  33,0
0827                *
0828  04E2    0000  NULL    RES  20,0
0829  04F6    C0C0          TEXT '@@'
0830                *
0831  04F7    C4C9  MAREA   TEXT 'DIMS. (THICK,WIDTH):: @'
      04F8    CDD3
      04F9    AEA0
      04FA    A8D4
      04FB    C8C9
      04FC    C3CB
      04FD    ACD7
      04FE    C9C4
      04FF    D4C8
      0500    A9BA
      0501    BAA0
      0502    C0A0
0832  0503    CDC9  MMSTPS  TEXT 'MIN. STRESS (KSI): @'
      0504    CEAE
      0505    A0D3
      0506    D4D2
      0507    C5D3
      0508    D3A0
      0509    A8CB
      050A    D3C9
      050B    A9BA
      050C    A0C0
0833  050D    D3D4  MSTRLM  TEXT 'STRAIN LMTS (+,-):: @'
      050E    D2C1
      050F    C9CE
      0510    A0CC
      0511    CDD4
```

```
PAGE  0028                          LOW CYCLE FATIGUE

      0512  D3A0
      0513  A8AB
      0514  ACAD
      0515  A9BA
      0516  BAA0
      0517  C0A0
0834  0518  D2C1  RNDMES TEXT 'RANDOM LMTS (Y,N): 0'
      0519  C2C4
      051A  CFCD
      051B  A0CC
      051C  CDD4
      051D  D3A0
      051E  A8D9
      051F  ACCE
      0520  A9BA
      0521  A0C0
0835  0522  D3D4  MRATE  TEXT 'STRAIN RATE (1/SEC): 0'
      0523  D2C1
      0524  C9CE
      0525  A0D2
      0526  C1D4
      0527  C5A0
      0528  A8B1
      0529  AFD3
      052A  C5C3
      052B  A9BA
      052C  A0C0
0836  052D  C5D8  MEXEC  TEXT 'EXECUTE0'
      052E  C5C3
      052F  D5D4
      0530  C5C0
0837  0531  D2C5  RESETM TEXT 'RESET RANDOM NOS. (Y,N): 0'
      0532  D3C5
      0533  D4A0
      0534  D2C1
      0535  CEC4
      0536  CFCD
      0537  A0CE
      0538  CFD3
      0539  AEA0
      053A  A8D9
      053B  ACCE
      053C  A9BA
      053D  A0C0
0838                *
0839  053E  C0C0  BUFFID RES  26,:C0C0
0840                *
0841  0558  C3D9  MHEAD  TEXT 'CYCLES MODULUS (+)STRESS(-)'
      0559  C3CC
      055A  C5D3
      055B  A0CD
      055C  CFC4
      055D  D5CC
```

```
PAGE  0029                        LOU CYCLE FATIGUE

      055E  D5D3
      055F  A0A3
      0560  ABA9
      0561  D3D4
      0562  D2C5
      0563  D3D3
      0564  A8AD
      0565  A9A0
0842  0566  A0A8        TEXT ' (+)T.DISPL.(-) '
      0567  ABA9
      0568  D4AE
      0569  C4C9
      056A  D3D0
      056B  CCAE
      056C  A8AD
      056D  A9A0
0843  056E  A3AB        TEXT '(+)PLASTIC(-)@'
      056F  A9D0
      0570  CCC1
      0571  D3D4
      0572  C9C3
      0573  A8AD
      0574  A9C0
0844  0575  C3D9  MLAST  TEXT 'CYCLES= @'
      0576  C3CC
      0577  C5D3
      0578  BDA0
      0579  C0A0
0845  057A  C1D6  MAVGS  TEXT 'AVG PEAK STRAIN= @'
      057B  C7A0
      057C  D0C5
      057D  C1CB
      057E  A0D3
      057F  D4D2
      0580  C1C9
      0581  CEBD
      0582  A0C0
0846  0583  D3CC  MSLOPE TEXT 'SLOPE(PSI)= @'
      0584  CFD0
      0585  C5A8
      0586  D0D3
      0587  C9A9
      0588  BDA0
      0589  C0A0
0847  058A  0000  CMPTBL RES  6,0
0848  0590  0000  TMPTBL RES  6,0
0849              *
0850              *
0851              * SUBROUTINE TO CONVERT FLOAT TO FIX POINT.
0852  0596  0300  OUFLFX ENT
0853              *
0854              * OUTPUT FIX POINT NUMBERS
0855              * AT CALL:  OUFLEN - CONTAINS (INT) FIELD LENGTH
```

```
PAGE  0030                    LOW CYCLE FATIGUE

0856                *          OUFLX  - X (F.P.) # TO BE OUTPUT (LOST)
0857                *         OUFLZ - Z(F.P.) NUM TO DIVIDE BY: Z=Z/10
0858                *
0859  0597  B256           LDA  OUFLEN   SAVE LENGTH
0860  0598  9A56           STA  OUFLN2
0861  0599  EA53           STX  OUSAVX   SAVE X-REG
0862  059A  0000           NOP
0863  059B  0000           NOP
0864  059C  0000           NOP
0865  059D  0000           NOP
0866  059E  0000           NOP
0867  059F  0000           NOP
0868  05A0  F944           FDVD OUFLX,OUFLZ,OUFLZ Z=X/Z (RIGHT UNITS)
      05A1  05F0
      05A2  05F2
      05A3  05F2
0869  05A4  0110           ZAP
0870  05A5  9A46           STA  OUPK     K=0
0871  05A6  C701           LAM  1
0872  05A7  3A47           ADD  OUFLN2   L=L-1
0873  05A8  2095           JAM  A        RETURN
0874  05A9  9A45           STA  OUFLN2
0875                *
0876                * PRINT SIGN (+ OR -)
0877                *
0878  05AA  F948           FCMP OUFLZ,F0 SEE IF Z<0 OR >0,A=-1,OR +1
      05AB  05F2
      05AC  006E
0879  05AD  3096           JAP  OU2      Z>0
0880  05AE  0043           TAX           (SAVE A)
0881  05AF  F942           FSUB F0,OUFLZ,OUFLZ Z=ABS(Z)
      05B0  006E
      05B1  05F2
      05B2  05F2
0882  05B3  0030           TXA           (RESTORE A)
0883  05B4  3101  OU2      JAN  $+2
0884  05B5  C601           LAP  1        A=1,IF Z=0
0885  05B6  0308           NAX           X=-A
0886  05B7  C22C           AXI  :2C      X=:2C -(A)
0887  05B8  0030           TXA           A=X = "+" OR "-"
0888  05B9  F90E           OTT           PRINT "+" OR "-"
0889  05BA  C601           LAP  1        A=1
0890  05BB  9A2F  OU1      STA  OUPJ     J=1
0891  05BC  C701  OULOOP   LAM  1        A=-1
0892  05BD  8A31           ADD  OUFLN2   L=L-1
0893  05BE  20AA  A        JAM  OUPET    RETURN
0894  05BF  9A2F           STA  OUFLN2
0895  05C0  F948  OU3      FCMP OUFLZ,F1
      05C1  05F2
      05C2  045E
0896  05C3  2088           JAM  OU3B     Z<1
0897  05C4  F944           FDVD OUFLZ,F10,OUFLZ Z=Z/10
      05C5  05F2
```

```
PAGE  0031                        LOW CYCLE FATIGUE

      05C6  0464
      05C7  05F2
0898  05C8  C601        LAP  1
0899  05C9  8A21        ADD  OUPJ      J=J+1
0900  05CA  9A20        STA  OUPJ
0901  05CB  F60B        JMP  OU3
0902  05CC  C601  OU3B  LAP  1
0903  05CD  8A1E        ADD  OUPK      K=K+1
0904  05CE  9A1D        STA  OUPK      STORE K
0905  05CF  921B        SUB  OUPJ      A=K-J
0906  05D0  3103        JAN  OU4
0907                    * PRINT DECIMAL POINT
0908  05D1  C62E        LAP  :2E
0909  05D2  F90E        OTT
0910  05D3  F617        JMP  OULOOP
0911  05D4  F943  OU4   FMPL OUFLZ,F10,OUFLZ Z=Z*10
      05D5  05F2
      05D6  0464
      05D7  05F2
0912  05D8  F945        FIX  OUFLZ,OUFLX X=INT(Z)
      05D9  05F2
      05DA  05F0
0913  05DB  F946        FLT  OUFLX,OUFLX BACK TO F.P.
      05DC  05F0
      05DD  05F2
0914  05DE  F942        FSUB OUFLZ,OUFLX,OUFLZ Z=10*Z-INT(10*Z)
      05DF  05F2
      05E0  05F0
      05E1  05F2
0915  05E2  F945        FIX  OUFLX,OUFLX BACK TO FIX
      05E3  05F0
      05E4  05F0
0916                    * PRINT DIGIT
0917  05E5  C630        LAP  :30
0918  05E6  8A09        ADD  OUFLX
0919  05E7  F90E        OTT
0920  05E8  F62C        JMP  OULOOP
0921                    * RETURN
0922  05E9  E203  OUPET  LDX  OUSAVX    RESTORE X
0923  05EA  F754        RTN  OUFLFX
0924                    *    DATA
0925                    *
0926  05EB  0000  OUPJ    DATA 0         DECIMAL POINT LOCATOR
0927  05EC  0000  OUPK    DATA 0         CHARACTER POINTER
0928  05ED  0000  OUSAVX  DATA 0         XREG
0929  05EE  0000  OUFLEN  DATA 0         FIELD LEN.
0930  05EF  0000  OUFLN2  DATA 0         TEMP
0931  05F0  0000  OUFLX   RES  2,0       (F.P.) X
0932  05F2  0000  OUFLZ   RES  2,0       (F.P) Z
0933  05F4  4A74  F1E6    DATA :4A74,:2400 1.E6
      05F5  2400
0934  05F6  3B83  F1E3    DATA :3B83,:126F 1.E-3
      05F7  126F
```

```
PAGE  0032                              LOW CYCLE FATIGUE

0935  05F8  39D1  F1E14   DATA :39D1,:B717 1.E-4
      05F9  B717
0936                    *
0937                          END
```

PAGE 0033 LOW CYCLE FATIGUE

ACMPTS	0425	AUGSTN	0450	A	05BE	BEGIN	001B
BRANCH	01C7	BREAK	016A	BUFFID	053E	CLEAR1	0057
CLEAR2	0076	CLKRT	044C	CLR2	007D	CMPTBL	058A
CNTN1	0169	CNT	0177	CPLF2	03AF	CUPLD	013D
CURSTN	013E	CURSTP	00C2	CYADJ	0141	CYAD2	014B
CYAD3	014F	DATA01	01AF	DATA02	024F	DATN1	0156
DATPX	0173	DATPY	0179	DLTLD	0139	DLTSTI	0139
DOWN	8000	EMPTY	02D6	FAC:1	0426	FAC:2	0276
FAC:3	0278	FAC:4	02F4	FAREA	0442	FCYCLE	043A
FINAL	027A	FUM1	00C4	FNM2	00C6	FNM3	00C8
FTCYC	013F	FTHICK	043C	FULLN1	0163	FULL	0260
FWIDTH	043E	F0	006E	F1EM3	05F6	F1EM4	05F8
F1E6	05F4	F1	045E	F10	0464	F1000	0466
F2	0070	F3	00CA	F32767	0074	F4	0460
F5	0462	F:PI	007A	GETNUM	0176	GETSTA	0097
HLIMIT	00BE	HPAGE	0458	INCDIE	0134	INCTBL	0125
INCTB2	0127	INDEX	0172	INDEX1	00DD	INITCX	0270
INITCY	00A8	I300	013B	LAST	03F3	LDVALP	00A2
LLIMIT	00C0	LOAD	0000	LOAD2	013C	LOOP3	028D
LPAGE	0454	LSI	0376	MAREA	04F7	MAVGS	057A
MAXLIM	0446	MDFLG	016D	MD	0274	MD2ND	01E3
MEXEC	052D	MHEAD	0558	MINLIM	0448	MLAST	0575
MMSTRS	05C3	MOD	045C	MPATE	0522	MSLOPE	0583
MSTRLM	05CD	NAME	0007	NMBPTS	0428	NMMESS	00CC
NN	0458	NOT1	01DC	NULL	04E2	NUM	016C
NUM1	016B	NIX	0155	N1	0150	OLDLD	0137
OUFLEN	05EE	OUFLFX	0596	OUFLN2	05EF	OUFLY	05F0
OUFLZ	05F2	OULOOP	05BC	OUPJ	05EB	OUPK	05EC
OURET	05E9	OUSAVX	05ED	OUTMP1	03B5	OUTMP2	03E7
OU1	05EB	OU2	05E4	OU3B	05CC	OU3	05C0
OU4	05D4	PRINTV	02AE	PRINT	02F6	PRTSB	0387
RANDOM	0369	RESETM	0531	RESET1	00E1	RESTRT	00D6
RESULT	0426	REVDTN	021E	REVUP	0195	RMPDN	025D
RMPUP	01C4	RNDFIN	037A	RNDFLG	0175	RNDMES	0518
RNDMLT	0270	RNDM	00C3	RNDTMP	0456	RNIPTR	0174
RNI	0385	RN2	0386	ROUND	004B	RSTEX	00ED
RSTRT0	00E5	RVDN	0224	SAVE2	00EB	SETPTR	0271
SETTBL	0112	SETTB2	011F	SLOPE1	03C8	SLOPE:	03B0
SPACE	03AB	SPRATE	044A	STAT:A	0266	STAT:B	0269
STRAIN	0002	STRESS	0272	STRESV	044E	STROKE	0291
STRSLM	0444	STVALP	00B4	SWAP	0398	SVLOOP	03A3
TABLE1	0469	TABLE2	0489	TABLE3	04AA	TABLE4	04C1
TEMPAV	0438	TEMP1	0432	TEMP2	0434	TMPTBL	0590
UPDATE	017A	UPEXIT	021D	UP	0000	UP:	01C8
UTEMP1	016E	UTEMP2	016F	VALPTR	00C4	VIDTH	044C
WINKER	026D	WTCLR	0072	XABCP	02F3	XABC	0170
XBPT	0171	XC	0173	XIT	021B	XSUM	042A
XXSUM	042E	XX	045A	XX2	0233	XX3	01A1
XYSUM	0430	YSUM	042C				

APPENDIX II

SOURCE LISTING OF FORTRAN PROGRAM FOR STRESS AND STRAIN COMPUTATIONS AND PLOTTING

```
      PROGRAM DATA (OUTPUT,TAPE1,TAPE2,TAPE3,TAPE4,                     000110
     1 TAPE5,TAPE6,INPUT=/7.)                                           000120
C                                                                       000130
C          ************************                                     000140
C          THIS PROGRAM DEVELOPED BY                                    000150
C             CAPT ROBERT SCHAFRIK                                      000160
C                  MAY,1979                                             000170
C          ************************                                     000180
C                                                                       000190
      COMMON /A/ N(1500),E(1500),SIGMA1(1500),SIGMA2(1500),ELONG1(1500),000200
     AELONG2(1500),PLST1(1500),PLST2(1500),TITL(60),R1(1500),           000210
     BDELTEP(1500)                                                      000220
      REAL N                                                            000230
C                                                                       000240
C     IFLAG = YES       FOR COMPUTER DATA                               000250
C     IFLAG = NO    FOR NO COMPUTER DATA                                000260
C     IFLAG1 = YES FOR COMPUTER DATA PRINT-OUT (DATA ON P.F.)           000270
C     IUNIT IS THE TAPE NUMBER                                          000280
C                                                                       000290
      READ 4,IFLAG,IUNIT,IFLAG1                                         000300
 4    FORMAT ( / A1,4X,I1,4X,A1)                                        000310
C                                                                       000320
      IF (IUNIT.LE.0.OR.IUNIT.GT.6) IUNIT=1                             000330
      PRINT  8,IFLAG,IUNIT,IFLAG1                                       000340
 8    FORMAT (1H1,T2,*FROM DATA :   COMPUTER DATA = *,A1,               000350
     A/T2,*TAPE UNIT IS *,I1  /                                         000360
     BT4,*COMPUTER DATA FLAG IS *,A1//)                                 000370
      IF (IFLAG.NE.1HY) GO TO 50                                        000380
C                                                                       000390
      READ (IUNIT,9) (TITL(JT),JT=1,60)                                 000400
 9    FORMAT(60A1)                                                      000410
C                                                                       000420
      IMAX=1500                                                         000430
      I=0                                                               000440
    1 CONTINUE                                                          000450
      I=I+1                                                             000460
      IF (I.GT.IMAX) GO TO 1000                                         000470
C                                                                       000480
      READ (IUNIT,10) N(I),E(I),SIGMA1(I),SIGMA2(I),ELONG1(I),ELONG2(I),000490
     1PLST1(I),PLST2(I)                                                 000500
 10   FORMAT (8(F7.0,1X))                                              000510
C                                                                       000520
      IF(N(I).LT.0.9)  GO TO 3                                          000530
      IF (EOF(IUNIT))2,1                                                000540
 3    CONTINUE                                                          000550
      PRINT 30                                                          000560
 30   FORMAT (T2,*READ TERMINATED BY ZERO VALUE*)                       000570
      I=I-1                                                             000580
      GO TO 40                                                          000590
 1000 CONTINUE                                                          000600
      I=IMAX                                                            000610
      PRINT 1001,I                                                      000620
 1001 FORMAT(T2,4H**** ,2X,*IMAX = *,I5,2X,                             000630
     1 *DATA PTS EXCEED ARRAY DIMENSIONS*,//)                           000640
      GO TO 40                                                          000650
 2    CONTINUE                                                          000660
      PRINT 31                                                          000670
 31   FORMAT (T2,*READ TERMINATED BY EOF*)                              000680
      I=I-1                                                             000690
 40   CONTINUE                                                          000700
      PRINT 18,(TITL(JA),JA=1,60)                                       000710
 18   FORMAT (// T2,60A1, /T2,60(1H*)//)                                000720
      PRINT 11,I                                                        000730
```

```
 11   FORMAT(                              /T2,*NUMBER OF DATA PTS = *,I5   000740
     1, ///)                                                               000750
      IF (I.EQ.0) STOP                                                     000760
      DO 20 J=1,I                                                          000770
      IF (IFLAG1.NE.1HY)  GO TO 45                                         000780
      PRINT 21,   N(J),E(J),SIGMA1(J),SIGMA2(J),ELONG1(J),                 000790
     1ELONG2(J),PLST1(J),PLST2(J)                                          000800
 21   FORMAT (T2,F7.0, 3(1X,F7.2), 4(1X,F7.3))                             000810
 45   CONTINUE                                                             000820
      E(J)=E(J)*1.E6                                                       000830
      ELONG1(J)=ELONG1(J)*1.E-3                                            000840
      ELONG2(J)=ELONG2(J)*1.E-3                                            000850
      PLST1(J)=PLST1(J)*1.E-3                                              000860
      PLST2(J)=PLST2(J)*1.E-3                                              000870
 20   CONTINUE                                                             000880
      CALL LCF(I)                                                          000890
      GO TO 51                                                             000900
 50   CONTINUE                                                             000910
      I=0                                                                  000920
      PRINT 55                                                             000930
 55   FORMAT (// T2,*NO COMPUTER DATA*, ///)                               000940
C                                                                          000950
      READ 9,TITL                                                          000960
C                                                                          000970
      PRINT 18, (TITL(JA),JA=1,50)                                         000980
      CALL LCF(I)                                                          000990
 51   CONTINUE                                                             001000
      CALL DATA1                                                           001010
      CALL SUBPLOT(I)                                                      001020
      STOP                                                                 001030
      END                                                                  001040
C                                                                          001050
C*************************************************************           001060
C                                                                          001070
      SUBROUTINE LCF(I)                                                    001080
      COMMON /A/ N(1500),E(1500),SIGMA1(1500),SIGMA2(1500),ELONG1(1500),   001090
     AELONG2(1500),PLST1(1500),PLST2(1500),TITL(50),R1(1500),              001100
     BDELTEP(1500)                                                         001110
      COMMON /D/ LPLST,LELST                                               001120
      REAL LPLST,LELST,N                                                   001130
      DIMENSION MSIG(1500)                                                 001140
      DIMENSION DELTSIG(1500),DELTEL(1500),DELTPL(1500),DELTEE(1500),      001150
     ADELTSTN(1500)                                                        001160
      EQUIVALENCE (E(1),DELTSIG(1)) , (ELONG1(1),DELTEL(1)) ,              001170
     A(ELONG2(1),DELTPL(1)) ,(PLST1(1),DELTEE(1)) ,                        001180
     B(PLST2(1),DELTSTN(1))                                                001190
C                                                                          001200
      DATA MSIG /1500*(1H )/                                               001210
      DATA IFLG /0/                                                        001220
C                                                                          001230
C                                                                          001240
      READ *,EACT,LELST,LPLST,SFACTOR,DFACTOR,IFLG                         001250
C                                                                          001260
C     EACT IS ACTUAL ELASTIC MODULUS IN E6 PSI                             001270
C     LELST IS AN ASSUMED ELASTIC EFFECTIVE GAGE LENGTH                    001280
C     LPLST IS EFFECTIVE PLASTIC GAGE LENGTH                               001290
C     SFACTOR - COMPUTER STRESS CORRECTION FACTOR                          001300
C     DFACTOR - DISPL CORRECTION FACTOR, COMPUTER                          001310
C     IFLG IS USED TO SPECIFY DATA PRINT-OUT                               001320
C      FOR PRINT-OUT, USE 1                                                001330
C                                                                          001340
C                                                                          001350
      PRINT 23,EACT,LELST,LPLST,SFACTOR,DFACTOR,IFLG                       001360
 23   FORMAT (T2,*FROM LCF* / T2,*EACT = *,E12.5,*, LELST = *, E12.5,      001370
     Z*  LPLST = *, E12.5 / T3,3H***,                                      001380
     1*, SFACTOR = *, E12.5, *, DFACTOR = *, E12.5 / ,                     001390
```

```
     AT3,*COMPUTER DATA PRINT-OUT FLAG IS = *,I1 //)                    001400
C                                                                       001410
      IF (I.EQ.0) RETURN                                                001420
C                                                                       001430
      EACT=EACT*1.E+6                                                   001440
      DELTEET=0.0                                                       001450
C                                                                       001460
      DO 9  J=1,I                                                       001470
      DELTEET=DELTEET+E(J)                                              001480
 9    CONTINUE                                                          001490
C     ASSUME MINI-COMPUTER INTERNAL ARITHMETIC IS OK                    001500
      DELTEET=DELTEET/I*(1.00/1.00)                                     001510
      LELST=EACT/DELTEET                                                001520
C                                                                       001530
      DO 10  J=1,I                                                      001540
      SIGMA1(J)=SIGMA1(J)*SFACTOR                                       001550
      SIGMA2(J)=SIGMA2(J)*SFACTOR                                       001560
      ELONG1(J)=ELONG1(J)*DFACTOR                                       001570
      ELONG2(J)=ELONG2(J)*DFACTOR                                       001580
      DELTSIF=SIGMA1(J)-SIGMA2(J)                                       001590
      DELTEK=ELONG1(J)-ELONG2(J)                                        001600
C     ELASTIC STRAIN = SIGMA/E = (UT-UP)/LELST                          001610
C                                                                       001620
      PL1=PLST1(J)                                                      001630
      PLST1(J)=ELONG1(J)-(LELST*SIGMA1(J)*1.E+3/EACT)                   001640
      PL2=PLST2(J)                                                      001650
      PLST2(J)=ELONG2(J)-(LELST*SIGMA2(J)*1.E+3/EACT)                   001660
      DELTPK=PLST1(J)-PLST2(J)                                          001670
      IF (DELTPK.LE.1.E-6)  GO TO 11                                    001680
 12   CONTINUE                                                          001690
      DELTED=(DELTEK-DELTPK)/LELST                                      001700
      DELTEP(J)=(DELTPK/LPLST)                                          001710
      DELTSTM=DELTED+DELTEP(J)                                          001720
      R1(J)=ABS(SIGMA1(J)/SIGMA2(J))                                    001730
      GO TO 8                                                           001740
 11   CONTINUE                                                          001750
      PLST1(J)=PL1*LELST                                                001760
      PLST2(J)=PL2*LELST                                                001770
      MSIG(J)=1H*                                                       001780
      DELTPK=PLST1(J)-PLST2(J)                                          001790
      RPL=DELTSIF/DELTEET                                               001800
      DISPDIF=RPL/DELTEK                                                001810
      DRATIO=DISPDIF*DFACTOR*1.E3                                       001820
      PRINT 101, N(J),DRATIO                                            001830
101   FORMAT(T3,*CORRECTION FACTOR FOR DISPLACEMENTS: N = *,            001840
     AF6.1,3X,*SUGGESTED DFACTOR = *,F6.4)                              001850
      IF (DELTPK.GT.1.E-6)  GO TO 12                                    001860
      MSIG(J)=1HX                                                       001870
      DELTPK=1.E-5                                                      001880
      GO TO 12                                                          001890
 8    CONTINUE                                                          001900
      E(J)=DELTSIF                                                      001910
      ELONG1(J)=DELTEK                                                  001920
      ELONG2(J)=DELTPK                                                  001930
      PLST1(J)=DELTED                                                   001940
      PLST2(J)=DELTSTM                                                  001950
 10   CONTINUE                                                          001960
C                                                                       001970
      PRINT 20,(TITL(JA),JA=1,31)                                       001980
 20   FORMAT(1H1,T40,*INSTRON COMPUTER*/ T28,                           001990
     Z*DATA FOR *, 3A1 / T28,40(1H*), 3(/),                             002000
     XT59, *RATIO*, /  T56, *MAX STRESS*,/                              002010
     1T11,*TOTAL*, T20,*PLASTIC*, T30 ,                                 002020
     2*STRESS*, T40,*MAX*, T49, *MIN*,T60, *TO*, T68, *ELASTIC*,        002030
     3T79, *PLASTIC*, T89,*STRAIN*  /                                   002040
     4 T2,*CYCLES*,                  T11, *ELONG*,  T21, *ELONG*,  T30, 002050
```

```
     5        *RANGE*,  T40,*STRESS*,                                          002060
     6  T48,  *STRESS*,  T56,  *MIN STRESS*,  T68,  *STRAIN*,                  002070
     7 T79,  *STRAIN*,  T89,  *RANGE*/,                                       002080
     8                  T10,*(INCHES)*,  T20,  *(INCHES)*,  T30,              002090
     9       *(KSI)*,  T4.,  *(KSI)*,  T48,                                   002100
     A *(KSI)*, T68, *(PCNT)*,  T79, *(PCNT)*,  T89, *(PCNT)* /)              002110
C                                                                             002120
      DO 30  K=1,I                                                            002130
      DELTEP(K)=DELTEP(K)*100.                                                002140
      DELTEE(K)=DELTEE(K)*100.                                                002150
      DELTSTN(K)=DELTSTN(K)*100.                                              002160
      NT=N(K)                                                                 002170
C                                                                             002180
C USE TO ELIMINATE PRINTING                                                   002190
C                                                                             002200
      IF (IFLG.NE.1)  GO TO 99                                                002210
C                                                                             002220
      PRINT 22,NT,     DELTEL(K),DELTPL(K),                                   002230
     1DELTSIG(K),SIGMA1(K),SIGMA2(K),R1(K),DELTEE(K),                         002240
     3DELTEP(K),DELTSTN(K),MSIG(K)                                            002250
 22   FORMAT (T2, I5,              T11,  F6.5,  T21,  F6.5, T30,              002260
     1    F7.2, T40,  F5.1, T48,  F6.1, T56,  F7.3,                          002270
     3  T68,F5.3,T79,F6.4,  T89,  F5.3,T120,A1)                              002280
C                                                                             002290
 99   CONTINUE                                                                002300
C                                                                             002310
 30   CONTINUE                                                                002320
      PRINT 40                                                                002330
 40   FORMAT(///  )                                                          002340
      PRINT 31,DELTEET,LELST                                                  002350
 31   FORMAT (1H1,                                                            002360
     1        T ,*THE AVERAGE MODULUS FOR THIS DATA WAS*,E12.5,*   PSI*,      002370
     2 / T2,*EFFECTIVE ELASTIC GAGE LENGTH IS *,E12.5,* INCHES*/)             002380
      RETURN                                                                  002390
      END                                                                     002400
C                                                                             002410
C*************************************************************              002420
C                                                                             002430
      SUBROUTINE DATA1                                                        002440
      COMMON /A/ BA(12000),TITL(60),BB(3000)                                  002450
      COMMON /C/ SIGC(70) ,STRT(70) ,STRP(70) ,STRNC(70) ,NC(70) ,KI,         002460
     ZDELTELC(70),DELTPLC(70)                                                 002470
      INTEGER UNITS,DATASTS                                                   002480
      REAL NC                                                                 002490
C                                                                             002500
      READ 11,DATASTS                                                         002510
 11   FORMAT(I1)                                                              002520
C                                                                             002530
      IF (DATASTS.LE.0)  GO TO 50                                             002540
C                                                                             002550
      KA=0                                                                    002560
      DO 15 M=1,DATASTS                                                       002570
C                                                                             002580
C     FOR CHART DIMENS IN M4,USE  M                                           002590
C     FOR CHART DIMENSIONS IN INCHES, USE  I                                  002600
C                                                                             002610
      READ 2,UNITS,FCTR                                                       002620
 2    FORMAT (A1,4X,F5.0)                                                     002630
C                                                                             002640
      PRINT 9,TITL                                                            002650
 9    FORMAT(/ T2,80(1H$)/ T2,60A1)                                           002660
      PRINT 6,UNITS,FCTR                                                      002670
 6    FORMAT (/T2,*FROM DATA1, UNITS = *,A1 ,/,                               002680
     AT2,*ADD THESE NUMBER OF CYCLES TO DATA *,1X,F5.0/)                      002690
      IF (UNITS.EQ.1HI.OR.UNITS.EQ.1HM) GO TO 51                              002700
      GO TO 50                                                                002710
```

```
 51   CONTINUE                                                          002720
C                                                                      002730
C     CALSIG IS CALIBRATION FACTOR FOR LOAD SCALE ON H-P CHART         002740
C     CALDIS1 IS EXTENSOMETER CALIB FACTOR                             002750
C     CALDIS2 IS CALIBRATION FACTOR FOR H-P CHART                      002760
C     SPECA IS SPECIMEN AREA                                           002770
      READ *,CALSIG,CALDIS1,CALDIS2,SPECA                              002780
C                                                                      002790
      PRINT 10,CALSIG,CALDIS1,CALDIS2,SPECA                            002800
 10   FORMAT (// T2,*FROM DATA1*/ T2,*H-P CHART LOAD SCALE CALIBRATION 002810
     1IS *, F7.5,                                                      002820
     2 /.T2,*EXTENSOMENTER CALIBRATION FACTOR IS *, F7.5,              002830
     4 / T2, *H-P CHART DISPLACEMENT SCALE CALIBRATION IS *,F7.5,      002840
     5 / T2,*SPECIMEN AREA = *,F7.5 /)                                 002850
      PRINT 29,UNITS                                                   002860
 29   FORMAT (T2,* UNITS DESIG IS *, A2/)                              002870
      CALDIS=CALDIS1*CALDIS2                                           002880
C                                                                      002890
      KT=KA                                                            002900
 100  CONTINUE                                                         002910
      KA=KA+1                                                          002920
      IF (KA.GT.70)  GO TO 70                                          002930
C                                                                      002940
      READ *,NC(KA),STRT(KA),STRP(KA),SIGC(KA)                         002950
C     USE -1. TO TERMINATE READING DATA STRING                         002960
C     PRINT *,NC(KA),STRT(KA),STRP(KA),SIGC(KA)                        002970
      IF(NC(KA).LT.0.3) GO TO 103                                      002980
      NC(KA)=NC(KA)+FCTR                                               002990
      GO TO 100                                                        003000
 70   CONTINUE                                                         003010
      PRINT 71                                                         003020
 71   FORMAT (4(/)  T3,*EXCEEDED ARRAY DIMENSIONS IN DATA1*,3(/))      003030
 103  CONTINUE                                                         003040
      PRINT 4                                                          003050
 4    FORMAT(// T2,*CYCLES*, T10,*T.DISP*, T18,*PL.DISP*,T28,          003060
     1*STRESS*/)                                                       003070
      KA=KA-1                                                          003080
      KI=KA                                                            003090
      KS=KT+1                                                          003100
C                                                                      003110
      DO 1 J=KS,KI                                                     003120
      PRINT 5,NC(J),STRT(J),STRP(J),SIGC(J)                            003130
 5    FORMAT (T2,F5.0,T10,F5.2,T18,F5.2,T28,F5.2)                      003140
 1    CONTINUE                                                         003150
      CALL DATA2 (CALSIG,CALDIS,SPECA,UNITS,KS)                        003160
 15   CONTINUE                                                         003170
C                                                                      003180
      PRINT 9                                                          003190
      PRINT 21,(TITL(JA),JA=1,31)                                      003200
 21   FORMAT (1H1,T28,*HYSTERESIS LOOP*,/                              003210
     AT16,*DATA FOR *, 31A1/                                           003220
     BT16,40(1H*),  3(/)                                               003230
     CT10,*TOTAL*,  T20,*PLASTIC*,T31,                                 003240
     D*STRESS*,  T42,*ELASTIC*,  T53,                                  003250
     E*PLASTIC*,  T65,*STRAIN*  /  T2                                  003260
     F,*CYCLES*,  T11,*ELONG*,  T21, *ELONG*,                          003270
     GT31, *RANGE*,  T42, *STRAIN*,  T53,                              003280
     H*STRAIN*,  T65,*RANGE*  ,  /   T10,                              003290
     I*(INCHES)*,  T20,  *(INCHES)*,  T31,                             003300
     J*(KSI)*, T42,  *(PCNT)*,  T53,*(PCNT)*,                          003310
     KT65, *(PCNT)* /)                                                 003320
C                                                                      003330
      DO 28  MC=1,KI                                                   003340
      NT=NC(MC)                                                        003350
      PRINT 22,NT,DELTELC(MC),DELTPLC(MC),SIGC(MC),                    003360
     ASTRT(MC),STRP(MC),STRNC(MC)                                      003370
```

```
 22   FORMAT(T2,I5,T11,F6.5,T21,F6.5,T30,F7.2,T42,F5.3                  003380
     AT53,F6.4,T65,F5.3)                                               003390
 28   CONTINUE                                                          003400
      PRINT 27                                                          003410
 27   FORMAT (1H1)                                                     003420
C                                                                       003430
      RETURN                                                            003440
 50   CONTINUE                                                          003450
      PRINT 7                                                           003460
 7    FORMAT (/ T2,*NO HYSTERESIS LOOP DATA* ,/)                        003470
      KI=0                                                              003480
      RETURN                                                            003490
      END                                                               003500
C                                                                       003510
C***********************************************************          003520
C                                                                       003530
      SUBROUTINE DATA2(CALSIG,CALDIS,SPECA,UNITS,KS)                    003540
      COMMON /C/ SIGC(70) ,STRT(70) ,STRP(70) ,STRNC(70) ,NC(70) ,KI    003550
     A,DELTELC(70),DELTPLC(70)                                          003560
      COMMON /D/ LP,LE                                                  003570
      INTEGER UNITS                                                     003580
      REAL NC                                                           003590
C  LE IS EFF ELAST GAGE LGTH,LP IS PL EFF GAGE LENGTH,                  003600
      REAL LE,LP                                                        003610
C                                                                       003620
      SIG( C,CAL,A,F)=C/F*CAL*500./A                                    003630
      E(C,CAL,F)=C/F*CAL                                                003640
      STNE(UTOT,UPL,EE)=(UTOT-UPL)/EE                                   003650
      STNP(UPL,EP)=UPL/EP                                               003660
C                                                                       003670
      PRINT 8,LE,LP,CALSIG,CALDIS                                       003680
 8    FORMAT (T2,* LE,LP,CALSIG,CALDIS  ARE = *, 4F9.5, //)             003690
      PRINT 6                                                           003700
 6    FORMAT (3(/), T2,*CYCLES*,  T9,*ELAST STN*, T22, *PL STRN*,       003710
     1 T35, *TOT STRN*,T48,*STRESS*,T57,*TOT DISPL* ,T70,*PL DISPL* /)  003720
      IF (UNITS.EQ.1HI)  FACTOR=1.00                                    003730
      IF (UNITS.EQ.1HM)  FACTOR=2.54                                    003740
C                                                                       003750
      DO 5 K=KS,KI                                                      003760
      SIGC(K)=SIG(SIGC(K),CALSIG,SPECA,FACTOR)*1.E-3                    003770
      UT=E(STRT(K),CALDIS,FACTOR)                                       003780
      UP=E(STRP(K),CALDIS,FACTOR)                                       003790
      STNEL=STNE(UT,UP,LE)*1.E2                                         003800
      STNPL=STNP(UP,LP)*1.E2                                            003810
      STRNC(K)=STNEL+STNPL                                              003820
C     STORE ELAS & PLAST STRAIN                                         003830
      STRT(K)=STNEL                                                     003840
      STRP(K)=STNPL                                                     003850
      DELTELC(K)=UT                                                     003860
      DELTPLC(K)=UP                                                     003870
      UT=UT*1.E3                                                        003880
      UP=UP*1.E3                                                        003890
      PRINT 7,NC(K),STRT(K),STRP(K),STRNC(K),SIGC(K),UT,UP              003900
 7    FORMAT (T2,F5.0,T9,F4.3,T22,F4.3   ,T35,F5.3,  T48,F5.1,T57,      003910
     1 F4.2,T70,F4.3)                                                   003920
 5    CONTINUE                                                          003930
      RETURN                                                            003940
      END                                                               003950
C                                                                       003960
C***********************************************************          003970
C                                                                       003980
      SUBROUTINE SUBPLOT(I)                                             003990
      COMMON /A/ N(1500),DELTSIG(1500),X(1500),Y(1500),DELTEL(1500),    004000
     ADELTPL(1500),DELTEE(1500),DELTSTN(1500),TITL(60),                 004010
     BR1(1500),DELTEP(1500)                                             004020
      COMMON /C/ SIGC(70),STRT(70),STRP(70),STRNC(70),NC(70),KI         004030
```

```
     A,DELTELC(70),DELTPLC(70)                                          004040
      REAL N,U(50),NC                                                   004050
      REAL XA(70),YA(70)                                                004060
      DIMENSION IPAK(50),MPLOT(10)                                      004070
      LOGICAL HYPLOT,COMPLOT,DUALPT                                     004080
C                                                                       004090
      PRINT 10,I,KI                                                     004100
 10   FORMAT (1H1//T2,*FROM SUBPLOT : NO. OF COMPUTER DATA PTS IS = *,  004110
     A15 / T17,*NO. OF HYSTERESIS LOOP DATA PTS IS = *, I5/)            004120
      CALL COMPRS                                                       004130
C                                                                       004140
      COMPLOT=.T.                                                       004150
      HYPLOT=.T.                                                        004160
      DUALPT=.F.                                                        004170
      IF (I.LE.0) COMPLOT=.F.                                           004180
      IF (KI.LE.0) HYPLOT=.F.                                           004190
      IF (HYPLOT.AND.COMPLOT) DUALPT=.T.                                004200
C                                                                       004210
      PRINT 6, COMPLOT,HYPLOT,DUALPT                                    004220
 6    FORMAT ( / *  COMPLOT = *, L3, 5X, *,HYPLOT = *, L3/,             004230
     AT3,*DUALPT = *,L3 /)                                              004240
C                                                                       004250
      IF (.NOT.COMPLOT.AND..NOT.HYPLOT) RETURN                          004260
C                                                                       004270
      LN2=1                                                             004280
      IF (DUALPT) LN2=2                                                 004290
C                                                                       004300
C  DEFINE MESSAG LTR HEIGHT & BLNK1 SIZE                                004310
      HT=0.14                                                           004320
C   ASSUMES 15 PLOTTED CHARACTERS                                       004330
C                                                                       004340
      XLNGTH=15.*HT+2.*HT                                               004350
      YLNGTH=2.*HT                                                      004360
      XORGIN=1.0                                                        004370
      YORGIN=1.0                                                        004380
C     ESTABLISH LENGTHS FOR BLANKING                                    004390
      XF=XORGIN+XLNGTH                                                  004400
      YF=YORGIN+YLNGTH                                                  004410
C     ESTABLISH MESSAG PRINT POSITIONS                                  004420
      XO=XORGIN+HT*2.                                                   004430
      YO=YORGIN+HT/2.                                                   004440
C                                                                       004450
C                                                                       004460
C     FOR PLOTS 1-10   USE  Y                                           004470
C                                                                       004480
      READ 1, (MPLOT(L),L=1,10)                                         004490
 1    FORMAT(10A1)                                                      004500
C                                                                       004510
      PRINT 9, (MPLOT(L),L=1,10)                                        004520
 9    FORMAT (T2, *MPLOT IS : *, 10(A1,1X) /)                           004530
C                                                                       004540
C     ASSUMES 15 CHARACTERS + $                                         004550
      ENCODE (15,20,U)  (TITL(KL),KL=1,15)                              004560
 20   FORMAT (15A1, "$")                                                004570
C                                                                       004580
C     YMIN2,YMAX2 - STRESS RANGE FOR PLOT 2                             004590
C     YMIN3,YMAX3 - STRAIN RANGE FOR PLOT 3                             004600
C     YMIN4,YMAX4 - STRESS RANGE FOR PLOT 4                             004610
C     YMIN5,YMAX5 - STRESS RANGE FOR PLOT 5                             004620
C     XMAX1 - DEFINED MAX NUMBER OF CYCLES FOR 2ND PLOT GROUP           004630
C                                                                       004640
      READ *,YMIN2,YINC2,YMAX2                                          004650
      READ *,YMIN3,YINC3,YMAX3                                          004660
      READ *,YMIN4,YINC4,YMAX4                                          004670
      READ *,YMIN5,YINC5,YMAX5                                          004680
      READ *,XSORGN,XCYCLE                                              004690
```

```
      READ *,XINC1,XMAX2                                                    004700
C                                                                           004710
      PRINT 8,YMIN2,YINC2,YMAX2,YMIN3,YINC3,YMAX3,YMIN4,YINC4,YMAX4,        004720
     AYMIN5,YINC5,YMAX5,XSORGN,XCYCLE,XINC1,XMAX2                           004730
  8   FORMAT (/T3,*YMIN2,YINC2,YMAX2 = *,3F10.2/                            004740
     AT3,*YMIN3,YINC3,YMAX3 = *,3F10.2/                                     004750
     BT3,*YMIN4,YINC4,YMAX4 = *,3F10.2 /                                    004760
     CT3,*YMIN5,YINC5,YMAX5 = *,3F10.2/                                     004770
     ET3,*XSORGN,XCYCLE = *,2F10.2/                                         004780
     DT3,*XINC1,XMAX2 = *,2F10.2/)                                          004790
C                                                                           004800
      JTEST=0                                                               004810
      DO 607  JRS=1,10                                                      004820
      IF (MPLOT(JRS).EQ.1HY) JTST=1                                         004830
      JTEST=JTEST+JTST                                                      004840
 607  CONTINUE                                                              004850
      IF (JTEST.EQ.0)   GO TO 1001                                          004860
      CALL BGNPL(-1)                                                        004870
      DO 1000  MINDEX=1,2                                                   004880
      IF (MINDEX.EQ.1.AND.COMPLOT) GO TO 400                                004890
      IF (MINDEX.EQ.1.AND..NOT.COMPLOT) GO TO 410                           004900
      IF (MINDEX.EQ.2.AND.COMPLOT) GO TO 405                                004910
      IF (MINDEX.EQ.2.AND..NOT.COMPLOT) GO TO 405                           004920
 400  CONTINUE                                                              004930
C     FIND XMAX                                                             004940
      XMAX=N(1)                                                             004950
      DO 30  M=2,I                                                          004960
      IF (N(M).GT.XMAX)  XMAX=N(M)                                          004970
 30   CONTINUE                                                              004980
      XMAX=XMAX/100.                                                        004990
      IXMAX=XMAX                                                            005000
      XMAX=(IXMAX+1)*100.                                                   005010
      IF (DUALPT)  GO TO 402                                                005020
      GO TO 401                                                             005030
 402  CONTINUE                                                              005040
      DO 32  M=1,KI                                                         005050
      IF (NC(M).GT. XMAX)  XMAX=NC(M)                                       005060
 32   CONTINUE                                                              005070
      XMAX=XMAX/100.                                                        005080
      IXMAX=XMAX                                                            005090
      XMAX=(IXMAX+1)*100.                                                   005100
      GO TO 401                                                             005110
C                                                                           005120
 410  CONTINUE                                                              005130
C     FIND NC-MAX                                                           005140
      XMAX=NC(1)                                                            005150
      DO 31  M=2,KI                                                         005160
      IF (NC(M).GT.XMAX)  XMAX=NC(M)                                        005170
 31   CONTINUE                                                              005180
      XMAX=XMAX/100.                                                        005190
      IXMAX=XMAX                                                            005200
      XMAX=(IXMAX+1)*100.                                                   005210
      GO TO 401                                                             005220
C                                                                           005230
 405  CONTINUE                                                              005240
 415  CONTINUE                                                              005250
      XMAX=XMAX2                                                            005260
      GO TO 401                                                             005270
C                                                                           005280
 401  CONTINUE                                                              005290
      PRINT 3, MINDEX,XMAX                                                  005300
  3   FORMAT (T2,*MINDEX= *, I3, 4X,*XMAX = *,F7.1 /)                       005310
C                                                                           005320
      IF (MPLOT(MINDEX*5-4).NE.1HY)  GO TO 502                              005330
 501  CONTINUE                                                              005340
C                                                                           005350
```

```
C PLOT S-MAX/S-MIN VS CYCLES          PLOT #1                                  005360
C$$$$$$$$$$$$$$$$$$$$$$$$$$$$$$$$$$$$$$$$$$$$$$$$$$$$$$$$$$$$$$$$$$$$$$$$$$ 005370
C                                                                              005380
      IF (.NOT.COMPLOT) GO TO 120                                              005390
      PRINT 7,I                                                                005400
 7    FORMAT(///* SUBPLOT *//,T2,* I= *,I5/)                                   005410
C     DO 10 J=1,I                                                              005420
C     PRINT 1,J, N(J), R1(J)                                                   005430
C1    FORMAT (T2,  *J= *,I5,3X,* N= *,F7.1,3X,* R1= *,F5.3)                    005440
C10   CONTINUE                                                                005450
C                                                                              005460
      XLTH=7.0                                                                 005470
      YLTH=5.0                                                                 005480
      XMIN=0.0                                                                 005490
      XINC=500.                                                                005500
      YINC=.1                                                                  005510
      YMIN=.4                                                                  005520
      YMAX=1.3                                                                 005530
C     ELIM OUT OF RANGE PTS                                                    005540
      IT=0                                                                     005550
      DO 210  IJ=1,I                                                           005560
      IF (R1(IJ).LT.YMIN.OR.R1(IJ).GT.YMAX) GO TO 211                          005570
      IF (N(IJ).LT.XMIN.OR.N(IJ).GT.XMAX) GO TO 211                            005580
      IT=IT+1                                                                  005590
      X(IT)=N(IJ)                                                              005600
      Y(IT)=R1(IJ)                                                             005610
      GO TO 210                                                                005620
 211  CONTINUE                                                                 005630
 210  CONTINUE                                                                 005640
C                                                                              005650
      CALL BASALF("STANDARD")                                                  005660
      CALL MIXALF ("INSTRUCTION")                                              005670
      CALL MX3ALF ("L/OGREEK" ,1H*)                                            005680
      CALL TITLE(1H ,-1,"CYCLES$",100,"RATIO (H2.)*S)(LH.5)MAX(LXHX) TO 005690
     1(H2.)*S)(LH.5)MIN(LXHX)$", 100, XLTH  ,YLTH)                             005700
      CALL HEADIN ("RATIO OF (H2.)*S)(LH.5)MAX(LXHX) TO (H2.)*S(LH.5)MIN005710
     1(LXHX)$",   100,3,2)                                                    005720
      CALL HEADIN ("VERSUS CYCLES$", +100, 3,2)                                005730
      CALL BLNK1(XORGIN,XF,YORGIN,YF,+1)                                       005740
      CALL INTAXS                                                              005750
      CALL FRAME                                                               005760
      CALL GRAF(XMIN,XINC,XMAX,YMIN,YINC,YMAX)                                 005770
      CALL SCLPIC(0.5)                                                         005780
      CALL CURVE (X,Y,IT,-1)                                                   005790
      CALL RESET("BLNK1")                                                      005800
      CALL HEIGHT (HT)                                                         005810
      CALL MESSAG(U,100,XO,YO)                                                 005820
      CALL ENDPL(MINDEX*5-4)                                                   005830
      CALL RESET ("HEIGHT")                                                    005840
C                                                                              005850
C                                                                              005860.
 502  CONTINUE                                                                 005870
      IF (MPLOT(MINDEX*5-3).NE.1HY)  GO TO 503                                 005880
C                                                                              005890
C                                                                              005900
C     PLOT STRESS RANGE VS CYCLES      PLOT #2                                 005910
C$$$$$$$$$$$$$$$$$$$$$$$$$$$$$$$$$$$$$$$$$$$$$$$$$$$$$$$$$$$$$$$$$$$$$$$$$$ 005920
C                                                                              005930
C     DO 11 J=1,I                                                              005940
C     PRINT 2, J, N(J),DELTSIG(J)                                              005950
C2    FORMAT(T2,*J= *,I5,3X,*N= *,F7.1,3X,*DELTSIG= *, F6.1)                   005960
C11   CONTINUE                                                                005970
C                                                                              005980
      XLTH=7.0                                                                 005990
      YLTH=5.0                                                                 006000
      YMIN=YMIN                                                                006010
```

```
      YINC=YINC2                                                        006020
      YMAX=YMAX2                                                        006030
      XMIN=0.0                                                          006040
      XINC=500.                                                         006050
      IF (MINDEX.EQ.1) XINC=XINC1                                       006060
C                                                                       006070
      IF (.NOT.COMPLOT)  GO TO 120                                      006080
      IT=0                                                              006090
      DO 220  IJ=1,I                                                    006100
      IF (DELTSIG(IJ).LT.YMIN.OR.DELTSIG(IJ).GT.YMAX) GO TO 221         006110
      IF (N(IJ).LT.XMIN.OR.N(IJ).GT.XMAX) GO TO 221                     006120
      IT=IT+1                                                           006130
      X(IT)=N(IJ)                                                       006140
      Y(IT)=DELTSIG(IJ)                                                 006150
      GO TO 220                                                         006160
 221  CONTINUE                                                          006170
 220  CONTINUE                                                          006180
C                                                                       006190
 120  CONTINUE                                                          006200
      IF (.NOT.HYPLOT) GO TO 227                                        006210
      JT=0                                                              006220
      DO 225 IJ=1,KI                                                    006230
      IF (SIGC(IJ).LT.YMIN.OR.SIGC(IJ).GT.YMAX) GO TO 226               006240
      IF (NC(IJ).LT.XMIN.OR.NC(IJ).GT.XMAX)  GO TO 226                  006250
      JT=JT+1                                                           006260
      XA(JT)=NC(IJ)                                                     006270
      YA(JT)=SIGC(IJ)                                                   006280
      GO TO 225                                                         006290
 226  CONTINUE                                                          006300
 225  CONTINUE                                                          006310
 227  CONTINUE                                                          006320
C                                                                       006330
C                                                                       006340
      CALL SCLPIC(1.0)                                                  006350
      CALL RESET ("MXALFS")                                             006360
      CALL BASALF("STANDARD")                                           006370
      CALL TITLE(1H  ,-1,  "CYCLES$",  100,  "STRESS RANGE (KSI)$",     006380
     1  100,XLTH, YLTH)                                                 006390
      CALL HEADIN ("STRESS RANGE  VS  CYCLES$", -100,3,1)               006400
      CALL BLNK1(XORGIN,XF,YORGIN,YF,+1)                                006410
      CALL BLNK2(0.35,4.25,1.95,2.65,+1)                                006420
      CALL INTAXS                                                       006430
      CALL FRAME                                                        006440
      CALL GRAF (XMIN,XINC,XMAX,YMIN,YINC,YMAX)                         006450
      CALL SCLPIC(0.5)                                                  006460
      IF (COMPLOT) CALL CURVE (X,Y,IT,-1)                               006470
      IF (HYPLOT)  CALL CURVE(XA,YA,JT,-1)                              006480
      CALL RESET("BLNK1")                                               006490
      CALL RESET("BLNK2")                                               006500
      CALL HEIGHT (HT)                                                  006510
      CALL MESSAG(U,100,XO,YO)                                          006520
      CALL SCLPIC(1.00)                                                 006530
      IF (COMPLOT) CALL LINES("COMPUTER GENERATED DATA$",IPAK,1)        006540
      IF (HYPLOT) CALL LINES ("HYSTERESIS LOOP DATA$",IPAK,LN2)         006550
      CALL LEGEND(IPAK,LN2,1.0,2.0)                                     006560
      CALL ENDPL(MINDEX*5-3)                                            006570
      CALL RESET ("HEIGHT")                                             006580
C                                                                       006590
 503  CONTINUE                                                          006600
      IF (MPLOT(MINDEX*5-2).NE.1HY)  GO TO 504                          006610
C                                                                       006620
C                                                                       006630
C     PLOT STRAIN RANGE VS CYCLES       PLOT #3                       006640
C$$$$$$$$$$$$$$$$$$$$$$$$$$$$$$$$$$$$$$$$$$$$$$$$$$$$$$$$$$$$$$$$$$$ 006650
C                                                                       006660
C     DO 12 J=1,I                                                       006670
```

```
C     PRINT 3, J,N(J),DELTSTN(J)                                        006680
C3    FORMAT(I2,*J= *,I5,3X,*N= *,F7.1,3X,*DELTSTN= *,F6.4)             006690
C12   CONTINUE                                                         006700
C                                                                       006710
      XLTH=7.0                                                          006720
      YLTH=5.0                                                          006730
      YMIN=YMIN3                                                        006740
      YINC=YINC3                                                        006750
      YMAX=YMAX3                                                        006760
      XMIN=0.0                                                          006770
      XINC=500.                                                         006780
      IF (MINDEX.EQ.1) XINC=XINC1                                       006790
C                                                                       006800
      IF (.NOT.COMPLOT) GO TO 130                                       006810
      IT=0                                                              006820
      DO 230  IJ=1,I                                                    006830
      IF (DELTSTN(IJ).LT.YMIN.OR.DELTSTN(IJ).GT.YMAX) GO TO 231         006840
      IF (N(IJ).LT.XMIN.OR.N(IJ).GT.XMAX) GO TO 231                     006850
      IT=IT+1                                                           006860
      X(IT)=N(IJ)                                                       006870
      Y(IT)=DELTSTN(IJ)                                                 006880
      GO TO 230                                                         006890
 231  CONTINUE                                                          006900
 230  CONTINUE                                                          006910
 130  CONTINUE                                                          006920
C                                                                       006930
      IF (.NOT.HYPLOT)  GO TO 237                                       006940
      JT=0                                                              006950
      DO 235 IJ=1,KI                                                    006960
      IF (STRNC(IJ).LT.YMIN.OR.STRNC(IJ).GT.YMAX) GO TO 236             006970
      IF (NC(IJ).LT.XMIN.OR.NC(IJ).GT.XMAX) GO TO 236                   006980
      JT=JT+1                                                           006990
      XA(JT)=NC(IJ)                                                     007000
      YA(JT)=STRNC(IJ)                                                  007010
      GO TO 235                                                         007020
 236  CONTINUE                                                          007030
 235  CONTINUE                                                          007040
 237  CONTINUE                                                          007050
C                                                                       007060
      CALL SCLPIC(1.0)                                                  007070
      CALL TITLE (1H , -1,"CYCLES$",  100, "STRAIN RANGE (PERCENT)$",   007080
     1 100,XLTH, YLTH)                                                  007090
      CALL HEADIN ("STRAIN RANGE  VS  CYCLES$",   -100, 3,1)            007100
      CALL FRAME                                                        007110
      CALL BLNK1(XORGIN,XF,YORGIN,YF,+1)                                007120
      CALL BLNK1(0.95,4.25,1.95,2.55,+1)                                007130
      CALL XINTAX                                                       007140
      CALL GRAF (XMIN,XINC,XMAX,YMIN,YINC,YMAX)                         007150
      CALL SCLPIC(0.5)                                                  007160
      IF (COMPLOT) CALL CURVE (X,Y,IT,-1)                               007170
      IF (HYPLOT)  CALL CURVE(XA,YA,JT,-1)                              007180
      CALL RESET("BLNK1")                                               007190
      CALL RESET ("BLNK2")                                              007200
      CALL HEIGHT (HT)                                                  007210
      CALL MESSAG(U,100,XO,YO)                                          007220
      CALL SCLPIC(1.0)                                                  007230
      IF (COMPLOT) CALL LINES("COMPUTER GENERATED DATA$",IPAK,1)        007240
      IF (HYPLOT) CALL LINES ("HYSTERESIS LOOP DATA$",IPAK,LN2)         007250
      CALL LEGEND (IPAK,LN2,1.0,2.0)                                    007260
      CALL ENDPL(MINDEX*5-2)                                            007270
      CALL RESET ("HEIGHT")                                             007280
C                                                                       007290
 504  CONTINUE                                                          007300
      IF (MPLOT(MINDEX*5-1).NE.1HY)  GO TO 505                          007310
C                                                                       007320
C ..  PLOT EXPLODED STRESS RANGE VS CYCLES  PLOT #4                     007330
```

```
C$$$$$$$$$$$$$$$$$$$$$$$$$$$$$$$$$$$$$$$$$$$$$$$$$$$$$$$$$$$$$$$$$
C
      XLTH=7.0
      YLTH=5.0
      YMIN=YMIN4
      YINC=YINC4
      YMAX=YMAX4
      XMIN=0.0
      XINC=500.
      IF (MINDEX.EQ.1) XINC=XINC1
C
      IF (.NOT.COMPLOT) GO TO 140
      IT=0
      DO 240  IJ=1,I
      IF (DELTSIG(IJ).LT.YMIN.OR.DELTSIG(IJ).GT.YMAX ) GO TO 241
      IF (N(IJ).LT.XMIN.OR.N(IJ).GT.XMAX) GO TO 241
      IT=IT+1
      X(IT)=N(IJ)
      Y(IT)=DELTSIG(IJ)
      GO TO 240
  241 CONTINUE
  240 CONTINUE
  140 CONTINUE
C
      IF (.NOT.HYPLOT) GO TO 247
      JT=0
      DO 245 IJ=1,KI
      IF (SIGC(IJ).LT.YMIN.OR.SIGC(IJ).GT.YMAX) GO TO 246
      IF (NC(IJ).LT.XMIN.OR.NC(IJ).GT.XMAX) GO TO  246
      JT=JT+1
      XA(JT)=NC(IJ)
      YA(JT)=SIGC(IJ)
      GO TO 245
  246 CONTINUE
  245 CONTINUE
  247 CONTINUE
C
      CALL SCLPIC(1.0)
      CALL TITLE(1H  ,-1,  "CYCLES$",  100,  "STRESS RANGE (KSI)$",
     1  100,XLTH, YLTH)
      CALL HEADIN ("STRESS RANGE  VS  CYCLES$", -100,3,1)
      CALL FRAME
      CALL BLNK1(XORGIN,XF,.30 ,.60 ,+1)
      CALL BLNK2(0.60,3.90,0.90,1.6,+1)
      CALL INTAXS
      CALL GRAF (XMIN,XINC,XMAX,YMIN,YINC,YMAX)
      CALL GRID (5,5)
      CALL SCLPIC(0.5)
      IF (COMPLOT) CALL CURVE (X,Y,IT,-1)
      IF (HYPLOT)   CALL CURVE(XA,YA,JT,-1)
      CALL RESET("BLNK1")
      CALL RESET ("BLNK2")
      CALL HEIGHT (HT)
      CALL MESSAG(U,100,XO,.38)
      CALL SCLPIC(1.0)
      IF (COMPLOT) CALL LINES("COMPUTER GENERATED DATA$",IPAK,1)
      IF (HYPLOT) CALL LINES ("HYSTERESIS LOOP DATA$",IPAK,LN2)
      CALL LEGEND (IPAK,LN2,.65,.95)
      CALL ENDPL (MINDEX*5-1)
      CALL RESET ("HEIGHT")
C
C
  505 CONTINUE
      IF (MPLOT(MINDEX*5).NE.1HY)  GO TO 99
C
C     PLOT STRESS RANGE VS LOG CYCLES  PLOT #5
```

```
C$$$$$$$$$$$$$$$$$$$$$$$$$$$$$$$$$$$$$$$$$$$$$$$$$$$$$$$$$$$$
C
      YMIN=YMIN5
      YMAX=YMAX5
      YLTH=5.
      XLTH=7.
      YSTEP=YINC5
      XMIN=0.0
      IF ((YMIN5+YLTH*YINC5).LT.YMAX5) YSTEP=(YMAX5-YMIN5)/YLTH
C
      IF (.NOT.COMPLOT) GO TO 150
      IT=0
      DO 250 IJ=1,I
      IF (DELTSIG(IJ).LT.YMIN.OR.DELTSIG(IJ).GT.YMAX)  GO TO 251
      IF (N(IJ).LT.XMIN.OR.N(IJ).GT.XMAX) GO TO 251
      IT=IT+1
      X(IT)=N(IJ)
      Y(IT)=DELTSIG(IJ)
      GO TO 250
  251 CONTINUE
  250 CONTINUE
      IF (IT.EQ.0) GO TO 260
  150 CONTINUE
C
      IF (.NOT.HYPLOT)  GO TO 257
      JT=0
      DO 255  IJ=1,KI
      IF (SIGC(IJ).LT.YMIN.OR.SIGC(IJ).GT.YMAX) GO TO 256
      IF (NC(IJ).LT.XMIN.OR.NC(IJ).GT.XMAX)  GO TO 256
      JT=JT+1
      XA(JT)=NC(IJ)
      YA(JT)=SIGC(IJ)
      GO TO 255
  256 CONTINUE
  255 CONTINUE
      IF (JT.EQ.0) GO TO 260
  257 CONTINUE
C
      PRINT 280,YMIN,YMAX,YLTH,XLTH,YSTEP
  280 FORMAT (T2 ,*YMIN5,YMAX5,YLTH,XLTH,YSTEP = *,5F7.1 /)
C
      CALL MIXALF ("L/CSTD")
      CALL TITLE  ("STRESS RANGE  VS  L(OG) CYCLES$", -100,
     1 "CYCLES$", 100,  "STRESS RANGE (()KSI())$",  100,
     2  XLTH,YLTH)
      CALL YINTAX
      CALL FRAME
      CALL BLNK1(XORGIN,XF,YORGIN,YF,+1)
      XINC5=XLTH/XCYCLE
      PRINT 281,X5ORGN,XINC5,YMIN,YSTEP
  281 FORMAT (T2,*X5ORGN,XINC5,YMIN,YSTEP = *,4F7.1/)
C
      CALL XLOG(X5ORGN,XINC5,YMIN,YSTEP)
      CALL SCLPIC(0.5)
      IF (COMPLOT) CALL CURVE (X,Y,IT,-1)
      IF (HYPLOT)   CALL CURVE(XA,YA,JT,-1)
      CALL RESET("BLNK1")
      CALL HEIGHT (HT)
      CALL MESSAG(U,100,XO,YO)
      CALL SCLPIC(1.0)
      IF (COMPLOT) CALL LINES("COMPUTER GENERATED DATA$",IPAK,1)
      IF (HYPLOT) CALL LINES ("HYSTERESIS LOOP DATA$",IPAK,LN2)
      CALL LEGEND (IPAK,LN2,1.,2.)
      CALL ENDPL (MINDEX*5)
C
      GO TO 99
```

```
 260  CONTINUE                                                          008660
      PRINT 264,IT,JT                                                   008670
 264  FORMAT (T3, 34*** , *NO DATA PTS WITH RANGE OF PLOT 5*/           008680
     AT4,*IT = *,I5, 3X, *,JT = *, I5/)                                 008690
C                                                                       008700
 99   CONTINUE                                                          008710
C                                                                       008720
C$$$$$$$$$$$$$$$$$$$$$$$$$$$$$$$$$$$$$$$$$$$$$$$$$$$$$$$$$$$$$$$$$$$$ 008730
 1000 CONTINUE                                                          008740
      CALL DONEPL                                                       008750
 1001 CONTINUE                                                          008760
      RETURN                                                            008770
      END                                                               008780
```

BIBLIOGRAPHY

1. M. N. Menon and W. H. Reimann, "Low Cycle Fatigue Crack Initiation Study in René 95," J. Mater. Sci. 10, 1571-1581 (1975).

2. B. Leis and A. Clauer, Investigation of Rejuvenation of Fatigue Damage in IN-718, Air Force Materials Laboratory Technical Report, AFML-TR-78-90, AF Contract F33615-76-C-5100 (Air Force Materials Laboratory, Wright-Patterson Air Force Base, Ohio, 1978).

3. S. S. Manson, Thermal Stress and Low Cycle Fatigue, McGraw-Hill (1966).

4. M. Gill, G. R. Leverant, and C. H. Wells, "The Fatigue Strength of Nickel-Base Superalloys," Achievement of High Fatigue Resistance in Superalloys, ASTM STP 467, American Society of Testing and Materials, 53-76 (1970).

5. C. H. Wells and C. P. Sullivan, "Low Cycle Fatigue of Udimet 700 at 1700 F," Trans. ASM 61, 149-155 (1968).

6. C. H. Wells and C. P. Sullivan, "The Effect of Temperature on the Low Cycle Fatigue Behavior of Udimet 700," Trans. ASM 60, 217-222 (1967).

7. C. H. Wells and C. P. Sullivan, "The Low Cycle Fatigue Characteristics of a Nickel-Base Superalloy at Room Temperature," Trans. ASM 57, 841-855 (1964).

8. M. Gell and G. R. Leverant, "The Fatigue of the Nickel-Base Superalloy MAR-M-200 in Single Crystal and Columnam Grain Forms at Room Temperature," Trans. AIME 242, 1869-1879 (1968).

9. P. Gauthier, H. DeRandy, and J. Auvinet, "Secondary Cracking Process During Fatigue Crack Propagation," Eng. Fract. Mech. 5, 977-981 (1973).

10. W. H. Vaughan, R. J. Sanford, J. M. Krofft, W. H. Cullen, and J. W. Dolly, Failure Studies of a Third Stage Fan Disk from a TF-30 Turbine Engine, NRL Memorandum Report 3874, Naval Research Laboratories (1978).

11. A. H. Cottrell, "Fracture," Proc. Roy. Soc. London A 276, 1-18 (1963).

12. A. W. Funkenbusch and L. F. Coffin, "Low Cycle Fatigue Crack Nucleation and Early Growth in Ti-17," Met. Trans. 9A, 1159-1167 (1978).

13. J. C. Grosskrentz, Phys. Stat. Solidi (B) 47, 359-396 (1971).

14. G. E. Dieter, Mechanical Metallurgy, McGraw-Hill, 403-450 (1976).

15. C. H. Wells and C. P. Sullivan, "The Low Cycle Fatigue Characteristics of a Nickel-Base Superalloy at Room Temperature," Trans. ASM 57, 841-847 (1964).

16. H. F. Merrick, "The Low Cycle Fatigue of Three Wrought Nickel-Base Alloys," Met. Trans. 5, 891-897 (1974).

17. D. R. Muzyka, "The Metallurgy of Iron Nickel Alloys," The Superalloys (C. T. Sims and W. C. Hagel, eds.), John Wiley and Sons, New York (1972).

18. R. F. Decker and S. Floreen, "Precipitation from Substitutional Iron-Base Austenitic and Martensitic Solid Solutions," Precipitation from Iron Base Alloys (G. R. Speich and J. B. Clark, eds.), Gordon and Breach Scientific Publishers, New York (1965).

19. E. F. Bradley and M. J. Donachie, "Forgings for Jet Engines: More Quality at Less Cost," Metals Prog. 106/2, 80-82 (July 1974).

20. D. Raynor and J. M. Silcock, "Strengthening Mechanisms in Gamma-Prime Precipitating Alloys," Metal Sci. J. 4, 121-130 (1970).

21. D. R. Muzyka, "Controlling Microstructure and Properties of Superalloys Via Use of Precipitated Phases," Metals Eng. Qtrly 11/4, 12-20 (1971).

22. G. R. Speich, "Cellular Precipitation in an Austenitic Fe-30Ni-6Ti Alloy," Trans. AIME 227, 754-762 (1963).

23. C. C. Clark and J. S. Iwanski, "Phase Changes in Precipitation Hardening Nickel-Chromium-Iron Alloys during Prolonged Heating," Trans. AIME 215, 648-651 (1959).

24. H. J. Beattie and W. C. Hagel, "Intragranular Precipitation of Intermetallic Compounds in Complex Austenitic Alloys," Trans. AIME 221, 28-35 (1961).

25. E. E. Brown, R. C. Boettner, and D. L. Ruckle, Minigrain Processing of Nickel-Base Alloys, presented at the Metallurgical Society of AIME Fall Meeting, Cleveland, 1970.

26. R. F. Decker and C. T. Sims, "The Metallurgy of Nickel-Based Superalloys," The Superalloys (C. T. Sims and W. C. Hagel, eds.) John Wiley and Sons, New York (1972).

27. C. T. Sims, "The Occurrence of Topologically Close-Packed Phases," The Superalloys (C. T. Sims and W. C. Hagel, eds.), John Wiley and Sons, New York (1972).

28. J. P. Dennison and B. Wilshire, "Mechanisms of Improving Creep Rupture Lives by Re-Heat Treatments," Fracture 2, 635-639 (1977).

29. J. P. Dennison, P. D. Holmes, and B. Wilshire, "The Creep and Fracture Behavior of the Cast Nickel-Based Superalloy IN-100," Mater. Sci. & Eng. 33, 35-47 (1978).

30. K. C. Anthony and J. F. Rodavitch, The Effects of HIP Rejuvenation of Turbine Blades, presented at the AIME Annual Meeting, Atlanta, Georgia.

31. Summary Report on the Powder Metallurgy Seminar, Air Force Materials Laboratory Technical Report AFML-TM-LT-74-4 (Air Force Materials Laboratory, Wright-Patterson Air Force Base, Ohio, 1974).

32. ASTM Standard E407-70, "Standard Methods for Microetching Metals and Alloys," Annual Book of ASTM Standards, American Society of Testing and Materials, Philadelphia (1974).

33. M. F. Henry, A Technique for Monitoring Time Dependent Surface Damage, General Electric Report No. 71-C-338, Schenectady, New York (1971).

34. Pratt and Whitney Aircraft Specification 1003H, East Hartford, Conn. (November 1973).

35. W. P. Koster and J. B. Kohls, Relationship of Surface Integrity to Cost and Reliability of Structural Components, SME Technical Paper IQ72-207 (1972).

36. R. L. Ketter and S. P. Prawel, Modern Methods of Engineering Computation, McGraw-Hill (1969).

37. L. G. Heroux and C. P. Sullivan, "Metallographic Replication of Curved Surfaces," Trans. ASM 56, 861-863 (1963).

38. L. K. Singhal and M. L. Vaidya, "Precipitation of Sigma Phase in a Duplex Fe-Cr-Ni-Ti Alloy," Trans. ASM Qtrly 62, 879-885 (1969).

39. W. H. Hill, K. D. Shimmin, and B. A. Wilcox, "Elevated Temperature Dynamic Moduli of Metallic Materials," ASTM Proc. 61, 890-906 (1961).

40. S. Spinner and W. F. Tefft, "A Method for Determining Mechanical Resonance Frequencies and for Calculating Elastic Moduli from These Frequencies," ASTM Proc. 61, 1221-1238 (1961).

41. W. E. Tefft, "Numerical Solution of the Frequency Equations for the Flexural Vibration of Cylindrical Rods," J. Research NBS 64B, 237-242 (1960).

42. ASTM Standard E112-61, "Standard Methods for Estimating the Average Grain Size of Metals," Annual Book of ASTM Standards, American Society of Testing and Materials, Philadelphia (1974).

43. Aerospace Structural Metals Handbook, Code 4107, Mechanical Properties Data Center, Traverse City, Michigan (December 1973).

44. A. Green, H. Sieber, D. Wells, and T. Wolfe, Research Investigation to Determine Mechanical Properties of Nickel and Cobalt-Base Alloys for Inclusion in Military Handbook 5, Air Force Materials Laboratory Technical Report ML-TDR-64-116, DDC AD-608813, V1, 500-508 (1964).

45. SEM/TEM Fractography Handbook, MCIC-HB-06, compiled by McDonnell Douglas Astronautics Co., published by Metals and Ceramics Information Center, Battelle-Columbus Laboratories, Columbus, Ohio (1975).

46. C. Laird, Mechanisms and Theories of Fatigue, presented at the Materials Science Seminar, American Society for Metals, St. Louis, Missouri (1978).

47. W. H. Kim and C. Laird, "Crack Nucleation and Stage I Propagation in High Strain Fatigue - I. Microscopic and Interferometric Observations," Acta Met. 26, 777-787 (1978).

48. W. H. Kim and C. Laird, "Crack Nucleation and Stage I Propagation in High Strain Fatigue - II. Mechanism," Acta Met. 26, 789-799 (1978).

49. D. Kuhlmann-Wilsdorf and C. Laird, "Dislocation Behavior in Fatigue," Mater. Sci. and Eng. 31, 137-156 (1977).

50. W. A. Wood, Fatigue in Aircraft Structures, Academic Press, New York (1956).

51. C. Laird, Fatigue Crack Propagation, ASTM 415, American Society for Testing and Materials, Philadelphia (1967).

52. A. S. Tetelman and A. J. McEvily, Fracture of Structural Materials, 347-400 (1967).

53. American Society for Metals, Failure Analysis and Prevention, vol. 10, Metals Handbook (8th ed.), Metals Park, Ohio (1975).

54. F. Petit, Personal Communication, Materials Research Laboratory, Pratt and Whitney Aircraft, Commercial Products Division, East Hartford, Conn. (June 1979).

55. R. Sandström, "Subgrain Growth Occurring by Boundary Migration," Acta Met. 25, 905-911 (1977).

56. R. Sandström, "On Recovery of Dislocations in Subgrains and Subgrain Coalescence," Acta Met. 25, 897-904 (1977).

57. J. P. Hirth and J. Lothe, Theory of Dislocations, McGraw-Hill, New York (1968).

58. M. R. James and A. W. Sleeswyk, "Influence of Intrinsic Stacking Fault Energy on Cyclic Hardening," Acta Met. 26, 1721-1726 (1978).

59. R. W. Landgraf, "The Resistance of Metals to Cyclic Deformation," Achievement of High Fatigue Resistance in Metals and Alloys, ASTM STP 467, American Society of Testing and Materials, 3-36 (1970).

60. R. W. Smith, M. H. Hirschberg, and S. S. Manson, Fatigue Behavior of Materials under Strain Cycling in Low and Intermediate Life Range, NASA Technical Note D-1574, Lewis Research Center, Cleveland, Ohio (1963).

61. T. J. Dolan, "Designing Structures to Resist Low-Cycle Fatigue," Metals Eng. Qtrly 10, 18-25 (November 1970).

62. D. Macha, Unpublished Research, Air Force Materials Laboratory, Metals Behavior Branch (AFML/LLN), Wright-Patterson Air Force Base, Ohio 45433 (1977).

63. G. R. Irwin, Plastic Zone Near a Crack and Fracture Toughness, Seventh Sagamore Ordinance Materials Research Conference (August 1960).

64. C. Calabrese and C. Laird, "High Strain Fatigue Fracture Mechanics in Two Phase Alloys," Met. Trans. 5, 1785-1793 (1974).

65. C. Calabrese and C. Laird, "Cyclic Stress-Strain Response of Two-Phase Alloys; Part I. Microstructures Containing Particles Penetrable by Dislocations," Mater. Sci. and Eng. 13, 141-157 (1974).

66. C. Calabrese and C. Laird, "Cyclic Stress-Strain Response of Two-Phase Alloys; Part II. Particles Not Penetrated by Dislocations," Mater. Sci. and Eng. 13, 159-174 (1974).

67. W. H. Kim and C. Laird, "The Role of Cyclic Hardening in Crack Nucleation at High Strain Amplitude," Mater. Sci. and Eng. 33, 225-231 (1978).

68. C. Laird, V. J. Langelo, M. Hallrah, N. C. Yang, and R. DeLaVeaux, "The Cyclic Stress-Strain Response of Precipitation Hardened Al-15 wt% Ag Alloy," Mater. Sci. and Eng. 32, 137-160 (1978).

69. H. J. Beattie, Jr., "The Crystal Structure of a M_3B_2-Type Double Boride," Acta Cryst. 11, 607-609 (1958).

70. M. J. Fleetwood and C. A. P. Horton, "The Use of the Microprobe Analyzer and the Electron Microscope for the Identification of Precipitate Particles in a Nickel-Chromium-Iron Alloy," J. Roy. Microsc. Soc. 83, 245-250 (1964).


DA
FILM